

**Marine palynological records in the southern South China Sea over the
last 44 kyr**

Dissertation
zur Erlangung des Doktorgrades der
Mathematisch-Naturwissenschaftlichen-Fakultät
der Christian-Albrechts-Universität
zu Kiel

vorgelegt von
Hiroshi Kawamura

Kiel 2002

Referent: Prof. Dr. Wolfgang Kuhnt

Koreferent: Dr. habil. Wolfram Brenner

Tag der mündlichen Prüfung: 11.12.2002

Zum Druck genehmigt: Kiel,

Der Dekan: Prof. Dr. Wulf Depmeier

ABSTRACT

Dinoflagellate cysts and pollen from the South China Sea (SCS) are investigated to test their applicability as paleoceanographic/paleoclimatic indicators. Modern distribution patterns and species composition of dinoflagellate cysts are determined in 86 surface sediment samples, collected during the R/V Sonne cruises 95, 115 and 140a.

A total of 45 dinoflagellate cyst species are identified. The highest concentrations are found in the shallow coastal areas (< 50 m water-depth) off middle Vietnam, where the highest surface water productivity is recorded. Similarly, the lowest surface water productivity recorded near the central SCS basin corresponds to the lowest cyst concentrations.

Multivariate statistical analysis of the dinoflagellate cyst assemblage show that the distribution patterns and the species compositions are strongly related to the distance of a surface sample from the coast. This relationship may be the result of offshore transport from the high productivity shallow coastal areas and/or of surface water productivity gradients in the SCS. The dinoflagellate cyst taxa can therefore be divided into three groups on the basis of surface water productivity, namely: eutrophic & coastal-slope, mesotrophic & shelf to slope, and oligotrophic & oceanic.

The eutrophic & coastal-slope group is dominated by protoperidinioids such as *Brigantedinium* spp. *Selenopemphix nephroids* and *Trinovantedinium capitatum*. The mesotrophic & shelf to slope group is characterized by high proportion of variety of *Spiniferites* species and *Protoceratium reticulatum*. The oligotrophic & oceanic group is characterized by the occurrence of *Impagidinium* species and *Nematosphaeropsis labyrinthus*.

To test if these groupings can be used to reconstruct past changes in surface water productivity, the dinoflagellate cyst and pollen content from the high resolution core GIK 18267-3 are investigated. This core was recovered from a winter upwelling area off the Sunda Shelf and contains a 44 kyr undisturbed pelagic record. The results indicate that the surface water productivity was moderately higher during Marine Isotope Stage (MIS) 3 than the present, and that the climate was slightly drier than the present. The highest surface water productivity during the last 44 kyr is recorded in MIS 2, corresponding to the coldest climate. From about 19 ka cal. BP until the early Holocene, the productivity gradually decreased as the climate rapidly became warm and wet.

The general trend is for eutrophic surface water to correspond to a cold/dry climate with a strong winter monsoon and a weak summer monsoon, and for oligotrophic surface water conditions to correspond to a warm/humid climate with a strong summer monsoon and a weak winter monsoon.

KURZFASSUNG

Um die Anwendbarkeit von Dinoflagellaten-Zysten für paläoozeanographische/klimatische Rekonstruktionen zu testen, wurden Dinoflagellaten-Zysten in Sedimenten aus dem Südchinesischen Meer untersucht. Die Artenzusammensetzung und die räumlichen Verteilungsmuster moderner Dinoflagellaten-Zysten wurden anhand von 86 Oberflächensedimentproben untersucht (RV SONNE Fahrten 95, 115, und 140a). Insgesamt konnten 45 Dinoflagellaten Arten bestimmt werden. Die Artendichte und Individuenzahl ist in den flachen Küstengewässern (< 50 m Wassertiefe) vor Mittel-Vietnam, in einem Gebiet mit hoher Oberflächenwasserproduktivität, am höchsten. Niedrigste Zysten-Konzentrationen treten im zentralen Beckenbereich des Südchinesischen Meeres auf, in denen die Oberflächenwasserproduktivität am niedrigsten ist.

Eine multivariate statistische Auswertung der Artengemeinschaften ergab, dass Artenzusammensetzung und Verteilungsmuster der Dinoflagellaten-Zysten dabei stark abhängig von der Entfernung einer Probe zur Küste sind. Dies ist vermutlich auf Umlagerung von Zysten aus den hochproduktiven Küstengewässern in die Tiefsee und/oder auf Produktivitätsgradienten im Oberflächenwasser des Südchinesischen Meeres zurückzuführen. Es konnten somit drei Artengruppen von Dinoflagellaten-Zysten unterschieden werden: Die Artengruppe der eutrophen Küstengewässer ("Eutroph/Küstengewässer"), die durch die Arten *Brigantidium* spp. *Selenopemphix nephroids* und *Trinovantedinium capitatum* dominiert wird, die Gruppe "Mesotroph/Schelf-Hang" mit den Arten *Spiniferites* species and *Protoceratium reticulatum*, sowie die Gruppe "Oligotroph/Ozean", die durch die Arten *Impagidinium* species und *Nematosphaeropsis labyrinthus* dominiert wird.

Um zu prüfen, ob diese Gruppierung für eine Rekonstruktion der Paläoproduktivität genutzt werden kann, wurden Dinoflagellaten-Zysten- und Pollengehalt im Kern GIK 18267 untersucht. Die Ergebnisse zeigen, dass die Produktivität im Oberflächenwasser und die klimatischen Verhältnisse im Vergleich zum heutigen Zustand während des Marinen Isotopenstadiums 3 leicht erhöht bzw. geringfügig trockener waren. Die höchsten Produktivitätswerte der letzten 44 ka vor heute werden im Marinen Isotopenstadium 2 erreicht, das gleichzeitig durch die kühlestn klimatischen Bedingungen gekennzeichnet ist. Zwischen ca. 19000 Jahre vor heute und dem frühen Holozän nahm Primärproduktion allmählich ab, und das Klima wurde feuchter und wärmer.

Generell entsprechen eutrophe und kühl/trockene klimatische Bedingungen Phasen mit einem verstärkten Winter- bzw. abgeschwächten Sommer-Monsun. Oligotrophe Verhältnisse im Oberflächenwasser und warm/feuchte klimatische Bedingungen korrespondieren mit einem verstärkten Sommer- bzw. abgeschwächten-Winter-Monsun.

ACKNOWLEDGEMENTS

I sincerely thank Prof. Dr. Wolfgang Kuhnt for the opportunity to come to Kiel, to pursue “Doktorarbeit” in Kiel, for the supervision of this thesis and countless invitations to his place for dinner, wine and other good food. I thank Dr. habil. Wolfram Brenner for allowing me to use his Palynology laboratory and his guest-friendliness at GEOMAR. I am also deeply indebted to Dr. Bernard K. Maloney who passed away in 2000 for his encouragement during the difficult time and for allowing me to sub-sample from his precious SE Asian pollen reference collections.

I wish to thank Prof. Dr. Michael Sarnthein for his constructive critics on my age-model. I thank “Sunda Sister” Dr. Renata Szarek and “Sunda Brother” Dr. Stephan Steinke for the last minute help for proof reading and for the German translations of abstract. You guys were very helpful although you guys are so far away (Poland and Taiwan).

Others equally worthy of note are “The Sunda Boys and Girls (Dr. Stephan Steinke, Dr. Renata Szarek, Dr. Till Hanebuth, Dr. Alex Schimanski and Dr. Charu “Honey” Sharma, Dr. Markus Kienast) and Dr. Christian “Crispy” Buehring for the countless discussions. My good friend in Canada Kevin E. Gostlin has helped me with English language and made some valuable comments on Chapter 2-3. Dr. Derek Dreger corrected English of my abstract.

Heartfelt thanks are extended to the current and former members of MIPA group (Dr. habili. Mara Weinelt, Dr. Ann Holbourn, Dr. Uta Wollenburg, Dr. Silvia Hess, Dr. Shirley van Kreveld, Prof. Dr. Zhimin Jian, Frau Brigitte Salomon, Frau Astrid Lueders, Dr. Uwe Pflaumann, Dr. Florian Luderer, Dr. Thorsten Kiefer, Dr. Thomas Pletsch, Dr. Mikael Gustafsson, Dr. Abder El Albani, Dr. habili. Holgar Gebhardt, Oran Costello, Harald Paulsen, Andrea Lorenz) for the helps here and there.

A debt of gratitude is owed to our non-MIPA lunch crew (Dr. Elke Vogelsang, Dr. Thomas Papenfuss, Dr. Johannes Simstich, Prof. Baohua Lee, Daniela Crudeli, Christian Millo, Gretta Bartoli) for listening my complain and sharing their lunchtime with me. Other former and current colleagues in our institute (Prof. Dr. Michael Schulz, Dr. Hanno Kinkel, Dr. Derek Dreger, Luciano Henrique de Oliverira Caldas, Prof. Dr. Karl Statterger, Frank Koesters, Maja Zuvella) for their help, colleagues from GEOMAR (Dr. Andre Kaiser, Arne Sturm, Anja Wolf, Silke Steph, Dr. Shungo Kawagata, Dr. Mari Sumita, Hans Jörg Meemkan, Natasja Brughmans, Reinhard Kozdon, Jeroen Groeneveld) for making me feel at home at GEOMAR.

I am also grateful to Prof. Dr. Kazumi Matsuoka, Dr. Hyun-Jin Cho, Prof. Dr. Francine McCarthy and Dr. Annemiek Vink for stimulating discussions and comments on dinoflagellate cyst taxonomy. Professor Xiangjun Sun and Professor Quanhong Zhao provided valuable Chinese literature.

I owe special thanks to Prof. Dr. Pieter M. Grootes and Dr. Helmut Erlenkeuser for carrying out the AMS 14C dating and the isotope measurements at the Leibniz Laboratory. I would like to thank the captains and the crew of the R/V SONNE cruise 115 and 140 for the wonderful cruises.

I thank DAAD for six-months of German language course at the Goethe Institute Göttingen and 4 years of survival funding.

At last but not least, I thank my family (Yukichi Kawamura, Tatsuko Kawamura, Yumiko Ogawa, Hiromi Satoh, Yoshimi Kawamura) for their supports.

Well, that’s it!! I can now say “Ich bin ein Kieler” (modified from JFK).

Ich habe fertig!! (Giovanni Trapattoni, 1998)

This thesis is dedicated to Dr. Bernard K. Maloney, a pioneer of the SE Asian pollen research.

I’ve never managed to identify pollen like you. Old Pal!!

TABLE OF CONTENTS

ABSTRACT.....	I
KURZFASSUNG.....	II
ACKNOWLEDGEMENTS.....	III
TABLE OF CONTENTS.....	IV
1. INTRODUCTION.....	1
1.1 Objectives and strategies	1
1.2 South China Sea	1
1.3 East Asian Monsoon system	2
1.4 Proxies	3
1.5 Material and method.....	6
2. Dinoflagellate cyst distribution along a shelf to slope transect of an oligotrophic tropical sea (Sunda Shelf, South China Sea) (Hiroshi Kawamura).....	11
3. Distribution patterns of organic-walled dinoflagellate cysts in the South China Sea (Hiroshi Kawamura).....	48
4. 44 kyr marine palynological records from the southern South China Sea: implications for the changes in the surface water productivity and climatic conditions (Hiroshi Kawamura, Wolfgang Kuhnt, Markus Kienast and Stephan Steinke)	101
5. CONCLUSIONS.....	143

CHAPTER 1. INTRODUCTION

1.1 OBJECTIVES AND STRATEGIES

The objectives of this study are 1) to investigate distribution patterns of dinoflagellate cysts, pollen and spores and to study taxa-environment relations and other possible factors affecting the distribution patterns in the South China Sea (SCS), and 2) to reconstruct past marine and terrestrial environments over the last 44 kyr in and around the southern SCS using dinoflagellate cysts and pollen as main proxies.

To achieve the first objective, 86 surface sediment samples collected during cruises SONNE 95, 115 and 140a were investigated palynologically (Figure 1). The results were analyzed with the help of multivariate analysis (Redundancy Analysis and Canonical Correspondence Analysis), and compared with sedimentological (% Total Organic Carbon, grain-size analysis) and oceanographic (surface water circulation patterns, annual primary productivity, sea surface temperature) parameters. The results are presented in Chapter 2 and 3.

To achieve the second objective, the core GIK 18267-3 was investigated for palynology and geochemistry. The core GIK 18267-3 was chosen because the core is located in an area that high sedimentation rate was reported (Wang, 1999) and the high sedimentation rate makes a high-resolution paleoenvironmental reconstruction possible. Age-model and stratigraphy of the core was first constrained by $\delta^{18}\text{O}$ of surface dwelling planktonic foraminifera (*Globigerinoides ruber*), three C^{14} AMS dates and four analogue points of $\text{d}18\text{O}$ isotopic events. The taxa-environment relations obtained in Chapter 2 and 3 were applied to the downcore dinoflagellate assemblages of core GIK 18267-3 in order to reconstruct paleo-environmental conditions in/around the southern SCS over the last 44 kyr. The stratigraphy of GIK 18267-3 and the results of palynological study are presented in Chapter 4. The comprehensive conclusions for the entire study are presented in Chapter 5.

1.2 SOUTH CHINA SEA

The SCS is a semi-enclosed marginal basin situated between the Pacific Ocean and the Indian Ocean. It is connected to the Pacific Ocean through the Luzon Strait and to the Indian Ocean through the shallow Sunda Shelf. The main oceanographic parameters such as sea surface temperature (SST), primary productivity and current directions are governed by a bi-annual reversal of East Asian monsoon regimes. During the last glacial period, the large continental shelf, “Sunda Shelf”, was emerged, and some large fluvial systems developed on the emerged Sunda Shelf (Tija, 1980). One of the large fluvial systems “Molengraaff River” was directly flowing into the southern SCS and discharging large loads of sediments (Tija, 1980).

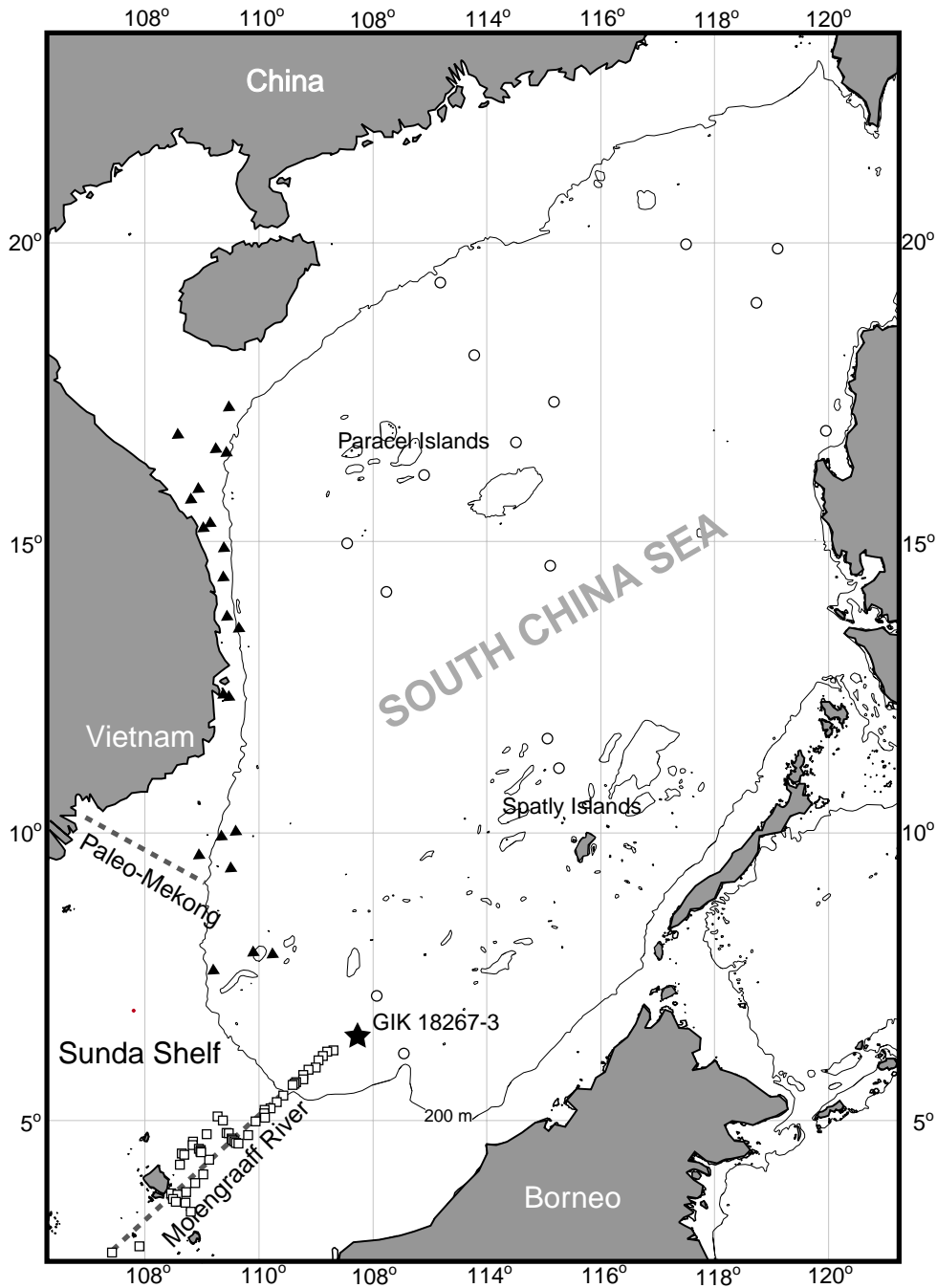


Figure 2. Locations of surface samples collected during the cruises SONNE 95 (empty circles), 115 (empty squares) and 140a (black triangles), and of core GIK 18267-3 (star). Dotted-lines indicate the speculated course of Molengraaff River and Paleo-Mekong River.

1.3 EAST ASIAN MONSOON SYSTEM

The East Asian Monsoon system is one of three subsystems of the Asian Monsoon system (Figure 2). This monsoon system affects the area from the east of the Bay of Bengal to

the Tibetan Plateau, and has strong influence on the most densely populated region (East Asia) in the world by bringing high precipitation during summer. Two primary driving forces of the East Asian Monsoon system are (a) the thermal gradient between the highly elevated Asian landmass and the Pacific and (b) the subsequent release of latent heat over the Tibetan plateau. East Asian Monsoon is closely related to climate in higher latitude, to SST in low latitude, to ocean-atmosphere interactions associated with the West Pacific Warm Pool (WPWP) and to dynamics of the Inter-tropical Convergence Zone (ITCZ)(An, 2000). During the northern hemisphere winter, the continental high pressure system over the Tibetan Plateau drives cold air from high latitude to lower latitude and form the strongest northerly dry and cold winter monsoon in the world. The northern hemisphere winter monsoon propagates over the equator into the southern hemisphere, and strengthens the summer monsoon in the southern hemisphere (An, 2000).

During the northern hemisphere summer, a warm and humid air mass originating from the low latitude oceans moves northward over the SCS and provides high precipitation in the area. The main origins of air masses are Australia, the South Pacific and the Indian Ocean. The air mass from the Indian Ocean is the main component affecting the SCS. It is an extension of the Indian southwest monsoon. The southeasterly trade wind from Australia and the south Pacific causes a dry season in the eastern parts of Indonesia. The dry air mass formed in the Australian continent picks up moisture over the seas and islands of Indonesia. When it reaches the SCS, the air mass becomes humid and unstable. Compared with the winter monsoon, the summer monsoon is much weaker (Nieuwolt. 1981).

1.4 PROXIES

Palynomorphs are used as proxies for paleoenvironmental reconstruction in this study. Palynomorphs are unique paleoenvironmental proxies in marine sediments. Marine sediments contain not only palynomorphs from marine origin but also those from terrestrial origin. Each palynomorph group contains different ecological information from the origins. Since preparation methods are very similar for different palynomorph groups, different palynomorphs from different origins can be counted at the same time in a slide from the same sample. Thus, the variations in different environmental conditions can be directly compared.

Dinoflagellate cysts

Dinoflagellates are single-celled organisms of a Division Pyrrhophyta. Perhaps, dinoflagellates are best known as one of the causal organisms for toxic algae bloom “red tide”. They occur in a wide range of aquatic environments from the poles to the equator but most diverse in tropical to temperate ocean. Over 2000 living species have been identified of which about 170 are known to produce fossilizable cysts. Dinoflagellates can be autotrophic

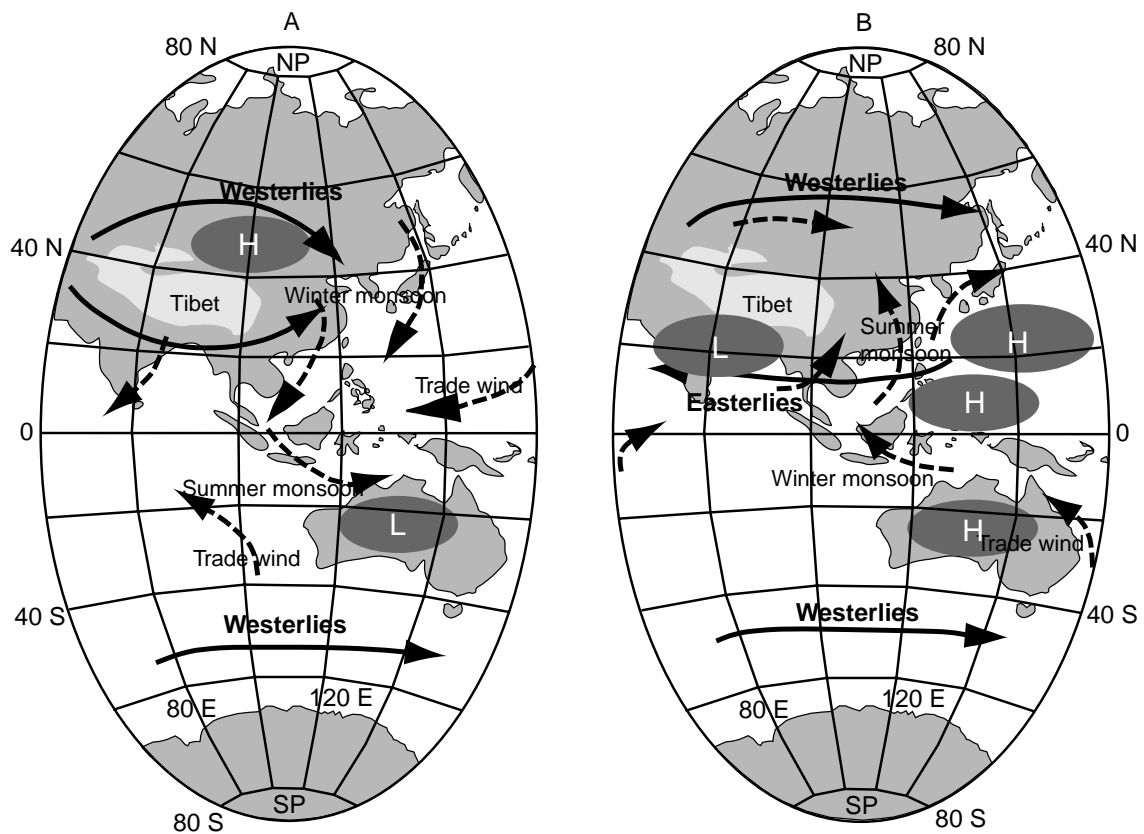


Fig. 2. Schematic view of the main atmosphere characteristics during the northern hemisphere winter (A) and summer (B). The dominant flows in the middle and low troposphere are indicated by closed and dashed arrows respectively. The most important pressure systems are marked with a dark ellipse (after Z. An, 2000).

or heterotrophic. Autotrophic dinoflagellates are important primary producer in the world ocean only second to the diatoms (Head, 1996).

Paleontologically, dinoflagellates themselves have low significance. They have very low fossilization potential. However, their resting cysts often have very high fossilization potential and can be used as proxies for past environmental variations. Dinoflagellate cysts occur abundantly in marine sediments from the Silurian to modern days and can be utilized for various geological purposes such as biostratigraphy and paleoecology.

For paleoceanographical purpose, dinoflagellate cysts have been successfully used as proxies for SST, sea surface salinity (SSS) and primary productivity in the North Atlantic and adjacent seas (e.g. de Vernal et al., 2001; de Vernal et al., 1998; Levac and de Vernal, 1997; Rochon et al., 1999; Versteegh, 1995; Versteegh et al., 1996). However, recent studies showed that certain taxa of dinoflagellate cysts are highly susceptible to degradation caused by dissolved oxygen level of the ambient water (Zonneveld and Brummer, 2000). Furthermore, presence of true oceanic cyst producing dinoflagellates have been often

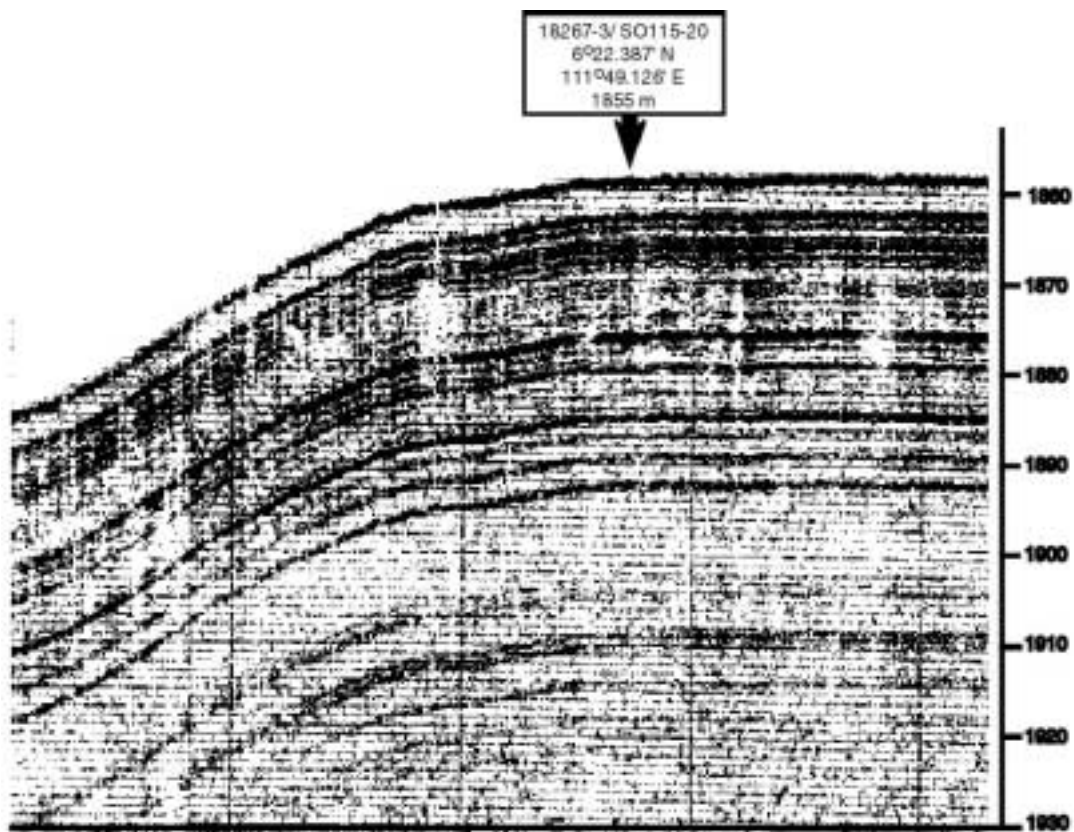


Figure 3. Parasound echo-sound record of the core location (GIK 18267-3) (after Stattegger et al, 1997).

questioned by Dale (Dale, 1996; Dale and Dale, 1992 and Dale and Fjellsa 1993). Thus, it is important to consider those points when dinoflagellate cyst data are interpreted.

Pollen, Spores and freshwater algae

Pollen, spores and freshwater algae in lake sediments are the most widely used proxies for terrestrial climate. Pollen grains are produced in the anthers of male flowers of gymnosperms and angiosperms. Spores are the dispersal unit of ferns and lower plants. Pollen, spores and freshwater algae are found widely in marine sediments. Despite of their abundant occurrence in marine sediments, these terrestrial palynomorphs have been seldom used as paleoclimate proxies. This is due to the complex transport paths and depositional processes that obscure original climate signals. However, recent studies showed that terrestrial palynomorphs in marine sediments (pollen, spores and freshwater algae) can be also utilized as proxies for large-scale climatic conditions, (Dupont, 1999; Dupont et al., 2000; Levac and de Vernal, 1997) and for the extent of freshwater plume when their transport paths are take into account (Matthiessen and Baumann, 1990; Matthiessen and Brenner, 1996).

1.5 MATERIAL AND METHOD

Surface sediments

Surface sediments were obtained using a Giant Box Corer or a multicorer during the cruises SONNE 95, 115 and 140 (Figure 1). Top 1 cm of sediments is carefully sampled using a pre-cleaned spoon immediately after the core recovery. Samples from the cruise SONNE 95 were sub-sampled from methanol preserved and rose-bengal stained samples for benthic foraminifer study. The details of sediment characters are listed in Chapter 2 & 3 as well as in Sarnthein et al (1994), Stattegger et al (1997) and Wiesner et al (1999). The samples from SONNE 95 and 115 are assumed to be of recent origins based on the abundant occurrences of Rose Bengal stained (living) benthic foraminifera (Hess, 1998, Szarek, 2001).

Core GIK 18267-3

Core GIK 18267-3 was obtained using a piston corer from the lower slope off Sunda Shelf (6°22.387 N; 111°49.126E, recovery 1409 cm) at the water-depth of 1885 m during the cruise SONNE 115 (Stattegger et al, 1997) (Figure 2). The core was recovered from a hemipelagic sediment sequence on a pelagic plateau (Figure 3). The core-location is in a present-day winter upwelling area. This winter upwelling is induced by the combination of southerly wind and the shoaling topography of the Sunda Shelf (Liu et al, 2001). The core location was within the distal part of the Molengraaff River delta during the last sealevel low-stand and high sedimentation rates were reported in the area (Wang, 1999).

The core consists of olive gray pelagic clays. Organic-rich lenses are occasionally observed in the intervals of 270- 780 cm and 1160- 1480 cm. Burrow-like structures suggest that sediments are moderately bioturbated. The detailed core descriptions and results of magnetic susceptibility measurements are provided in Stattegger et al (1997).

Palynological preparation

Samples are prepared using a standard method for marine palynology. Surface sediment samples from SO 95 and 140a are freeze-dried. Three grams of dry-sediments (samples from SO 95, 140a and core GIK 18267-3) or five milliliters of wet-sediments (samples from SO 115) are treated with 10% HCl to dissolve carbonate sediments. During the HCl treatment, a tablet of *Lycopodium clavatum* is added to each sample in order to determine the concentration of palynomorphs (Stockmarr, 1971). Then the samples are sieved and concentrated through a 5µm mesh nylon sieve. During sieving, an ultrasonic treatment of less than 30 seconds is applied to the sediments in order to disaggregate clay contents of sediments. The residues are then treated with 40% HF to remove siliceous sediments. The samples are left in HF without agitations until all siliceous sediments are dissolved. The

samples are again sieved through 5 μ m nylon sieve with distilled water. The residues are mounted on slides with glycerine gel and sealed with paraffin. No hot acids and oxidizing agents are used during the sample preparation in order to avoid selective degradations of certain dinoflagellate cyst taxa.

Major types of palynomorphs (dinoflagellate cysts, pollen, spores, tintinomorphs and algae) are identified and counted using a light microscope with magnifications of x400 and x800. Most of organic-walled dinoflagellate cysts are identified up to species level in accordance with the classifications of Lentin and Williams (1993) and Rochon et al. (1999). Non-use of hot acids and oxidizing agents, in turn, makes identification of pollen difficult. Therefore, only certain major taxa of pollen are identified to lower taxonomic levels.

Stable Isotope Analysis

Stable Oxygen and Carbon isotope analysis were performed on samples composed of 15-25 specimens of the near surface dwelling planktonic foraminifer *Globigerinoides ruber* (D'ORBIGNY) s.s. (white) in the 250-400 μ m size fraction. Before isotopic measurements, foraminiferal tests were manually crushed and then washed in ethanol (99.8 %) in an ultrasonic bath. Samples were dried at 40 °C over night. Isotopic measurements were performed using a Finnigan MAT-251 mass-spectrometer with Kiel-CARBOPREP automatic carbonate preparation line at the Leibniz Laboratory in Kiel University. The analytical precision of isotopic measurements was better than 0.04 ‰ PDB for $\delta^{13}\text{C}$ and 0.08 ‰ for $\delta^{18}\text{O}$ (Erlenkeuser, pers. comm.).

Geochemical Analysis

Total Organic Carbon (TOC) and total nitrogen (N) were measured at the University of British Columbia using flash-combustion gas chromatography on a Carlo-Erba elementary analyzer. Detailed descriptions are available from Verardo et al. (1990). Acetanelide ($\text{CH}_3\text{CONHC}_6\text{H}_5$) was used as a standard. Duplicate measurements confirm the analytical precision within $\pm 1.25\%$.

REFERENCES

- An, Z., 2000. The history and variability of the East Asian paleomonsoon climate. *Quaternary Science Reviews*; Past global changes and their significance for the future.,19(1-5), 171-187.
- Dale, B., 1996. Dinoflagellate cyst ecology: modeling and geological applications. In: J. Jansonius and D.C. McGregor (Editors), *Palynology: principles and applications*. American Association of Stratigraphical Palynologists Foundation, Salt Lake City, pp. 1249-1276.
- Dale, B. and Dale, A.L., 1992. *Dinoflagellate Contributions to the Deep Sea*. Ocean Biocoenosis Series, 5. Woods Hole Oceanographic Institution, 75 pp.
- Dale, B. and Fjellsa, A., 1993. Dinoflagellate cysts as paleoproductivity indicators; state of the art, potential, and limits. In: Zahn et al. (Editors), *Carbon cycling in the glacial ocean; constraints on the ocean's role in global change; quantitative approaches in paleoceanography*. NATO ASI Series. Series I: Global Environmental Change. Springer Verlag, Berlin, Federal Republic of Germany, pp. 521-537.
- de Vernal, A. et al., 2001. Dinoflagellate cyst assemblages as tracers of sea-surface conditions in the northern North Atlantic, Arctic and sub-Arctic seas: the new 'n=677' data base and its application for quantitative palaeoceanographic reconstructions. *Journal of Quaternary Science*, 16(7), 681-698.
- de Vernal, A., Rochon, A., Turon, J.-L. and Matthiessen, J., 1998. Organic-walled dinoflagellate cysts: palynological tracers of sea-surface conditions in the middle to high latitude marine environments. *GEOBIOS*, 30, 905-920.
- Dupont, L.M., 1999. Pollen and spores in marine sediments from the East Atlantic- a view from the ocean into the African continent. In G. Fischer and G. Wefer(Editors), *Use of proxies in paleoceanography: examples from the South Atlantic*. Springer Verlag, Berlin Heidelberg, pp.523-546.
- Dupont, L.M., Jahns, S., Marret, F. and Ning, S., 2000. Vegetation change in equatorial West Africa: time-slices for the last 150 ka. *Palaeogeography, Palaeoclimatology, Palaeoecology*,155,95-122.
- Head, M.J., 1996. Modern dinoflagellate cysts and their biological affinities. In: J. Jansonius and D.C. McGregor (Editors), *Palynology: principles and applications*. American Association of Stratigraphical Palynologists Foundation, Dallas, pp. 1197-1248.
- Hess, S., 1998. Distribution patterns of recent benthic foraminifera in the South China Sea. *Berichte - Reports*, Geologisch-Palaeontologisches Institut und Museum, Christian-Albrechts-Universitaet Kiel, 91.Christian-Albrechts-Universitaet Kiel, Geologisch-Palaeontologisches Institut und Museum,Kiel, Federal Republic of Germany, 173 pp.
- Levac, E. and de Vernal, A., 1997. Postglacial changes of terrestrial and marine environments along the Labrador coast; palynological evidence from cores 91-045-005 and 91-045-006, Cartwright Saddle. *Canadian Journal of Earth Sciences = Journal Canadien des Sciences de la Terre*,34(10),1358-1365.
- Levac, E. and de Vernal, A., 1997. Postglacial changes of terrestrial and marine environments along the Labrador coast: palynological evidence from cores 91-045-005 and 91-045-006, Cartwright Saddle. *Canadian Journal of Earth Sciences*,34(10),1358-1365.
- Matthiessen, J. and Baumann, K.H., 1990. *Dinoflagellaten-Zysten und Coccolithophoriden-Floren im Holozan*

- des Europaeischen Nordmeeres; Synoekologie und Oekostratigraphie. Nachrichten - Deutsche Geologische Gesellschaft, 43,62-63.
- Matthiessen, J. and Brenner, W., 1996. Chlorococcalean algae and dinoflagellate cysts in recent sediments from Greifswald Bay (southern Baltic Sea).
- Nieuwolt, S., 1981. The climates of continental Southeast Asia. In: K. Takahashi and H. Arakawa (Editors), *Climates of southern and western Asia. World Survey of Climatology*. Elsevier Scientific Publishing, Amsterdam, pp. 1-38.
- Rochon, A., de Vernal, A., Turon, J.-L., Matthiessen, J. and Head, M.J., 1999. Distribution of recent dinoflagellate cysts in surface sediments from the North Atlantic Ocean and adjacent seas in relation to sea-surface parameters. *American Association of Stratigraphical Palynologists Contribution Series*, 35. American Association of Stratigraphical Palynologists, Dallas, 152, pp.
- Sarnthein, M., Pflaumann, U., Wang, P.X. and Wong, H.K., 1994. Preliminary report on Sonne-95 cruise "Monitor Monsoon" to the South China Sea; Manila - Guangzhou - Hongkong - Kota Kinabalu - Hongkong; 16 April-8 June 1994. *Berichte - Reports, Geologisch-Palaeontologisches Institut und Museum, Christian-Albrechts-Universitaet Kiel*, 68. Christian-Albrechts-Universitaet Kiel, Geologisch-Palaeontologisches Institut und Museum, Kiel, Federal Republic of Germany, 226, pp.
- Stattegger, K., Kuhnt, W., Wong, H.K., Bühring, C., Haft, C., Hanebuth, T., Kawamura, H., Kienast, M., Lorenz, S., Lotz, B., Lüdmann, T., Lurati, M., Mühlhan, N., Paulsen, A.M., Paulsen, J., Pracht, J., Putar-Roberts, A., Hung, H.Q., Richter, A., Salomon, B., Schimanski, A., Steinke, S., Szarek, R., Nhan, N.V., Weinelt, M., Winguth, C., 1997. Cruise Report SONNE 115 "SANDAFLUT". *Berichte - Reports, Geologisch-Palaeontologisches Institut und Museum, Christian-Albrechts-Universitaet Kiel*, 86. Christian-Albrechts-Universitaet Kiel, Geologisch-Palaeontologisches Institut und Museum, Kiel, Federal Republic of Germany, 211, pp.
- Szarek, R., 2001. Biodiversity and biogeography of recent benthic foraminiferal assemblages in the south-western South China Sea (Sunda Shelf). Ph.D. Thesis, Institut fuer Geowissenschaften, Christian Albrechts Universitaet zu Kiel, Kiel, 273 pp.
- Tijja, H.D., 1980. The Sunda Shelf, Southeast Asia. *Zeitschrift fuer Geomorphologie*. N.F., 24, 405-427.
- Versteegh, G., 1995. Palaeoenvironmental changes in the Mediterranean and North Atlantic in relation to the onset of northern hemisphere glaciations (2.5 Ma B.P.) -a palynological approach-, Ph.D. thesis, Universiteit Utrecht.
- Versteegh, G.J.M., Brinkhuis, H., Visscher, H. and Zonneveld, K.F., 1996. The relation between productivity and temperature in the Pliocene North Atlantic at the onset of northern hemisphere glaciation: a palynological study. *Global and Planetary Change*, 11, 155-165.
- Wang, P.X., 1999. Response of Western Pacific marginal seas to glacial cycles: paleoceanographic and sedimentological features. *Marine Geology*, 156(1-4), 5-40.
- Wiesner, M.G., Stattegger, K., Kuhnt, W., Arpe, C., Bracker, E., Catene, S., de Leon, M., Duyanen, J., Faber, U., Gerbich, C., Hess, S., Holbourn, A., Jagodzinski, R., Kaminski, M., Kawamura, H., Kuueger, O.,

- Lorenc, S., Nguyen, H.-S., Nguyen, H.-P., Nguyen, T.-T., Nguyen, V.-B., Paulsen, H., Peleo-Alampay, A., Richter, A., Rimek, R., Schimanski, A., Seeman, B., Sharma, C., Siringan, ., Steen, E., Steinke, S., Szarek, R., Szczucincki, W., Vo, D.-S., Von Wersch, V., Wetzel, A., Witzki, D., 1999. Cruise report SONNE 140 Suedmeer III, Berichte - Reports, Institut fuer Geowissenschaften, Christian-Albrechts-Universitaet Kiel, 7, Institut fuer Geowissenschaften, Christian Albrechts Universitaet zu Kiel, Kiel. 155 pp.
- Zonneveld, K.A.F. and Brummer, G.A., 2000. (Palaeo-)ecological significance, transport and preservation of organic-walled dinoflagellate cysts in the Somali Basin, NW Arabian Sea. *Deep Sea Research II*, 47,2229-2256.

CHAPTER 2. Dinoflagellate cyst distribution along a shelf to slope transect of an oligotrophic tropical sea (Sunda Shelf, South China Sea)

Hiroshi Kawamura

Institut fuer Geowissenschaften der Christian Albrechts Universitaet zu Kiel
Olshausenstr. 40, 24118 Kiel, Germany

ABSTRACT

Thirty-five taxa of organic-walled dinoflagellate cysts are identified from fifty surface samples collected along a shelf to slope transect of the Sunda Shelf, South China Sea (SCS). Oligotrophic tropical shelf assemblages on the Sunda Shelf are dominated by gonyaulacoids such as *Spiniferites* species, *P. reticulatum* and *O. israelianum*. Concentrations of dinoflagellate cysts in the shelf sediments are generally low and correlate well with the content of fine-grained (clay and silt fraction) sediments. Detailed comparisons of sediment grain-size distributions to concentrations of dominant dinoflagellate taxa (*Spiniferites* species, *P. reticulatum* and *O. israelianum*) in the shelf sediments indicate that these taxa behave in water like sediment particles with size range ϕ^0 5.75-6.25. In contrast, slope assemblages in fine-grained sediments are dominated by protoperidinioids. This may reflect higher nutrient availability due to weak winter upwelling. The concentrations of dinoflagellate cysts in the shelf sediments are mainly controlled by transport and winnowing processes and are probably not representative of surface water conditions.

1.1 INTRODUCTION

In recent years, the knowledge regarding dinoflagellate cyst distribution patterns in the world oceans has significantly improved. This is partially due to the needs for such knowledge in interpreting paleoceanographical records and in toxic phytoplankton bloom studies. The knowledge is also significantly improved recently in the Pacific marginal seas: Matsuoka (1981) in the Philippine Sea, Cho and Matsuoka, (1999) Cho and Matsuoka (2001) and Matsuoka *et al.*, (1999) in the East China Sea, Qi *et al.* (1996) in shallow Chinese coastal water in the East and South China Sea, Wu and Sun (2000) in the SCS basin, Wu and Tocher (1995) in Okinawa Trough, Lirdwitayaprasit (1998, 2000) in the Gulf of Thailand and coastal water along northern Borneo, McMinn, (1991, 1992) in coastal Tasmanian Sea. Kobayashi *et al.*, (1986), Kobayashi and Yuki (1991), Matsuoka (1992), Matsuoka (1994) in the Japanese coast water, Lee and Matsuoka (1994) in the southern Korean waters, Biebow (1996) in the Peruvian upwelling area. However, most of these studies have concentrated on either shallow neritic/ coastal areas (<50 m water depth) or deep oceanic area (>1000 m) and the studies on intermediate areas have been often neglected.

This study concentrates on a transect covering the outer-shelf to lower continental slope of the Sunda Shelf with closely spaced site intervals (Fig.1). The studied area has unique settings. The area is remote from the land, a main source of nutrient supply. Unlike narrow continental shelves (e.g. New Jersey Margins and Vietnamese Shelf) with significant primary productivity gradients, it has low productivity gradients.

The aims of this paper are: a) to document the distribution of dinoflagellate cysts and other major marine palynomorph groups (foraminiferal linings, tintinomorphs, spore and some algae group) in the sediments on the oligotrophic Sunda Shelf and its slope; b) to investigate possible environmental and taphonomical factors controlling the distribution patterns of dinoflagellate cysts. Also, sediment size distributions are compared to the absolute abundances of dinoflagellate cyst taxa in order to gain insight into the potential taphonomical processes influencing the assemblages.

1.2 STUDY AREA

The studied area is located at the northern tip of the Sunda Shelf and its continental slope. Physical oceanography of the SCS is generally controlled by the East Asian Monsoon System. The surface current direction and velocity change semi-annually (Fig. 2ab). The winter monsoon begins in September with a sharp increase in wind speed towards southwest (Liu and Xie, 1999). During the winter monsoon, an anti-clockwise circulation prevails. The predominant current direction is west in the deeper part and southwest on the shelf. The current velocity reaches up to ca. 0.5 m/s (Liu and Xie, 1999) (Fig. 2a).

The summer monsoon is relatively weak compared to the winter monsoon. It begins in May with a sharp increase in atmospheric water vapor contents (Wyrski, 1961). A clockwise surface circulation develops in summer in the SCS. In the studied area, the current direction varies from north to east. The current velocity is up to 0.3 m/s but commonly it is less than 0.2 m/s (Liu and Xie, 1999)(Fig. 2b).

A weak winter upwelling has been reported in the slope area off Sunda Shelf (Liu *et al.*, 2002). However the upwelling is so weak that it does not translate into higher annual productivity in the study area. The annual primary productivity varies from ca. 100 gCm⁻²y⁻¹ in the basin to 166 gCm⁻²y⁻¹ on the shelf (SeaWifs) (Fig. 3). The sea surface temperature (SST)

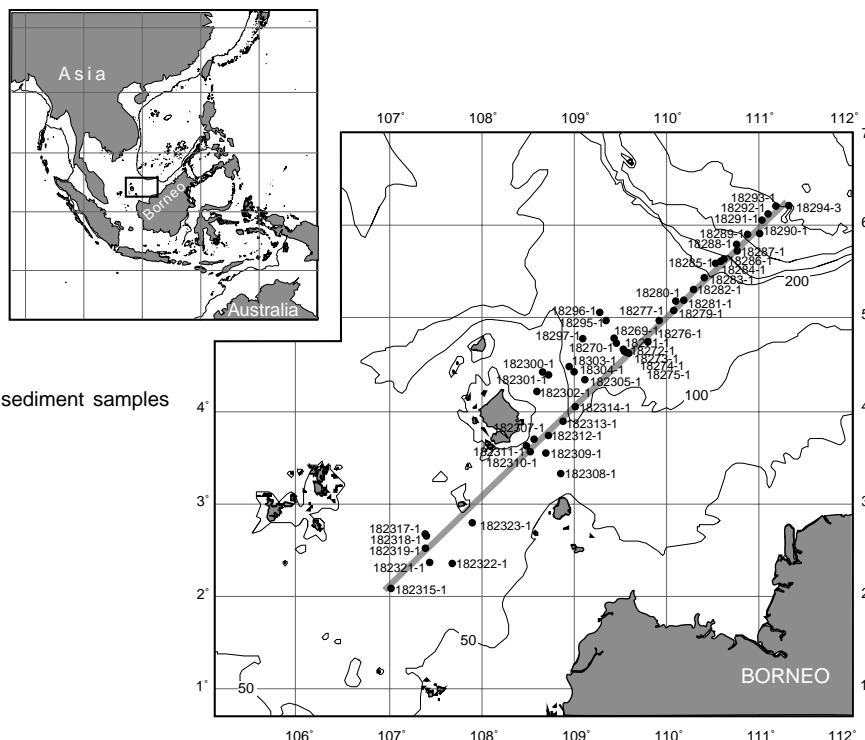


Figure 1. Locations of the surface sediment samples studied in this chapter.

and salinity (SSS) of the area is relatively constant throughout a year (SST 27-29 C, SSS 33 psu).

Paulsen (1998) studied various sedimentological properties (Total Organic Carbon, CaCO_3 content, sediment grain-sizes and rare elements) of surface sediments and divided the area into 3 zones; proximal, intermediate and distal. The proximal zone (inner shelf) contains the sites south and southeast of Natuna Island with water-depth less than 109 m. This zone is characterized by medium TOC values (0.32-0.76 %) and relatively high clay and sand content (Fig. 4). The intermediate zone (outer shelf) contains the sites north of Natuna Island with water-depth 90-200 m. The intermediate zone is characterized by slightly lower TOC values (0.26-0.72 %) and high silt and sand content. The distal zone (slope) contains the sites on the continental slope with water-depth deeper than 200 m. This distal part is characterized by high TOC value (0.46-1.27 %) and high silt and clay content.

Nino and Emery (1966) reported the presence of relict sediments on the Sunda Shelf. Thus, sediments may be of significantly older origin. However the sediments are considered as of recent origin due to the abundant occurrence of Rose Bengal stained (living) benthic foraminifera in same samples (Szarek, 2001). Grain-size analyze by Paulsen (1998) indicates that sediments on the shelf are partially winnowed.

Hydrographically, the studied area are under influence of two different water masses with a seasonally changing boundary near the shelf break (neritic water and oceanic water). The neritic water mass in the studied area is characterized by lower temperature, salinity and density values than these in the transitional area (Saadon *et al.*, 1998).

2.1 MATERIAL AND METHODS

Surface sediments from 51 sites are collected by a giant box corer or a multi-corer during the cruise SONNE115 'Sundaflut' in 1996-1997 (Stattegger *et al* 1997). The water-depth of sites varies from 69 m to 1409 m. Top 1 cm sediments are carefully collected using a

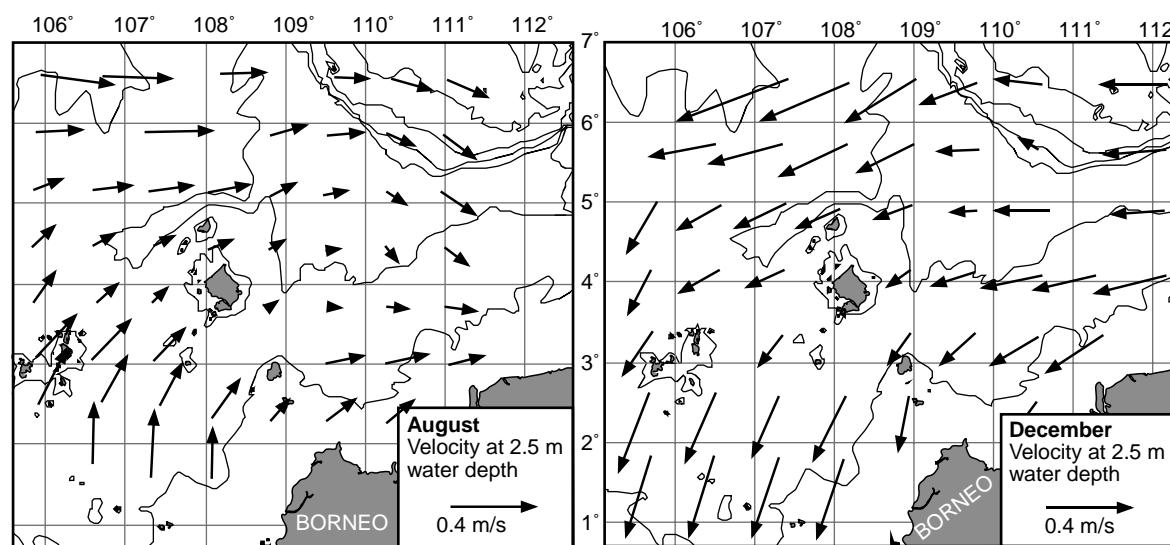


Figure 2 a & b. General circulation patterns and velocities of surface water during: **a)** August and **b)** December (modified from Liu & Xie, 1999).

spoon. The water-depth and lithological character of the sediments from each site is shown in Table 1. Total Organic Carbon (TOC) data shown in Figure 4 is from Statterger *et al* (1997).

For palynological investigations, 5 ml of wet sediments is first treated with 10% HCl for maximum of 3 hours to remove carbonate contents. A *Lycopodium clavatum* tablet (batch # 124961) is added to each sample in order to measure the concentrations of palynomorphs (Stockmarr, 1971). The samples are then concentrated using a 5 μ m nylon sieve. During the sieving, a short ultrasonic treatment (<30 seconds) is applied in order to disaggregate clay contents of the samples. The samples are then treated with 38% HF to remove the siliceous fraction and left without agitation until dissolution is completed. The samples are sieved again with a 5 μ m nylon sieve with distilled water. The residue is embedded in glycerine jelly and sealed from air with paraffin wax. The use of oxidizing reagents and hot acids are avoided because these can significantly damage certain dinoflagellate cysts (Dale, 1976). Major palynomorph groups (dinoflagellate cysts, pollen, spore, benthic foraminiferal lining, tintinomorphs and algae) are identified and counted using a Zeiss Oxilab microscope at x400 and x 800 magnifications. Selected cysts were photographed using attached digital camera (AVT MC-1009S/F)(Plate 1-2).

Counts were carried out until a minimum of 100 cysts per sample was identified. Taxonomic classification follows the systematics of Lentin and Williams (1993) and Rochon *et al.* (1999). Some *Spiniferites* cysts could not always be identified to species level due to the poor preservation or orientation, and are simply counted as *Spiniferites* spp. *Brigantedinium* spp. is also only identified only to the genus level.

The slides and samples are stored at Micropaleontology Group, Institute of Geosciences, Universität Kiel, Germany and are available on request.

2.2 STATISTICAL ANALYSIS

A Redundancy Analysis (RA) is used to help interpreting the distribution patterns and controlling factors on the shelf. A RA is a canonical form of Principal Component Analysis (PCA). A RA is run using the CANOCO software (ter Braak and Smilauer, 1998). A RA is chosen because it assumes that species abundance has a linear response to changing

environmental gradients. The studied area is relatively small and no large environmental gradients have been reported. Thus, a linear response of species is expected. Theoretical details of RA can be obtained from Rao (1964). Concentrations of main dinoflagellate cysts groups and palynomorph groups are used as input data and fractions of each sediment sizes, water-depth and TOC of each site are used as passive parameters.

Table 1. List of samples used in this study with location, water-depth, coring device (GBC=Giant Box Corer, MC= Multi-Corer) sediment type, number of dinoflagellatecysts counted, concentration of dinoflagellate cysts (cyst ml⁻¹ wet sediment), and Total Organic Carbon (TOC)

Sample	Latitude	Longitude	WD (m)	Coring device	Sediment type	Total cyst counted	Cyst Concentration	TOC (%)
18269-1	4:46.042 N	109:26.353 E	114	GBC	sandy mud	140	88.90	0.446
18270-1	4:43.481 N	109:28.607 E	106	GBC	silty sand	161	141.70	0.554
18271-1	4:38.341 N	109:32.949 E	116	GBC	clayish silty sand	184	242.15	0.276
18272-1	4:37.635 N	109:33.607 E	121	GBC	clayish sand	190	196.53	0.721
18273-1	4:37.280 N	109:33.949 E	127	GBC	sandy mud	109	238.37	0.633
18274-1	4:36.324 N	109:34.824 E	117	GBC	clayish sand	42	100.53	0.333
18275-1	4:35.699 N	109:35.560 E	109	GBC	clayish sand	104	173.45	0.264
18276-1	4:44.946 N	109:44.862 E	120	GBC	clayish sand	147	218.12	0.416
18277-1	4:56.341 N	109:56.283 E	134	GBC	sandy mud	182	399.06	0.68
18279-1	5:02.586 N	110:02.504 E	139	GBC	sandy mud	279	383.27	2.396
18280-1	5:05.975 N	110:06.007 E	144	GBC	sandy mud	363	434.34	0.659
18281-1	5:07.751 N	110:07.754 E	145	GBC	sandy mud	128	321.72	0.527
18282-1	5:14.702 N	110:14.643 E	152	GBC	sandy mud	142	258.49	N/A
18283-1	5:25.139 N	110:25.093 E	166	GBC	sandy mud	140	223.35	0.466
18284-1	5:32.506 N	110:32.424 E	226	GBC	silty sand	23	255.73	0.418
18284-1 MC	5:32.486 N	110:32.423 E	226	MC	sandy mud	112	232.89	0.418
18285-1	5:34.464 N	110:34.369 E	291	MC	sandy mud	188	256.43	0.46
18286-1	5:36.365 N	110:36.240 E	404	MC	mud	239	301.77	1.151
18287-1	5:39.759 N	110:39.691 E	595	MC	mud	113	502.59	1.281
18288-1	5:44.401 N	110:44.324 E	790	MC	mud	278	336.64	1.066
18289-1	5:49.772 N	110:49.741 E	978	MC	mud	252	490.39	1.288
18290-1	5:55.025 N	110:54.939 E	1124	MC	mud	144	188.06	1.025
18291-1	5:57.923 N	110:57.717 E	1208	MC	mud	100	235.53	1.145
18292-1	6:03.564 N	111:03.515 E	1309	MC	mud	248	309.38	1.263
18293-1	6:09.419 N	111:09.411 E	1404	MC	mud	309	222.89	1.244
18294-3	6:07.806 N	111:18.182 E	846	GBC	mud	36	41.65	1.129
18295-1	4:55.556 N	109:17.868 E	117	GBC	sandy mud	174	196.96	0.436
18296-1	4:59.754 N	109:14.435 E	118	GBC	silty mud	121	126.53	0.587
18297-1	4:44.332 N	109:01.902 E	112	GBC	clayish silt	141	242.92	0.567
18300-1	4:21.770 N	108:39.211 E	94	GBC	clayish sand	99	119.28	0.547
18301-1	4:21.304 N	108:38.824 E	92	GBC	clayish sand	128	269.36	0.438
18302-1	4:09.588 N	108:34.531 E	83	GBC	clayish silt	189	234.12	0.425
18303-1	4:26.360 N	108:55.516 E	107	GBC	clayish sand	22	122.91	0.46
18304-1	4:21.788 N	109:00.155 E	104	GBC	silty mud	159	152.81	1.33
18305-1	4:17.314 N	109:04.594 E	109	GBC	mud	101	182.00	0.603
18306-1	3:35.277 N	108:26.540 E	88	GBC	mud	157	241.02	0.735
18307-1	3:37.620 N	108:31.630 E	100	GBC	mud	157	203.73	0.755
18308-1	3:17.830 N	108:47.143 E	80	GBC	silty sand	73	73.01	0.328
18309-1	3:27.958 N	108:41.196 E	84	GBC	sandy mud	64	259.77	0.32
18310-1	3:32.149 N	108:32.160 E	101	GBC	mud	141	158.05	0.44
18312-1	3:42.355 N	108:42.383 E	101	GBC	silty mud	111	113.14	0.484
18313-1	3:52.183 N	108:52.231 E	99	GBC	sandy mud	118	92.38	0.237
18314-1	3:59.463 N	108:59.466 E	100	GBC	clayish sand	93	118.42	0.412
18315-1	2:01.672 N	107:02.016 E	69	GBC	mud	127	186.08	0.63
18316-1	2:29.262 N	107:22.527 E	71	GBC	sandy mud	118	153.05	0.579
18317-1	2:36.598 N	107:22.515 E	96	GBC	mud	81	214.14	0.671
18318-1	2:36.609 N	107:22.505 E	86	GBC	mud	101	197.62	0.741
18319-1	2:36.620 N	107:22.502 E	81	GBC	mud	130	199.57	0.679
18321-1	2:18.457 N	107:25.327 E	109	GBC	mud	114	231.17	0.699
18322-1	2:18.410 N	107:37.911 E	70	GBC	mud	167	280.91	0.599
18323-1	2:47.040 N	107:53.197 E	92	GBC	sandy mud	178	280.46	0.587

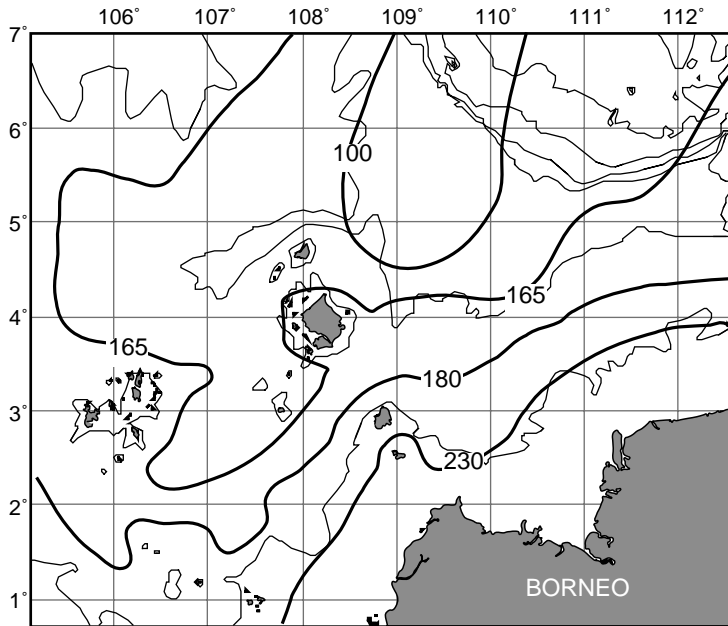


Figure 3. Annual primary productivity of the studied area (modified from SeaWifs, 2001).

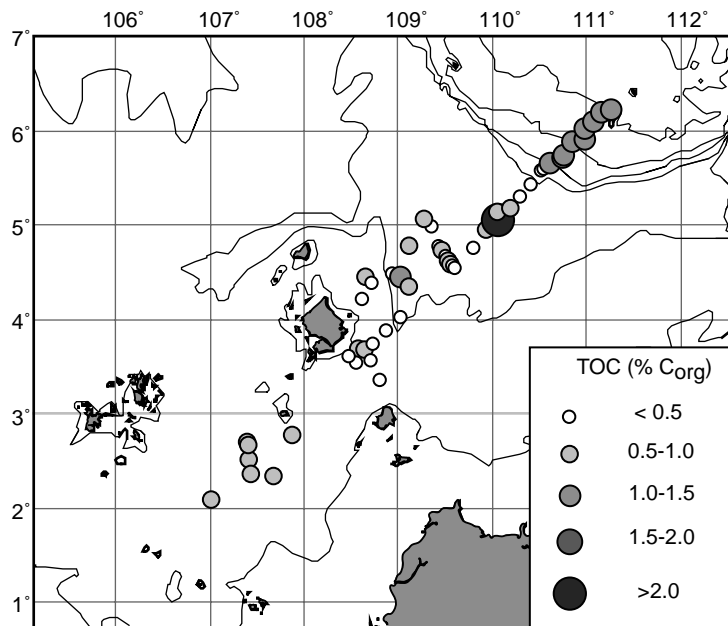


Figure 4. Total Organic Carbon (TOC) of the surface sediments (after Paulsen, 1998).

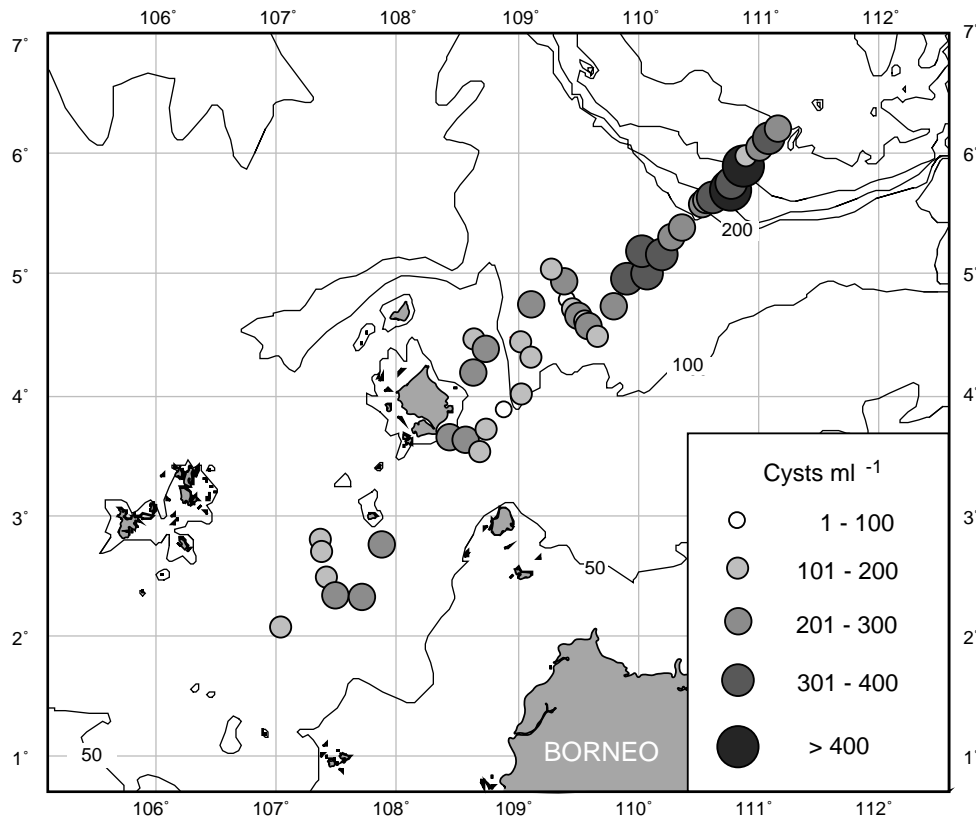


Figure 5. Concentrations of dinoflagellate cysts (cysts ml⁻¹ wet sediments) in the surface sediments from the Sunda Shelf, South China Sea.

3. RESULTS

3.1 Distribution patterns of dinoflagellate cysts

Concentrations of the dinoflagellate cysts vary from 86.1 cysts ml⁻¹ to 817.3 cysts ml⁻¹ (Fig. 5). Generally, higher concentrations are observed on the continental slope than on the continental shelf. Comparisons of dinoflagellate cyst concentrations to silts fractions of sediments show a fair correlation ($R=0.59$) (Figure 9). The concentrations of dinoflagellate

A total of 35 taxa of dinoflagellate cysts were identified from 51 sites. (Table 2) Twenty-one species belong to the gonyaulacoid group, ten species belongs to the protoperinioid group, one species of each of the tuberculodinioid group, diplopsalid group, gymnodinioid group and calciodinellid group were identified. Gonyaulacoid and Protoperidinioid groups dominate the assemblages at all sites (89.0-99.1%)(Fig. 6). Gonyaulacoids typically dominate the shelf assemblage with values ranging from 42.0% to 81.3%, whereas the continental slope assemblages are dominated by protoperidinioids with values ranging from 43.9% to 77.0%(Fig. 6). Diplopsalids (*Diplopelta parva*) occur at most sites with relatively low percentages (<11.2%). Highest proportions are observed on the shelf however. Tuberculodinioids (*Tuberculodinium vancampoae*) appears only at 22 sites mainly on the shelf with small proportions (<2.88%). Gymnodinioids (*Polykrikos hartmannii*) and Calciodinellids (*Scrippsiella* spp.) occur only sporadically with low proportions. (<6.5 %).

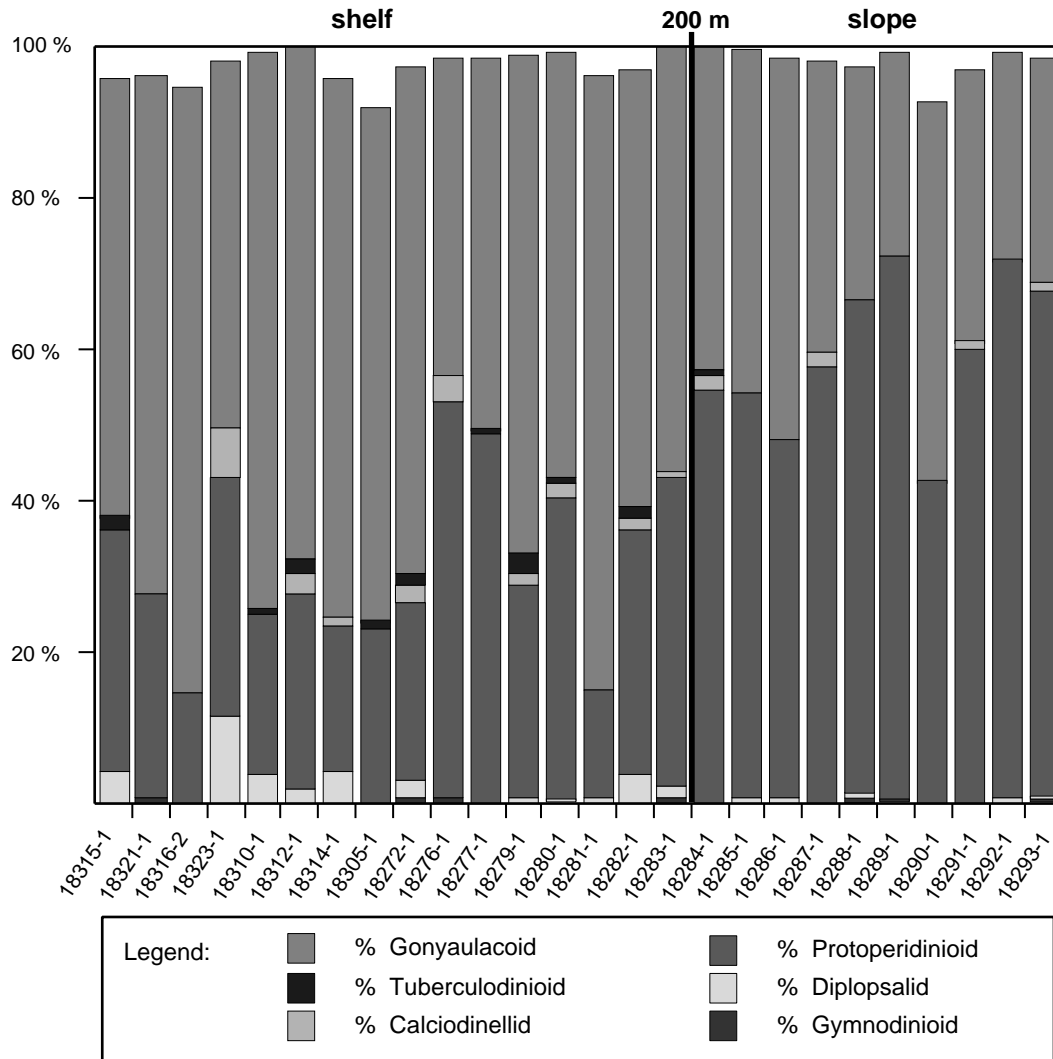


Figure 6. Changes in the relative abundances of major cyst groups.

In the gonyaulacoid group, five main *Spiniferites* species (*Spiniferites bulloideus*, *Spiniferites ramosus*, *Spiniferites mirabilis*, *Spiniferites hyperacanthus* and *Spiniferites membranaceus*), *Protoperidinium reticulatum* and *Operculodinium* species (*Operculodinium longispinigerum* and *Operculodinium israelianum*) account for up to 85.8%. Eight species of *Spiniferites* are identified (Table 2). *Spiniferites* occurs at all sites (Fig. 7a) with concentrations varying from 12.3 to 181.3 cysts ml^{-1} . High concentrations of *Spiniferites* are observed on the shelf and the concentrations decrease sharply towards the slope. *P. reticulatum* also occurs at all sites (Fig. 7b) with concentrations varying from 4.5 to 39.5 cysts ml^{-1} . The highest concentrations are observed in the vicinity of the shelf break. The concentrations sharply decline on the slope.

The distribution patterns of *O. israelianum* and *O. longispinigerum* roughly mirror the distribution pattern of *P. reticulatum*. They are common on shelf and are scarce or absent on slope (Fig. 7cd). Five *Impagidinium* species are identified (Table 2). *Impagidinium* species are not common on the shelf and the concentrations generally increase towards the slope (Fig. 7e). *Nematosphaeropsis labyrinthus* is observed only on the continental slope with low concentrations (2.3-4.3 cysts ml^{-1}) (Fig. 7f).

In the protopteridinioid group, ten species are identified (Table 1). *Brigantedinium* spp. is present at every site (Fig. 7g) and account for up to 91.2% of the protopteridinioid group. The concentrations of *Brigantedinium* spp. vary from 2.6 to 321.1 cysts ml⁻¹ and generally increase towards the lower slope. *Votadinium calvum*, *Trivantedinium capitatum*, *Selenopemphix quanta* and *Selenopemphix nephroides* occur at most sites with low concentrations (max. values 17.5, 10.2, 7.8 and 23.1 cysts ml⁻¹ respectively)(Fig. 6hijk). The higher concentrations of *V. calvum* and *T. capitatum* are observed on the outer shelf and the upper slope. The higher concentrations of *S. quanta* and *S. nephroides* are found on the slope. Pre-encysted protopteridinioids are normally present on the shelf and the upper slope (Fig. 7k). The concentrations vary from 0-27.5 cysts ml⁻¹. The concentrations decrease sharply towards the lower slope. The four other species (*Stelladinium stelladium*, *Protopteridinium latissimum*, *L. sabrina* and *Quinquecuspis concretum*) occur sporadically and have low concentrations.

Diplopsalid (*D. parva*) occurs at 28 sites with low concentrations (0-29.74 cysts ml⁻¹)(Fig. 7l). Although Diplopsalid occurs inconsistently in the studied area, higher concentrations (>4 cysts/ml) are observed only on the shelf. Calciodinellid (*Scripsiella* spp.) and Gymnodinioid (*P. hartmannii*) occur at some sites irregularly.

Table 2. List of dinoflagellate cysts identified in the surface sediments from the Sunda Shelf, South China Sea

GONYAULACALES

Gonyaulacaceae

Gonyaulacoid Group

Achomosphaera spp.
Alexandrium tamarense Dale 1977
Impagidinium paradoxum (Wall) Stover & Evitt 1978
Impagidinium patulem (Wall) Stover & Evitt 1978
Impagidinium striatum (Wall) Stover & Evitt 1978
Impagidinium sphaericum (Wall) Lentin & Williams 1981
Impagidinium spp.
Lingulodinium machaerophorum (Deflandre & Cookson) Wall 1967
Nematosphaeropsis labyrinthus (Ostenfeld) Reid 1974
Protoceratium reticulatum (Claparede & Lachmann) Buetchli
Operculodinium israelianum (Rossignol) Wall 1967
Operculodinium longispinigerum Matsuoka 1983
Spiniferites bulloideus (Deflandre & Cookson) Sarjeant 1970
Spiniferites bentori (Rossignol) Wall & Dale 1970
Spiniferites delicatus Reid 1974
Spiniferites hypercanthus (Deflandre & Cookson) Cookson & Eisenack 1974
Spiniferites ramosus (Rossignol) Mantel 1854
Spiniferites mirabilis (Rossignol) Sarjeant 1970
Spiniferites membranaceus (Rossignol) Sarjeant 1970
Spiniferites spp.
Tectatodinium spp.

Pyrophacaceae

Tuberculodinioid Group

Tuberculodinium vancampoae (Rossignol) Wall 1967

GYMNODINIALES

Gymnodinioid Group

Pheopolykrikos hartmannii Fukuyo 1982
Cochlodinium spp.

PERIDINIALES

Protopteridiniaceae

Protopteridinioid Group

Brigantedinium spp.
Protopteridinium latissimum Wall & Dale 1968
 Pre-encysted *Protopteridinium*
Selenopemphix nephroides Benedek 1972
Selenopemphix quanta (Bradford) Matsuoka 1985
Stelladinium stellatum (Wall & Dale) Reid 1977
Trinovantedinium capitatum Reid 1977
Votadinium calvum Reid 1977
Lejeunecysta sabrina Reid 1977
Quinquecuspis concretum (Reid) Harland 1977

Diplopsalid Group

Diplopelta parva Matsuoka 1988

Calciodineliaceae

Calciodinellid Group

Scripsiella spp.

3.2 Redundancy Analysis (RA) of shelf samples

A RA shows that first 2 axis explain 39.8 and 12.7% of total variance and 69.1 and 22.0 % of species-environmental relation of data (Figure 10). Gradients of size phi⁰ 5.25 sediment fractions are closely correlated with 1st RA axis (Figure 10). The correlations

coefficiencies between the 1st RA axis and different sediment grain size decrease as increasing/decreasing fractions of sediments with grain-size ϕ° 5.25. Concentrations of total dinoflagellate cysts, *P. reticulatum* and *Spiniferites* spp. are especially closely related to the amount of size ϕ° 5.75-6.25 sediments. *Brigantedinium* spp. is strongly related to coarser sediments (ϕ° 3.75). Concentration spore is strongly related with finer grain size (ϕ° 9.75). Concentrations of Tintinomorphs and pollen are negatively correlated with water-depth.

3.3 Distribution patterns of other palynomorphs

Three taxa of acritarchs (*Halodinium major*, *Cyclopsiella* spp. and *Cladopyxis* spp.) occur along the transect. *Halodinium major* is commonly present on the shelf. *Cladopyxis* spp. is found only on the outer shelf and slope sites in small concentrations. *Cyclopsiella* spp. occurs only at 5 sites mainly on the shelf.

Foraminiferal linings are present at every site and are abundant on the shelf and upper slope sites (598.13-3199.59 linings ml⁻¹) but the concentrations become lower on the lower slope (Fig. 8a). Tintinomorphs are present at all sites (Fig. 8b). High concentrations of tintinomorphs are recorded on both inner shelf and slope. Spore and pollen are also present at all sites (Fig. 8cd). High concentrations are also observed on both inner shelf and slope.

4. DISCUSSION

4.1 Climatic assemblage classification

Dinoflagellate cyst distribution patterns, as other planktonic phytoplankton, are largely controlled by latitudinal temperature gradient. This study area has narrow latitude gradients (ca. 4 degree) where the SST does not vary significantly throughout the year. The assemblages are dominated by temperate to tropical species (e.g. *S. bulloideus*, *S. mirabilis*, *S. membranaceus*, *L. machaerophorum*, *I. striatum*, *O. israelianum*, *T. vancampoae*, *T. capitatum*, *Q. concreta*, *V. calvum*) and cosmopolitan species (*S. ramosus*, *P. reticulatum* and *P. zoharyi*) (according to the classification of Mudie and Harland (1996)). Minor components of cool temperate to temperate species (*S. stellatum*, *S. delicatus*, *N. labyrinthus* and *I. paradoxum*) are observed in slope sediments. The dinoflagellate assemblages from the studied area are in good accordance with the climatic assemblage classification of Edwards and Andrieu (1992) and Mudie and Harland (1996).

4.2 Oligotrophic Tropical Shelf Assemblage

There are only few studies on the distribution patterns of dinoflagellate cysts on a broad oligotrophic tropical shelf to date (e.g. McMinn, 1992). The oligotrophic tropical shelf assemblage on the Sunda Shelf is characterized by low overall concentrations of cysts and higher proportions of gonyaulacoids (*Spiniferites*, *P. reticulatum*, *O. longispinigerum* and *O. israelianum*) than protoperinoids (*T. capitatum* and Pre-encysted protoperidinoid) and diplopsalids.

The cyst concentrations on the Sunda Shelf are low compared with studies from other parts of the world (e.g. Biebow, 1996; Cho and Matsuoka, 1999; Cho and Matsuoka, 2001; Vink *et al.*, 2000). This may be because of low dinoflagellate production in surface waters due to low primary productivity and/or of high energy winnowing environments in the area. McMinn (1992) studied three samples from the Bass Strait (between Australia and Tasmania),

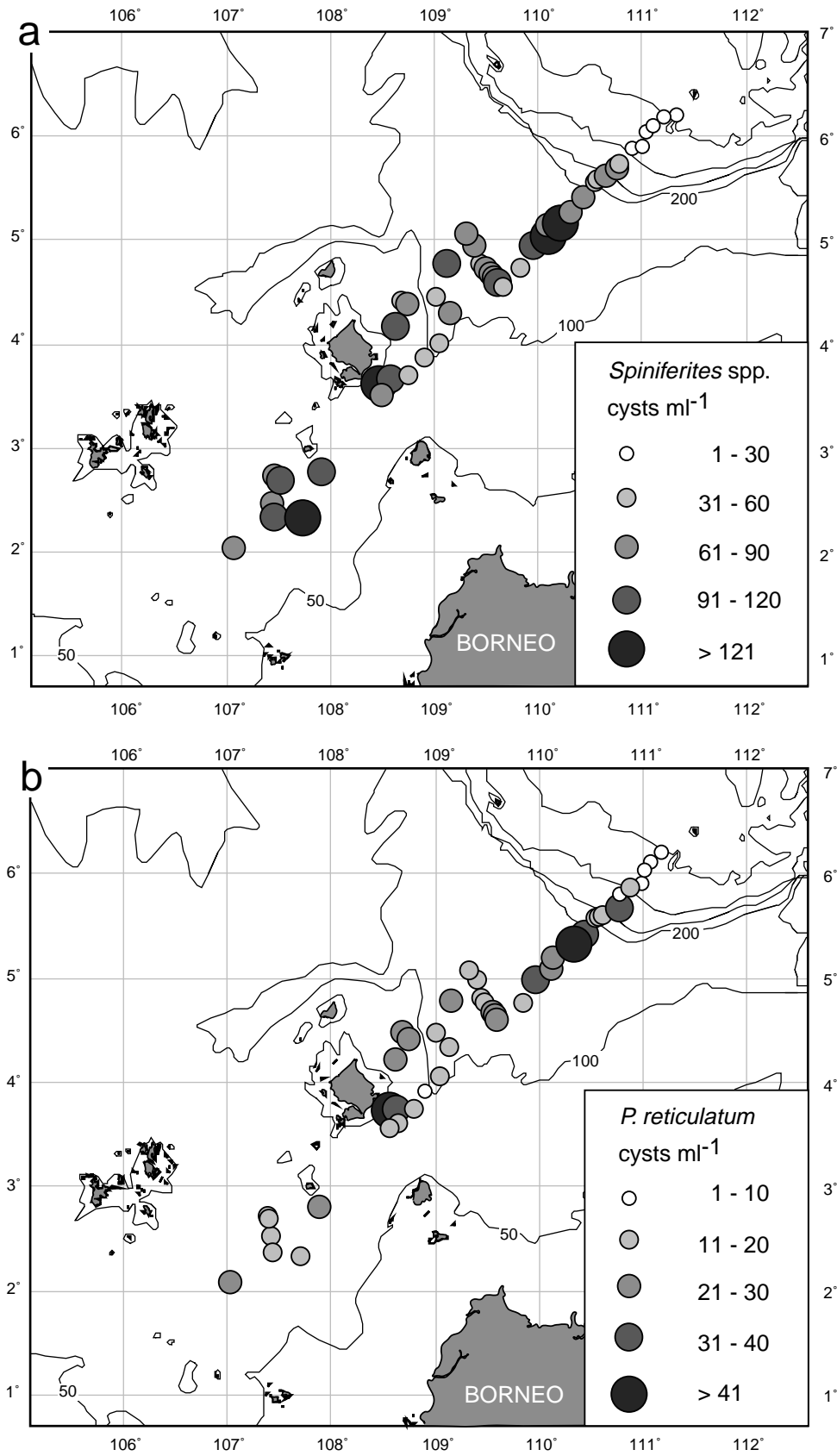


Figure 7 a-b. Distribution maps of (a) *Spiniferites* combined and (b) *Protoceratium reticulatum*.

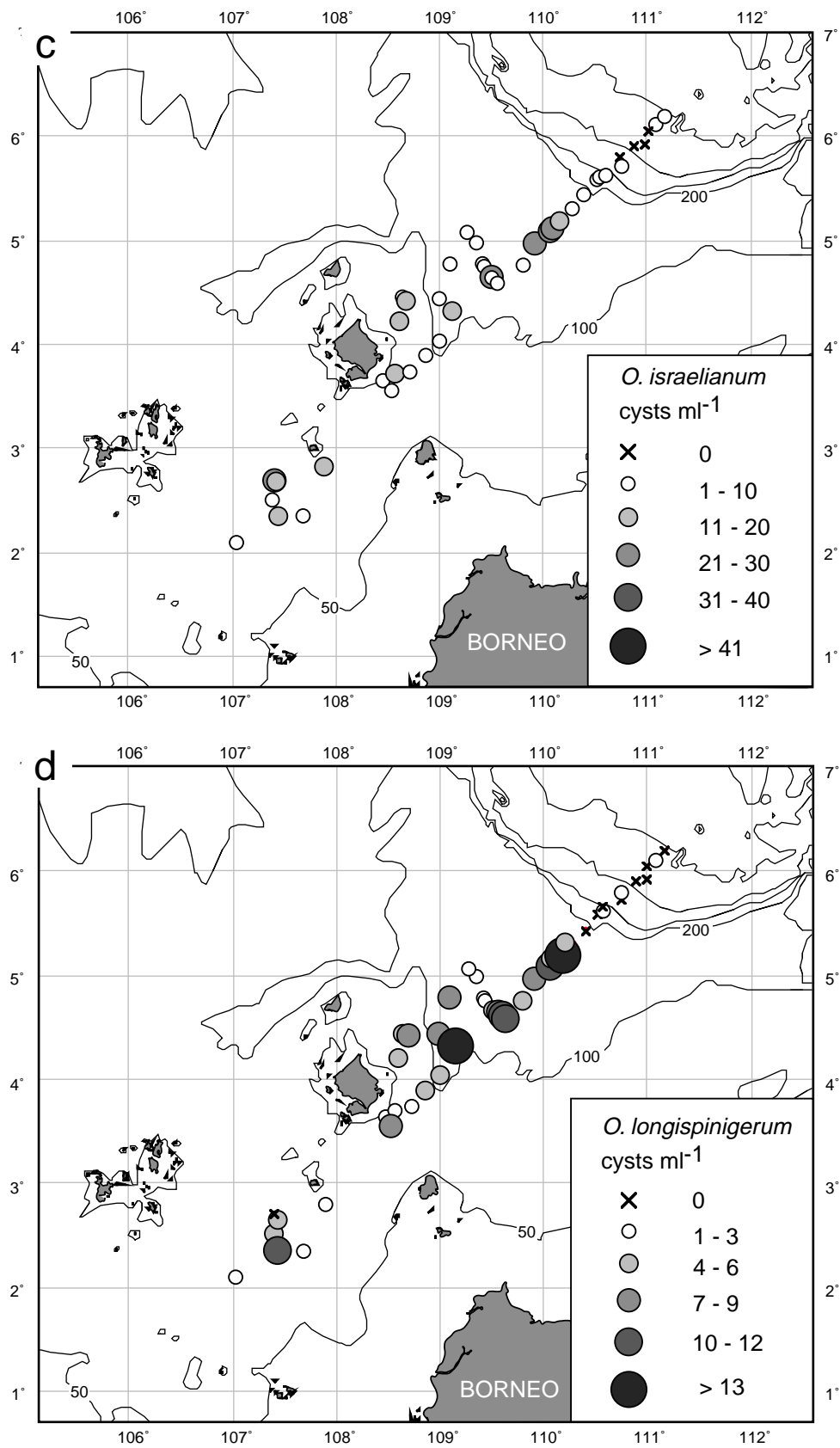


Figure 7 c-d. Distribution maps of (c) *Operculodinium israelianum* and (d) *Operculodinium longispinigerum*.

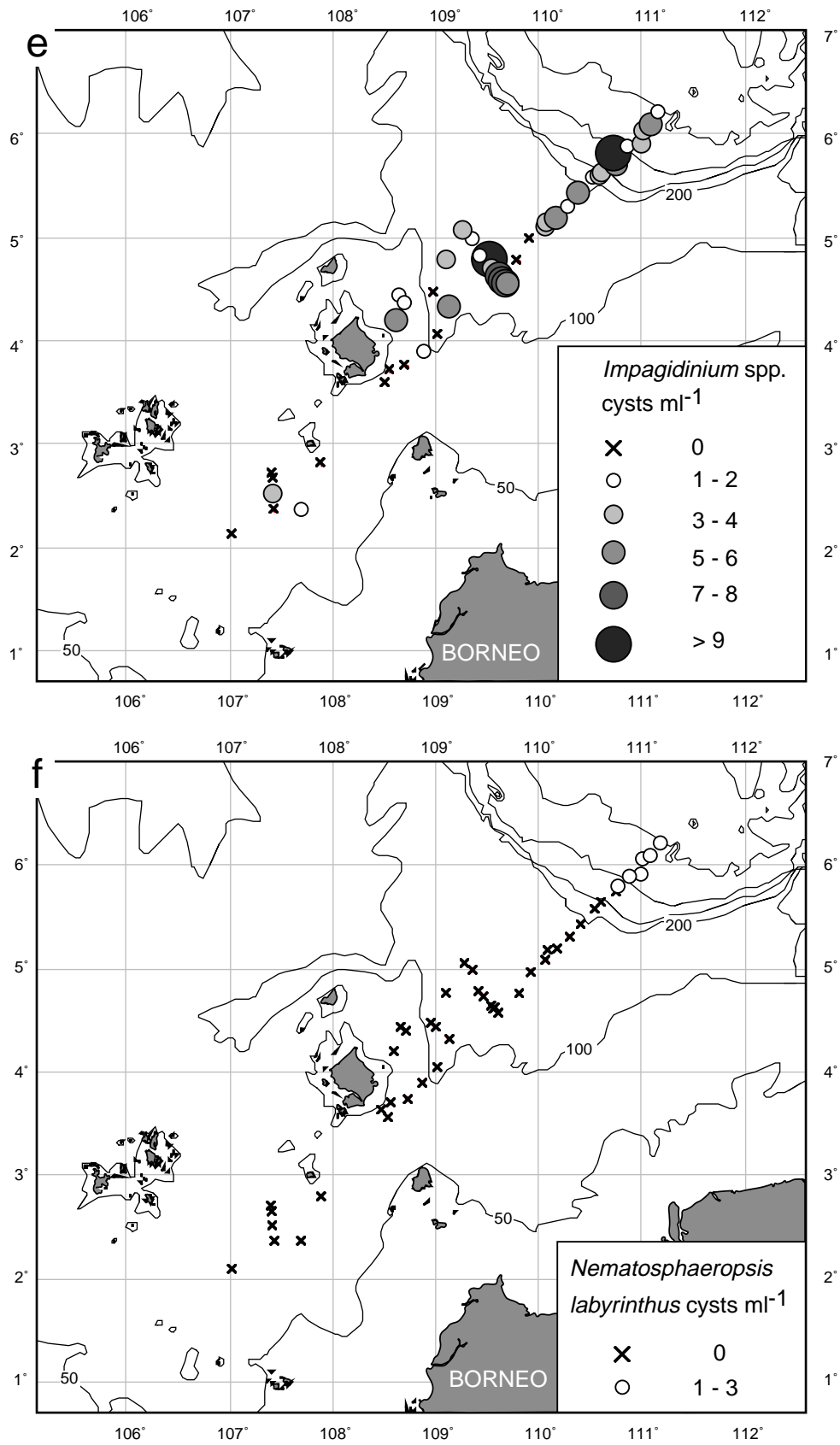


Figure 7 e-f. Distribution maps of (e) *Impagidinium* combined and (f) *Nematosphaeropsis labyrinthus*.

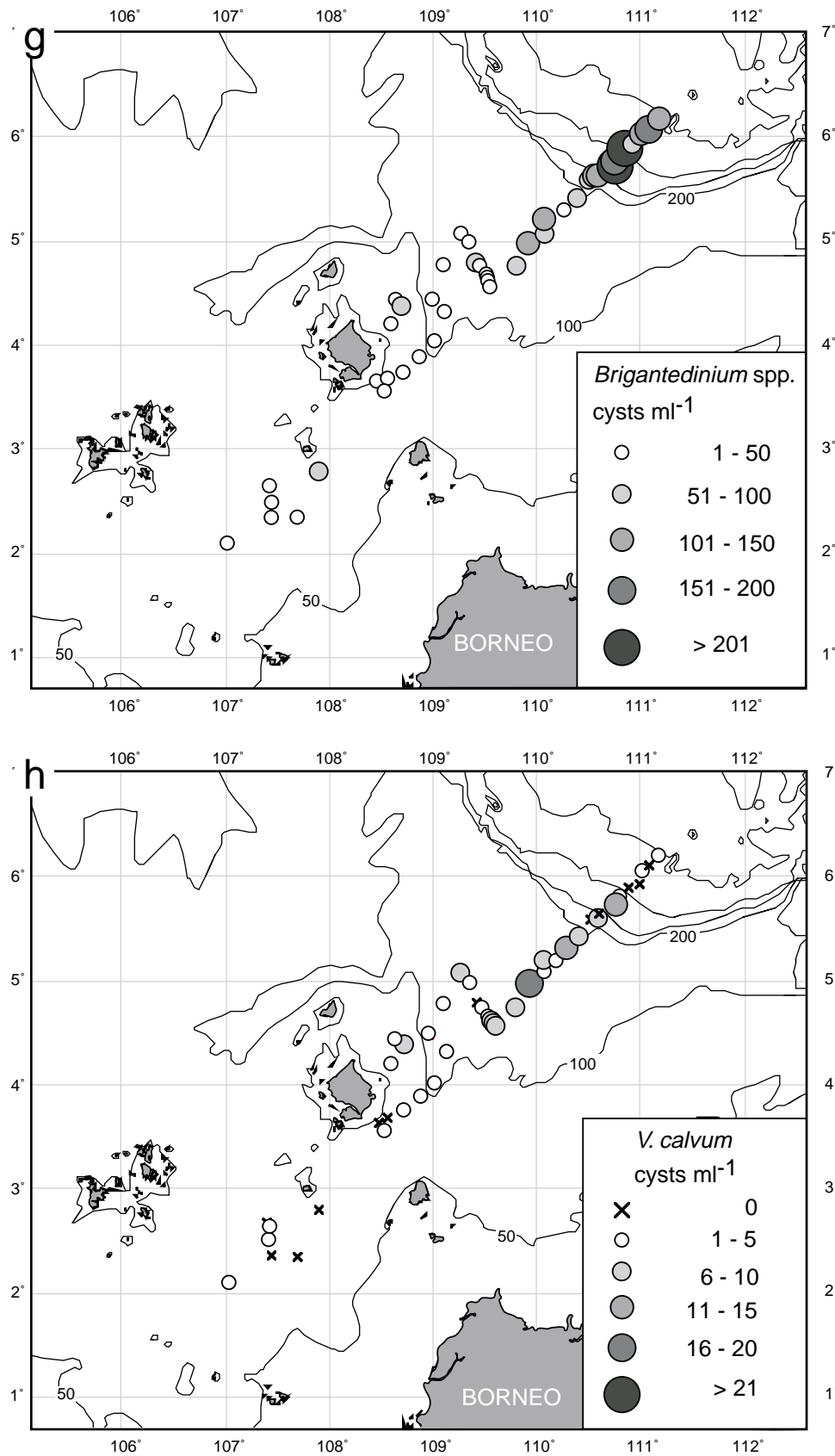


Figure 7 g-h. Distribution maps of (g) *Brigantedinium* combined and (h) *Votadinium calvum*.

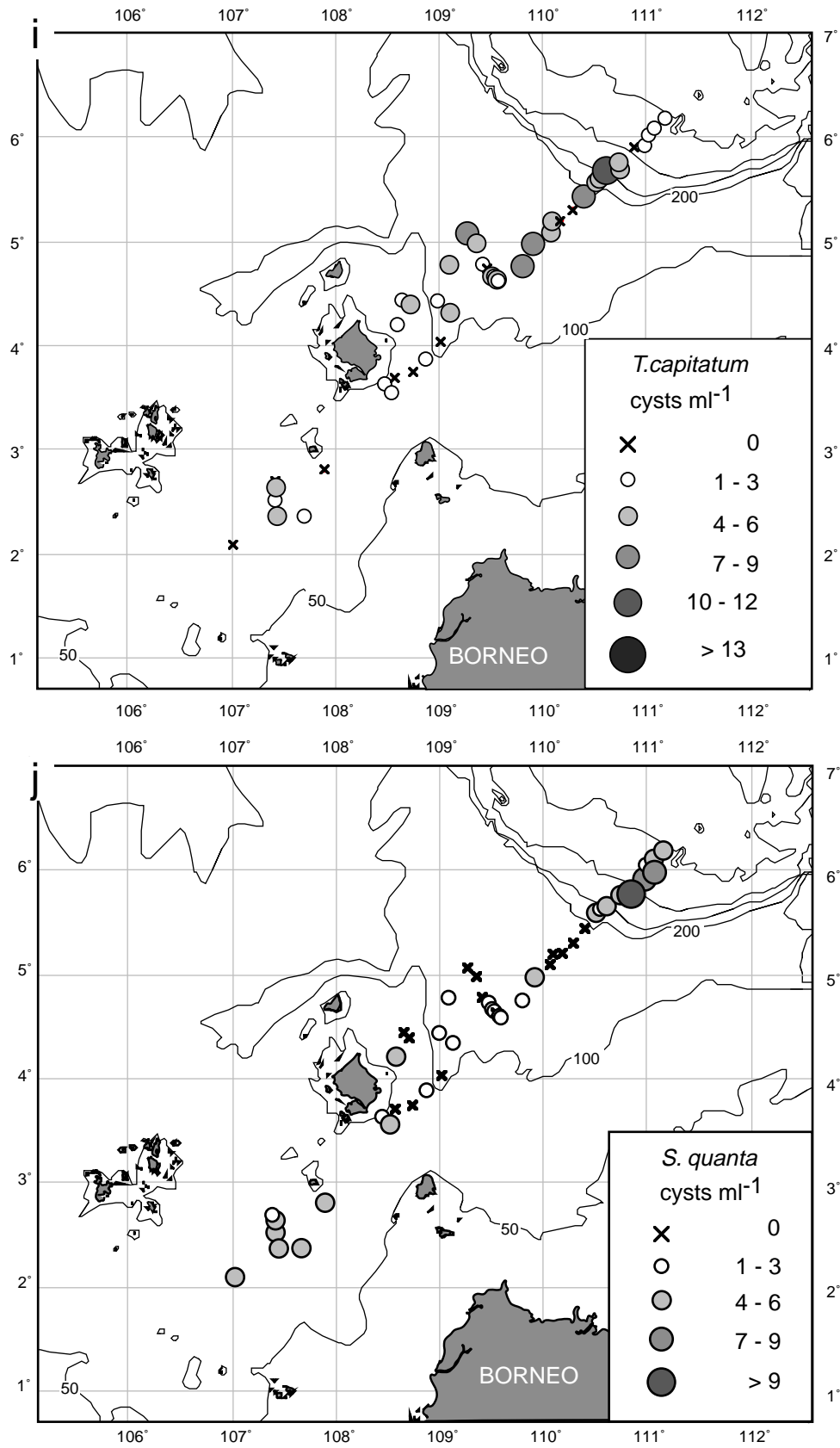


Figure 7 i-j. Distribution maps of (i) *Trinovantedinium capitatum* and (j) *Selenopemphix quanta*.

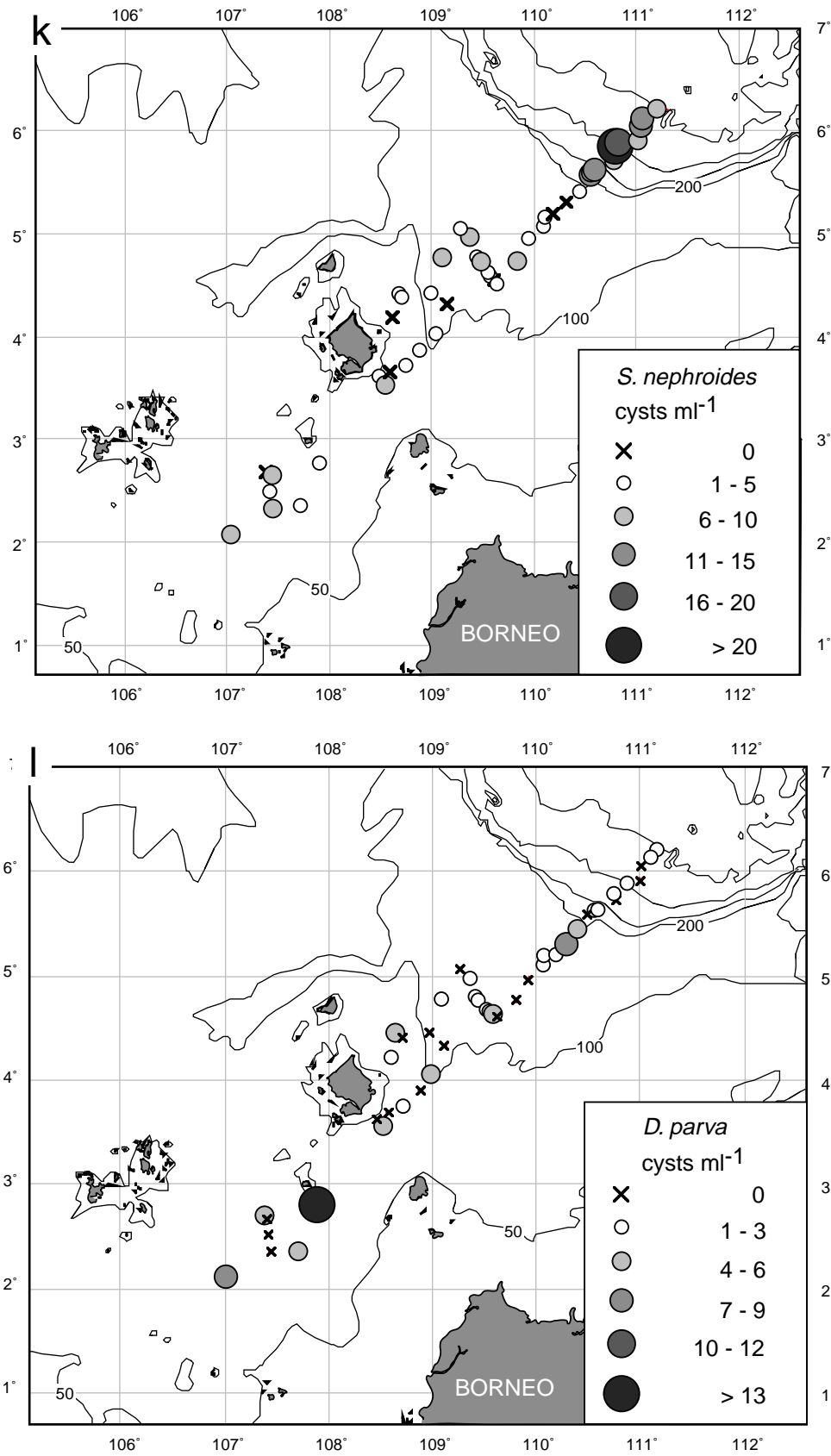


Figure 7 k-l. Distribution maps of (k) *Selenopemphix nephroides* and (l) *Diplopelta parva*.

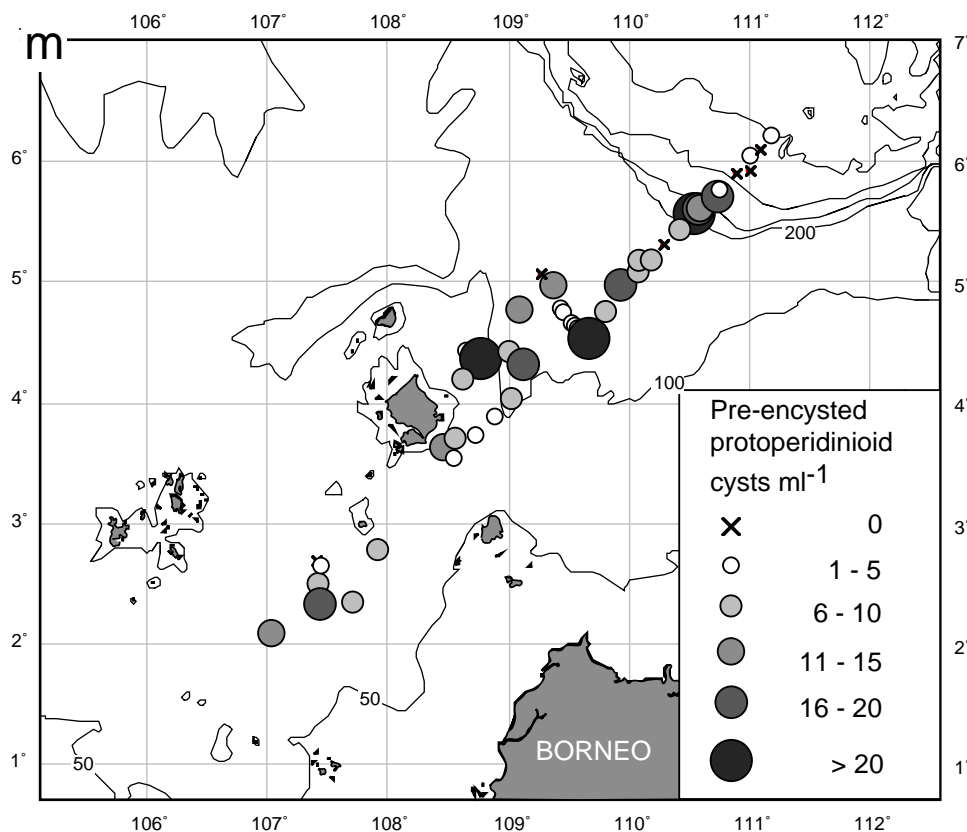


Figure 7 m. Distribution maps of (m) *Pre-encysted protoperidinioids*.

a broad and relatively oligotrophic shelf from middle latitude. The dinoflagellate cyst assemblages from the Basi Strait are similar to the Sunda Shelf assemblages except for the absence of *O. israelianum*. The absence of *O. israelianum* is perhaps related to the SST. *O. israelianum* is assigned to warm water to tropical species (Mudie and Harland, 1996) and it is unlikely to occur in middle latitudes such as the Basi Strait.

Compared with eutrophic shelf assemblages from the Yellow Sea and the East China Sea from Cho and Matsuoka (1999) and Cho and Matsuoka (2001), the oligotrophic assemblages from the Sunda Shelf contain much lower cyst concentrations and less consistent occurrences of *Alexandrium* spp. The assemblages from the Sunda Shelf have higher concentrations and more consistent occurrences of *O. israelianum*, *S. hyperacanthus*, *S. mirabilis*, *S. membranaceus* and *S. ramosus*. The differences in cyst concentrations may be related to the difference in primary productivity. In the Yellow Sea and the East China Sea, the annual primary productivity varies from 225 to over 450 $\text{gCm}^{-2}\text{y}^{-1}$ (SeaWifs). These values are significantly higher than these from the studied area. Cho and Matsuoka (2001) reported the higher concentrations of *Alexandrium* spp. in the northern Yellow Sea where highest annual primary productivities are recorded. In addition, occurrences of *Alexandrium* spp. are usually reported from the coastal area (e.g. Bolch and Hallegraeff, 1990; Kobayashi *et al.*, 1986; Kobayashi and Yuki, 1991; Nehring, 1997; Sonneman and Hill, 1997). The differences in the concentrations and occurrences of *Alexandrium* spp. may also result from the differences in primary productivity. Thus *Alexandrium* sp. may be classified as neritic/high productivity species. The differences in the concentrations and occurrences of *O. israelianum*, *S. hyperacanthus*, *S. mirabilis*, *S. membranaceus* and *S. ramosus* are probably related to the

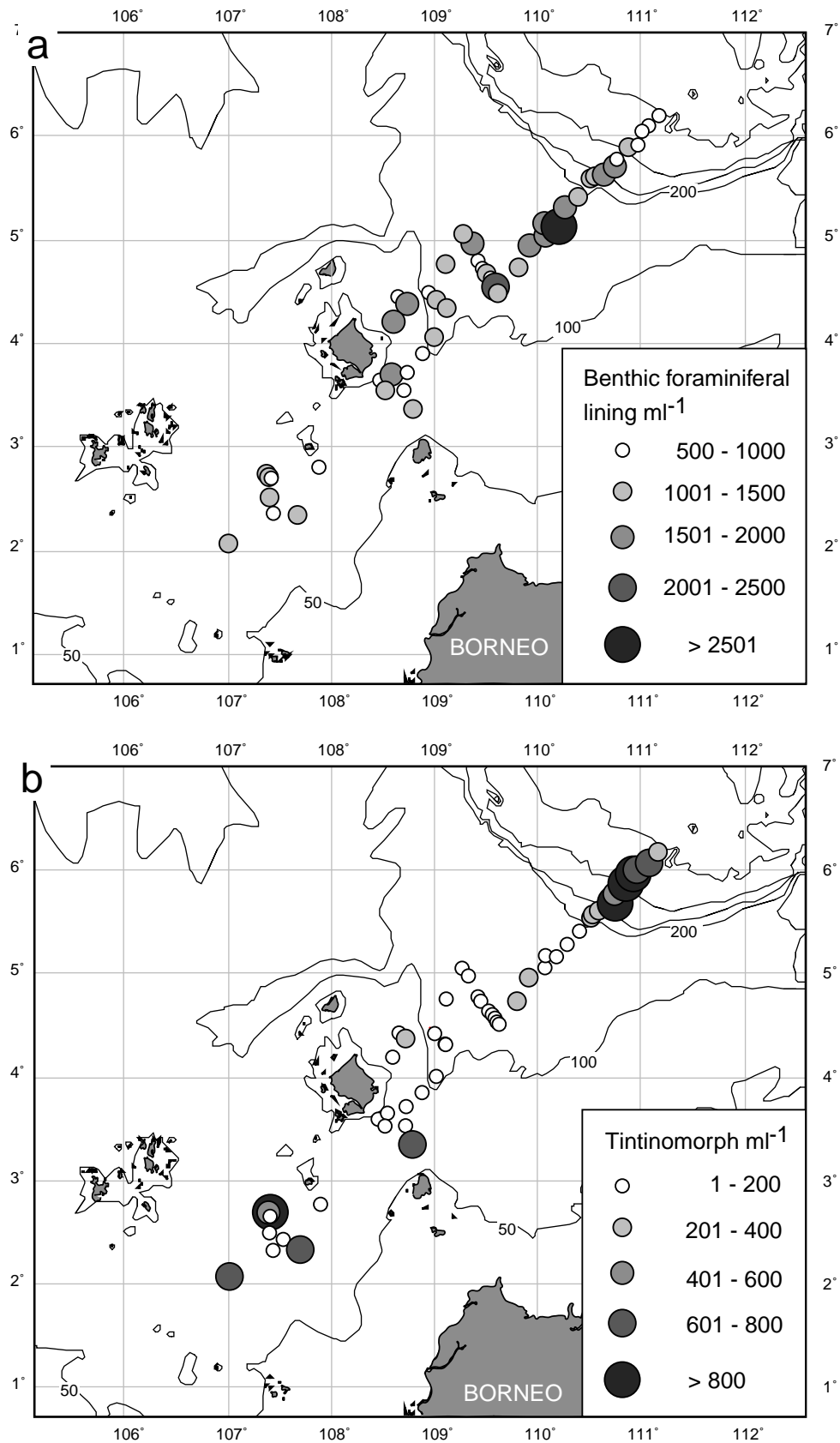


Figure 8 a-b. Distribution maps of (a) benthic foraminiferal linings and (b) tintinomorphs; expressed in individuals/grains ml^{-1} wet sediments.

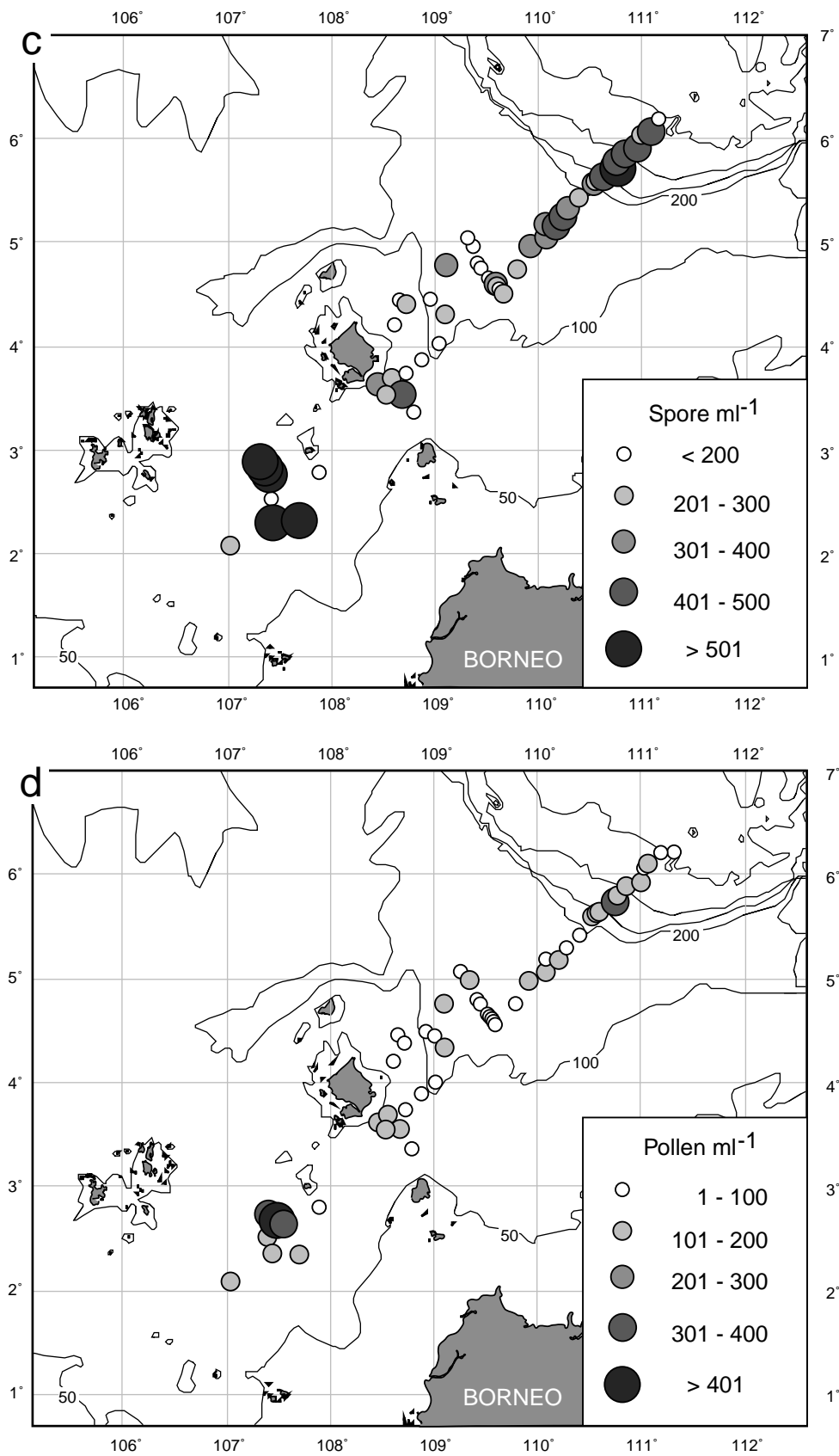


Figure 8 c-d. Distribution maps of (c) spores and (d) pollens; expressed in individuals/grains ml^{-1} wet sediments.

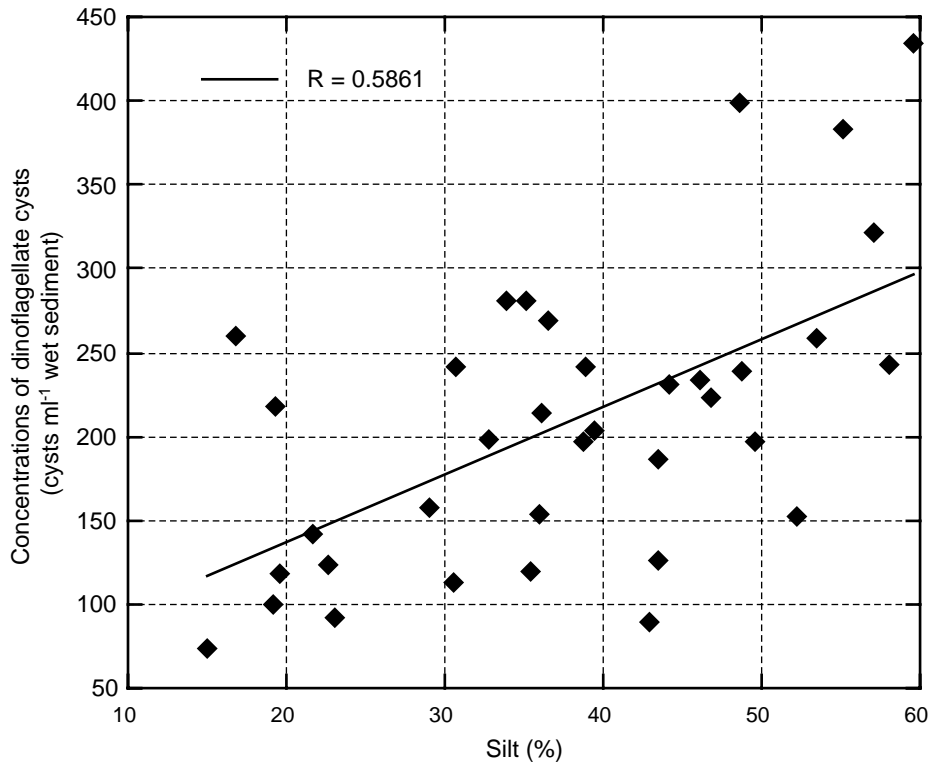


Figure 9. Concentrations of dinoflagellate cysts vs. clay/silt contents on the Sunda Shelf (R - the linear correlation coefficient). Data for sediment grain sizes is from Paulsen (1998).

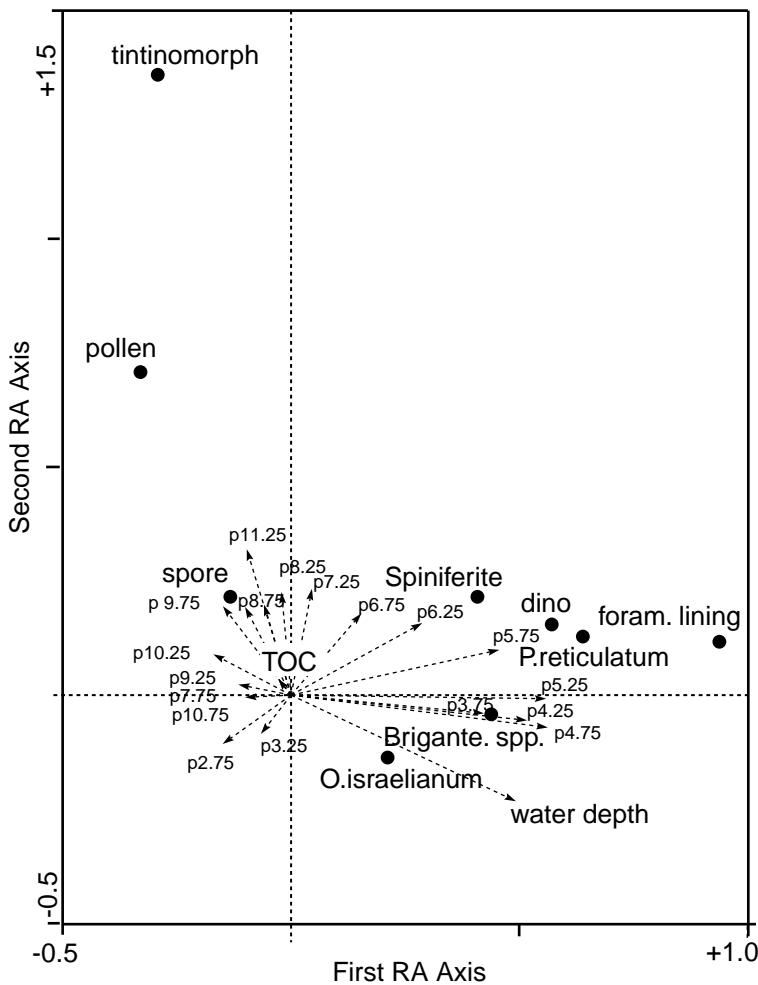


Figure 10. RA diagram of main taxa concentration values (cysts ml⁻¹) in relation to the variations in surface sediment grain sizes (dashed arrows). Scales of axes are given in standard deviations. Black circles indicate main taxa of dinoflagellate cysts and palyno-morph groups. Sediment grain-size data is from Paulsen (1998) and TOC data is from Stattegger *et al.* (1997).

winter SST. The winter SST in the Yellow Sea and the East China Sea varies from 11 in the northern Yellow Sea to 23 C in the East China Sea (SeaWifs). These temperatures are much lower than these from the Sunda Shelf. (Mudie and Harland, 1996) classified *O. israelianum* as warm water to tropical species, *S. mirabilis* (*S. hyperacanthus*) and *S. membranaceus* as cool temperate to tropical species and *S. ramosus* as cosmopolitan species.

4.3 Slope assemblage

The slope assemblage is characterized by high cyst concentrations and high proportions of protoperidinioids (*Brigantedinium* spp., *S. nephroides* and *S. quanta*) with low proportions of gonyaulacoids (*Lingulodinium machaerophorum* (short processes), *N. labyrinthus* and *Impagidinium* species). *Impagidinium* species and *N. labyrinthus* are classified as outer neritic-oceanic and inner neritic to oceanic species respectively (Mudie and Harland, 1996). Frequent and abundant occurrences of these species have been reported from the deep ocean basin in the western Pacific regions (Matsuoka, 1981; Wu and Sun, 2000; Wu and Tocher, 1995). These species are not reported from shelf sediments of the Yellow Sea and the East China Sea (Cho and Matsuoka, 1999; Cho and Matsuoka, 2001). Thus, the results presented here with respect to *Impagidinium* spp. and *N. labyrinthus* are not unexpected.

Beside occurrence of these oceanic species, the slope assemblages show many similarities to reported upwelling assemblages with higher concentrations of dinoflagellate cysts and dominance of protoperidinioids (mainly *Brigantedinium* spp.) and *L. machaerophorum*. (e.g. Dale and Fjellsa, 1993; Targarona *et al.*, 1999). A weak winter upwelling occurs in the studied area (Liu *et al.*, 2002). Thus, the cyst assemblages on the slope and high cyst concentrations may be results of the winter upwelling.

4.4 Dinoflagellate cysts as sediment particles

Palynomorphs can be transported laterally by surface current, bottom current and downslope by turbidity currents. In general, pollen, spore and dinoflagellate cysts are believed to have the hydrodynamic characteristics of fine silt-sized particles (Dale, 1983). In the studied area, the concentrations of different palynomorph groups correlate roughly with the abundances of silt size particles (Fig. 9). These results indicate that winnowing mechanisms play major role on the distribution and concentration of cysts on the shelf.

The results of RA show that total dinoflagellate cyst concentrations and *P. reticulatum* in the winnowed shelf sediments are best correlated to amounts of sediment with size $\phi^{10} 5.75$ and of *Spiniferites* spp. is best correlated with $\phi^{10} 6.25$. These results indicate that dinoflagellate cysts behave best like sediment particle size $\phi^{10} 5.75-6.25$ in water and confirm that dinoflagellate cysts behave best like silt particles.

The negative correlation of concentration of pollen to the increasing water-depth may indicate that concentrations of pollen are related to the distance from the source areas (land).

5. CONCLUSIONS AND IMPLICATION

Surface sediments from the Sunda Shelf and its slope in the SCS are examined palynologically in order to study the distribution patterns of organic-walled dinoflagellate cysts and of other major palynomorph groups. Thirty-seven taxa of dinoflagellate cysts are identified. The comparisons of cysts concentrations to the sediments grain-sizes suggest that organic-walled dinoflagellate cysts from the shelf area are highly altered by winnowing processes. Despite winnowing processes some new knowledge are gained and summarized below.

- 1) The studied area can be palynologically divided into the shelf area and the slope area and these two areas are governed by two different depositional environment.
- 2) Organic-walled dinoflagellate cyst assemblages from the oligotrophic tropical Sunda Shelf are characterized by high proportions of *Spiniferites* species (*S. bulloideus*, *S. mirabilis*, *S. ramosus*, *S. hyperacanthus*, *S. membranaceus*), *P. reticulatum* and *O. israelianum*.
- 3) Cysts of *Spiniferites* and *P. reticulatum* act generally like sediments with grain-size ϕ° 5.75-6.25 (fine to medium silt) in water. These sizes are slightly larger than often cited "fine-silt" size.
- 4) The slope assemblage shows a mixed signal of estuary/neritic high productivity species and oceanic low productivity species. This assemblage may reflect a weak winter upwelling in the studied area.
- 5) *A. tamarense* is probably a high productive and coastal species.

REFERENCES

- Biebow, N., 1996. Dinoflagellatenzysten als indikatoren der spaet- und postglazialen entwicklung des auftriebsgeschehens vor Peru. GEOMAR-Report, 57. GEOMAR, Forschungszentrum fur Marine Geowissenschaften der Christian-Albrechts-Universitaet zu Keil, Kiel, Federal Republic of Germany, 100 pp.
- Bolch, C.J. and Hallegraeff, G.M., 1990. Dinoflagellate cysts in recent marine sediments from Tasmania, Australia. *Botanica Marina*, 33: 173-192.
- Cho, H.-J. and Matsuoka, K., 1999. Dinoflagellate cyst composition and distribution in the surface sediments from the Yellow Sea and the East China Sea. In: T. Matsuno, K. Matsuoka and J. Ishizaka (Editors), *The East China Sea*. Nagasaki University, Nagasaki, pp. 73-82.
- Cho, H.-J. and Matsuoka, K., 2001. Distribution characteristics of dinoflagellate cysts in the surface sediments collected from the Yellow Sea and the East China Sea. *Marine Micropaleontology*, 42: 103-123.
- Dale, B., 1976. Cyst formation, sedimentation, and preservation; factors affecting dinoflagellate assemblages in Recent sediments from Trondheimsfjord, Norway. *Review of Palaeobotany and Palynology*, 22(1): 39-60.
- Dale, B., 1983. Dinoflagellate resting cysts: "benthic plankton". In: G.A. Fryxell (Editor), *Survival strategies of the algae*. Cambridge University Press, Cambridge, pp. 69-136.
- Dale, B. and Fjellsa, A., 1993. Dinoflagellate cysts as paleoproductivity indicators; state of the art, potential, and limits. In: Zahn *et al.* (Editors), *Carbon cycling in the glacial ocean; constraints on the ocean's role in global change; quantitative approaches in paleoceanography*. NATO ASI Series. Series I: Global Environmental Change. Springer Verlag, Berlin, Federal Republic of Germany, pp. 521-537.
- Edwards, L.E. and Andrieu, V.A.S., 1992. Distribution of selected dinoflagellate cysts in modern marine sediments. In: M.J. Head and J.H. Wrenn (Editors), *Neogene and Quaternary Dinoflagellate Cysts and Acritarchs*. AASP Foundation, Salt Lake City, pp. 259-288.
- Kobayashi, S., Matsuoka, K. and Iizuka, S., 1986. Distribution of dinoflagellate cysts in surface sediments of Japanese coastal water. I. Omura Bay, Kyushu. *Bulletin of Plankton Society of Japan*, 33(2): 81-93.
- Kobayashi, S. and Yuki, K., 1991. Distribution of dinoflagellate cysts in surface sediments of Japanese surface water II. Matoya Bay. *Bulletin of Plankton Society of Japan*, 38(1): 9-23.
- Lee, J.B. and Matsuoka, K., 1994. Distribution of dinoflagellate cyst from surface sediments in southern Korea water, 2nd International Symposium on the Marine Science Exploitation of Marine Resources. Unesco, Cheju National University, Korea, pp. 1-20.
- Lentin, J.K. and Williams, G.L., 1993. *Fossil Dinoflagellates: Index to Genera to Species*, 1993 Edition. AASP Contribution Series, 28. American Association of Stratigraphical Palynologists, Dallas, 864 pp.
- Lirdwitayaprasit, T., 1998. Distribution of dinoflagellate cysts in the surface sediment of South China Sea: Area 2. Off Sabah, Sarawak and Brunei Darussalam, Second Technical Seminar on Marine Fishery Resources Survey in the South China Sea, Area II: West coast of Sabah, Sarawak and Brunei Darussalam, Kuala Lumpur, pp. 310-322.
- Lirdwitayaprasit, T., 1998. Distribution of Dinoflagellate Cysts in the Surface Sediment of the South China Sea, Area I: Gulf of Thailand and East Coast of Peninsula, First Technical Seminar on Marine Fishery Resources Survey in the South China Sea, Area I: Gulf of Thailand and east coast of Peninsula Malaysia, Kuala Lumpur, pp. 311-326.
- Liu, W.T. and Xie, X., 1999. Spacebased observations of the seasonal changes of South Asian monsoon and oceanic responses. *Geophysical Research Letters*, 26(10): 1473-1476.
- Marret, F., 1994. Distribution of dinoflagellate cysts in recent marine sediments from the east Equatorial Atlantic (Gulf of Guinea). *Review of Palaeobotany and Palynology*, 84: 1-22.
- Matsuoka, K., 1981. Dinoflagellate cysts and pollen in pelagic sediments of the northern part of the Philippine Sea. *Bulletin of Faculty of Liberal Arts, Nagasaki University*, 21: 59-70.
- Matsuoka, K., 1992. Species diversity of modern dinoflagellate cysts in surface sediments around the Japanese Islands. In: Head, Martin, J ; Wrenn, John (Editors), *Neogene and Quaternary dinoflagellate cysts and acritarchs*. Publishers Press, Salt Lake City, UT, United States, pp. 33-55.
- Matsuoka, K., 1994. Geographical distribution of the toxic dinoflagellate *Gymnodinium catenatum* Grehm in Japanese Coastal Waters. *Botanica Marina*, 37: 495-503.

- Matsuoka, K. *et al.*, 1999. Marine palynomorphs found in surface sediments and a core sample collected from off Changjiang River, western part of the East China Sea. In: T. Matsuno, K. Matsuoka and J. Ishizaka (Editors), *The East China Sea*. Nagasaki University, Nagasaki.
- McMinn, A., 1991. Recent dinoflagellate cysts from estuaries on the central coast of New South Wales, Australia. *Micropaleontology*, 37(3): 269-287.
- McMinn, A., 1992. Recent and late Quaternary dinoflagellate cyst distribution on the continental shelf and slope of Southeastern Australia. *Palynology*, 16: 13-24.
- Mudie, P.J. and Harland, R., 1996. Chapter 21. Aquatic Quaternary. In: J. Jansonius and D.C. McGregor (Editors), *Palynology: principles and applications*. AASP Foundation, Salt Lake City, pp. 843-877.
- Nehring, S., 1997. Dinoflagellate resting cysts from recent German coastal sediments. *Botanica Marina*, 40: 307-324.
- Nino, H. and Emery, K.O., 1966. Continental shelf sediments off northeastern Asia. *Journal of Sedimentary Petrology*, 36(1): 152-161.
- Paulsen, J., 1998. Statistische Analyse Geochemischer und Sedimentologischer Daten von Oberflaechenproben de3s Vietnam- und Sunda-Schelfs (Sued-Chna-See). Diplom Thesis, Christian Albrecht Universitaet zu Kiel, Kiel, 36 pp.
- Qi, Y.Z., Hong, Y., Zheng, L., Kulis, D.M. and Anderson, D.M., 1996. Dinoflagellate cysts from recent marine sediments of the South and east China Seas. *Asian Marine Biology*, 13: 87-103.
- Rao, C.R., 1964. The use and interpretation of principal component analysis in applied research. *Sankhya*, A 26: 329-358.
- Rochon, A., de Vernal, A., Turon, J.-L., Matthiessen, J. and Head, M.J., 1999. Distribution of recent dinoflagellate cysts in surface sediments from the North Atlantic Ocean and adjacent seas in relation to sea-surface parameters. *American Association of Stratigraphical Palynologists Contribution Series*, 35. American Association of Stratigraphical Palynologists, Dallas, 152 pp.
- Saadon, N., Kin, L.P., Snidvongs, A. and Rojana-Anawat, P., 1998. Physical characteristics of watermass in the South China Sea, Area II: Sarawak, Sabah and Brunei Darussalam Water, First Technical Seminar on Marine Fishery Resources Survey in the South China Sea, Area I: Gulf Of Thailand and east coast of Peninsula Malaysia , pp. 1-22.
- Sarnthein, M., Pflaumann, U., Wang, P.X. and Wong, H.K., 1994. Preliminary report on Sonne-95 cruise "Monitor Monsoon" to the South China Sea; Manila - Guangzhou - Hongkong - Kota Kinabalu - Hongkong; 16 April-8 June 1994. *Berichte - Reports, Geologisch-Palaeontologisches Institut und Museum, Christian-Albrechts-Universitaet Kiel*, 68. Christian-Albrechts-Universitaet zu Kiel, Geologisch-Palaeontologisches Institut und Museum, Kiel, Federal Republic of Germany, 226 pp.
- Schoenfeld, J. and Kudrass, H.R., 1993. Hemipelagic sediment accumulation rates in the South China Sea related to late Quaternary sea-level changes. *Quaternary Research (New York)*, 40(3): 368-379.
- Seawifs, 2001. Ocean Primary Productivity Study. <http://marine.rutgers.edu/opp/>
- Sonneman, J.A. and Hill, D.R.A., 1997. A taxonomic survey of cyst-producing dinoflagellates from recent sediments of Victorian coastal waters, Australia. *Botanica Marina*, 40: 149-177.
- Stattegger, K., Kuhnt, W., Wong, H.K., Buehring, C. Haft, C., Hanebuth, T., Kawamura, H., Kienast, M., Lorenc, S., Lotz, B., Luedman, T., Lurati, M., Muelhan, N., Paulsen, A.M., Paulsen, J., Pracht, J., Putar-Roberts, A., Hung, H.Q., Richter, A., Salomon, B., Schimanski, A., Steinke, S., Szarek, R., Nhan, N.V., Weinelt, M., Winguth, C., 1997. Cruise Report SONNE 115 „SANDAFLUT“ *Berichte - Reports, Geologisch-Palaeontologisches Institut und Museum, Christian-Albrechts-Universitaet Kiel*, 86. Christian-Albrechts-Universitaet Kiel, Geologisch-Palaeontologisches Institut und Museum, Kiel, Federal Republic of Germany, p.211
- Steinke, S., 2001. Sedimentological and climate changes during the Last Deglaciation recorded in cores from the Sunda Shelf margin and continental slope (southern South China Sea). Ph.D. Thesis, Institut fuer Geowissenschaften, Christian Albrechts Universitaet zu Kiel, Kiel.
- Stockmarr, J., 1971. Tablets with spores used in absolute pollen analysis. *Pollen et Spores*, 13: 615-621.
- Szarek, R., 2001. Biodiversity and biogeography of recent benthic foraminiferal assemblages in the south-western South China Sea (Sunda Shelf). Ph.D. Thesis, Institut fuer Geowissenschaften, Christian Albrechts Universitaet zu Kiel, Kiel, 273 pp.
- Targarona, J., Warnaar, J., Boessenkool, K.P., Brinkhuis, H. and Canals, M., 1999. Recent dinoflagellate cyst distribution in the North Canary Basin, NW Africa. *Grana*, 38: 170-178.

- ter Braak, C.J.F. and Smilauer, P., 1998. CANOCO 4. Center of Biometry, Washington, 351 pp.
- Vink, A., Zonneveld, K.A.F. and Willems, H., 2000. Organic-walled dinoflagellate cysts in western Equatorial Atlantic surface sediments; distributions and their relation to environment. *Review of Palaeobotany and Palynology*, 112(4): 247-286.
- Wall, D., Dale, B., Lohmann, G.P. and Smith, W.K., 1977. The environmental and climatic distribution of dinoflagellate cysts in modern marine sediments from regions in the north and south Atlantic Oceans and adjacent seas. *Marine Micropaleontology*, 2: 121-200.
- Waveren, v., 1993. Planktonic organic matter in surficial sediments of the Banda Sea (Indonesia) - a palynological approach-. Ph.D Thesis, Universiteit Utrecht, Utrecht, 239 pp.
- Wiesner, M.G., Zheng, L., Wong, H.K., Wang, Y. and Chen, W., 1996. Fluxes of particulate matter in the South China Sea. In: V. Ittekkot, P. Schaefer, S. Honjo and P.J. Depetris (Editors), *Particle Flux in the Ocean*. John Wiley & Sons Ltd, pp. 293-312.
- Wu, G. and Sun, X., 2000. Distribution of dinoflagellate cysts in surface sediments from South China Sea. *Tropical Oceanology*, 19(1): 7-16.
- Wu, G. and Tocher, B., 1995. Organic-wall dinoflagellate from the surface sediments in southern Okinawa Trough. *Chinese Science Bulletin*, 40(6): 545-547.
- Wyrtki, K., 1961. *Physical oceanography of Southeast Asian Waters*, NAGA Report, Scientific Results of Marine Investigations of the South China Sea and the Gulf of Thailand, Scripps Institute of Oceanography, La Jolla, USA.
- Zonneveld, K.A.F., Versteegh, G.J.M. and de, L.G.J., 2001. Palaeoproductivity and post-depositional aerobic organic matter decay reflected by dinoflagellate cyst assemblages of the eastern Mediterranean S1 sapropel. *Marine Geology*, 172(3-4): 181-195.
- Zonneveld, K.A.F., Versteegh, G.J.M., de Lange, G.J., 1997. Preservation of organic-walled dinoflagellate cysts in different oxygen regimes: a 10,000 year natural experiment. *Marine Micropaleontology*, 29: 393-405.

Appendix I. Dinoflagellate cysts counted

Sample	18269	18270	18271	18272	18273	18274	18275	18276	18277	18279
Sediment Quantity (ml wt)	6	5	5	5	5	5	5	4.9	5	5
Lycopodium	3292	2850	1906	2425	1147	1048	1504	1725	1144	1826
Benthic foraminiferal lining	1226	893	1096	743	987	494	888	940	855	1141
Tintinomorphs	12	2	47	13	1	18	14	161	101	7
Spore	168	216	142	312	92	62	127	151	153	267
Gonyaulacoid Group										
<i>Spiniferites bulloideus</i>	7	29	17	18	10	7	8	13	10	20
<i>S. ramosus</i>	7	11	9	9	14	1	6	2	9	24
<i>S. mirabilis</i>	10	5	11	15	1	0	1	2	3	24
<i>S. hypercanthus</i>	8	17	9	7	6	3	7	4	5	22
<i>S. membrane</i>	8	13	6	7	6	4	4	0	3	14
<i>S. delicatus</i>	1	0	1	0	0	1	0	0	0	1
<i>S. bentori</i>	0	0	0	0	0	0	0	0	0	0
<i>Spiniferites spp.</i>	17	19	16	15	11	3	6	10	14	27
<i>Achomosphaera spp.</i>	0	0	0	3	0	0	0	1	1	0
<i>Protoceratium reticulatum</i>	29	18	16	25	23	2	5	9	18	21
<i>O. longispinigerum</i>	1	1	3	9	5	0	6	4	4	9
<i>O. crassum</i>	16	5	17	8	8	3	2	6	12	15
<i>Lingulodinium machaerophorum</i>	1	0	0	2	0	0	1	1	0	0
<i>L. machaerophorum (short process)</i>	0	0	7	2	0	2	2	7	8	3
<i>Impagidinium paradoxum</i>	0	0	2	2	0	0	0	0	0	1
<i>I. patulum</i>	0	0	0	1	1	0	0	0	0	0
<i>I. sphaericum</i>	0	1	0	0	1	0	1	0	0	2
<i>I. striatum</i>	0	0	0	1	0	0	0	0	0	0
<i>Impagidinium spp.</i>	1	9	0	2	1	0	2	0	0	0
<i>Nematopshaeropsis labyrinthus</i>	0	0	0	0	0	0	0	0	0	0
<i>Tectatodinium spp.</i>	0	0	0	0	0	0	0	1	1	0
<i>Alexandrium tamarensis</i>	0	0	3	2	1	0	1	3	1	0
Tuberculodinioid Group										
<i>Tuberculodinium vancampoeae</i>	2	2	1	3	0	1	1	0	1	8
Calciodinellid group										
<i>Scrippsiella trochoidea</i>	3	4	3	4	0	0	0	5	0	4
Protoperidinioid Group										
<i>Brigantedinium spp.</i>	17	10	47	27	9	10	18	49	62	64
<i>Selenopemphix quanta</i>	1	0	0	2	0	1	1	2	2	0
<i>S. nephroides</i>	3	8	1	3	0	1	3	7	2	4
<i>Stelladium stellatum</i>	1	0	0	0	0	0	1	0	0	1
<i>Trinovantedinium capitatum</i>	2	0	4	2	2	0	1	5	4	3
Pre-encysted Protoperidium	1	2	3	2	1	1	13	7	9	5
<i>Protoperidinium latissimum</i>	1	0	0	0	0	0	0	0	0	0
<i>Votadinium calvum</i>	0	1	4	6	3	0	6	5	8	1
<i>Lejeunecysta sabrina</i>	0	0	1	2	0	1	0	0	1	0
<i>Quinquecuspis concret</i>	0	0	0	0	0	0	0	0	0	0
<i>Diplopelta parva</i>	1	1	1	5	2	0	0	0	0	2
Gymnodiniales										
<i>Phepolykrikos hartmannii</i>	0	0	0	1	0	0	0	0	0	0
Other										
<i>Cladopyxis spp.</i>	0	0	0	0	0	0	0	0	0	0
<i>Halodinium major</i>	0	2	1	4	3	4	1	0	1	2
<i>Pediastrum</i>	0	0	0	0	2	0	0	0	0	0
<i>Cyclopsiella spp.</i>	0	0	0	0	0	0	0	0	0	0
Total number of dino	138	156	182	185	105	41	96	143	178	275

Sample	18269	18270	18271	18272	18273	18274*	18275	18276	18277	18279
Sediment Quantity (ml wt)	6	5	5	5	5	5	5	4.9	5	5
Lycopodium	3292	2850	1906	2425	1147	1048	1504	1725	1144	1826
Benthic foraminiferal lining	1226	893	1096	743	987	494	888	940	855	1141
Tintinomorphs	12	2	47	13	1	18	14	161	101	7
Spore	168	216	142	312	92	62	127	151	153	267
Gonyaulacoid Group										
<i>Spiniferites bulloideus</i>	7	29	17	18	10	7	8	13	10	20
<i>S. ramosus</i>	7	11	9	9	14	1	6	2	9	24
<i>S. mirabilis</i>	10	5	11	15	1	0	1	2	3	24
<i>S. hypercanthus</i>	8	17	9	7	6	3	7	4	5	22
<i>S. membrane</i>	8	13	6	7	6	4	4	0	3	14
<i>S. delicatus</i>	1	0	1	0	0	1	0	0	0	1
<i>S. bentori</i>	0	0	0	0	0	0	0	0	0	0
<i>Spiniferites spp.</i>	17	19	16	15	11	3	6	10	14	27
<i>Achomosphaera spp.</i>	0	0	0	3	0	0	0	1	1	0
<i>Protoceratium reticulatum</i>	29	18	16	25	23	2	5	9	18	21
<i>O. longispinigerum</i>	1	1	3	9	5	0	6	4	4	9
<i>O. crassum</i>	16	5	17	8	8	3	2	6	12	15
<i>Lingulodinium machaerophorum</i>	1	0	0	2	0	0	1	1	0	0
<i>L. machaerophorum (short process)</i>	0	0	7	2	0	2	2	7	8	3
<i>Impagidinium paradoxum</i>	0	0	2	2	0	0	0	0	0	1
<i>I. patulum</i>	0	0	0	1	1	0	0	0	0	0
<i>I. sphaericum</i>	0	1	0	0	1	0	1	0	0	2
<i>I. striatum</i>	0	0	0	1	0	0	0	0	0	0
<i>Impagidinium spp.</i>	1	9	0	2	1	0	2	0	0	0
<i>Nematopshaeropsis labyrinthus</i>	0	0	0	0	0	0	0	0	0	0
<i>Tectatodinium spp.</i>	0	0	0	0	0	0	0	1	1	0
<i>Alexandrium tamarensis</i>	0	0	3	2	1	0	1	3	1	0
Tuberculodinioid Group										
<i>Tuberculodinium vancampoae</i>	2	2	1	3	0	1	1	0	1	8
Calcioidinellid group										
<i>Scripsiella trochoidea</i>	3	4	3	4	0	0	0	5	0	4
Protopteridinioid Group										
<i>Brigantedinium spp.</i>	17	10	47	27	9	10	18	49	62	64
<i>Selenopemphix quanta</i>	1	0	0	2	0	1	1	2	2	0
<i>S. nephroides</i>	3	8	1	3	0	1	3	7	2	4
<i>Stelladium stellatum</i>	1	0	0	0	0	0	1	0	0	1
<i>Trinovantedinium capitatum</i>	2	0	4	2	2	0	1	5	4	3
Pre-encysted Protopteridium	1	2	3	2	1	1	13	7	9	5
<i>Protopteridium latissimum</i>	1	0	0	0	0	0	0	0	0	0
<i>Votadinium calvum</i>	0	1	4	6	3	0	6	5	8	1
<i>Lejeunecysta sabrina</i>	0	0	1	2	0	1	0	0	1	0
<i>Quinquecuspis concret</i>	0	0	0	0	0	0	0	0	0	0
<i>Diplopelta parva</i>										
Gymnodiniales	1	1	1	5	2	0	0	0	0	2
<i>Phepolykrikos hartmannii</i>										
Other	0	0	0	1	0	0	0	0	0	0
<i>Cladopyxis spp.</i>										
<i>Halodinium major</i>	0	0	0	0	0	0	0	0	0	0
<i>Pediastrum</i>	0	2	1	4	3	4	1	0	1	2
<i>Cyclopsiella spp.</i>	0	0	0	0	2	0	0	0	0	0
Total number of dino	0	0	0	0	0	0	0	0	0	0
Gonyaulacoid Group	138	156	182	185	105	41	96	143	178	275

Sample	18301	18302	18303*	18304	18305	18306	18307	18308*	18309*	18310
Sediment Quantity (ml wt)	5	5	5	4.5	5	5	5	5	5	4.8
Lycopodium	1192	2025	449	2900	1392	1634	1933	2508	618	2331
Benthic foraminiferal lining	933	1334	174	1210	639	531	1200	1186	245	1008
Tintinomorphs	152	85	0	55	3	0	3	619	0	50
Spore	107	130	36	189	129	248	215	156	114	195
Gonyaulacoid Group										
<i>Spiniferites bulloideus</i>	17	23	5	21	11	40	25	5	10	23
<i>S. ramosus</i>	4	20	3	9	5	9	28	4	10	13
<i>S. mirabilis</i>	2	11	0	0	2	3	4	1	1	11
<i>S. hypercanthus</i>	3	11	1	6	7	18	7	5	5	4
<i>S. membrane</i>	6	5	2	12	3	7	8	8	5	15
<i>S. delicatus</i>	0	0	0	0	0	0	1	0	0	0
<i>S. bentori</i>	1	0	0	0	0	0	1	0	0	0
<i>Spiniferites spp.</i>	9	18	2	5	8	17	18	5	5	7
<i>Achomosphaera spp.</i>	0	0	0	0	0	0	0	0	0	0
<i>Protoceratium reticulatum</i>	13	22	2	17	11	32	24	6	9	14
<i>O. longispinigerum</i>	4	3	5	8	9	2	2	0	1	6
<i>O. crassum</i>	5	10	0	10	8	4	14	4	1	7
<i>Lingulodinium machaerophorum</i>	0	0	0	2	0	1	0	0	0	0
<i>L. machaerophorum (short process)</i>	7	6	0	6	1	0	0	6	0	0
<i>Impagidinium paradoxum</i>	0	0	0	0	1	0	0	0	0	0
<i>I. patulum</i>	0	1	0	0	0	0	0	0	0	0
<i>I. sphaericum</i>	0	0	0	0	1	0	0	0	0	0
<i>I. striatum</i>	0	0	0	0	0	0	0	0	0	0
<i>Impagidinium spp.</i>	1	3	0	0	1	3	0	0	0	0
<i>Nematopshaeropsis labyrinthus</i>	0	0	0	0	0	0	0	0	0	0
<i>Tectatodinium spp.</i>	0	0	0	0	0	0	0	0	0	0
<i>Alexandrium tamarensis</i>	4	4	0	1	0	0	0	6	0	1
Tuberculodinioid Group										
<i>Tuberculodinium vancampoae</i>	0	0	0	1	1	0	2	0	1	1
Calcioidinellid group										
<i>Scripsiella trochoidea</i>	0	3	0	0	0	0	2	0	3	0
Protopteridinioid Group										
<i>Brigantedinium spp.</i>	27	22	0	33	6	8	13	8	10	13
<i>Selenopemphix quanta</i>	0	3	0	1	1	1	0	2	0	3
<i>S. nephroides</i>	2	0	0	5	0	1	0	1	0	7
<i>Stelladium stellatum</i>	0	0	0	0	2	0	0	4	1	0
<i>Trinovantedinium capitatum</i>	3	2	0	2	2	1	0	0	2	2
Pre-encysted Protopteridium	10	8	1	9	11	8	4	1	0	1
<i>Protopteridium latissimum</i>	0	0	0	0	0	0	0	0	0	0
<i>Votadinium calvum</i>	3	4	1	1	1	0	0	1	0	3
<i>Lejeunecysta sabrina</i>	0	0	0	0	0	0	0	0	0	0
<i>Quinquecuspis concret</i>	1	1	0	0	0	0	0	1	0	0
<i>Diplopelta parva</i>										
Gymnodiniales	0	2	0	0	0	0	0	1	0	5
<i>Phepolykrikos hartmannii</i>										
Other	0	0	0	0	0	0	0	0	0	0
<i>Cladopyxis spp.</i>										
<i>Halodinium major</i>	0	0	0	0	0	0	0	0	0	0
<i>Pediastrum</i>	2	4	0	1	2	1	1	2	0	5
<i>Cyclopsiella spp.</i>	0	0	0	0	0	0	0	0	0	0
Total number of dino	0	0	0	4	0	0	0	0	0	0
Gonyaulacoid Group	122	182	22	149	92	155	153	69	64	136

Sample	18312	18313	18314	18315	18316	18317*	18318	18319	18321	18322
Sediment Quantity (ml wt)	5	5	5	5	5	4	5	5	5	5.1
Lycopodium	2461	3204	1970	1712	1934	1186	1282	1634	1237	1462
Benthic foraminiferal lining	860	764	873	736	872	545	669	400	312	842
Tintinomorphs	29	3	83	500	366	41	658	25	75	435
Spore	131	126	80	160	151	371	346	777	125	230
Gonyaulacoid Group										
<i>Spiniferites bulloideus</i>	13	11	10	16	18	6	8	23	24	25
<i>S. ramosus</i>	7	6	8	4	12	9	9	12	5	19
<i>S. mirabilis</i>	3	5	3	1	3	4	6	3	7	9
<i>S. hypercanthus</i>	11	9	6	11	7	4	5	4	5	25
<i>S. membrane</i>	8	4	6	9	7	11	3	23	4	17
<i>S. delicatus</i>	2	1	2	2	0	0	1	0	0	0
<i>S. bentori</i>	0	2	0	0	0	1	0	0	0	0
<i>Spiniferites spp.</i>	8	17	7	8	10	7	8	8	8	2
<i>Achomosphaera spp.</i>	0	0	0	0	4	0	0	0	0	1
<i>Protoceratium reticulatum</i>	12	12	14	17	15	6	9	13	6	17
<i>O. longispinigerum</i>	2	7	3	1	4	3	0	3	6	2
<i>O. crassum</i>	5	3	3	1	5	8	11	7	10	5
<i>Lingulodinium machaerophorum</i>	2	1	0	0	0	0	0	0	0	0
<i>L. machaerophorum (short process)</i>	1	0	5	2	1	1	5	0	0	5
<i>Impagidinium paradoxum</i>	0	0	0	0	0	0	0	0	0	1
<i>I. patulum</i>	0	0	0	0	0	0	0	0	0	0
<i>I. sphaericum</i>	0	0	0	0	0	0	0	0	0	0
<i>I. striatum</i>	0	0	0	0	0	0	0	0	0	0
<i>Impagidinium spp.</i>	0	1	0	0	2	1	0	0	0	0
<i>Nematopshaeropsis labyrinthus</i>	0	0	0	0	0	0	0	0	0	0
<i>Tectatodinium spp.</i>	0	0	0	0	0	0	0	0	0	0
<i>Alexandrium tamarensis</i>	1	4	0	2	2	2	0	3	2	2
Tuberculodinioid Group										
<i>Tuberculodinium vancampoe</i>	2	0	0	2	0	1	0	1	0	0
Calciodinellid group										
<i>Scrippsiella trochoidea</i>	3	1	1	0	0	0	2	0	0	4
Protoperidinioid Group										
<i>Brigantedinium spp.</i>	25	11	11	19	2	6	21	5	12	16
<i>Selenopemphix quanta</i>	0	2	0	4	4	1	1	3	2	3
<i>S. nephroides</i>	1	3	1	6	1	1	0	4	3	2
<i>Stelladium stellatum</i>	0	1	0	0	0	0	5	0	0	1
<i>Trinovantedinium capitatum</i>	0	3	0	0	2	0	0	4	2	2
Pre-encysted Protoperidium	1	5	4	8	6	4	0	1	9	3
<i>Protoperidinium latissimum</i>	0	0	0	0	0	0	0	0	0	1
<i>Votadinium calvum</i>	1	2	1	3	1	0	0	1	0	0
<i>Lejeunecysta sabrina</i>	0	0	1	0	0	0	0	0	0	1
<i>Quinquecuspsis concret</i>	0	0	0	0	0	0	0	0	1	0
<i>Diplopelta parva</i>										
Gymnodiniales	2	0	4	5	0	3	2	0	0	3
<i>Phepolykrikos hartmannii</i>										
Other	0	0	0	0	0	0	0	0	0	0
<i>Cladopyxis spp.</i>										
<i>Halodinium major</i>	0	0	0	0	0	0	0	0	0	0
<i>Pediastrum</i>	0	5	1	1	5	2	0	8	4	1
<i>Cyclopsiella spp.</i>	0	0	0	0	0	0	0	1	0	0
Total number of dino	1	0	0	0	3	0	0	0	0	0
Gonyaulacoid Group	110	111	90	121	106	79	96	118	106	166

Sample	18323-1
Sediment Quantity (ml wt)	5
Lycopodium	1592
Benthic foraminiferal lining	566
Tintinomorphs	7
Spore	181
Gonyaulacoid Group	
<i>Spiniferites bulloideus</i>	12
<i>S. ramosus</i>	13
<i>S. mirabilis</i>	4
<i>S. hypercanthus</i>	9
<i>S. membrane</i>	8
<i>S. delicatus</i>	0
<i>S. bentori</i>	0
<i>Spiniferites spp.</i>	13
<i>Achomosphaera spp.</i>	0
<i>Protoceratium reticulatum</i>	11
<i>O. longispinigerum</i>	0
<i>O. crassum</i>	9
<i>Lingulodinium machaerophorum</i>	0
<i>L. machaerophorum (short process)</i>	3
<i>Impagidinium paradoxum</i>	0
<i>I. patulum</i>	0
<i>I. sphaericum</i>	0
<i>I. striatum</i>	0
<i>Impagidinium spp.</i>	0
<i>Nematopshaeropsis labyrinthus</i>	0
<i>Tectatodinium spp.</i>	0
<i>Alexandrium tamarensis</i>	1
Tuberculodinioid Group	
<i>Tuberculodinium vancampoae</i>	0
Calciodinellid group	
<i>Scrippsiella trochoidea</i>	11
Protopteridinioid Group	
<i>Brigantodinium spp.</i>	39
<i>Selenopemphix quanta</i>	4
<i>S. nephroides</i>	1
<i>Stelladium stellatum</i>	5
<i>Trinovantedinium capitatum</i>	0
Pre-encysted Protopteridium	5
<i>Protopteridium latissimum</i>	0
<i>Votadinium calvum</i>	0
<i>Lejeunecysta sabrina</i>	0
<i>Quinquecuspis concret</i>	0
<i>Diplopelta parva</i>	
Gymnodiniales	19
<i>Pheopolykrikos hartmannii</i>	
Other	0
<i>Cladopyxis spp.</i>	
<i>Halodinium major</i>	0
<i>Pediastrum</i>	8
<i>Cyclopsiella spp.</i>	0
Total number of dino	0
Gonyaulacoid Group	167

Chapter 1 Appendix II

Spec: Species scores (adjusted for species variance)

N	NAME	AX1	AX2	AX3	AX4	WEIGHT	1
	EIG	0.398	0.1266	0.0416	0.007		
1	Spiniferites	0.4084	0.2141	0.7809	1.3916	1	1
2	P. reticu	0.6388	0.1291	0.4516	0.7223	1	1
3	O.israel	0.2124	-0.1368	0.4121	1.9392	1	1
4	Bri. spp.	0.4393	-0.0414	-0.113	2.1796	1	1
5	dino	0.5693	0.1567	0.4696	1.9185	1	1
6	foramlin	0.9385	0.1184	0.0121	-0.0384	1	1
7	tintinom	-0.2928	1.3573	-0.1695	0.0097	1	1
8	spore	-0.1332	0.2163	1.3721	-0.1028	1	1
9	pollen	-0.3292	0.7067	1.0671	-0.2807	1	1

Samp: Sample scores

N	NAME	AX1	AX2	AX3	AX4	WEIGHT	1
	EIG	0.398	0.1266	0.0416	0.007		
1	269	-0.9652	-0.6767	-0.664	-0.2466	1	1
2	270	-0.9475	-0.6505	-0.3349	-0.0172	1	1
3	271	0.3224	-0.2053	-0.2777	0.1812	1	1
4	272	-0.9913	-0.5691	0.1498	0.178	1	1
5	273	1.7183	-0.0368	-0.1226	-0.3553	1	1
6	275	0.3889	-0.287	-0.2186	-0.3218	1	1
7	276	0.1621	0.2412	-0.2601	0.0114	1	1
8	277	1.1215	0.4613	0.2641	0.7142	1	1
9	279	0.5897	-0.1955	0.4866	0.8162	1	1
10	280	0.5279	-0.1956	0.5983	1.1904	1	1
11	281	3.7213	0.5084	0.722	-0.6	1	1
12	282	1.1703	0.0112	0.0564	-0.1088	1	1
13	283	-0.2914	-0.1492	-0.2265	0.1967	1	1
14	295	1.2804	0.2831	-0.4181	-0.352	1	1
15	296	-0.3897	-0.5227	-0.3626	-0.2762	1	1
16	297	-0.1422	-0.3946	0.2902	0.1056	1	1
17	300	-0.7948	-0.6131	-0.4913	-0.1918	1	1
18	301	1.2406	0.7161	-0.1752	-0.0978	1	1
19	302	0.7139	-0.0081	-0.3571	-0.019	1	1
20	304	-0.2361	-0.3544	-0.3513	-0.2116	1	1
21	305	-0.246	-0.4501	-0.1117	-0.1298	1	1
22	306	-0.8918	-0.5571	0.3969	0.3878	1	1
23	307	0.5366	-0.2437	0.1439	-0.2213	1	1
24	310	-0.3065	-0.3325	-0.1829	-0.2014	1	1
25	312	-0.7827	-0.5575	-0.5397	-0.186	1	1
26	313	-1.3143	-0.7582	-0.6684	-0.1621	1	1
27	314	-0.3456	-0.282	-0.6904	-0.2709	1	1
28	315	-0.6093	1.3663	-0.5124	0.039	1	1
29	316	-0.4413	0.7528	-0.4172	-0.2715	1	1
30	318	-0.4092	3.1231	0.938	-0.4403	1	1
31	319	-1.41	-0.2239	3.1821	-0.412	1	1
32	321	-1.2932	-0.2537	-0.0368	0.4104	1	1
33	322	0.0437	1.5953	0.1541	0.287	1	1
34	323	-0.7293	-0.5413	0.037	0.5756	1	1
35	ORIGIN	-2.4707	-1.0877	-1.1567	-0.2016	0	0

CFit: Cumulative fit per species as fraction of variance of species

N	NAME	AX1	AX2	AX3	AX4	VAR(y)	% EXPL
	FR FITTED	0.398	0.1266	0.0416	0.007		
1	Spiniferites	0.1052	0.1215	0.2459	0.4082	0.03	55.87
2	P. reticul	0.2574	0.2634	0.3049	0.3487	0	81.22
3	O.israeli	0.0285	0.0351	0.0698	0.385	0	59.86
4	Bri. spp.	0.1217	0.1223	0.1249	0.5232	0.02	65.47
5	dino	0.2045	0.2132	0.2582	0.5668	0.15	56.78
6	foramli	0.5556	0.5606	0.5606	0.5608	6.19	56.08
7	tintino	0.0541	0.7095	0.7154	0.7154	1.63	71.55
8	spor e	0.0112	0.0278	0.4117	0.4126	0.84	41.42
9	pollen	0.0684	0.2461	0.4783	0.4849	0.13	56.5

BipE: Biplot scores of environmental variables

N	NAME	AX1	AX2	AX3	AX4
	R(SPEC,ENV)	0.7676	0.7725	0.6615	0.7495
1	wd	0.4736	-0.2213	-0.0078	0.0973
2	TOC (.)	-0.0156	0.0176	0.1605	0.143
3	p2.75	-0.1325	-0.0954	-0.1827	-0.0647
4	p3.25	-0.0518	-0.0688	-0.2255	-0.0361
5	p3.75	0.3997	-0.0373	-0.078	-0.0378
6	p4.25	0.4964	-0.0516	-0.093	0.0016
7	p4.75	0.5421	-0.069	-0.0768	0.0565
8	p5.25	0.5379	-0.0082	-0.0762	0.1086
9	p5.75	0.4364	0.0946	-0.058	0.1701
10	p6.25	0.2671	0.1463	-0.0537	0.1728
11	p6.75	0.139	0.1636	-0.0533	0.1581
12	p7.25	0.0421	0.2107	-0.051	0.1239
13	p7.75	-0.0936	0.0205	-0.0869	0.001
14	p8.25	-0.0186	0.2036	-0.0771	0.1128
15	p8.75	-0.0531	0.1798	-0.077	0.1157
16	p9.25	-0.1501	0.0784	-0.1684	0.0362
17	p 9.75	-0.1364	0.1783	-0.0846	0.1142
18	p10.25	-0.0893	0.1744	-0.1004	0.1181
19	p10.75	-0.0792	-0.0026	-0.0603	0.0043
20	p11.25	-0.0906	0.2982	-0.0632	0.0884

Summary

Axes	1	2	3	4	Total variance
Eigenvalues :	0.398	0.127	0.042	0.007	1
pecies-environment correlations :	0.768	0.773	0.661	0.749	
Cumulative percentage variance					
of species data	39.8	52.5	56.6	57.3	
of species-environment relation:	69.1	91.1	98.4	99.6	
Sum of all unconstrained eigenvalues					1
Sum of all canonical eigenvalues					0.576

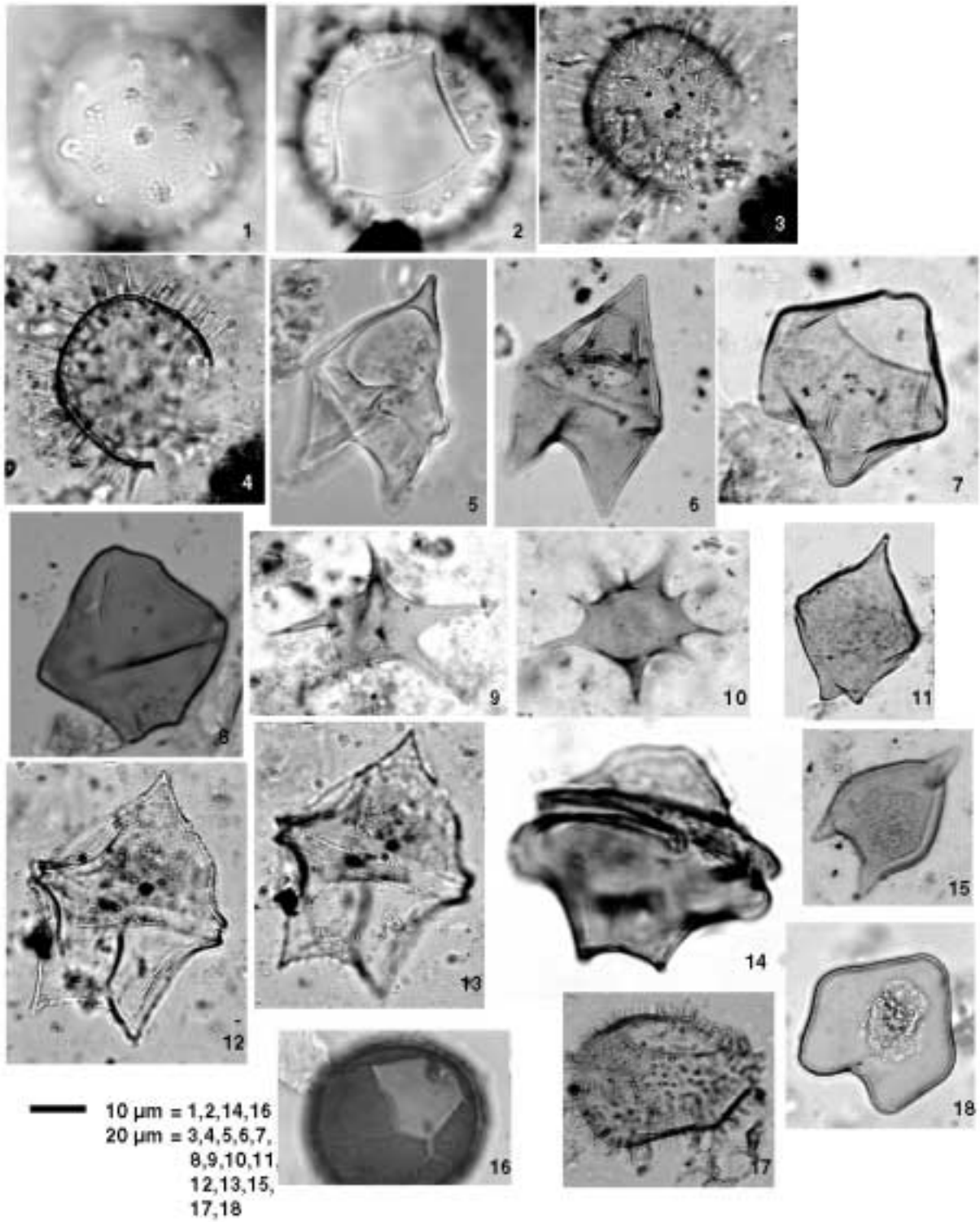


Plate I

Plate I.

1 - 4. *Operculodinium israelianum*

5 & 6. *Votadinium calvum*

7. *Lejeunecysta sabrina*

8 & 11. *Protoperidinium latissimum*

9 & 10. *Stelladinium cf. stallatum*

12-13. *Trinovantedinium capitatum*

14. *Selenopemphix nephroides*

15 & 18. Pre-encysted protoperidinioids

17. *Votadinium spisosum*

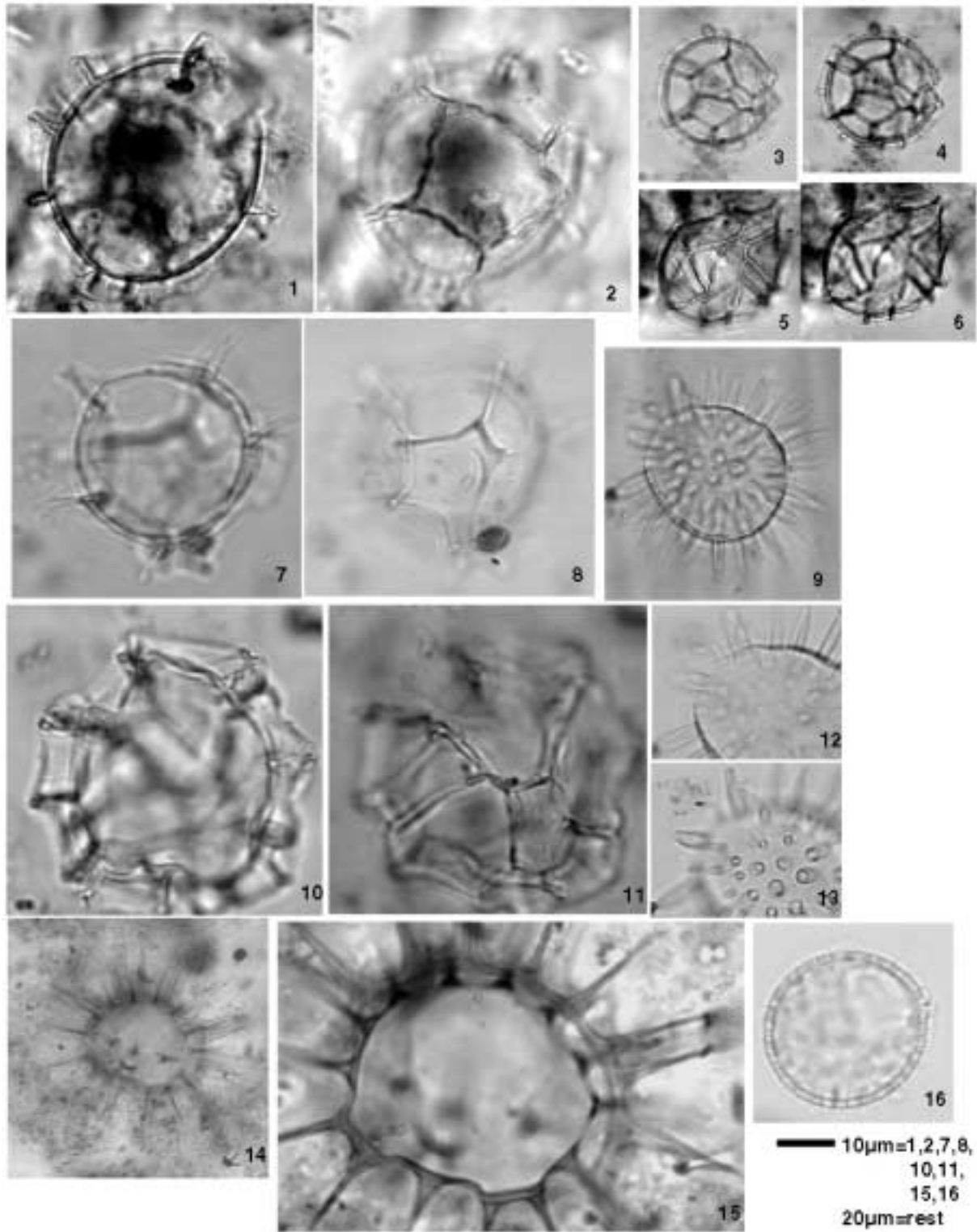


Plate II

Plate II

1-4. *Impagidinium patulum*

5-6. *Impagidinium sphaericum*

7-8. *Impagidinium striatum*

10-11. *Impagidinium* spp.

9, 12&13. *Lingulodinium machaerophorum*

14-15. *Selenopemphix quanta*

16. *Scripsiella* sp.

CHAPTER 3. Distribution patterns of organic-walled dinoflagellate cysts in the South China Sea

Hiroshi Kawamura

Institut fuer Geowissenschaften der Christian Albrechts Universitaet zu Kiel

Olshausenstr. 40, 24118 Kiel, Germany

ABSTRACT

Forty taxa of organic-walled dinoflagellate cysts are identified from thirty-six surface samples collected from the South China Sea (SCS). The concentrations of dinoflagellate cysts are low (39.5 to 1828.2 cysts g⁻¹). Dinoflagellate cyst assemblages in the SCS are mainly composed of temperate to tropical taxa of Mudie and Harland (1996). Cyst concentrations in sediments from shallow coastal areas are much higher than those from deep basin area. In coastal areas (<50 m wd), the assemblages are characterized by high concentration of protoperidinioids, *Spiniferites* species, *P. reticulatum* and *L. machaerophorum*. Vietnamese Shelf assemblages are characterized by dominances of *Spiniferites* species, *P. reticulatum* and cysts from protoperidinioid group. The assemblages on slope and oceanic basin are characterized by occurrences of *Impagidinium* species and *N. labyrinthus*. A Correspondence Analysis of the results revealed that the distribution patterns of dinoflagellate cysts are strongly related to distances from the landmasses. This relation can be explained with either gradients of surface water primary productivity or effect of offshore cyst transport processes in the South China Sea.

1.1 INTRODUCTION

Dinoflagellate cysts have been successfully used in paleoceanographic research as a proxy for sea surface conditions since 1970's (McCarthy et al., 1999; Rochon et al., 1998; Rochon et al., 1999; Versteegh and Zonneveld, 1994; Zonneveld, 1995). However, these studies are mainly limited in the Atlantic Ocean and the Southern Ocean and in other oceans such as the Pacific Ocean and the Indian Ocean, dinoflagellate cysts are underutilized as paleoceanographical proxies. This may be partially due to the poor understanding of its distributions in these oceans and their marginal seas. Furthermore, most studies on the distributions of dinoflagellate cysts are restricted to either shallow coastal areas (<50m water-depth (wd)) where dinoflagellate can be counted as up to 50 % of primary productions (Dale, 1996) and where the highest concentrations of dinoflagellate cysts are commonly recorded, or deep oceanic areas (>1000 m wd) where no complete life cycles of cyst-producing dinoflagellate have been observed to date (Sarjeant and Taylor, 1999). Studies in transitional areas are seldomly carried out. Samples were collected from the shelf, slope and ocean basin areas and sampling area covered whole South China Sea (SCS). These samples provide unique opportunity to document the assemblage changes through different water depths with various oceanographic and sedimentological parameters. The objectives of this study are to document the recent distribution patterns of organic-walled dinoflagellate cysts in the South China Sea and to investigate possible environmental and taphonomical factors controlling the distribution patterns.

1.2 STUDY AREA

The SCS is a marginal sea located in the tropical/subtropical climatic zones surrounded by southern China, Philippines, Vietnam, Borneo (Malaysia) and Indonesia (Figure 1). The southern part of the SCS belongs to the western end of the West Pacific Warm Pool (WPWP) with high sea surface temperature (SST). The oceanography of the SCS is strongly controlled by semi-annual reversal of monsoon regimes.

During winter monsoon (September-May), the predominant current direction is to the southwest (Figure 2a). An anticlockwise gyre develops off middle Vietnam. The main incoming surface water enters through the Luzon Strait (between Taiwan and Philippines), Taiwan Strait (between Taiwan and China), Balabac and Mindoro Strait (from the Sulu Sea). The surface water exits the SCS through the Karimata Strait (between Borneo and Sumatra) to the Java Sea. During summer monsoon (June-August), the inflow water comes from the Java Sea through the Karimata Strait and forms NE-trending currents along Vietnamese coast. A clockwise eddies develop in the central SCS in April (Wyrki, 1961) (Figure 2b).



Figure 1. Locations of the surface sediment samples studied in this chapter.

Sea surface temperature (SST) varies from 20 to 28.8 °C during winter monsoon in the SCS (Figure 2c). The SST has north-south gradients with low SST in northern SCS. The gradient is steeper along Chinese and Vietnamese coasts due to low temperature on the land. During a summer monsoon, the temperature gradient in the South China Sea is low varying from 27 to 29 °C (Figure 2d). The SST is slightly lower off mid-Vietnamese coast because of seasonal upwelling activity in this region.

Sea surface salinity (SSS) during winter monsoon ranges from 32.8 to 34.6 psu. Lower salinity is found in the Mekong Delta and the Gulf of Tonkin reflecting the freshwater influx. The SSS increases towards the Luzon Strait. This is reflecting the inflow of the saline western pacific water. The SSS during a summer monsoon ranges from 31.8 to 34.0 psu. Relatively low SSS during the summer monsoon is a result of the higher precipitation during summer months.

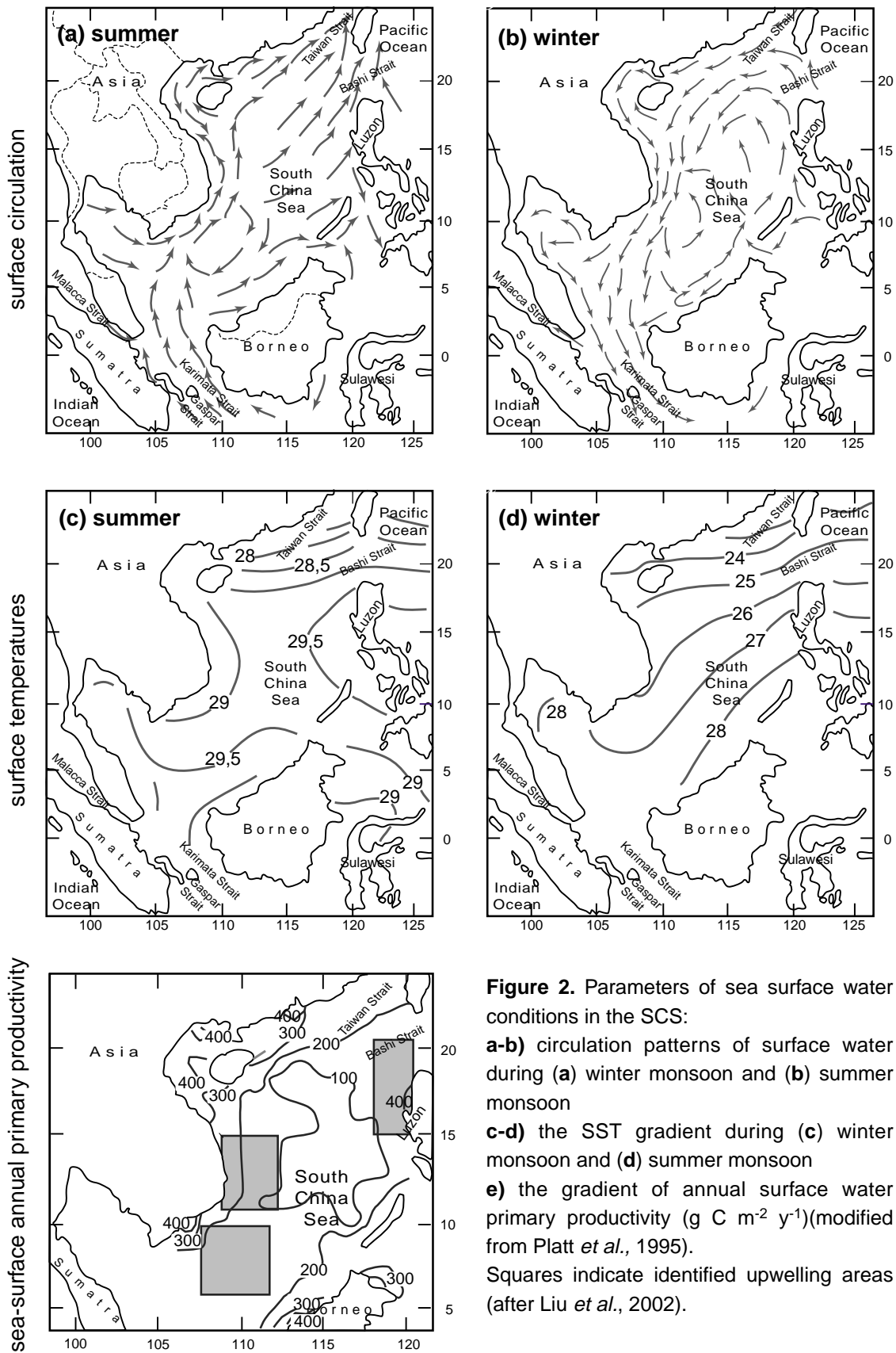


Figure 2. Parameters of sea surface water conditions in the SCS:
a-b) circulation patterns of surface water during **(a)** winter monsoon and **(b)** summer monsoon
c-d) the SST gradient during **(c)** winter monsoon and **(d)** summer monsoon
e) the gradient of annual surface water primary productivity ($\text{g C m}^{-2} \text{y}^{-1}$) (modified from Platt *et al.*, 1995). Squares indicate identified upwelling areas (after Liu *et al.*, 2002).

The annual primary productivity of the South China Sea is low ($<100 \text{ gCm}^{-1}\text{y}^{-1}$ in the central SCS)(Platt et al, 1995). High annual primary productivity ($>300 \text{ gCm}^{-1}\text{y}^{-1}$) is only observed in a narrow band along coasts (Figure 2e). Three seasonal upwelling areas are identified in the South China Sea. One meso-scale winter upwelling area is located at northwest of Luzon (Furio and Borja, 1998; Udarbe-Walker and Villanoy, 2001). This upwelling is not driven by local winds but by basin circulation (Shaw et al., 1996) and is characterized by obscure temperature gradient and offshore location of upwelling core (Udarbe-Walker and Villanoy, 2001). Another obscure winter upwelling was identified off Sunda Shelf (Liu et al, 2003). One summer upwelling is identified off southern Vietnam (Faughn, 1974; La Fond, 1963; La Fond, 1966; La Violette and Frontenac, 1967; Vo, 1995). This upwelling is induced by southwest wind.

2. METHODS AND MATERIALS

Thirty-six sediment samples covering spanning much of the SCS are collected using a multicorer or a giant box corer during R/V SONNE 95 and 140 cruises (Figure 1). Of thirty-six samples, two samples are from coastal area ($<50 \text{ m wd}$), twelve samples are from continental shelf ($50\text{-}200 \text{ m wd}$), eighteen samples are from continental slope ($201\text{-}3000 \text{ m wd}$) and two samples are from ocean basin ($>3001 \text{ m wd}$). Two major unsampled areas are off southern Philippines due to heavy turbidite activities and a part of ocean basin off southern Vietnam (no sample is available). The water-depth of the sites varies from 40 to 4309 m.

Characteristics of the surface sediments are described before samples are collected from the corers (Table 1). The sediments are sub-sampled carefully from the corers using a pre-cleaned spoon. The presence of relict sediments is reported on the shelf area near the mouth of the Mekong River (Emery, 1968). However, sediments are considered of recent origins due to the presence of Rose-Bengal stained (living) benthic foraminifera (Hess, 1998 and Szarek, 2001).

In the laboratory, sediments are freeze-dried. Three grams of dry sediments are treated with 10% HCl to dissolve carbonate sediments. During the HCl treatment, a tablet of *Lycopodium clavatum* is added to each sample in order to determine the concentration of palynomorphs (Stockmarr, 1971). The samples are then sieved and concentrated through a $5\mu\text{m}$ -mesh nylon sieve. During sieving, an ultrasonic treatment of less than 30 seconds is applied to the sediments in order to disaggregate clay contents of sediments. The residues are then treated with 40% HF to remove siliceous sediments. The samples are left in HF without agitation until all siliceous sediment is dissolved. The samples are again sieved through $5\mu\text{m}$ -nylon sieve with distilled water. The residues are mounted on slides with glycerin gel and sealed with paraffin. The use of

Table 1. List of samples used in this study with geographical and sedimentological characteristics.

Sample	Latitude	Longitude	Water Depth (m)	Sediment type	Sedi. rate (cm kyr-1)	Total cyst counted
18374-1	06.54.77 N	107.39.91 E	74.4	silty sand		29
18381-1	07.29.86 N	109.07.64 E	213.9	clayey silt		130
18384-1	07.46.33 N	109.48.68 E	829.1	clay		266
18386-1	07.54.09 N	110.07.85 E	380.4	sandy silt		66
18392-1	09.37.08 N	108.54.36 E	116.1	silty sand		130
18394-1	09.47.67 N	109.10.88 E	183	silty clay		327
18395-1	09.59.22 N	109.28.73 E	280.1	clayey silt		126
18397-1	12.14.71 N	109.19.91 E	44.5	silty clay		299
18401-1	13.30.12 N	109.33.67 E	134.2	clay		206
18404-1	13.41.11 N	109.27.02 E	169.1	clayey sand		61
18405-1	14.14.90 N	109.20.20 E	129.3	clay		267
18408-1	15.41.21 N	108.40.79 E	116.5	clay		253
18409-1	15.13.35 N	109.00.74 E	40	clay		264
18412-1	15.12.18 N	109.00.21 E	58.4	clayey silt sand and gravel		88
18413-1	14.44.81 N	109.17.61 E	52	clayey silt sand and gravel		40
18421-1	15.44.94 N	108.53.33 E	82.5	sandy silty clay		22
18426-1	16.44.40 N	108.27.77 E	92.9	sandy silt		135
18427-1	16.28.55 N	109.11.47 E	114.8	silty clay		123
18428-1	16.23.59 N	109.25.04 E	196.6	sandy silt		224
17925-1	19.51.2 N	119.02.8 E	2980	clay		49
17926-1	19.00.0 N	118.44.0 E	3761	clay		75
17927-1	17.15.0 N	119.27.2 E	2800	clay		69
17939-1	19.58.2 N	117.27.3 E	2473	clay	33.33	219
17942-1	19.20.0 N	113.12.1 E	329	sandy silt		231
17945-1	18.07.6 N	113.46.6 E	2404	clay	10	94
17949-1	17.20.9 N	115.10.1 E	2195	clay	6.67	130
17950-1	16.05.6 N	112.53.8 E	1868	sandy silt	6.67	180
17952-1	16.40.0 N	114.28.4 E	2340	clay	5	114
17953-1	14.36.2 N	115.07.2 E	4309	clay		94
17954-1	14.45.5 N	111.31.6 E	1517	clay	6.67	117
17958-1	11.37.1 N	115.04.9 E	2581	clay	15	102
17959-1	11.08.3 N	115.17.2 E	1957	clay	8.33	203
17962-1	07.10.9 N	112.04.9 E	1970	clay	6.67	385
17965-1	06.09.4 N	112.33.1 E	889	silty clay		317

oxidizing agents and hot acid are avoided since these can significantly degrade certain palynomorph groups (Dale, 1976).

Major types of palynomorphs (dinoflagellate cyst, pollen, spore, tintinomorphs and algae) are identified and counted using a light microscope with magnifications of x400 and x800. Organic-walled dinoflagellate cysts are identified up to a species level in accordance with the classifications of Lentin and Williams (1993) and Rochon et al. (1999). *Brigantedinium* spp. was identified only up to a genus level because many *Brigantedinium* cysts show poor cyst orientations that make positive identification of

their archeopyle difficult. Some *Spiniferites*, which are difficult to identified, are counted as *Spiniferites* spp. Pre-excysted Protoperidinioid cysts was not identified to the species level and was counted as a whole. The counts are made until minimum of 70 cysts or 6 slides.

2.2 STATISTICAL ANALYSIS

A Correspondence Analysis (CA) is used to analyze dinoflagellate cyst assemblages and to assist interpreting possible environmental/taphonomical factors controlling distributions. A CA is run using the CANOCO software (ter Braak and Smilauer, 1998). A CA is chosen from various multivariate statistical analyses (e.g. Principal Component Analysis, Redundancy Analysis, Canonical Variety Analysis) because of the assumption that species respond unimodally to the changing environmental parameters (Hill and Gauch, 1980; Jungman et al., 1995). Detailed descriptions of CA are available in Jungman et al. (1995). Only samples with greater than 70 cysts counted (26 samples) are included in the analysis. Concentrations of dinoflagellate cyst species are used as input data. Rare species are down-weighted using a built-in feature of the program in order to avoid over-influencing the sensitivities of the CA (ter Braak and Smilauer, 1998).

3. RESULTS

3.1 DISTRIBUTION PATTERNS OF DINOFLAGELLATE CYSTS

A total of forty different taxa of dinoflagellate cysts are identified from thirty-six samples (Table 2). Twenty-three taxa belong to the gonyaulacoid group, eleven taxa belong to the protoperidinioid group, and one taxon of each belonging to the tuberculodinioid, calciodinellid and gymnodinellid groups. The concentrations of dinoflagellate cysts vary from 39.5 to 1828.2 cysts g^{-1} (dry sediments)(Figure 3). The lowest value is observed on the shelf off mid-Vietnam at the water-depth of 82.5 m. The two highest concentrations are found in sites near coastal area (44 and 44.5 m wd). Cysts of the gonyaulacoid group commonly dominate the assemblages in the southern SCS (Figure 4). The proportion of the protoperidinioid group increases northward (Figure 4).

The calciodinellid group (*Scripsiella* spp.) is commonly present on the slope and basin and is rare on the shelf. The tuberculodinioid group (*Tuberculodinium vancampoe*) and the gymnodinioid group (*Pheopolykrikos hartmannii*) occur on the shelf with small relative abundance.

The gonyaulacoid group is characterized by high relative and absolute abundance of genus *Spiniferites* species (*Spiniferites bulloideus*, *Spiniferites ramosus*,

Table 2. List of dinoflagellate cysts identified in the surface sediments from the South China Sea

GONYAULACALES

Gonyalulacaceae

Gonyaulacoid Group

Achomosphaera spp.

Impagidinium aculeatum (Wall) Lentin & Williams 1981

Impagidinium paradoxum (Wall) Stover & Evitt 1978

Impagidinium patulum (Wall) Stover & Evitt 1978

Impagidinium spahericum (Wall) Lentin & Williams
1981

Impagidinium striatum (Wall) Stover & Evitt 1978

Impagidinium spp.

Lingulodinium machaerophorum (long processes)
(Deflandre & Cookson) Wall 1967

Lingulodinium machaerophorum (short processes)
(Deflandre & Cookson) Wall 1967

Nematosphaeropsis labyrinthus (Ostenfeld) Reid 1974

Protoceratium reticulatum (Claparede & Lachmann)
Buetchli

Operculodinium israelianum (Rossignol) Wall 1967

Operculodinium janduchenei Head et al 1989

Operculodinium longispinigerum Matsuoka 1983

Spiniferites bulloideus (Deflandre & Cookson) Sarjeant
1970

Spiniferites bentori (Rossignol) Wall & Dale 1970

Spiniferites delicatus Reid 1974

Spiniferites hypercanthus (Deflandre & Cookson)
Cookson & Eisenack 1974

Spiniferites ramosus (Rossignol) Mantel 1854

Spiniferites mirabilis (Rossignol) Sarjeant 1970

Spiniferites membranaceus (Rossignol) Sarjeant 1970

Spiniferites spp.

Tectatodinium spp.

Pyrophacaceae

Tuberculodinioid Group

Tuberculodinium vancampoae (Rossignol) Wall 1967

GYMNODINIALES

Gymnodinellid Group

Cyst of *Pheopolykrikos hartmannii*

PERIDINIALES

Protopteridiniaceae

Protopteridinioid Group

Brigantedinium spp.

Selenopemphix nephroides Benedek 1972

Selenopemphix quanta (Bradford) Matsuoka 1985

Stelladinium stellatum (Wall & Dale) Reid 1977

Trinovantedinium capitatum (Bradford) Bujak & Davies
1983

Votadinium calvum Reid 1977

Votadinium spinosa Reid 1977

Lejeunecysta sabrina (Reid) Bujak 1984

Pre-excysted protopteridinioids

Polysphaeridium zoharyi (Rossignol) Bujak et al 1980

Quinquecuspis concreta (Reid) Harland 1977

Calciodinellaceae

Calciodinellid Group

Scrippsiella spp.

Spiniferites hyperacanthus, *Spiniferites membranaceus* and *Spiniferites mirabilis*), *Protoceratium reticulatum*, *Operculodinium israelianum*, *Impagidinium* sp., *Lingulodinium machaerophorum* (short & long processes) in the SCS. *Spiniferites* sp.

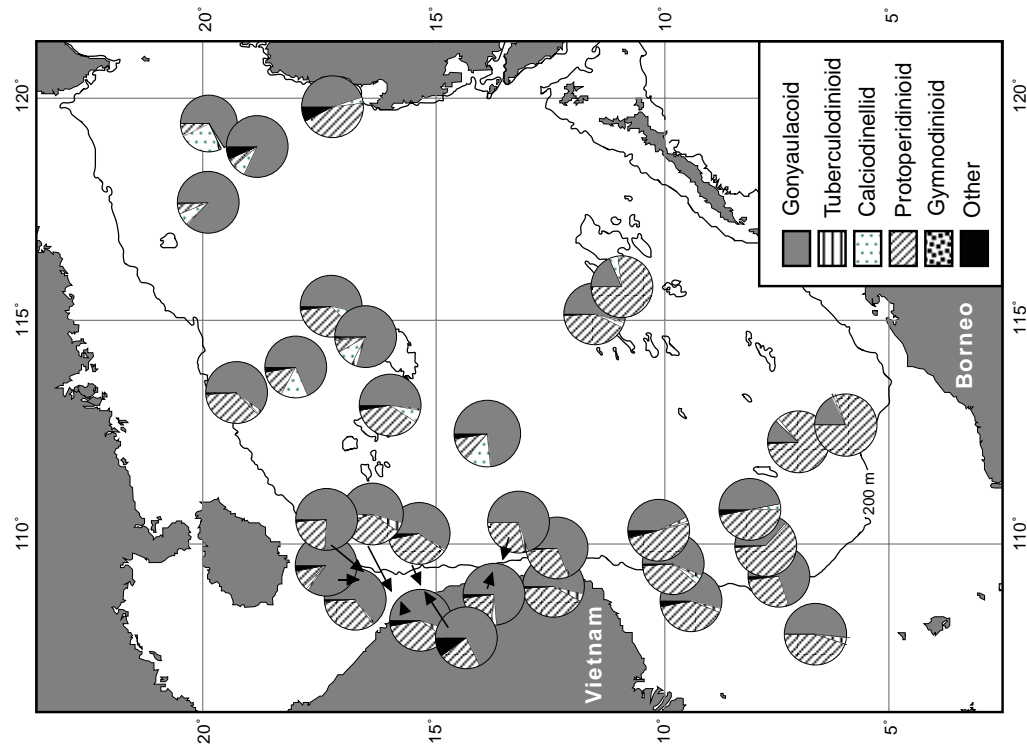


Figure 4. Relative abundances of dinoflagellate cyst groups in the surface sediments from the SCS.

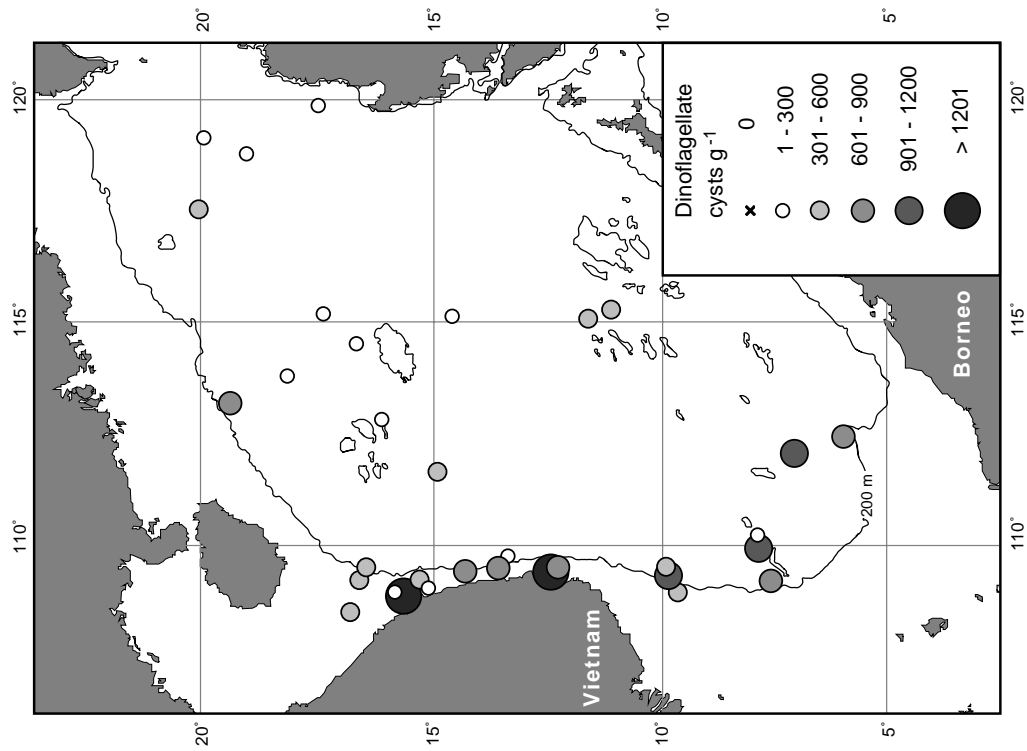


Figure 3. Concentration of dinoflagellate cysts (cysts g⁻¹ dry sediment) in the surface sediments from the SCS.

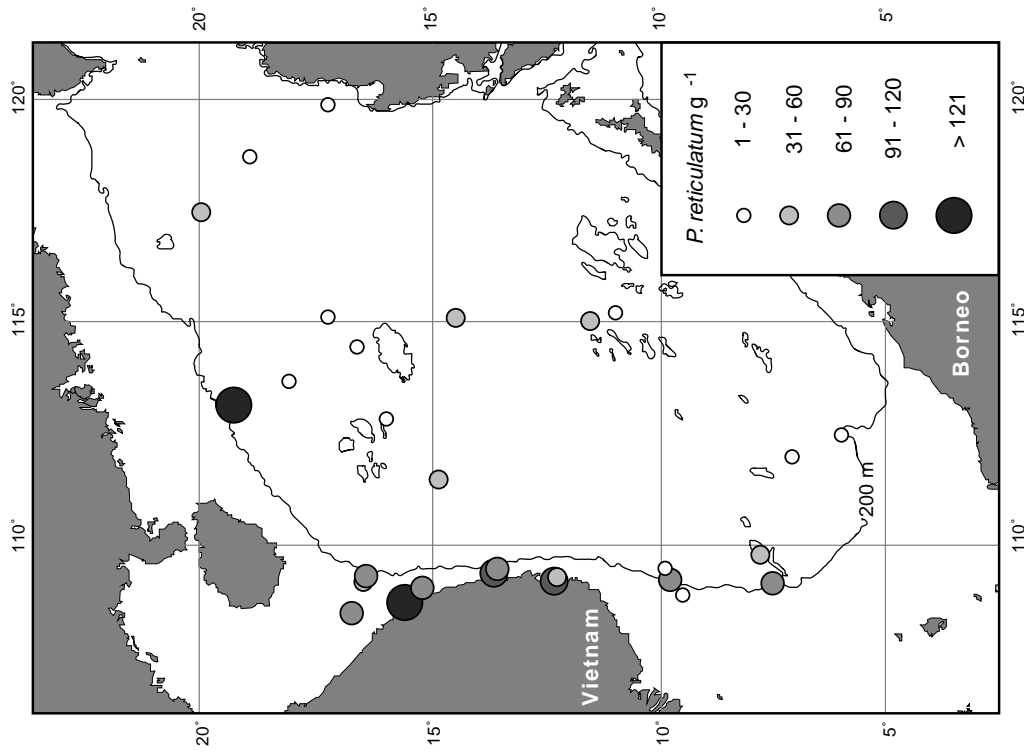


Figure 5b. Distribution map of *Protocestratium reticulatum*.

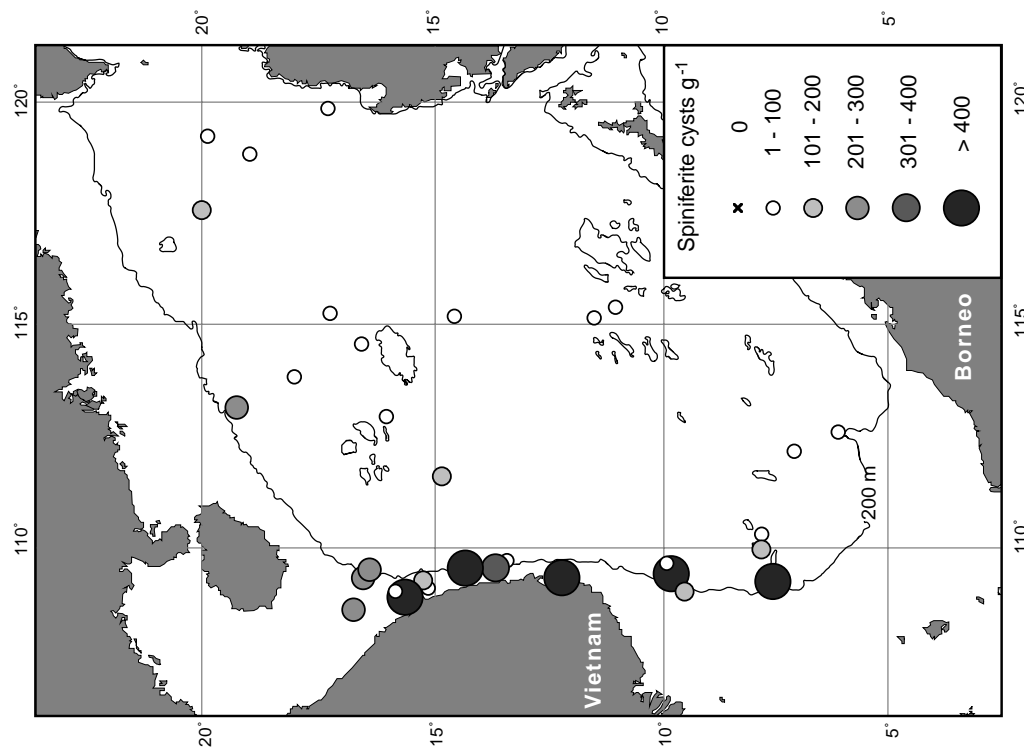


Figure 5a. Distribution map of *Spiniferites* species combined.

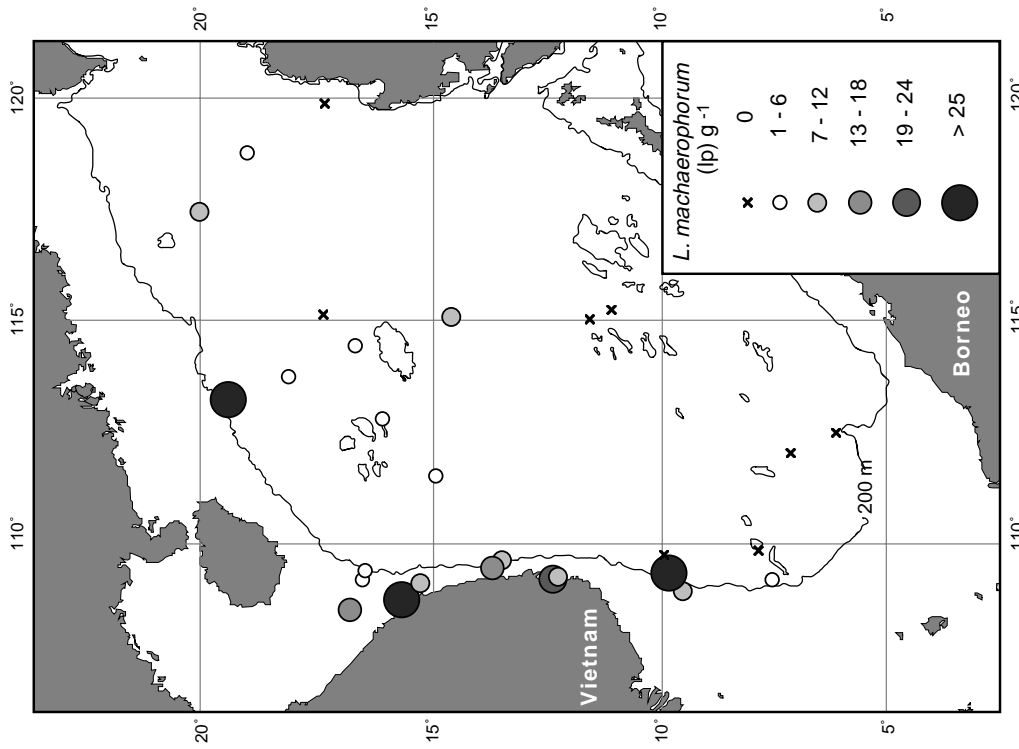


Figure 5d. Distribution map of *Lingulodinium machaerophorum* (long processes).

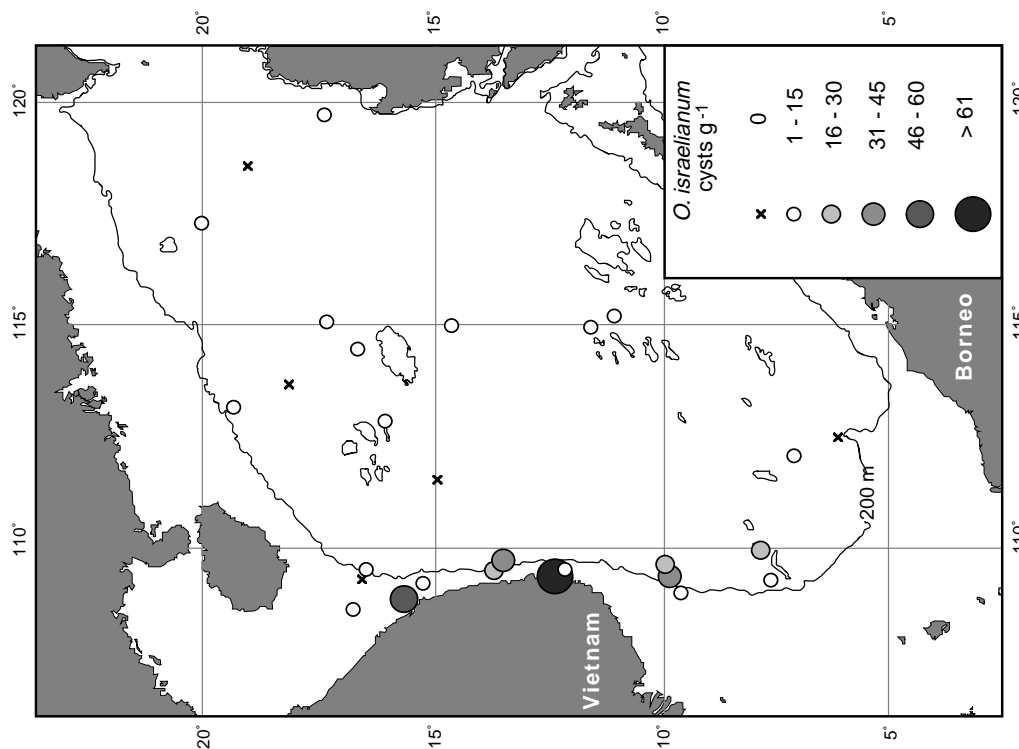


Figure 5c. Distribution map of *Operculodinium israelianum*.

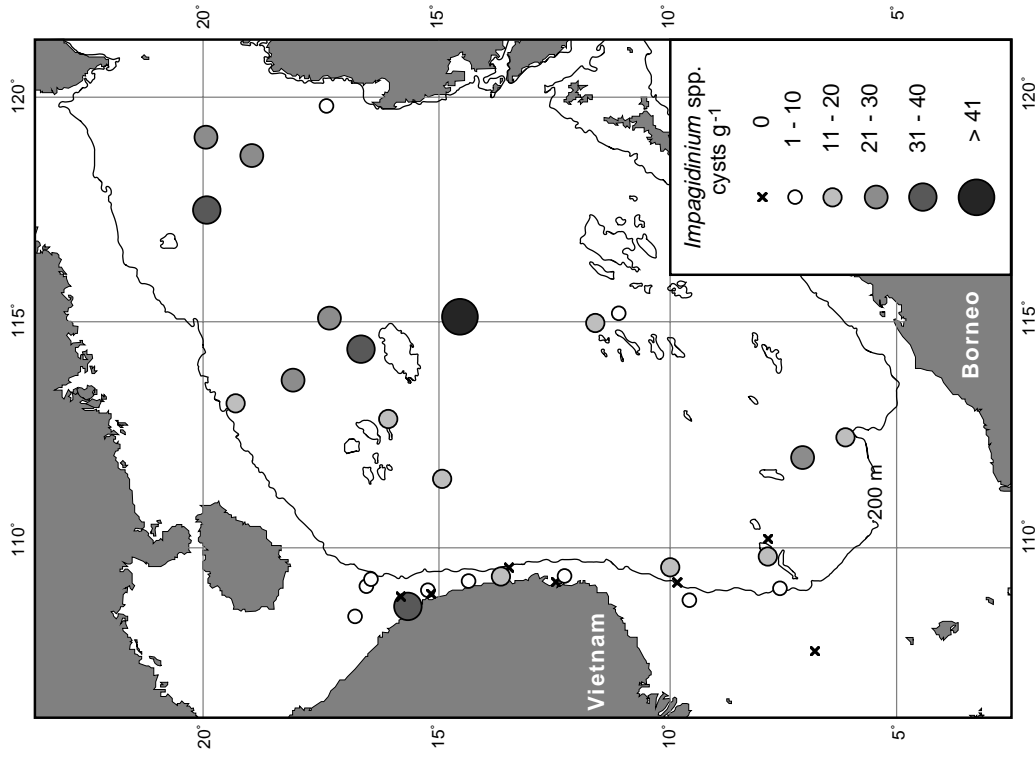


Figure 5f. Distribution map of *Impagidinium* species combined.

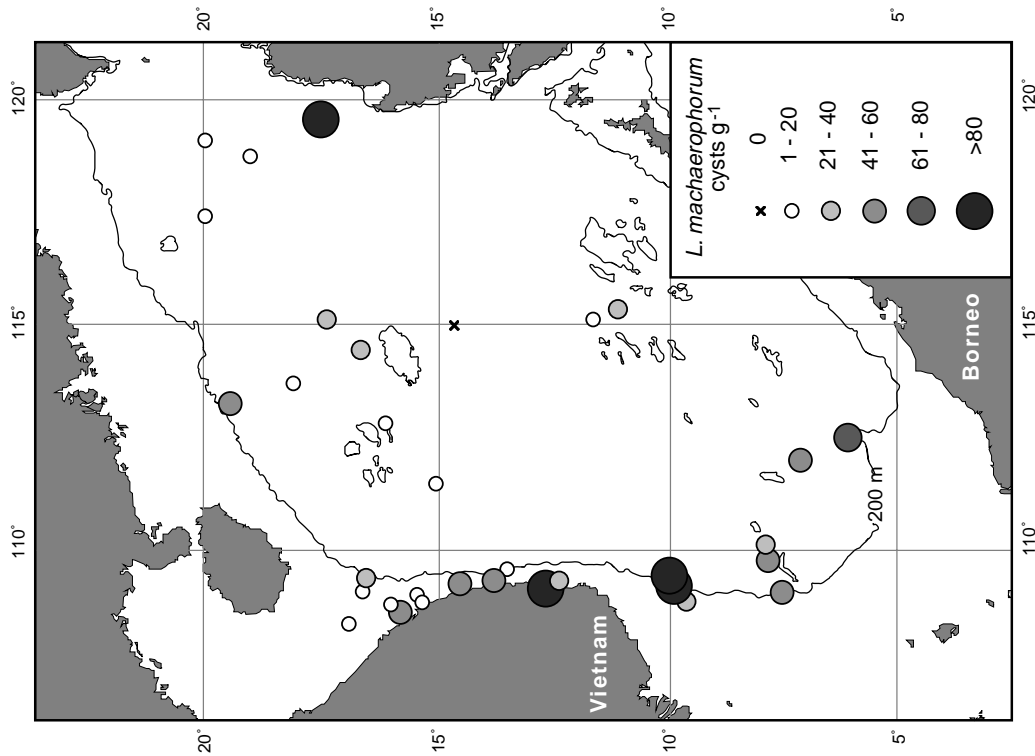


Figure 5e. Distribution map of *Lingulodinium machaerophorum* (short processes).

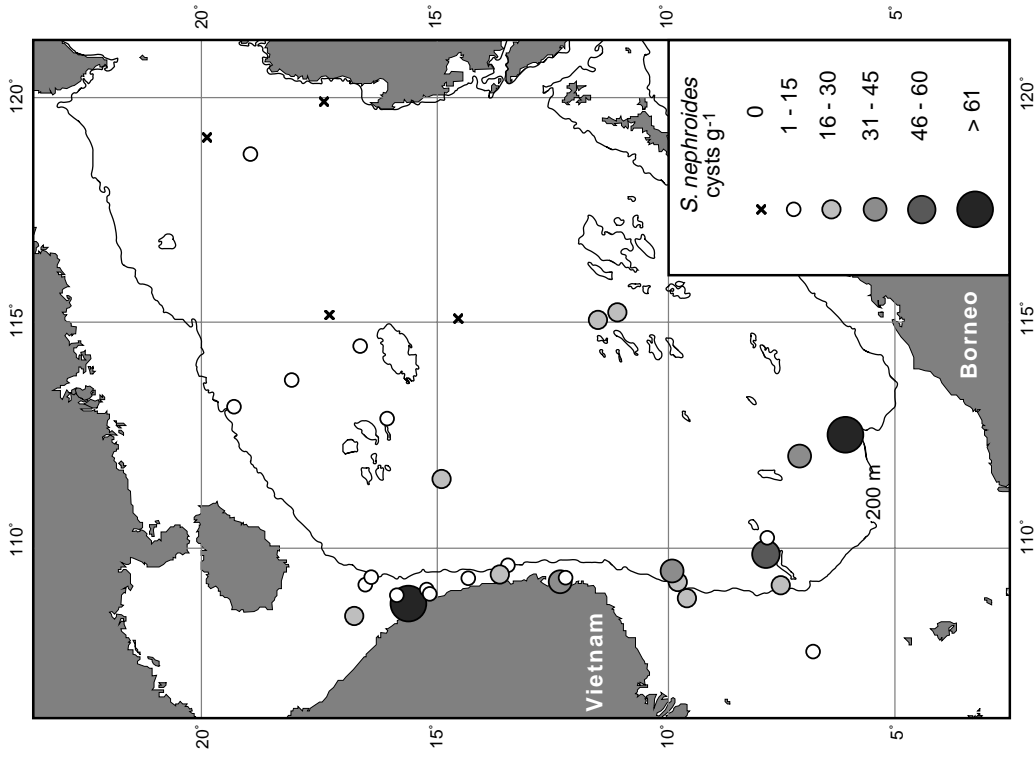


Figure 5h. Distribution map of *Selenopemphix nephroides*.

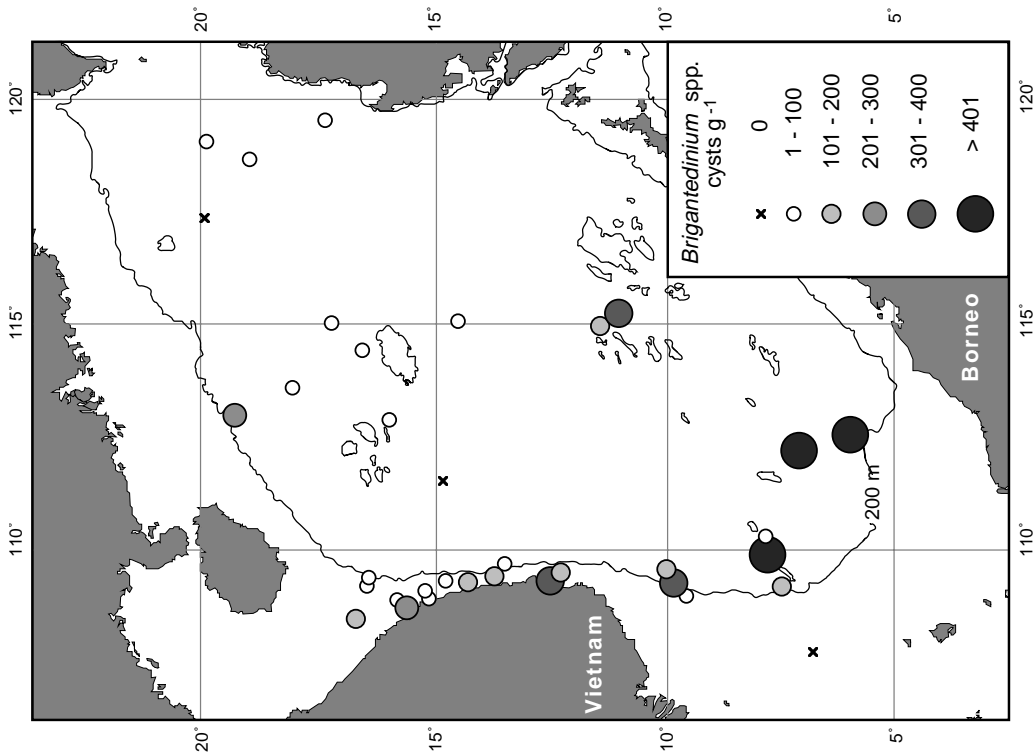


Figure 5g. Distribution map of *Brigantedinium* species combined (including round brown cysts).

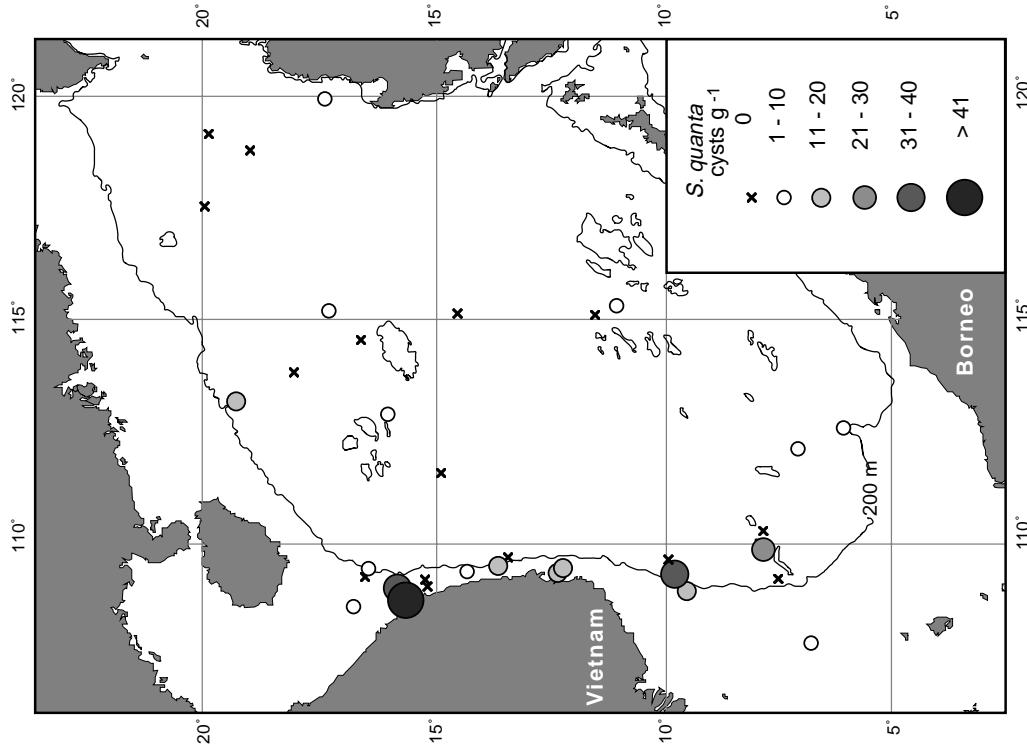


Figure 5j. Distribution map of *Selenopemphix quanta*.

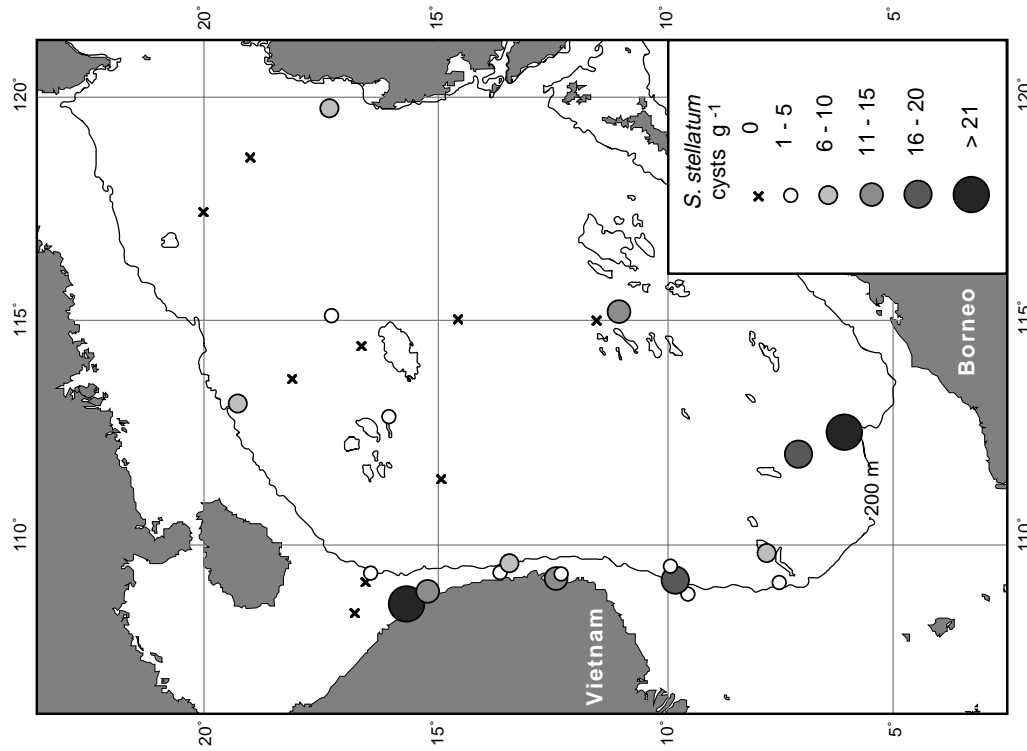


Figure 5i. Distribution map of *Stelladinium stellatum*.

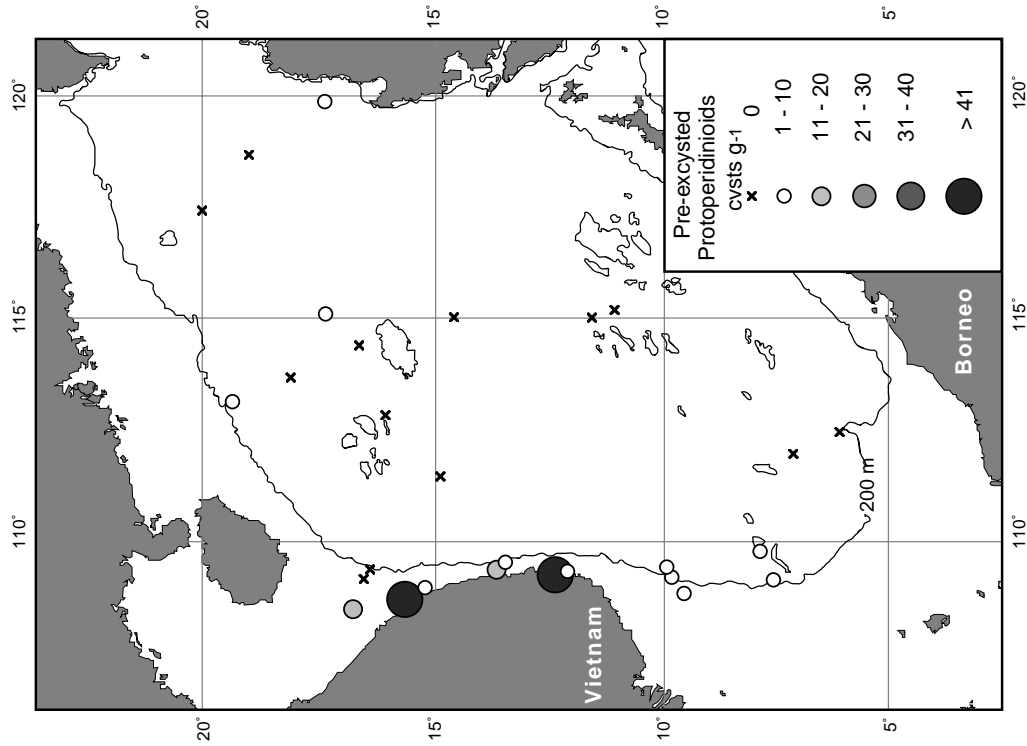


Figure 5i. Distribution map of pre-encysted Proto-peridinioid.

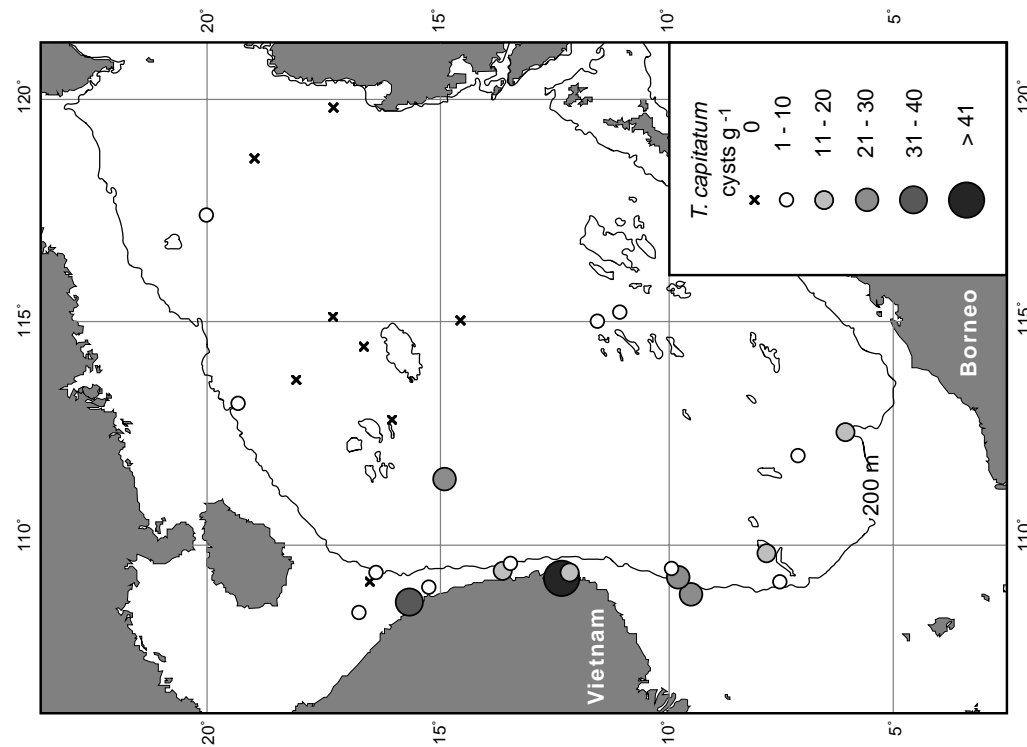


Figure 5k. Distribution map of *Trinovantedinium capitatum*.

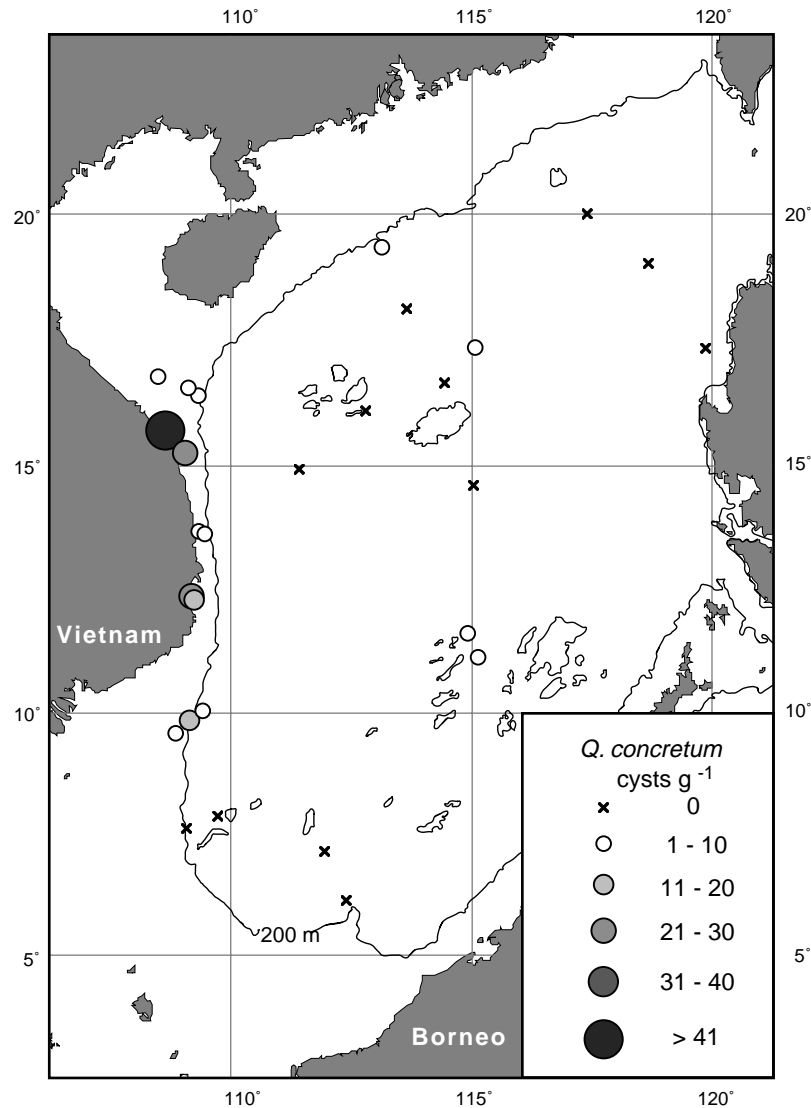


Figure 5m. Distribution map of *Quinquecuspis concretum*.

and *P. reticulatum* occur at every site. The concentrations of *Spiniferites* species and *P. reticulatum* vary from 12.1 to 564.7 cysts g⁻¹ (Figure 5a) and 2.5 to 172.5 cysts g⁻¹ (Figure 5b) respectively. The general trend shows that high concentrations of these taxa are recorded on the Vietnamese Shelf and its continental slope. *O. israelianum* (Figure 5c) and *L. machaerophorum* (Figure 5de) occur commonly in the SCS, and these taxa also mirror the distribution patterns of *Spiniferites* species and *P. reticulatum* with the two highest concentrations in the coastal area.

Impagidinium species occurs at most sites with low concentrations (<70.1 cysts g⁻¹) (Figure 5f). To the contrary to other taxa in the protoperidinioid group, high concentrations are observed on the slope and the oceanic basin. The highest

concentration is found at the deepest site (17953) situated at the center of the SCS.

The protoperidinioid group is characterized by consistent occurrences of *Brigantedinium* spp, *Selenopemphix nephroid*, *Selenopemphix quanta*, *Trivantedinium capitatum*, *Stelladinium stellatum* and restricted occurrences of *Quinquecuspis concreta*, *Votadinium spinosum* and pre-excysted protoperidinioids in the SCS. The highest concentrations of the protoperidinioid cysts are observed in the coastal area (<50 m wd) and on the continental slope sites. At four sites in the deepest area in the SCS, protoperidinioid cysts were not observed.

Brigantedinium spp. occurs at every site but two sites. It dominates the protoperidinioid group with high relative and absolute abundance (Figure 5g). The highest concentrations are found at the most southern sites of the SCS. High concentrations of *Brigantedinium* spp. are also observed in the coastal area. *S. nephroid* occurs commonly in the SCS (Figure 5h). High concentrations of *S. nephroid* are observed on the Vietnamese Shelf and its continental slope. The concentrations decrease towards the center of the basin. *S. stellatum* shows also similar distribution pattern with *S. nephroid* with lower concentrations (Figure 5i). *S. quanta* and *T. capitatum* rarely occur at sites with high water depth in the northern SCS (Figure 5j & k). The highest concentrations of these taxa are observed in the coastal area. Pre-excysted protoperidinioids and *Q. concret* occur mainly on the Vietnamese Shelf and its continental slope (Figure 5l & m). Highest concentrations of these taxa are observed in the coastal area and the values commonly decrease with increasing water depth.

3.2 OTHER PALYNOMORPHS

Pollen: The concentrations of pollen vary from 65.3 to 6026.2 grains g⁻¹. High concentrations of pollen (>500 grains g⁻¹) are found in the proximity of the Vietnamese and Philippines coastal areas (Figure 6a). Pollen assemblages are dominated by high relative and absolute abundance of Pinaceae (*Pinus*, *Picea* and *Abies*), *Dacrydium* and *Podocarpus*. High concentrations of *pinus* (>2001 grains g⁻¹) and *Graminae* (>100 grains g⁻¹) are observed in the proximity of Vietnamese and Phillipines coast (Figure 6b & c). *Dacrydium* and *Podocarpus* occur at most sites. High concentrations (>41 grains g⁻¹ and >31 grains g⁻¹ respectively) are found only on the Vietnamese Shelf (Figure 6d & 6e).

Spore: The concentrations of spore vary from 173.72 to 7521.23 spore g⁻¹. In general, high concentrations (>1001 grains g⁻¹) are observed in the northern half of the SCS. The highest concentrations are observed in the most proximal areas to the land (Figure 9).

Tintinomorphs: The concentrations of tintinomorph vary from 81.4 to 8314.9

tintinomorphs g^{-1} . High concentrations of tintinomorphs (< 901 tintinomorphs g^{-1}) are observed in the shelf to slope area along the Vietnamese coasts (see Fig. 7).

Benthic foraminiferal linings: The concentrations of benthic foraminiferal linings vary from 102.37 to 14324.98 linings g^{-1} . High concentrations (>6001 lining g^{-1}) are found on the shelf and slope area along the Vietnamese coasts (Figure 8).

3.3 RESULTS OF CORRESPONDENCE ANALYSE

A CA of active 564 clusters (26 samples with 34 different taxa of dinoflagellate cysts) shows that the variances of clusters can be explained mainly with the first two CA axes. The first axis (x-axis) explains 27.6 % of total variances. Only first axis is regarded as significant in this study because number of total cyst counted were low at some sites (70 cysts) and reliability of lower axes are questionable. Two ordination diagrams are generated and displayed in figure 10 a & b. The first ordination diagram (Figure 10a) shows that most sites situated on the Vietnamese Shelf are located in the lower half of the ordination diagrams and most sites situated in the central to the northern SCS basin are in the upper right part of the ordination diagram. Two sites on the slope off north-western Sunda Shelf, two sites situated in the vicinity of the Spratly Islands and one site in the vicinity of the Paracel Islands are in the upper left part of the ordination diagram. The second ordination diagram shows that species with high absolute abundance for the Vietnamese Shelf are situated in the lower half of the diagram. The taxa with high absolute abundance in the central to northern SCS basin are situated in the upper right part of the diagram. The taxa with high absolute abundance in the slope off northwestern Sunda Shelf are situated in the upper left part of the diagram.

On the basis of CA results, dinoflagellate cyst taxa are divided into three groups (see Fig. 10 b). Group I consists of *Lingulodinium* spp. (short processes), *Brigantedinium* sp., *O. israelianum*, *S. stellatum*, *S. quanta*, *Q. concreta*, pre-excysted protoperidinioids, *V. carvum*, *V. spinosum* and *S. nephroides*. Group II contains the highest numbers of taxa and consists of all taxa of genus *Spiniferites*, *P. reticulatum*, *T. vancampoae*, *T. capitatum*, *Impagidinium* spp., *O. longispigerum*, *Lejeunecysta sabrina* and *L. machaerophorum*. Group III consists of *I. aculeatum*, *I. striatum*, *P. zoharyi*, *O. janduchenei*, *I. paradoxum*, *I. patulum*, *I. sphaericum*, *N. labyrinthus* and *Scripsiella* spp.

Figure 11a shows the 1st CA scores for each site. Figure 11b and 11c shows the relations of 1st CA scores to measured distances from closest landmass and to annual primary productivity. Figure 11b shows that the scores correlate roughly with the distances ($R=0.606$) and only sites 17942 and 17949 are widely off from the linear

regression line. Figure 11c shows also rough correlation between the scores and

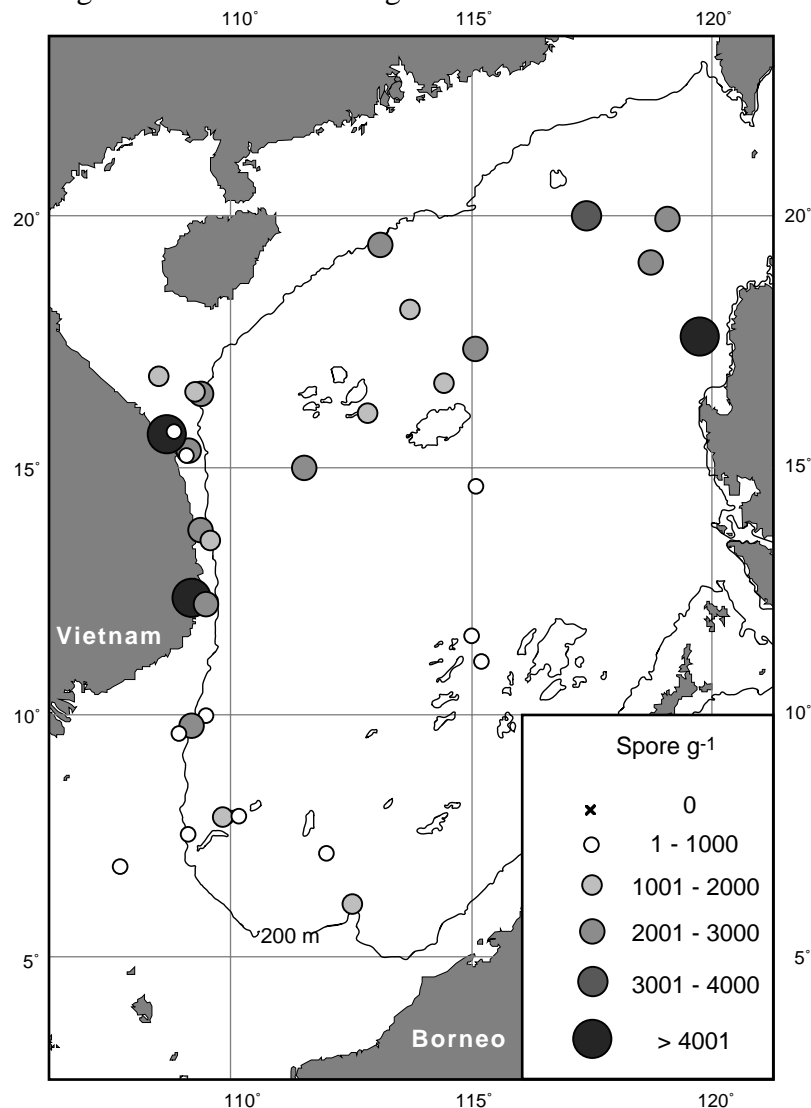


Figure 9. Distribution map of spores.

estimated primary productivity. The sites with low primary productivity near landmass (e.g. sites 17950, 17958, 17959 and 17927) are found far from the regression line.

4. DISCUSSION

4.1 NON-ECOLOGICAL FACTORS CONTROLLING DINOFLAGELLATE CYST DISTRIBUTIONS

Distribution patterns of dinoflagellate cysts can be altered by non-ecological factors such as transport, preservation and concentrations of dinoflagellate cysts and other palynomorphs may be susceptible to dilution process. Thus, observed cyst distribution patterns may not be totally depending on environmental factors.

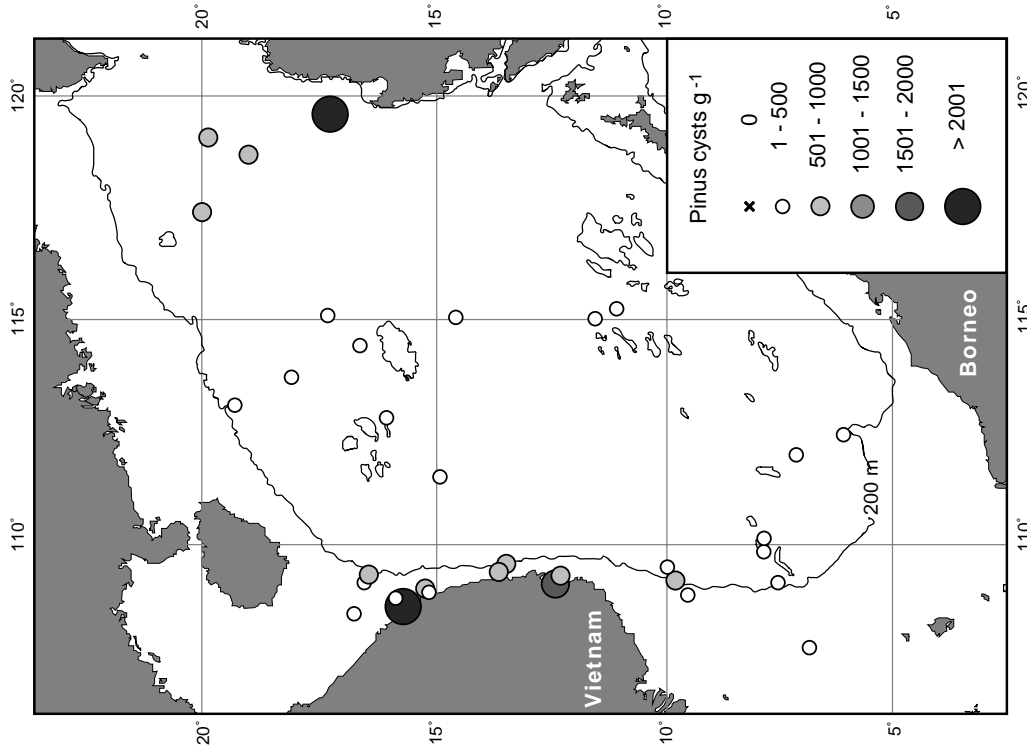


Figure 6b. Distribution map of Pinus cysts.

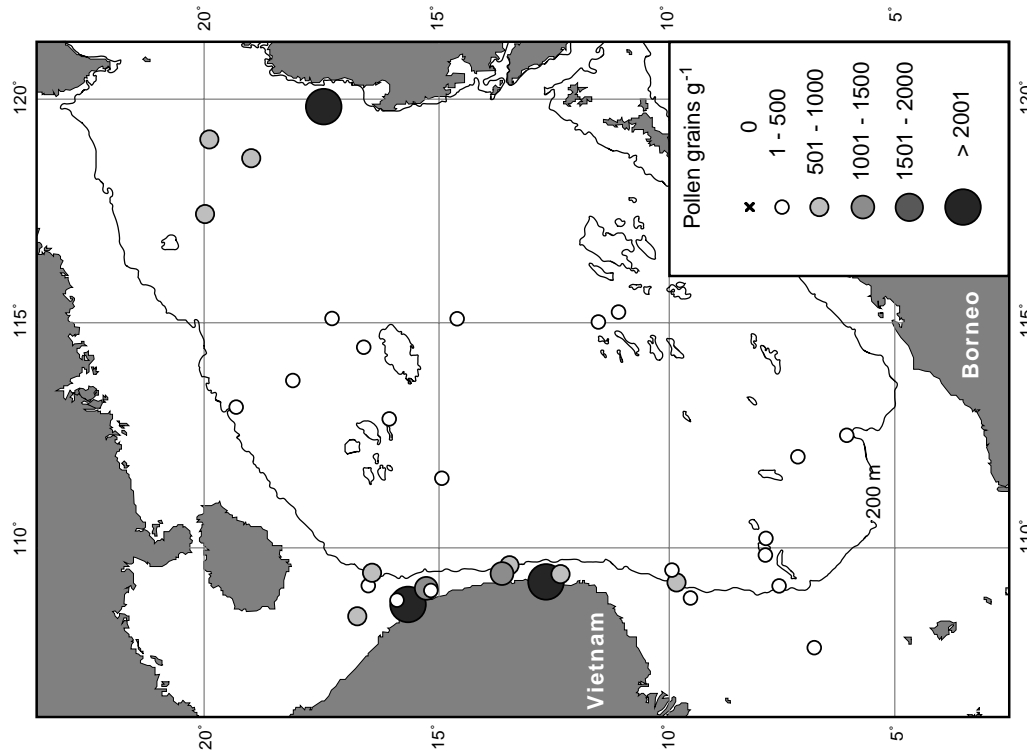


Figure 6a. Distribution map of pollen.

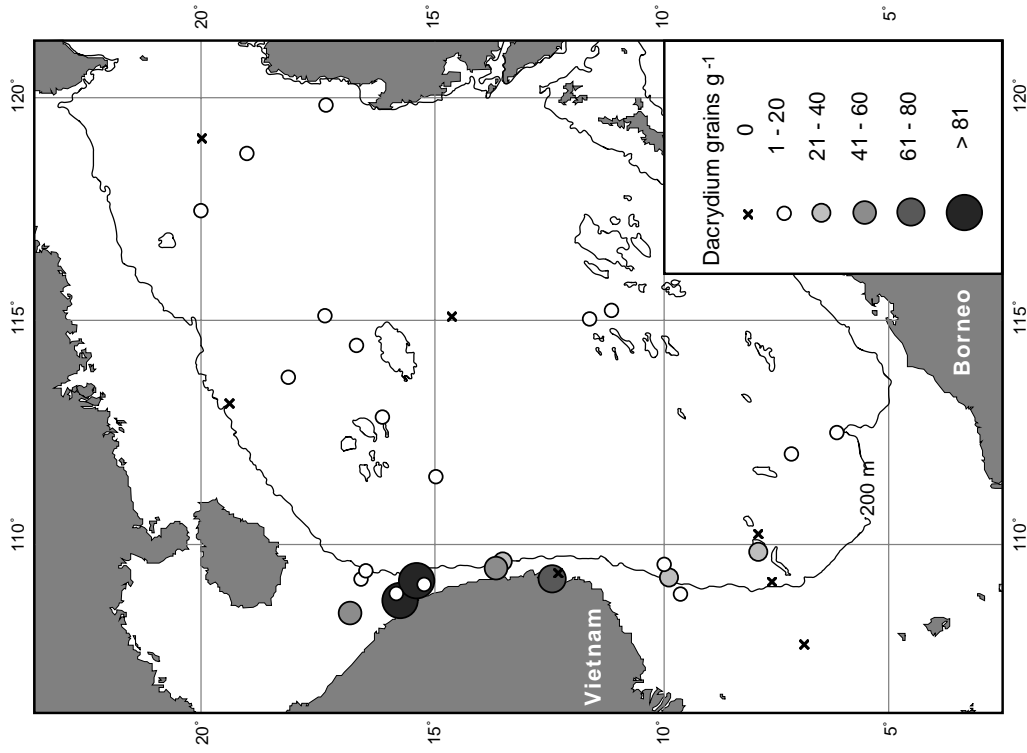


Figure 6d. Distribution map of Dactyidium.

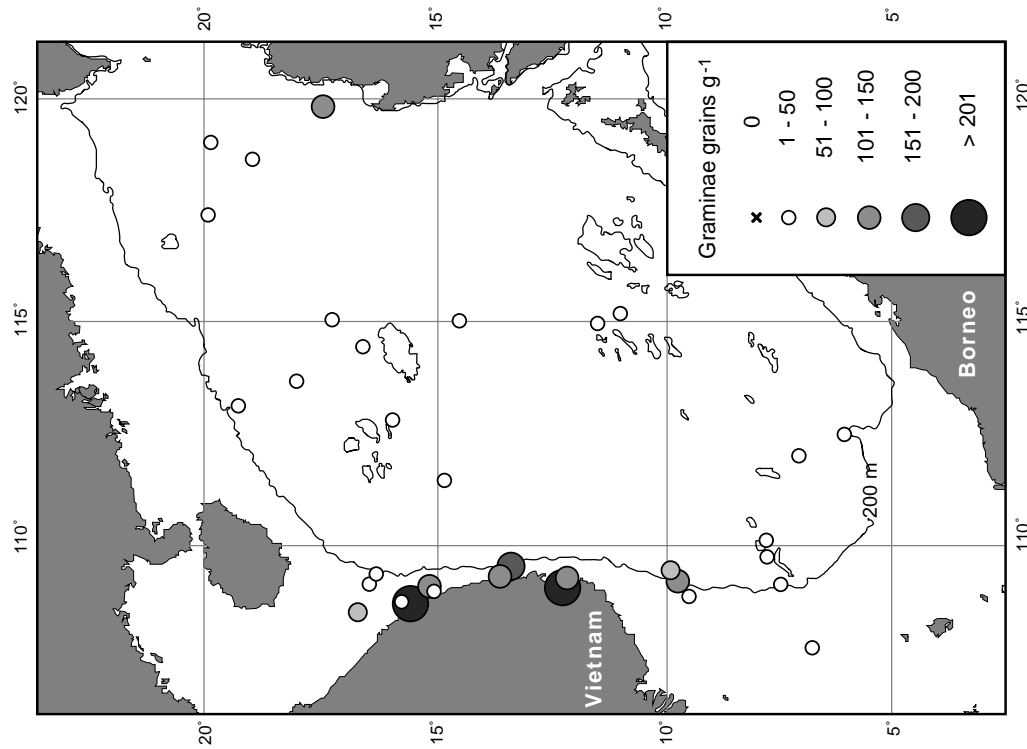


Figure 6c. Distribution map of Graminae.

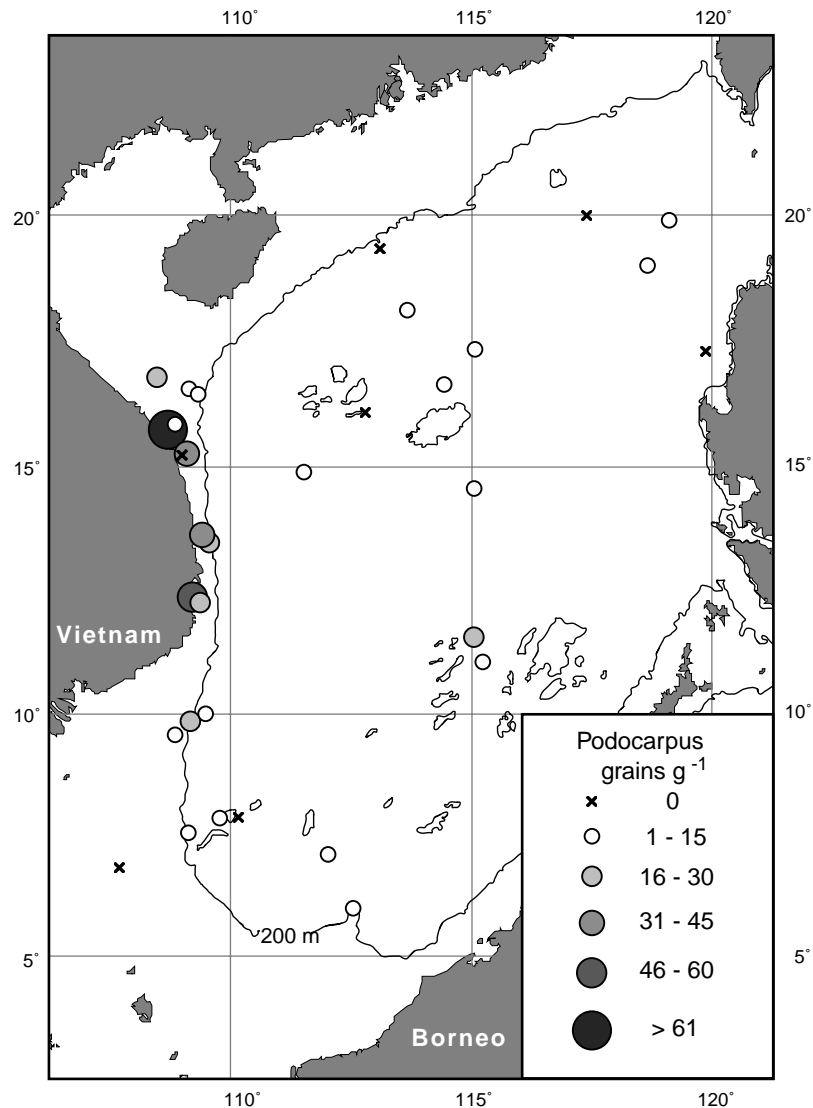


Figure 6e. Distribution map of Podocarpus.

Transport: As discussed in Chapter 2, winnowing processes play major roles on the distribution patterns of cysts on the Sunda Shelf. The influences of cyst transport on the distribution patterns can be inferred from the distribution patterns of pre-excysted protoperidinioids in this study. In dinoflagellate life cycles, pre-excysted dinoflagellate cysts (resting cysts) settle on the sea floor after encystment in water column. Then, excystment occurs after a certain period of cyst dormancy (Fensome et al, 1996). Therefore, distribution patterns of pre-excysted protoperidinioids probably represent better distribution patterns of dinoflagellates in the motile stage than of excysted dinoflagellate cysts. Thus, if excysted protoperidinioids are not biased by lateral transport processes, occurrence of both excysted and pre-excysted protoperidinioids should coincide. In the studied area, pre-excysted protoperidinioids are commonly

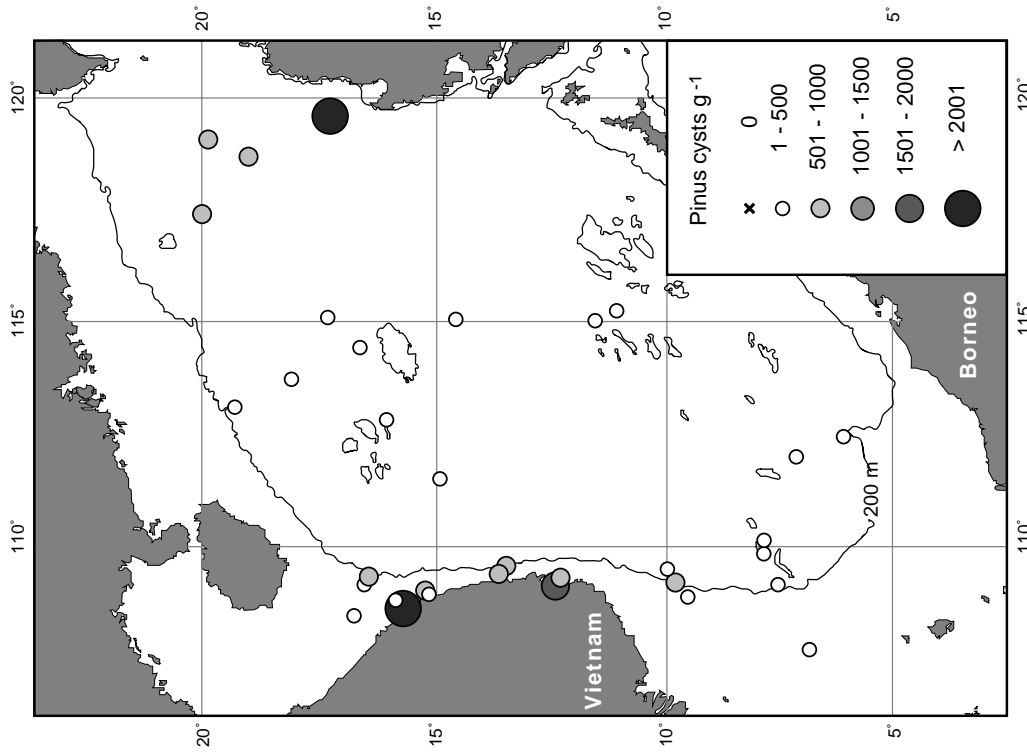


Figure 6b. Distribution map of Pinus cysts.

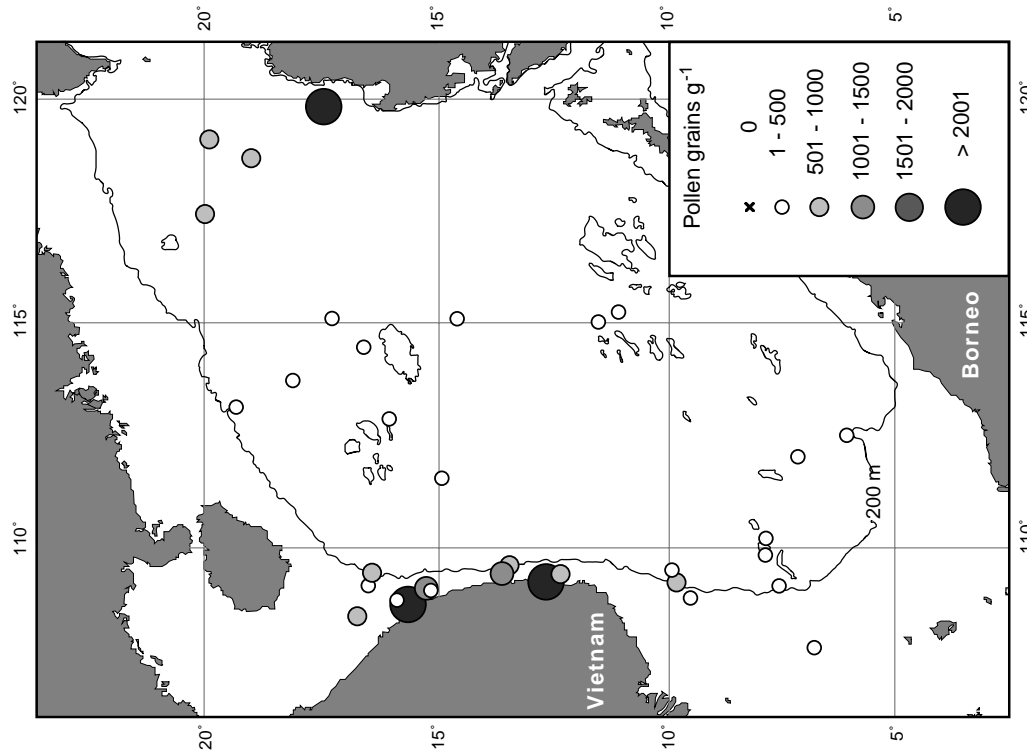


Figure 6a. Distribution map of pollen.

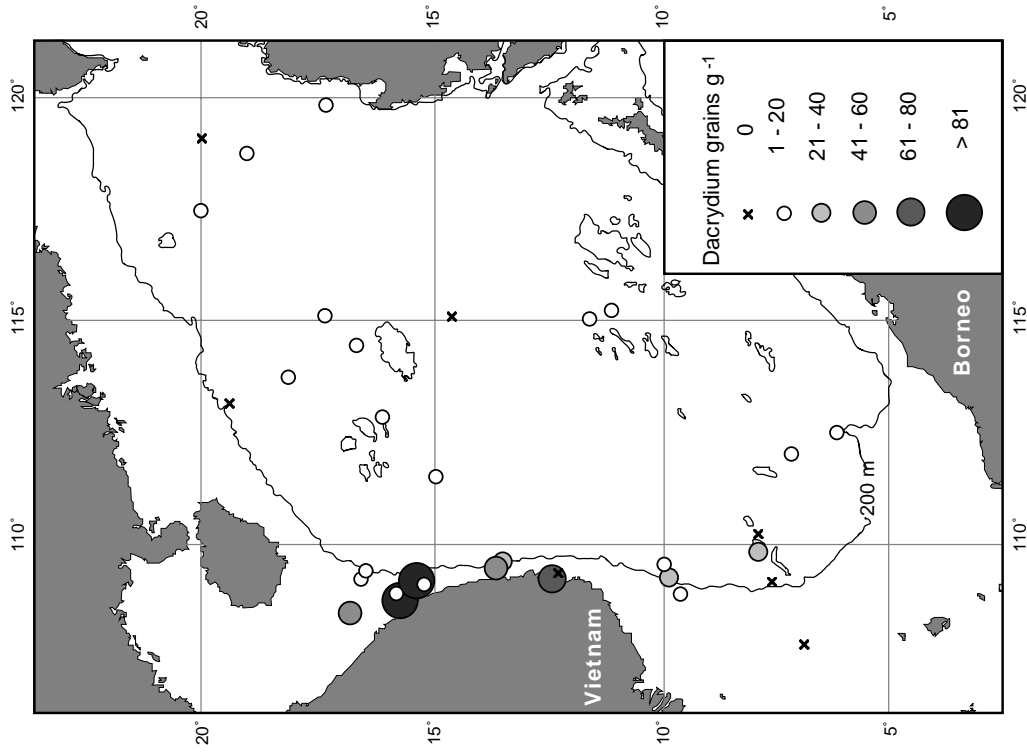


Figure 6d. Distribution map of Dactyidium.

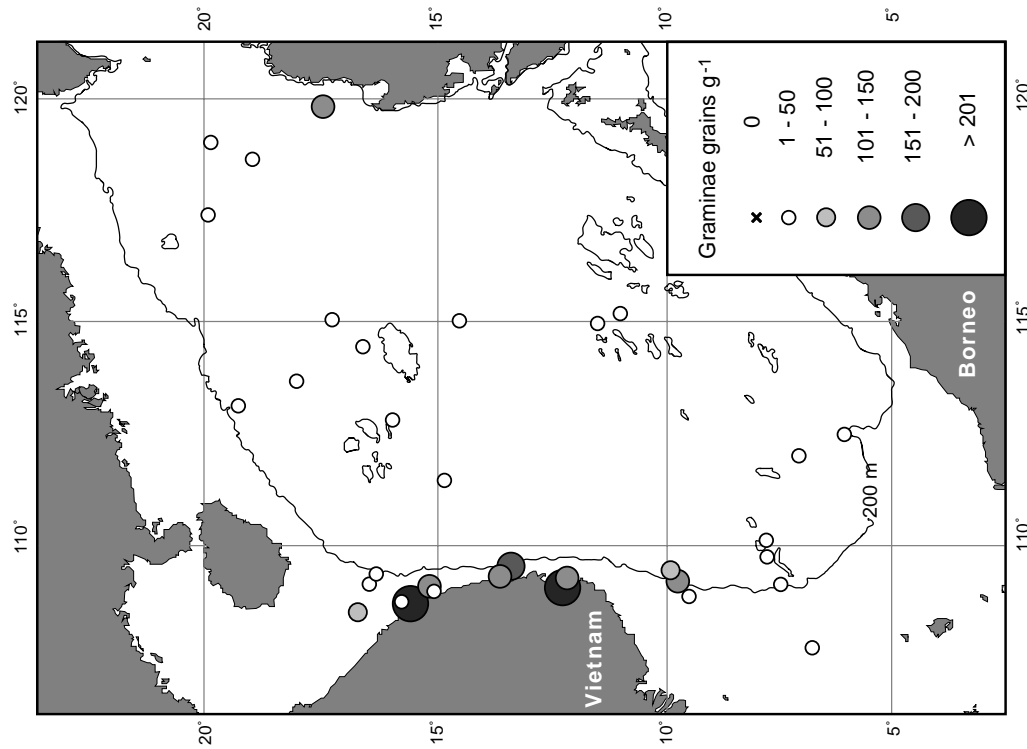


Figure 6c. Distribution map of Graminae.

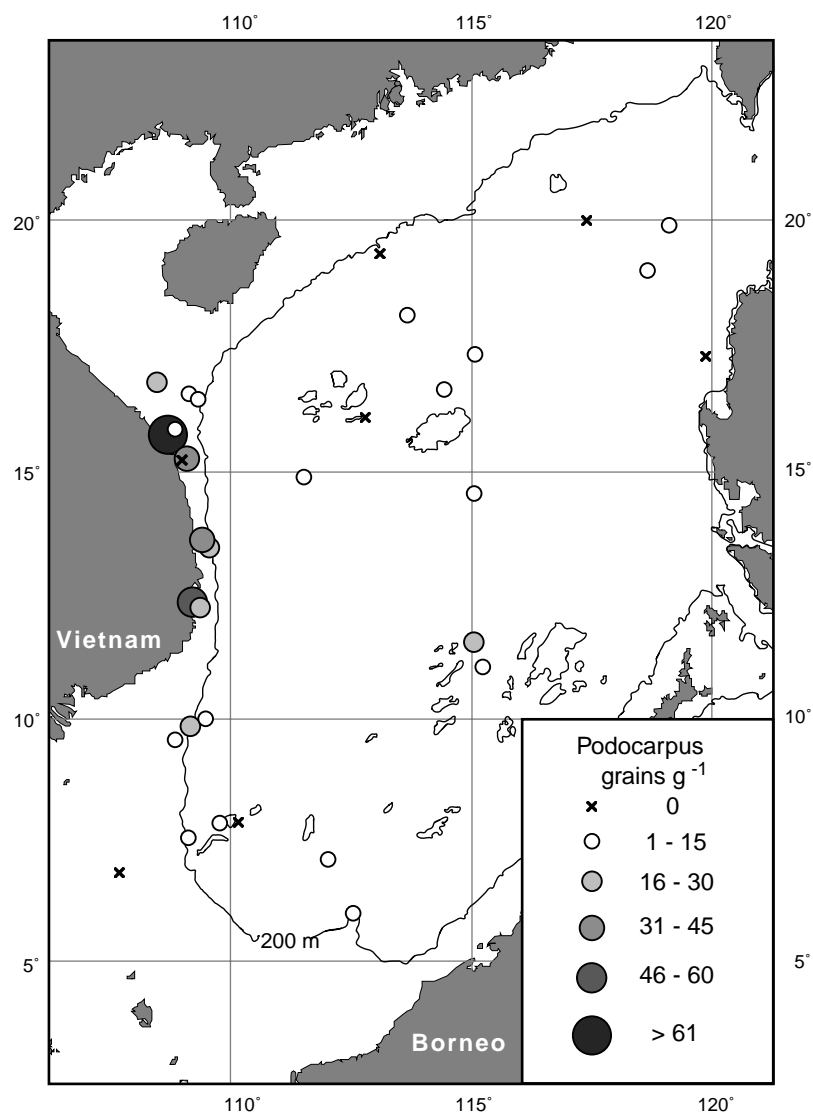


Figure 6e. Distribution map of Podocarpus.

found in high concentrations near the Vietnamese coast and are rarely recorded at sites below the shelf break. A comparison of distribution patterns of pre-excysted protoperidinioids to post-excysted protoperidinioids indicates that cyst transport has minor influence on the cyst distribution patterns on the Vietnamese Shelf. However, in the central and southern SCS, the occurrences of these two taxa do not always coincide (compare Figure 5k to 5f,g, h, I, j, l). This result indicates a potential bias resulting from lateral cyst transport in the central and southern SCS.

Clastic dilution: Sedimentation rates can significantly influence concentrations of dinoflagellate cysts and other palynomorphs. Only a few Holocene sedimentation rates are reported from the Vietnamese Shelf sites, however, available data suggest that the sedimentation rates generally decrease with increasing distance from landmasses

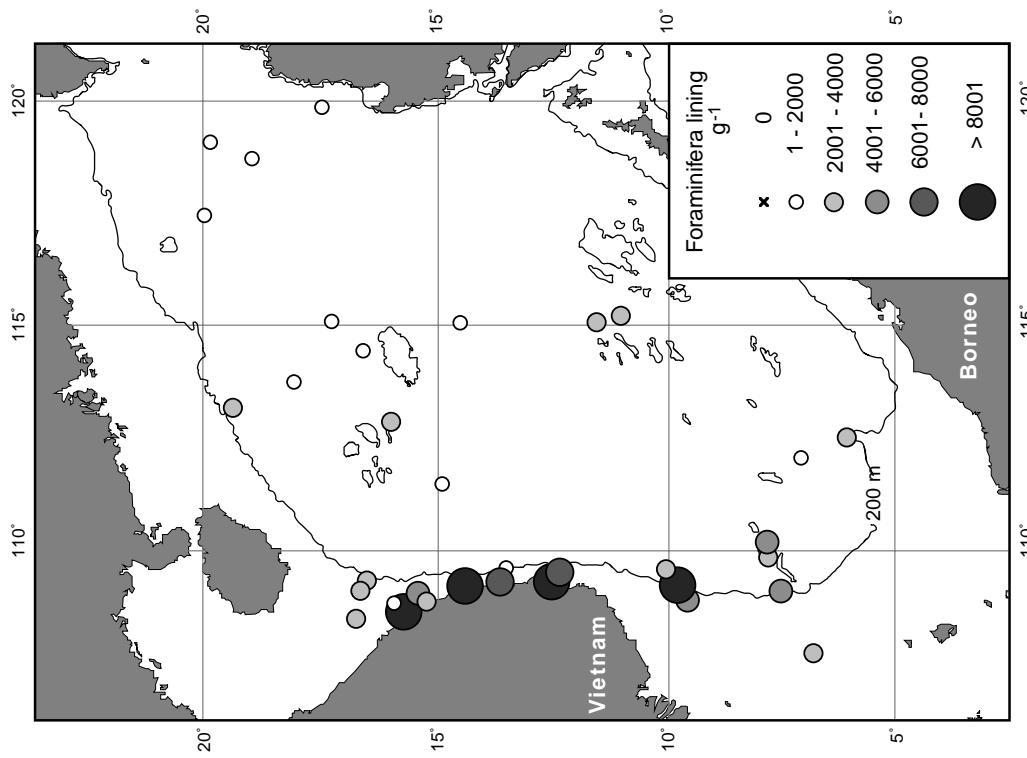


Figure 8. Distribution map of Foraminifera linings.

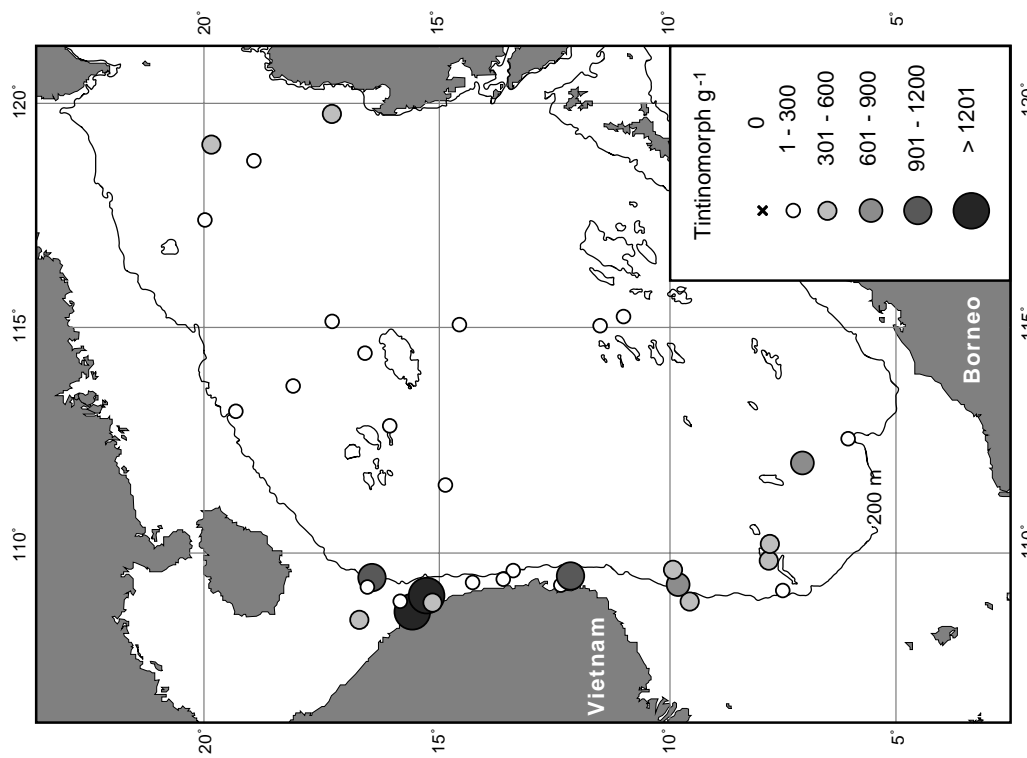


Figure 7. Distribution map of tintinomorphs.

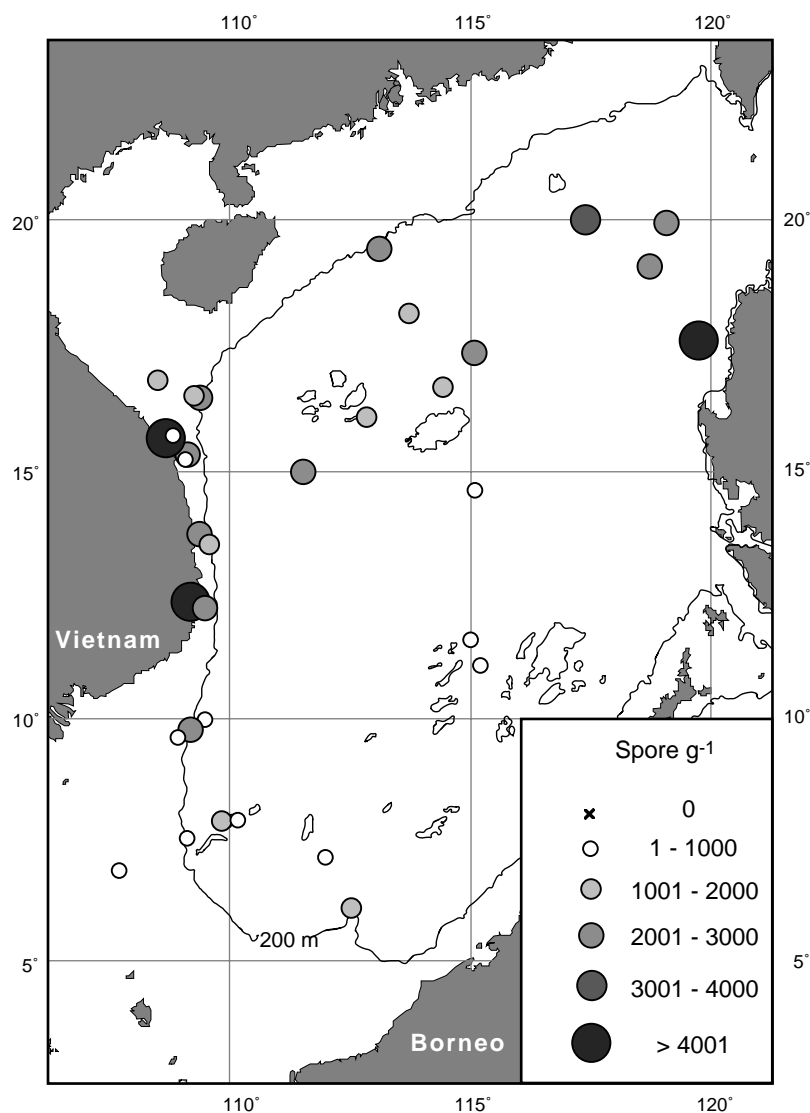


Figure 9. Distribution map of spores.

(Schimanski, 2002, Szczucinski and Stattegger, 2001). On the Vietnamese slope and in the basin, the sedimentation rates are usually low ($<10 \text{ cm kyr}^{-1}$) (Wang, 1999).

The highest concentrations of dinoflagellate cysts are observed in the coastal area. If the sedimentation rates in the coastal area are also highest, the cyst concentrations in the coastal area are lowered by clastic dilution, and thus, underrepresented. Thus, dinoflagellate cyst productions may be much higher than these represented as cyst concentrations in sediments.

Preservation: Zonneveld and Brummer (2000) and Zonneveld (1997b) reported that dinoflagellate cysts are susceptible to high dissolved oxygen content (DOC) of ambient water and classified that protoperidinioid taxa are the most susceptible to degradation. The DOC below the shelf break of the SCS ranges from ca. 2.0 to 5.0 mg l^{-1} (Sarnthein

et al., 1994). DOC values at the shelf sites are not available but it is expected to be high due to high-energy environments. High concentrations of protoperidinioids are found in the coastal area off Vietnam (<50 m wd) and the lower slope off Borneo. Thus, it is unlikely that degree of cyst preservation have major influences on the cyst assemblages in the SCS.

4.2 ENVIRONMENTAL FACTORS

SST gradients: Like other planktonic organisms, the distribution patterns of dinoflagellate are also primarily controlled by latitudinal gradients of SST. The distribution patterns of most dinoflagellate cysts identified in the tropical-subtropical SCS are in good accordance with the Atlantic based classification by Edwards and Andrieu (1992) and Mudie and Harland (1996) as cool temperate- tropical, warm temperate- tropical and broad thermal tolerance taxa. *S. stellatum* and *N. labyrinthus* are assigned by Mudie and Harland (1996) as temperate species. However, both species occur commonly in the SCS. The occurrences of these species are reported from east and west equatorial Atlantic (Marret, 1994; Vink et al., 2000b). Thus, these species are not restricted to temperate areas.

P. zoharyi and *O. janduchenei* have been assigned as tropical species (Edwards and Andrieu, 1992 and Mudie and Harland 1996). However, in the SCS, *P.*

zoharyi and *O. janduchenei* may not be tropical species. Occurrence of *P. zoharyi* and *O. janduchenei* is only recorded at the two northernmost sites in this study. Wu and Sun (2000) recorded occurrences of *P. zoharyi* and *O. janduchenei* in surface sediments in the sites north of 16°N in the SCS (Wu and Tocher, 1995). Occurrence of *P. zoharyi* was not recorded in the coastal area off Sabah, Sarawak (Borneo), in Gulf of Thailand, at the east coast of Malaysia peninsula (Lirdwitayaprasit, 1998a; Lirdwitayaprasit, 1998b) and on the Sunda Shelf (Chapter 2). This observation is also comparable to the study by (Harland, 1983) in the Atlantic, where occurrence of *P. zoharyi* was commonly limited to sites north of 6°N latitude.

4.3 FACTORS CONTROLLING THE VARIATIONS IN CA AXIS

A comparison of the CA results with available environmental data shows that the variations of the first CA axis (x-axis) seem to be related to the distance from landmass (Figure 10b). Either variation in primary productivity or a taphonomic

signature resulting from a transportation bias may explain this relation to the distance from landmass.

High values of annual surface primary productivity ($>300 \text{ gCm}^{-2}\text{y}^{-1}$) are observed in narrow coastal area and the values decrease as increasing distance from the coastal zone (Platt et al, 1995)(Figure 11a). The scores of the first CA axis correlate roughly with the gradient of surface water primary productivity (Figure 11c). Only these sites situated near the Paracel Islands and the Spatley Islands show negative values although the overlying surface water productivity is low. This may be results of the weak winter upwelling in those area.

Alternatively, transport effects from coastal area could be skewing the original assemblage. Biocoenosis of cyst producing dinoflagellate in the open ocean is not well understood (Harland, 1983). Dwelling of cyst producing dinoflagellate in open ocean has been repeatedly questioned by Dale (Dale, 1996; Dale and Dale, 1992 and Dale and Fjellsa 1993). Although transport processes of fine organic matter from shallow coastal area to deeper areas can be far more complicated than simple relation of distance to shoreline, it is roughly assumed that the transport effect decreases with increasing distance from the source area. Scores of 1st CA axis correlate to the distance to the closest landmass ($R= 0.693$)(Figure 11b). Thus, if dinoflagellate cysts are produced and then transported from the coastal area of the Paracel Islands and the Spatley Islands, the negative scores for these sites can be explained with the transport scenario. Furthermore, very high concentrations of dinoflagellate cysts are observed at the sites with less than 50m wd in the SCS and these concentrations generally decrease with increasing distance from the landmass (Figure 13). Despite of the presence of neritic/oceanic biogeographical boundary near the shelf break, most of observed taxa occur in sediments from both shelf and oceanic basin. Only taxa commonly found in sediments from the oceanic basins are *Impagidinium* species and *N. labyrinthus*, both of which have been classified as oceanic species (Dale, 1996; Mudie and Harland, 1996). The distribution patterns of pre-excysted protoperidinioids indicate that cyst assemblage in the central and southern SCS may be influenced by transport processes (see sec. 4.1 for discussions). For those reasons, first CA axis can be interpreted as a gradient of lateral transport processes. At this moment, sample size is too small to determine which of the two is the main controlling factor in the SCS.

4.4 RELATIONS OF GROUPS TO ENVIRONMENTAL CONDITIONS

Assuming that cysts found in the oceanic area are autochthonous and that cyst assemblages in sediments reflect overlying surface water conditions, relations between surface water conditions and the cysts assemblages in surface sediments can be

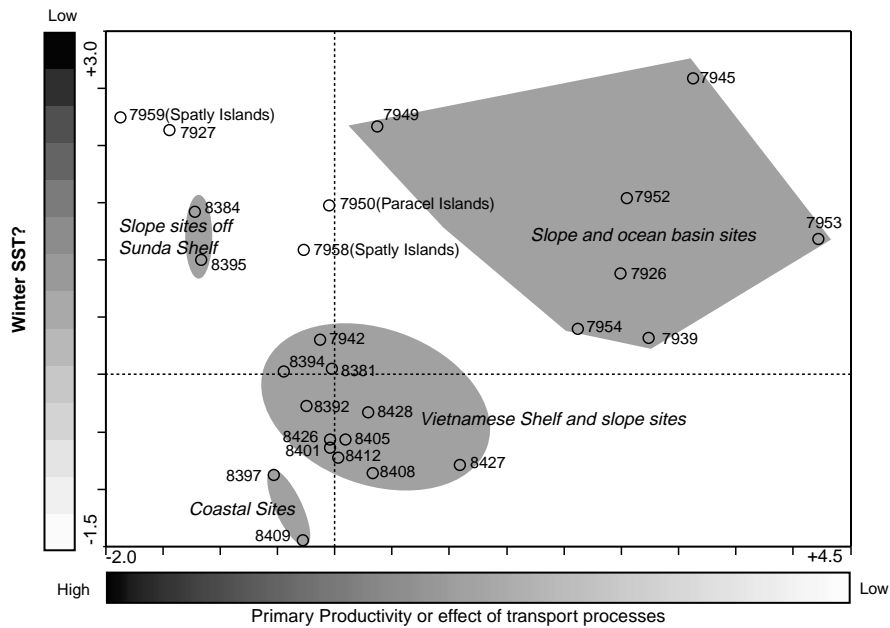


Figure 10a. Results of a CA; the variation within the site distribution (four digit numbers represent last four numbers of the sample sites).

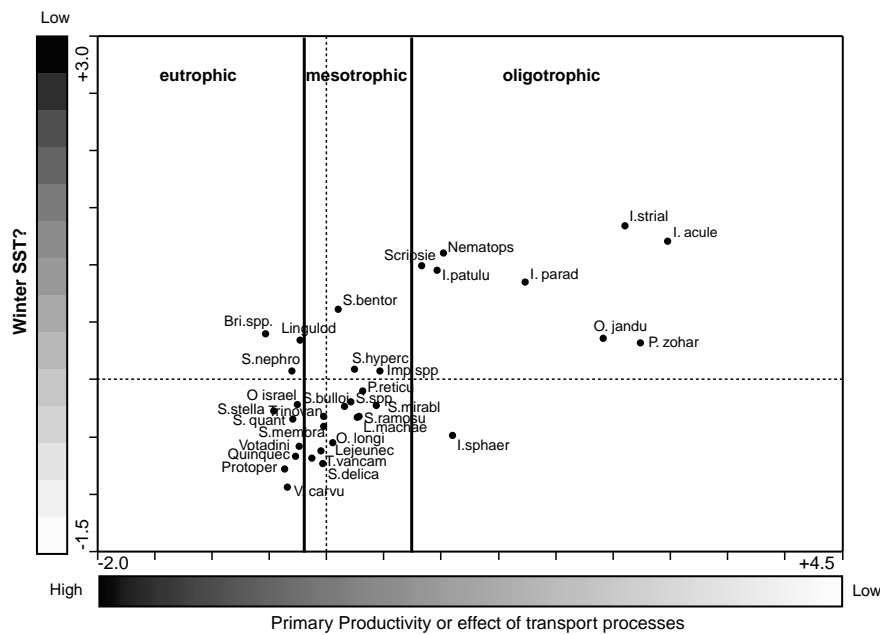


Figure 10b. Results of a CA; the variation within the species distribution.

Figure 10b. Results of a CA; the variation within the species distribution; Bri.spp= Brigantedinium species combined; I. acule= Impagidinium aculeatum; I. parad= Impagidinium paradoxum ; I. patulu= Impagidinium patulum; I. sphaer= Impagidinium sphaericum; I. strial= Impagidinium striatum; I.spp= Impagidinium spp.; Lejeunec= Lejeunecysta sabrina; Lingulod= Lingulodinium machaerophorum (short processes); L.machae= Lingulodinium machaerophorum (long processes); Nematops= Nematosphaeropsis labyrinthus; O. jandu= Operculodinium janduchenei; O.Israel= Operculodinium israelianum; P. reticu= Protoceratium reticulatum; Protooper= Pre-excysted Protopteridinioid; P.zohari= Polysphaeridium zoharyi; Quinquec= Quinquecupis concreta; Scripsie= Scripsella spp.; S. bentor= Spiniferites bentori; S. bulloid= Spiniferites bulloideus; S. delica= Spiniferites delicatus; S. hyperc= Spiniferites hypercanthus; S. membra= Spiniferites membranaceus; S. mirabl= Spiniferites mirabilis; S.ramos= Spiniferites ramosus; S. nephro= Selenopemphix nephroides; S. stella= Stelladinium stellatum; S. quant= Selenopemphix quanta; S.spp= Spiniferites spp.; Trinoven= Trinovantedinium appalanatum; T. vancam= Tuberculodinium vancampoae; V. carvu= Votadinium calvum;

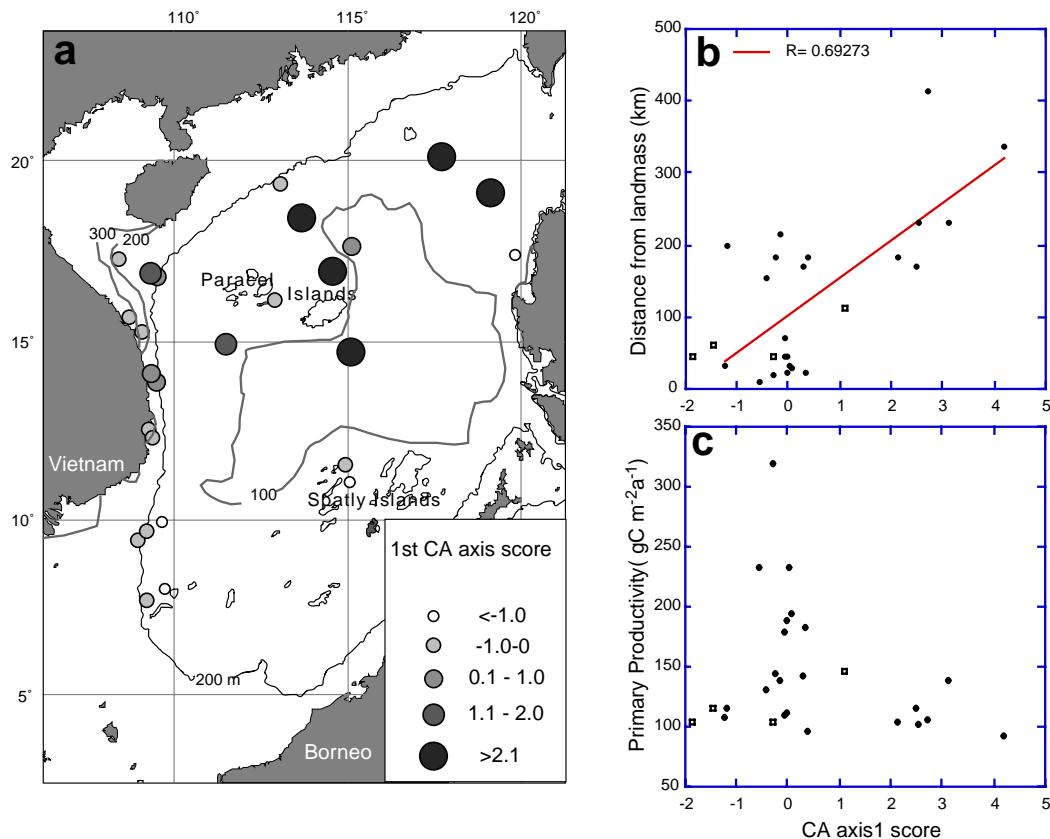


Figure 11. (a) 1st CA axis score of each sites; comparisons of 1st CA axis scores to the distances from the nearest landmass (b) and to the primary productivity of overlying surface water (c) ; empty triangles indicate sites near Parcel Islands and Spatly Islands

established. On the basis of 1st CA axis, cyst taxa are grouped into three (eutrophic & coastal to slope, mesotrophic & shelf to slope and oligotrophic & oceanic)(Figure 10b).

4.4.1 Group I Eutrophic & coastal to slope taxa

Consistent occurrences of *L. machaerophorum* in eutrophic coastal area are in good accordance with the classification of Vink et al. (2000b) as being eutrophic and shelf-ward taxon, and with the descriptions of (Dale and Fjellsa, 1993; Lewis and Hallett, 1997; Marret, 1994) as an indicator species for nutrient enrichment. The relation of process length of *L. machaerophorum* to the SSS gradient has been discussed (Ellegaard, 2000; Mudie et al., 2001). *L. machaerophorum* (short processes) is described as an indicator species for low salinity (Ellegaard, 2000; Matthiessen and Brenner, 1996; Mudie et al., 2001). The SSS gradients in the SCS are varying from ca. 32 psu to 34 psu. No correlation can be observed between relative and absolute abundance of *L. machaerophorum* (short processes) and the SSS

gradient.

The protoperidinioids such as *Brigantedinium* spp., *Q. concreta*, pre-excysted protoperidinioids, *V. carvum*, *V. spinosum*, *S. quanta* and *S. nephroides* have also been described as indicator species for nutrient-enriched water (Dale and Fjellsa, 1993; Lewis et al., 1990; Matsuoka and Kim, 1999). High concentrations of these species are recorded on the Vietnamese Shelf and on the slope off northern Sunda Shelf and may reflect the high nutrient level of the surface water in these regions.

4.4.2 Group II Mesotrophic & shelf to slope taxa

Twenty-three taxa in the Group II are ordinated around the origin of the diagram (Figure 10b). These taxa are common at the shelf sites and are interpreted to be mesotrophic, shelf to slope taxa. The taxa in Group II are roughly in accordance with the inshore- offshore cyst classifications of Mudie and Harland (1996) where *T.*

vancampoae is considered estuary to outer neritic species, *O. centrocarpum* (*P. reticulatum*), *S. bulloideus*, *S. membranaceus*, *S. ramosus*, *S. bentorii* and *L. machaerophorum* (long process) are considered estuary to oceanic taxa, *S. mirabilis* is considered inner neritic to oceanic taxa, and *S. delicatus* and *T. capitatum* are considered inner to outer neritic taxa.

4.4.3 Group III Oligotrophic & oceanic taxa

The CA based interpretations of all *Impagidinium* species and *N. labyrinthus* are in good accordance with the classifications of Edwards and Andrieu (1992); Mudie and Harland (1996); Vink et al., (2000b) and Zonneveld et al. (2001b) as oceanic species, and of Devillers and de Vernal (2000) and Vink et al. (2000b) as oligotrophic species. *P. zoharyi* is described as estuary-outer neritic species (Mudie and Harland, 1996). However, in the studied area, occurrences of *P. zoharyi* are recorded at two northernmost sites in the oceanic basin with low concentrations (<16 cyst g⁻¹) and are not recorded on the Vietnamese Shelf. The occurrences are reported by Borja *et al.*, (2000) and Furio *et al.* (2000) in the surface sediments from the Manila Bay (14 °N) and Malampaya Sound (11°N), Palawan, Philippines with high concentrations (<420 cyst cm⁻³). Thus, *P. zoharyi* found in the studied area may be transported from these shallow coastal areas.

Occurrences of *Scripsiella* spp. are mainly limited to the area below shelf break in the SCS. However, *Scripsiella* spp. have been reported from wide ranges of environments from coastal areas (Bolch and Hallegraeff, 1990; Kobayashi et al., 1986; Kobayashi and Yuki, 1991; Matsuoka et al., 1999; Nehring, 1997), from shelf areas (Cho and Matsuoka, 1999; Cho and Matsuoka, 2001), from oceanic basin (Vink et al.,

2000a) and from sediment traps from tropical and temperate Atlantic and tropical Pacific (Dale and Dale, 1992).

4.5 INTER-REGIONAL COMPARISONS AND IMPLICATIONS FOR THE BIOGEOGRAPHY OF CYSTS IN THE WESTERN PACIFIC

4.5.1 Shelf assemblage

The assemblages on the Vietnamese Shelf show many similarities to the assemblages from the oligotrophic Sunda Shelf (chapter 2). A marked difference between two areas is the cyst concentration. Unfortunately, different units are used to measure the cyst concentrations in Chapter 2 (cysts ml⁻¹ wet sediments for the Sunda Shelf study and cyst g⁻¹ dry sediments for present study). Thus, direct comparison of these results may not be accurate. However, even considering the inaccuracies associated with different methods used, samples from the Vietnamese Shelf show significantly higher concentration than those from the Sunda Shelf. Especially, two sites in the coastal area (<50 wd) off Vietnam show very cyst high concentrations for the SCS (>1600 cysts g⁻¹). Considering strong winnowing activity (Chapter 2) and very low Holocene sedimentation rates (Steinke, 2001) on the Sunda Shelf, there may be even bigger difference in the cyst production between two regions. The differences in concentrations between them may be due to differences in the primary productivity of overlying surface water. Several studies suggest that dinoflagellate cyst accumulation rate or dinoflagellate cyst concentration correlate positively with the primary productivity of overlying surface water (e.g. Hoell et al., 2000). However, Kawamura (Chapter 2) noted that the concentrations of dinoflagellate cysts on the Sunda Shelf correlate negatively with increasing sediment grain-sizes and may be controlled by winnowing activities. The dominant sediment-type on the Vietnamese Shelf is clay (Wiesner et al., 1999). Thus, high cyst concentration on the Vietnamese Shelf may be result of finer grain size.

Compared with the eutrophic shelf assemblages from the Yellow Sea and East China Sea (Cho and Matsuoka 1999 , Cho and Matsuoka 2001), the Vietnamese Shelf assemblages contain less *S. bulloideus* and *Alexandrium* cysts. *Spiniferites* species are more diverse on the Vietnamese Shelf than these in the Yellow Sea and the ECS. *O.israelianum* and *T. vancampoae* occur more consistently on the Vietnamese Shelf than in Yellow Sea or the ECS. This may be due to the difference in SST. *O. israelianum* and *T. vancampoae* are classified as warm temperate to tropical taxa (Mudie and Harland, 1996). According to Matsuoka (1985), occurrences of *O. israelianum* and *T. vancampoae* are not recorded north of 35°N in the Japanese coastal area and are not recorded at all in the Bering Sea (Redi et al , 2001). These results agree

with the study along Atlantic coast by Dale (1996) and may suggest that occurrences of *O. israelianum* and *T. vancampoe* are limited south of ca. 35°N with their acme in the subtropical to tropical areas in the western Pacific coastal area.

The cyst concentration in the Yellow Sea and the East China Sea sediments varies from 0 to 5006 cyst g⁻¹ (Cho and Matsuoka, 1999 ; Cho and Matsuoka 2001). This range is much wider than the one on the Vietnamese Shelf. This may be explained with difference in sedimentation rates and/or in cyst production rates due to the difference in primary productivity.

4.5.2 Oceanic assemblage

Distribution patterns of dinoflagellate cysts are not well documented in the Pacific Ocean and adjacent seas. Comparable studies in the vicinity of the SCS were performed only in the Okinawa Trough, East China Sea (ECS) by Wu and Tocher (1995) and in the Philippine Sea by Matsuoka (1981). However, these studies do not contain either count tables or concentration values. Thus, comparisons can be made only with the relative abundance of major taxa.

Spiniferites species and *T. vancampoe* occur in all three areas with similar relative abundance (6-66 % and <5% respectively). *P. reticulatum* occurs with higher absolute abundance in ECS than in the Philippines Sea and in the SCS. *L. machaerophorum* occurs with higher relative abundance in the SCS and ECS than in the Philippines Sea. This was expected since *L. machaerophorum* is classified as coastal to slope species (this study and Mudie and Harland, 1996) and the sampling sites in are distant from any landmass. *Impagidinium* species are thought to prefer oceanic and oligotrophic conditions (Mudie and Harland, 1996), and dominate cyst assemblages in the Philippines Sea. The dominance of *Impagidinium* species is probably due to prevailing oceanic and oligotrophic conditions in the Philippines Sea.

5. CONCLUSIONS

Thirty-six sediment surface samples from SCS are investigated palynologically in order to study distribution patterns of dinoflagellate cysts and factors controlling their distribution patterns. Forty taxa of dinoflagellate cysts are identified. The highest concentrations of dinoflagellate cysts are observed in shallow coastal area where the highest primary productivity was recorded. The CA diagram with sites shows that distribution patterns of dinoflagellate cysts are closely related with the distance from nearest landmass in the SCS. Ecologically, this relation can be explained with gradients of surface water primary productivity. Sample scores of 1st CA axis correlate roughly with annual primary productivity of each site. However, as pointed out by Dale (1996)

and Sarjeant and Taylor (1999), this relation may be product of offshore transport effect. Comparison of site scores of 1st CA axis with distances from nearest landmass of each sites show equally convincing results with the comparison with surface water productivity. More samples are necessary to determine which of the two scenarios are the main factors.

Assuming that cysts found in oceanic area are autochthonous and distribution patterns of dinoflagellate are controlled by surface water productivity in the SCS, cyst species are divided into three main groups. Group I: Eutrophic & coastal- slope species *Lingulodinium* spp. (short processes), *Brigantedinium* sp., *O. israelianum*, *S. stellatum*, *S. quanta*, *Q. concreta*, pre-excysted protoperidinioids, *V. calvum*, *V. spinosum* and *S. nephroides*. Group II: Mesotrophic & shelf to slope species all taxa of genus *Spiniferites*, *P. reticulatum*, *T. vancampoae*, *T. capitatum*, *O. longispigerum*, *L. sabrina* and *L. machaerophorum*. Group III Oligotrophic & oceanic: *I. aculeatum*, *I. striatum*, *O. janduchenei*, *I. paradoxum*, *I. patulum*, *I. sphaericum* and *N. labyrinthus*. These groups can be useful in the reconstruction of temporal changes in surface water productivity.

The results are compared with other published records in the western Pacific. The comparisons revealed that the occurrences of *O. israelianum* and *T. vancampoae* are limited in the areas south of 35°N in the western pacific shelf area. *P. zoharyi* is not a tropical species and its distribution is limited north of 16° N in the SCS. *N. labyrinthus* and *S. stellatum* is not limited in temperate regions. These species extend well into the tropical southern SCS with high concentrations.

REFERENCES

- Bolch, C.J. and Hallegraeff, G.M., 1990. Dinoflagellate cysts in recent marine sediments from Tasmania, Australia. *Botanica Marina*, 33: 173-192.
- Borja, V.M., Furio, E.F. and Rodriguez, A.K., 2000. Horizontal and vertical distribution of *Pyrodinium bahamense* cysts in sediments of Malampaya Sound, Palawan, Philippines, Conference proceeding on the Ninth Conference Harmful Algae Blooms, Tasmania.
- Cho, H.-J. and Matsuoka, K., 1999. Dinoflagellate cyst composition and distribution in the surface sediments from the Yellow Sea and the East China Sea. In: T. Matsuno, K. Matsuoka and J. Ishizaka (Editors), *The East China Sea*. Nagasaki University, Nagasaki, pp. 73-82.
- Cho, H.-J. and Matsuoka, K., 2001. Distribution characteristics of dinoflagellate cysts in the surface sediments collected from the Yellow Sea and the East China Sea. *Marine Micropaleontology*, 42: 103-123.
- Dale, B., 1976. Cyst formation, sedimentation, and preservation; factors affecting dinoflagellate assemblages in Recent sediments from Trondheimsfjord, Norway. *Review of Palaeobotany and Palynology*, 22(1): 39-60.
- Dale, B., 1996. Dinoflagellate cyst ecology: modeling and geological applications. In: J. Jansonius and D.C. McGregor (Editors), *Palynology: principles and applications*. American Association of Stratigraphical Palynologists Foundation, Salt Lake City, pp. 1249-1276.
- Dale, B. and Dale, A.L., 1992. *Dinoflagellate Contributions to the Deep Sea*. Ocean Biocoenosis Series, 5. Woods Hole Oceanographic Institution, 75 pp.
- Dale, B. and Fjellsa, A., 1993. Dinoflagellate cysts as paleoproductivity indicators; state of the art, potential, and limits. In: Zahn et al. (Editors), *Carbon cycling in the glacial ocean; constraints on the ocean's role in global change; quantitative approaches in paleoceanography*. NATO ASI Series. Series I: Global Environmental Change. Springer Verlag, Berlin, Federal Republic of Germany, pp. 521-537.
- Devillers, R. and de, V.A., 2000. Distribution of dinoflagellate cysts in surface sediments of the northern North Atlantic in relation to nutrient content and productivity in surface waters. *Marine Geology*, 166(1-4): 103-124.
- Edwards, L.E. and Andrieu, V.A.S., 1992. Distribution of selected dinoflagellate cysts in modern marine sediments. In: M.J. Head and J.H. Wrenn (Editors), *Neogene and Quaternary Dinoflagellate Cysts and Acritarchs*. AASP Foundation, Salt Lake City, pp. 259-288.
- Ellegaard, M., 2000. Variations in dinoflagellate cyst morphology under conditions of changing salinity during the last 2000 years in the Limfjord, Denmark. *Review of Palaeobotany and Palynology*, 109: 65-81.
- Emery, K.O., 1968. Relict sediments on the continental shelves of the world. *Bulletin of American*

- Association of Petroleum Geologists, 52: 445-464.
- Faughn, J.L., 1974. NAGA Expedition: Station Index and Data. NAGA Report, Vol. 1, Scripps Institute of Oceanography, La Jolla.
- Fensome, R.A., Riding, J.B. and Taylor, F.J.R., 1996. Dinoflagellates. In: Jansonius, J., McGregor, D.C. (Eds.), *Palynology: principles and applications*, Vol. 3. American Association of Stratigraphic Palynologists Foundation, Salt Lake City, UT, pp. 107-169.
- Furio, E.F. and Borja, V.M., 1998. The primary productivity in the South China sea, Area III: Western Philippines, SEAFDEC Seminar on Fishery Resources in the South China Sea, Area III: Western Philippines, Kuala Lumpur, pp. 235-250.
- Furio, E.F., Matsuoka, K., Fukuyo, Y. and Borja, V.M., 2000. Distribution of *Pyrodinium bahamense* var. *compressum* cysts in the surface sediments of Manila Bay, Philippines, Ninth Conference Harmful Algae Blooms, Tasmania.
- Harland, R., 1983. Distribution maps of Recent dinoflagellate cysts in bottom sediments from the North Atlantic Ocean and adjacent seas. *Palaeontology*, 26(Part 2): 321-387.
- Hess, S., 1998. Distribution patterns of recent benthic foraminifera in the South China Sea. *Berichte - Reports*, Geologisch-Palaeontologisches Institut und Museum, Christian-Albrechts-Universitaet Kiel, 91. Christian-Albrechts-Universitaet Kiel, Geologisch-Palaeontologisches Institut und Museum, Kiel, Federal Republic of Germany, 173 pp.
- Hill, M.O. and Gauch, H.G.J., 1980. Detrend Correspondence Analysis: an improved ordination technique. *Vegetatio*, 42: 47-58.
- Hoell, C., Zonneveld, K.A.F. and Willems, H., 2000. Organic-walled dinoflagellate cyst assemblages in the tropical Atlantic Ocean and oceanographical changes over the last 140 ka. *Palaeogeography, Palaeoclimatology, Palaeoecology*, 160(1-2): 69-90.
- Jungman, R.H.G., ter Braak, C.J.F. and van Tongeren, O.F.R., 1995. *Data Analysis in Community and landscape Ecology*. Cambridge University Press, Cambridge, 299 pp.
- Kobayashi, S., Matsuoka, K. and Iizuka, S., 1986. Distribution of dinoflagellate cysts in surface sediments of Japanese coastal water. I. Omura Bay, Kyushu. *Bulletin of Plankton Society of Japan*, 33(2): 81-93.
- Kobayashi, S. and Yuki, K., 1991. Distribution of dinoflagellate cysts in surface sediments of Japanese surface water II. Matoya Bay. *Bulletin of Plankton Society of Japan*, 38(1): 9-23.
- La Fond, E.C., 1963. Physical oceanography and its relation to marine production in the South China sea. In: S.I.O. *Oceanography* (Editor), *Ecology of the Gulf of Thailand and the South China Sea, a report on the results of the NAGA expedition, 1959-1961*. Scripps Institute of Oceanography Contribution Series, La Jolla, USA, pp. 5-33.
- La Fond, E.C., 1966. *South China Sea*, The Encyclopedia of Oceanography. Reinhold Publishing Corp., New York, pp. 829-836.

- La Violette, P.E. and Frontenac, T.R., 1967. Temperature, Salinity and Density of the World's Oceans: South China Sea and adjacent Gulfs. US Naval Oceanographic Office, Washington D.C., 134 pp.
- Lentin, J.K. and Williams, G.L., 1993. Fossil dinoflagellates: index to genera and species. American Association of Stratigraphical Palynologists Contribution Series, 24. American Association of Stratigraphical Palynologists, Dallas, 856 pp.
- Lewis, J., Dodge, J.D. and Powell, A.J., 1990. Quaternary dinoflagellate cysts from the upwelling system offshore Peru, Hole 686B, ODP Leg 112. In: Suess et al. (Editors), Proceedings of the Ocean Drilling Program, Peru continental margin; covering Leg 112 of the cruises of the Drilling Vessel JOIDES Resolution, Callao, Peru to Valparaiso, Chile, sites 679-688, 20 October 1986-25 December 1986. Proceedings of the Ocean Drilling Program, Scientific Results. Texas A & M University, Ocean Drilling Program, College Station, TX, United States, pp. 323-328.
- Lewis, J. and Hallett, R., 1997. *Lingulodinium polyedrum* (*Gonyaulax polyedra*) a blooming dinoflagellate. *Oceanography and Marine Biology: Annual Review*, 35: 97-161.
- Lirdwitayaprasit, T., 1998a. Distribution of dinoflagellate cysts in the surface sediment of South China Sea: Area 2. Off Sabah, Sarawak and Brunei Darussalam, Second Technical Seminar on Marine Fishery Resources Survey in the South China Sea, Area II: West coast of Sabah, Sarawak and Brunei Darussalam, Kuala Lumpur, pp. 310-322.
- Lirdwitayaprasit, T., 1998b. Distribution of Dinoflagellate Cysts in the Surface Sediment of the South China Sea, Area I: Gulf of Thailand and East Coast of Peninsula, First Technical Seminar on Marine Fishery Resources Survey in the South China Sea, Area I: GULF OF THAILAND AND EAST COAST OF PENINSULAR MALAYSIA, Kuala Lumpur, pp. 311-326.
- Marret, F., 1994. Distribution of dinoflagellate cysts in Recent marine sediments from the East Equatorial Atlantic (Gulf of Guinea). In: Zonneveld, Karin, F ; Versteegh and Gerard (Editors), *Dino 5; 5th international conference on Modern and fossil dinoflagellates. Review of Palaeobotany and Palynology*. Elsevier, Amsterdam, Netherlands, pp. 1-22.
- Matsuoka, K., 1981. Dinoflagellate cysts and pollen in pelagic sediments of the northern part of the Philippine Sea. *Bulletin of Faculty of Liberal Arts, Nagasaki University*, 21: 59-70.
- Matsuoka, K., 1985. Distribution of the Dinoflagellate cyst in surface sediments of the Tsushima warm current. *The Quaternary Research (Japan)*, 24: 1-12.
- Matsuoka, K., Fukuyo, Y., Praseno, D.P., Adnan, Q. and Kodama, M., 1999. Dinoflagellate Cysts in Surface Sediments of Jakarta Bay, off Ujung Pandang and Larantuka of Flores Islands, Indonesia with Special Reference of *Pyrodinium bahamense*. *Reports of fakulity of fishry, Nagasaki University*, 80: 49-54.
- Matsuoka, K. and Kim, H.S., 1999. Process of eutrophication in enclosed seas recorded in

- dinoflagellate cyst assemblages and sediments; the case in Nagasaki Bay, West Japan. *Fossils*, 66: 1-15.
- Matthiessen, J. and Brenner, W., 1996. Chlorococcalean algae and dinoflagellate cysts in recent sediments from Greifswald Bay (southern Baltic Sea).
- McCarthy, F.M.G., Gostlin, K.E. and Gauthier, M.E., 1999. Terrestrial and marine palynomorphs as sea-level proxies. In: Anonymous (Editor), American Association of Petroleum Geologists 1999 annual meeting. Annual Meeting Expanded Abstracts - American Association of Petroleum Geologists. American Association of Petroleum Geologists and Society of Economic Paleontologists and Mineralogists, Tulsa, OK, United States, pp. A91.
- Mudie, P.J., Aksu, A.E. and Yasar, D., 2001. Late Quaternary dinoflagellate cysts from the Black, Marmara and Aegean seas: variation in assemblages, morphology and paleosalinity. *Marine Micropaleontology*, 43: 155-178.
- Mudie, P.J. and Harland, R., 1996. Chapter 21. Aquatic Quaternary. In: J. Jansonius and D.C. McGregor (Editors), *Palynology: principles and applications*. AASP Foundation, Salt Lake City, pp. 843-877.
- Nehring, S., 1997. Dinoflagellate resting cysts from recent German coastal sediments. *Botanica Marina*, 40(307-324).
- Platt, T., Sathyendranath, S. and Longhurst, A., 1995. Remote sensing of primary production in the ocean: promise and fulfillment. *Philosophical Transactions of the Royal Society of London, Series A: Mathematical and Physical Sciences*, B248: 191-202.
- Redi, T., de Vernal, A. and Peyron, O., 2001. Relationships between dinoflagellate cyst assemblages in surface sediment and hydrographical condition in the Bering and Chukchi seas. *Journal of Quaternary Science*, 16(7): 667-680.
- Rochon, A., De, V.A., Sejrup, H.P. and Hafliðason, H., 1998. Palynological evidence of climatic and oceanographic changes in the North Sea during the last deglaciation. *Quaternary Research*, 47: 197-207.
- Rochon, A., de Vernal, A., Turon, J.-L., Matthiessen, J. and Head, M.J., 1999. Distribution of recent dinoflagellate cysts in surface sediments from the North Atlantic Ocean and adjacent seas in relation to sea-surface parameters. *American Association of Stratigraphical Palynologists Contribution Series*, 35. American Association of Stratigraphical Palynologists, Dallas, 152 pp.
- Sarnthein, M., Pflaumann, U., Wang, P.X. and Wong, H.K., 1994. Preliminary report on Sonne-95 cruise "Monitor Monsoon" to the South China Sea; Manila - Guangzhou - Hongkong - Kota Kinabalu - Hongkong; 16 April-8 June 1994. *Berichte - Reports, Geologisch-Palaeontologisches Institut und Museum, Christian-Albrechts-Universität Kiel*, 68. Christian-Albrechts-Universität Kiel, Geologisch-Palaeontologisches Institut

- und Museum, Kiel, Federal Republic of Germany, 226 pp.
- Shaw, P.-T., Chao, S.-H., Liu, K.-K., Pai, S.-C. and Liu, C.-T., 1996. Winter upwelling off Luzon in the northeastern South China Sea. *Journal of Geophysical Research*, 101: 16435-16448.
- Schimanski, A., 2002. Holocene Sedimentation on the Vietnamese Shelf: From Source to Sink. Ph.D. thesis Thesis, Institut fuer Geowissenschaften, Christian Albrechts Universitaet zu Kiel, Kiel, 110 pp.
- Steinke, S., 2001. Sedimentological and climate changes during the Last Deglaciation recorded in cores from the Sunda Shelf margin and continental slope (southern South China Sea). Ph.D. Thesis, Institut fuer Geowissenschaften, Christian Albrechts Universitaet zu Kiel, Kiel.
- Stockmarr, J., 1971. Tablets with spores used in absolute pollen analysis. *Pollen et Spores*, 13: 615-621.
- Szarek, R., 2001. Biodiversity and biogeography of recent benthic foraminiferal assemblages in the south-western South China Sea (Sunda Shelf). Ph.D. Thesis, Institut fuer Geowissenschaften, Christian Albrechts Universitaet zu Kiel, Kiel, 273 pp.
- Szczucinski, W. and Stattegger, K., 2001. Style and rate of sedimentation offshore Nha Trang, Vietnam, South China Sea. *Meyniana*, 53: 143-162.
- ter Braak, C.J.F. and Smilauer, P., 1998. CANOCO 4. Center of Biometry, Washington, 351 pp.
- Udarbe-Walker, M.J.B. and Villanoy, C.L., 2001. Structure of potential upwelling areas in the Philippines. *Deep-Sea Research I*, 48: 1499-1518.
- Versteegh, G.J.M. and Zonneveld, K.A.F., 1994. Determination of (palaeo-)ecological preferences of dinoflagellates by applying detrended and canonical correspondence analysis to late Pliocene dinoflagellate cyst assemblages of the south Italian Singa section. In: Zonneveld, Karin, F ; Versteegh and Gerard (Editors), *Dino 5; 5th international conference on Modern and fossil dinoflagellates. Review of Palaeobotany and Palynology*. Elsevier, Amsterdam, Netherlands, pp. 181-199.
- Vink, A., Zonneveld, K.A.F. and Willems, H., 2000a. Distributions of calcareous dinoflagellate cysts in surface sediments of the western equatorial Atlantic Ocean, and their potential use in palaeoceanography. *Marine Micropaleontology*, 38(2): 149-180.
- Vink, A., Zonneveld, K.A.F. and Willems, H., 2000b. Organic-walled dinoflagellate cysts in western Equatorial Atlantic surface sediments; distributions and their relation to environment. *Review of Palaeobotany and Palynology*, 112(4): 247-286.
- Vo, V.L., 1995. Coastal Upwelling off Southern Central Vietnam. Science and Technics Publishing House, Hanoi, pp. 207.
- Wang, P., 1999. Response of Western Pacific marginal seas to glacial cycles; paleoceanographic and sedimentological features. In: M. Sarnthein and P. Wang (Editors), *Response of West Pacific marginal seas to global climate change. Marine Geology*. Elsevier, Amsterdam,

- Netherlands, pp. 5-39.
- Wiesner, M.G., Stattegger, K., Kuhnt, W., Arpe, C., Bracker, E., Catene, S., de Leon, M., Duyanen, J., Faber, U., Gerbich, C., Hess, S., Holbourn, A., Jagodzinski, R., Kaminski, M., Kawamura, H., Kuueger, O., Lorenc, S., Nguyen, H.-S., Nguyen, H.-P., Nguyen, T.-T., Nguyen, V.-B., Paulsen, H., Peleo-Alampay, A., Richter, A., Rimek, R., Schimanski, A., Seeman, B., Sharma, C., Siringan, ., Steen, E., Steinke, S., Szarek, R., Szczucincki, W., Vo, D.-S., Von Wersch, V., Wetzal, A., Witzki, D., 1999. Cruise report SONNE 140 Suedmeer III, Berichte - Reports, Institut fuer Geowissenschaften, Christian-Albrechts-Universitaet Kiel, 7, Institut fuer Geowissenschaften, Christian Albrechts Universitaet zu Kiel, Kiel. 155 pp.
- Wiesner, M.G., Zheng, L., Wong, H.K., Wang, Y. and Chen, W., 1996. Fluxes of particulate matter in the South China Sea. In: V. Ittekkot, P. Schaefer, S. Honjo and P.J. Depetris (Editors), Particle Flux in the Ocean. John Wiley & Sons Ltd, pp. 293-312.
- Wu, G. and Sun, X., 2000. Distribution of dinoflagellate cysts in surface sediments from South China Sea. *Tropical Oceanology*, 19(1): 7-16.
- Wu, G. and Tocher, B., 1995. Organic-wall dinoflagellate from the surface sediments in southern Okinawa Trough. *Chinese Science Bulletin*, 40(6): 545-547.
- Wyrtki, K., 1961. Physical oceanography of Southeast Asian Waters, NAGA Report, Scientific Results of Marine Investigations of the South China Sea and the Gulf of Thailand, Scripps Institute of Oceanography, La Jolla, USA.
- Zonneveld, K.A.F., 1995. Palaeoclimatic and palaeo-ecological changes during the last deglaciation in the eastern Mediterranean; implications for dinoflagellate ecology. *Review of Palaeobotany and Palynology*, 84(3-4): 221-253.
- Zonneveld, K.A.F., 1997a. Dinoflagellate cyst distribution in surface sediments from the Arabian Sea (northwestern Indian Ocean) in relation to temperature and salinity gradients in the upper water column. In: Van, Weering, E ; Helder and W ; Schalk (Editors), Netherlands Indian Ocean Program 1992-1993; first results. *Deep-Sea Research. Part II: Topical Studies in Oceanography*. Pergamon Press, Oxford - New York, International, pp. 1411-1443.
- Zonneveld, K.A.F. and Brummer, G.A., 2000. (Palaeo-)ecological significance, transport and preservation of organic-walled dinoflagellate cysts in the Somali Basin, NW Arabian Sea. *Deep Sea Research II*, 47: 2229-2256.
- Zonneveld, K.A.F., Hoek, R.P., Brinkhuis, H. and Willems, H., 2001a. Geographical distributions of organic-walled dinoflagellate cysts in surface sediments of the benguela upwelling region and their relationship to upper ocean conditions. *Progress in Oceanography*, 48: 25-72.
- Zonneveld, K.A.F., Versteegh, G.J.M. and de, L.G.J., 2001b. Palaeoproductivity and post-depositional aerobic organic matter decay reflected by dinoflagellate cyst

assemblages of the eastern Mediterranean S1 sapropel. *Marine Geology*, 172(3-4): 181-195.

Zonneveld, K.A.F., Versteegh, G.J.M., de Lange, G.J., 1997b. Preservation of organic-walled dinoflagellate cysts in different oxygen regimes: a 10,000 year natural experiment. *Marine Micropaleontology*, 29: 393-405.

Appendix I Dinoflagellate cysts counted

Sample	18409	18397	18413	18412	18374	18421	18426	18427	18392	18408
Sediment weight (dry g)	3	3	3	3	3	3	3	3.1	3	3
Lycopodium	606	770	1260	811	2214	2328	993	1462	1563	1240
Foramling	1259	1744	668	829	1242	496	782	882	2134	2535
Tintinomorphs	225	15	132	1613	60	92	82	92	216	39
Spore	932	860	105	488	92	198	356	375	328	849
Gonyaulacoid Group										
<i>Spiniferites bulloideus</i>	23	21	4	5	2	3	11	42	13	27
<i>S. ramosus</i>	20	24	5	3	2	2	8	12	6	25
<i>S. mirabilis</i>	8	9	1	8	1	3	15	8	9	24
<i>S. hypercanthus</i>	7	7	1	8	2	0	4	13	4	19
<i>S. membranaceus</i>	9	9	2	2	3	0	8	1	2	13
<i>S. delicatus</i>	6	2	0	1	1	0	0	0	1	1
<i>S. bentoni</i>	0	0	0	1	0	0	0	0	0	0
<i>Spiniferites spp.</i>	20	32	6	7	1	1	12	6	9	21
<i>Achomosphaera spp.</i>	0	0	0	0	0	0	0	0	0	1
<i>Protoceratium reticulatum</i>	25	19	2	11	1	1	17	18	9	28
<i>Operculodinium longispinigerum</i>	5	1	0	0	0	0	1	0	0	2
<i>O. israelianum</i>	7	14	0	1	0	0	1	0	3	6
<i>O. janduchenei</i>										
<i>Lingulodinium machaerophorum</i>	5	4	4	2	0	0	3	1	3	4
<i>L. machaerophorum (short process)</i>	6	21	2	2	2	2	6	1	9	13
<i>Impagidinium paradoxum</i>	0	0	0	1	0	0	0	2	2	0
<i>I. patulum</i>	0	0	0	0	0	0	0	0	0	0
<i>I. sphaericum</i>	0	0	0	0	0	0	0	0	0	1
<i>I. aculeatum</i>										
<i>I. striatum</i>	0	0	0	0	0	0	0	0	0	0
<i>Impagidinium spp.</i>	4	0	0	0	0	0	1	1	1	0
<i>Nematopshaera labyrinthus</i>	0	0	0	0	0	0	0	0	0	0
Tuberculoidinioid										
<i>Tuberculodinium vancamptoeae</i>	14	11	0	1	1	1	1	1	2	6
Calciodinellid										
<i>Scripsiella trochoidea</i>	0	1	0	0	0	0	0	2	0	2
Protoperidinioid Group										
<i>Brigantedinium spp.</i>	39	64	5	14	8	4	29	8	29	34
<i>Selenopemphix quanta</i>	7	3	0	6	2	0	2	0	5	1
<i>S. nephroides</i>	9	6	2	2	2	2	5	1	6	1
<i>Stelladium stellatum</i>	9	2	1	3	1	1	0	0	1	1
<i>Trinovantedinium capitatum</i>	5	9	1	2	0	0	2	0	8	6
Pre-excysted Protoperidium	9	25	0	2	0	0	4	0	1	4
<i>Votadinium calvum</i>	8	1	0	0	0	0	1	0	1	0
<i>Votadinium spinosum</i>	3	6	0	0	0	0	1	1	0	5
<i>Lejeunecysta sabrina</i>	0	1	0	0	0	0	0	0	0	0
<i>Quinquecuspis concret</i>	10	5	0	4	0	1	2	1	3	2
<i>P. zoharyi</i>										
Gymnodiniales										
<i>Polykrikos kofoidii</i>	0	1	0	0	0	1	0	0	0	0
Other										
Unidentified dinoflagellate cysts	6	1	4	2	0	0	1	4	3	6
Total number of dino	264	299	40	88	29	22	135	123	130	253
<i>Cymatiosphaera</i>	5	7	0	0	0	0	0	1	0	4
<i>Cyclopsiella spp.</i>	23	19	2	16	1	4	9	2	3	9
<i>Cladopyxis spp.</i>	1	1	0	1	0	0	0	0	1	0

Sample	18408	18405	18401	18404	18394	18428	18381	18395	17942	18386
Sediment weight (dry g)	3	3	3	3	3	3	3	3	3	3
Lycopodium	1240	1540	1182	2304	1163	2158	939	1233	1223	1741
Foramling	2535	2629	2211	660	3985	1246	996	986	1075	1934
Tintinomorphs	39	84	309	54	215	597	35	112	18	154
Spore	849	654	599	265	576	1298	123	259	637	60
Gonyaulacoid Group										
<i>Spiniferites bulloideus</i>	27	49	27	5	54	40	18	6	12	2
<i>S. ramosus</i>	25	20	21	1	17	16	7	6	11	2
<i>S. mirabilis</i>	24	22	12	7	7	19	5	2	15	4
<i>S. hypercanthus</i>	19	19	10	3	11	15	8	2	15	1
<i>S. membranaceus</i>	13	6	8	3	7	4	8	0	8	3
<i>S. delicatus</i>	1	0	0	0	0	1	1	0	0	0
<i>S. bentori</i>	0	0	0	0	0	0	0	0	0	0
<i>Spiniferites spp.</i>	21	7	27	8	17	13	11	1	19	2
<i>Achomosphaera spp.</i>	1	0	1	0	0	0	0	0	1	0
<i>Protoceratium reticulatum</i>	28	22	15	4	22	34	14	7	36	4
<i>Operculodinium longispinigerum</i>	2	2	0	1	0	0	1	0	0	0
<i>O. israelianum</i>	6	12	3	1	10	1	3	5	3	1
<i>O. janduchenei</i>									0	
<i>Lingulodinium machaerophorum</i>	4	4	3	3	9	3	1	0	8	0
<i>L. machaerophorum (short process)</i>	13	17	10	7	30	20	10	24	14	12
<i>Impagidinium paradoxum</i>	0	2	0	0	0	0	0	1	4	0
<i>I. patulum</i>	0	0	0	0	0	2	1	0	0	0
<i>I. sphaericum</i>	1	0	0	0	0	0	0	0	0	0
<i>I. aculeatum</i>									0	
<i>I. striatum</i>	0	0	0	0	0	0	1	0	0	0
<i>Impagidinium spp.</i>	0	2	1	0	0	1	0	2	0	0
<i>Nematopshaera labyrinthus</i>	0	0	0	0	0	0	1	0	0	0
Tuberculoidinioid										
<i>Tuberculodinium vancampoae</i>	6	6	3	1	7	1	0	2	4	0
Calcioidinellid										
<i>Scrippsiella trochoidea</i>	2	1	0	0	9	0	0	1	3	2
Protoperidinioid Group										
<i>Brigantedinium spp.</i>	34	41	41	9	85	34	29	45	72	24
<i>Selenopemphix quanta</i>	1	7	5	0	9	3	0	0	6	0
<i>S. nephroides</i>	1	9	3	2	4	6	4	10	4	2
<i>Stelladium stellatum</i>	1	3	1	0	5	1	1	1	2	2
<i>Trinovantedinium capitatum</i>	6	3	3	2	7	2	1	2	1	0
Pre-excysted Protoperidium	4	1	2	3	2	0	2	1	1	1
<i>Votadinium calvum</i>	0	1	0	0	1	1	0	1	1	2
<i>Votadinium spinosum</i>	5	2	2	0	6	4	0	2	0	0
<i>Lejeunecysta sabrina</i>	0	5	0	0	0	1	0	0		0
<i>Quinquecuspis concret</i>	2	2	5	1	5	0	0	3	2	0
<i>P. zoharyi</i>									0	
Gymnodiniales										
<i>Polykrikos kofoidii</i>	0	1	1	0	0	0	0	0	0	0
Other										
Unidentified dinoflagellate cysts	6	1	2	0	3	2	3	2	1	2
Total number of dino	253	267	206	61	327	224	130	126	231	66
<i>Cymatiosphaera</i>	4	0	0	0	0	0	1	0	7	0
<i>Cyclopsiella spp.</i>	9	52	28	6	19	5	3	4	12	0
<i>Cladopyxis spp.</i>	0	0	1	0	0	0	0	3	2	0

Sample	18384	17965	17954	17950	17959	17962	17949	17952	17945	17939
Sediment weight (dry g)	3	3	2.99	3	3	3	3.02	3	3	3.02
Lycopodium	1196	1507	1466	3340	1659	1711	1914	2178	3184	2637
Foramling	978	806	142	1606	1467	668	300	244	109	65
Tintinomorphs	132	71	13	32	49	294	24	29	21	7
Spore	371	633	901	1378	140	329	1265	732	1523	2335
Gonyaulacoid Group										
<i>Spiniferites bulloideus</i>	13	3	19	13	10	2	3	9	4	30
<i>S. ramosus</i>	6	4	19	6	4	1	1	7	6	22
<i>S. mirabilis</i>	2	3	10	6	0	1	5	14	8	25
<i>S. hypercanthus</i>	10	1	8	16	6	0	16	15	4	21
<i>S. membranaceus</i>	3	2	0	6	1	1	0	4	1	1
<i>S. delicatus</i>	1	0	2	0	0	0	0	0	0	0
<i>S. bentori</i>	1	0	0	1	0	0	0	0	0	2
<i>Spiniferites spp.</i>	15	4	7	9	3	4	9	5	4	25
<i>Achomosphaera spp.</i>	0	0	0	0	0	0	0	0	0	0
<i>Protoceratium reticulatum</i>	16	10	18	22	1	3	7	8	15	36
<i>Operculodinium longispinigerum</i>	1	0	2	0	0	0	0	0	0	3
<i>O. israelianum</i>	6	0	0	3	3	4	1	2	0	3
<i>O. janduchenei</i>		0	3	0	0	0	0	0	0	5
<i>Lingulodinium machaerophorum</i>	0	0	1	1	0	0	0	1	2	6
<i>L. machaerophorum</i> (short process)	16	24	5	10	10	20	18	15	6	7
<i>Impagidinium paradoxum</i>	4	5	4	2	0	7	5	6	5	14
<i>I. patulum</i>	0	0	0	4	0	0	0	0	1	1
<i>I. sphaericum</i>	0	0	0	0	0	0	0	0	0	1
<i>I. aculeatum</i>		0	2	0	0	0	2	5	4	5
<i>I. striatum</i>	0	0	0	0	0	0	0	4	6	3
<i>Impagidinium spp.</i>	0	0	0	2	1	2	3	1	1	3
<i>Nematopshaera labyrinthus</i>	1	0	2	2	0	0	1	2	2	0
Tuberculoidinioid										
<i>Tuberculodinium vancampoae</i>	1	0	0	1	0	0	0	3	0	3
Calciodinellid										
<i>Scrippsiella trochoidea</i>	3	4	18	13	10	9	12	11	14	16
Protoperidinioid Group										
<i>Brigantedinium spp.</i>	135	220	0	68	147	304	44	6	13	0
<i>Selenopemphix quanta</i>	6	3	0	1	1	1	1	0	0	0
<i>S. nephroides</i>	15	23	6	5	7	16	0	2	1	1
<i>Stelladium stellatum</i>	2	8	0	2	6	8	1	0	0	0
<i>Trinovantedinium capitatum</i>	5	4	10	0	1	2	0	0	0	3
Pre-excysted Protoperidium	1	0	0	0	0	0	1	0	0	0
<i>Votadinium calvum</i>	0	1	0	0	1	2	0	0	0	0
<i>Votadinium spinosum</i>	0	0	0	0	0	0	0	0	0	0
<i>Lejeunecysta sabrina</i>	0									
<i>Quinquecuspis concret</i>	0	0	0	0	1	0	1	0	0	0
<i>P. zoharyi</i>		0	0	0	0	0	0	0	0	10
Gymnodiniales										
<i>Polykrikos kofoidii</i>	0	0	0	0	0	0	0	1	0	0
Other										
Unidentified dinoflagellate cysts	3	1	0	0	0	0	1	0	1	3
Total number of dino	266	317	117	180	203	385	129	112	94	219
<i>Cymatiosphaera</i>	1	0	6	0	0	0	0	5	0	32
<i>Cyclopsiella spp.</i>	7	11	0	13	7	16	21	2	8	0
<i>Cladopyxis spp.</i>	1	0	3	5	1	3	1	1	2	0

Sample	17958	17927	17925	17926	17953
Sediment weight (dry g)	3	3.04	2.95	3.12	3.2
Lycopodium	1014	1198	2110	1544	1733
Foramling	617	151	107	45	47
Tintinomorphs	19	136	161	93	6
Spore	208	2184	1334	1021	277
Gonyaulacoid Group					
<i>Spiniferites bulloideus</i>	10	1	7	4	7
<i>S. ramosus</i>	1	0	2	9	7
<i>S. mirabilis</i>	2	0	1	3	5
<i>S. hypercanthus</i>	9	2	2	3	1
<i>S. membranaceus</i>	1	0	0	2	1
<i>S. delicatus</i>	1	0	0	1	0
<i>S. bentori</i>	2	0	0	0	0
<i>Spiniferites spp.</i>	8	1	1	14	18
<i>Achomosphaera spp.</i>	0	0	0	0	0
<i>Protoceratium reticulatum</i>	13	3	2	11	20
<i>Operculodinium longispinigerum</i>	1	1	0	0	0
<i>O. israelianum</i>	3	1	0	0	2
<i>O. janduchenei</i>	0	0	2	0	0
<i>Lingulodinium machaerophorum</i>	0	0	0	2	4
<i>L. machaerophorum</i> (short process)	4	24	6	6	0
<i>Impagidinium paradoxum</i>	1	0	7	6	14
<i>I. patulum</i>	0	1	0	0	2
<i>I. sphaericum</i>	0	0	0	0	0
<i>I. aculeatum</i>	0	0	4	3	9
<i>I. striatum</i>	0	0	1	0	2
<i>Impagidinium spp.</i>	2	0	1	0	4
<i>Nematopshaera labyrinthus</i>	3	0	2	2	1
Tuberculoidinioid					
<i>Tuberculodinium vancampoae</i>	1	0	1	0	1
Calciodinellid					
<i>Scrippsiella trochoidea</i>	3	2	13	5	0
Protoperidinioid Group					
<i>Brigantedinium spp.</i>	40	29	3	3	1
<i>Selenopemphix quanta</i>	0	1	0	0	0
<i>S. nephroides</i>	4	0	0	1	0
<i>Stelladium stellatum</i>	0	2	0	0	0
<i>Trinovantedinium capitatum</i>	1	0	0	0	0
Pre-excysted Protoperidium	0	1	0	0	0
<i>Votadinium calvum</i>	0	0	0	0	0
<i>Votadinium spinosum</i>	1	0	0	0	0
<i>Lejeunecysta sabrina</i>					
<i>Quinquecuspis concret</i>	1	0	0	0	0
<i>P. zoharyi</i>	0	0	1	0	0
Gymnodiniales					
<i>Polykrikos kofoidii</i>	0	0	0	0	0
Other					
Unidentified dinoflagellate cysts	0	1	0	4	2
Total number of dino	102	69	49	75	94
<i>Cymatiosphaera</i>	1	1	0	1	0
<i>Cyclopsiella spp.</i>	1	0	6	0	7
<i>Cladopyxis spp.</i>	1	5	0	1	0

Chapter 3. Appendix II.

Spec: Species scores

	NAME	AX1	AX2	AX3	AX4	WEIGHT	N2
	EIG	0.1833	0.1356	0.0649	0.045		
1	S.bulloi	0.1569	-0.2348	-0.405	-0.0664	1516.9	14.98
2	S.ramosu	0.2673	-0.3286	-0.0689	0.1433	955.21	13.49
3	S.mirabl	0.4343	-0.2225	-0.2688	-0.1069	738.09	16.53
4	S.hyperc	0.2427	0.0876	-0.3295	-0.1013	753.25	19.87
5	S.membra	-0.0244	-0.4109	0.0158	-0.133	390.03	11.27
6	S.delica	-0.0363	-0.7354	0.5705	0.2651	80.68	3.74
7	S.bentor	0.1042	0.6134	-0.0916	-0.7741	20.56	3.83
8	S.spp	0.2142	-0.1953	0.2098	-0.101	1106.51	13.77
10	P.reticu	0.3147	-0.0982	-0.043	-0.1578	1421.26	17.76
11	O. longi	0.0557	-0.5479	0.257	0.3308	82.25	4.74
12	O. israel	-0.2563	-0.2178	0.1778	0.1556	346.91	9.7
13	O. jandu	2.4162	0.3604	-1.0571	1.8113	8.26	2
14	L.machae	0.2845	-0.3246	0.1143	-0.1812	227.23	11.53
15	Lingulod	-0.2307	0.3426	-0.0521	0.3359	972.99	15.94
16	I. parad	1.7324	0.8541	0.6837	-0.3494	168.84	10.6
17	I.patulu	0.9641	0.9498	0.3832	-0.4324	24.17	6.06
18	I.sphaer	1.096	-0.4841	-0.7711	0.0978	2.2	1.77
19	I. acule	2.9781	1.2077	1.4806	-0.2386	60.94	5.24
20	I.strial	2.6011	1.3432	0.799	0.3284	29.25	4.66
21	Imp spp	0.4677	0.0725	0.5686	-0.2498	91.72	7.52
22	Nematops	1.0211	1.1053	0.1605	0.1541	44.65	7.05
23	T.vancam	-0.1308	-0.6884	0.3928	0.209	290.07	5.71
24	Scripsie	0.8321	0.9945	-0.3042	0.8279	292.88	11.58
25	Bri.spp.	-0.5295	0.4029	0.0506	-0.0931	3507.06	14
26	S. quant	-0.2936	-0.3463	0.0682	-0.2668	246.37	9.41
27	S.nephro	-0.3011	0.0711	0.07	0.0235	393.96	12.79
28	S.stella	-0.4582	-0.2777	0.3548	0.0229	174.39	6.02
29	Trinovan	-0.0226	-0.3191	-0.0235	0.4247	263.59	10.38
30	Protoper	-0.3622	-0.7843	0.6364	0.5151	246.76	3.47
31	V. calvu	-0.3423	-0.9363	0.759	0.1545	49.13	2.29
32	Votadini	-0.2373	-0.5835	-0.0066	0.2807	129.84	6.83
33	Lejeunec	-0.0491	-0.6249	-0.7258	0.009	10.63	2.02
34	Quinquec	-0.2676	-0.6685	0.3544	0.0062	209.61	6.32
35	P. zohar	2.74	0.3182	-0.5781	0.3379	3.96	1

Samp: Sample scores

N	NAME	AX1	AX2	AX3	AX4	WEIGHT	N2
	EIG	0.1833	0.1356	0.0649	0.045		
1	8409	-0.2813	-1.4458	1.2216	0.2272	1746.17	14.31
2	8397	-0.5323	-0.8753	0.9675	1.1905	1589.58	10.51
3	8412	0.034	-0.7262	0.1146	-1.4168	441.48	11.89
4	8426	-0.0429	-0.5702	-0.2024	-0.7878	560.21	9.5
5	8427	1.0924	-0.7847	-2.739	-1.1538	329.33	5.49
6	8392	-0.2463	-0.2712	0.0279	-0.2138	338.02	10.28
7	8408	0.3301	-0.8579	-0.861	-0.014	825.59	11.56
8	8405	0.096	-0.567	-1.2922	-0.3594	711.19	10.47
9	8401	-0.0378	-0.6352	-0.4486	-0.6462	713.55	9.43
10	8394	-0.4409	0.0259	-0.6896	0.3674	1162.22	8.12
11	8428	0.2883	-0.329	-1.5038	-0.7216	428.2	9.01
12	8381	-0.0208	0.0502	-0.5435	-0.5095	564.02	8.82
13	8395	-1.1668	1.0009	0.3914	1.0992	418.55	5.28
14	7942	-0.1297	0.3063	-0.0765	-1.1591	821.97	7.23
15	8384	-1.2205	1.4195	0.3369	-0.7839	918.57	3.52
17	7954	2.1193	0.399	-1.4965	3.1627	384.5	10.15
18	7950	-0.0452	1.4776	-0.4887	-0.3027	241.54	6.14
19	7959	-1.8669	2.2467	0.1982	-0.2687	535.7	2.05
21	7949	0.3716	2.1675	0.1273	0.8834	283.98	5.97
22	7952	2.5459	1.5374	0.1919	1.3988	230.36	12.66
23	7945	3.1242	2.588	1.0325	1.6896	127.36	10.9
24	7939	2.74	0.3182	-0.5781	0.3379	370.69	11.07
25	7958	-0.2738	1.0895	-0.1563	-0.8648	461.23	5.98
26	7927	-1.4412	2.1367	0.1732	2.0815	237.16	3.28
27	7926	2.4953	0.8849	1.3313	0.079	195.11	10.01
28	7953	4.219	1.1865	4.1832	-3.0486	223.88	8.35

Tol : Species tolerance (root mean squared deviation for species)

N	NAME	AX1	AX2	AX3	AX4	RMSTOL	N2
	FR FITTED	0.2756	0.2039	0.0976	0.0677		
1	S.bulloi	0.997	0.8472	1.1548	0.9781	100.02	14.98
2	S.ramosu	1.1374	0.871	1.1753	1.1103	108.01	13.49
3	S.mirabl	1.1028	0.8563	1.0537	1.07	102.53	16.53
4	S.hyperc	1.0598	1.0408	0.9414	0.9996	101.14	19.87
5	S.membra	0.7249	0.8192	0.9063	0.7659	80.69	11.27
6	S.delica	0.7959	0.8966	0.9047	1.0048	90.35	3.74
7	S.bentor	1.172	0.8277	0.2938	0.5468	78.17	3.83
8	S.spp	1.2122	0.9515	1.1654	1.0597	110.18	13.77
10	P.reticu	1.2101	0.9565	1.2246	1.1231	113.36	17.76
11	O. longi	0.9776	1.0384	0.9964	1.0036	100.42	4.74
12	O. israel	0.8365	0.9905	0.9558	0.8608	91.32	9.7
13	O. jandu	0.3101	0.0404	0.4588	1.4111	75.82	2
14	L.machae	1.1841	0.7868	1.2067	1.0148	106.15	11.53
15	Lingulod	1.0071	1.1164	0.756	1.0068	98.05	15.94
16	I. parad	1.7954	0.8121	1.8803	1.7097	160.79	10.6
17	I.patulu	1.9301	0.9224	1.9171	1.5748	163.79	6.06
18	I.sphaer	1.1221	0.5476	0.1317	0.1639	63.31	1.77
19	I. acule	1.0657	0.6511	2.0568	2.1473	161.25	5.24
20	I.strial	1.2361	0.9247	1.5689	1.6337	137.05	4.66
21	Imp spp	1.5735	1.3031	1.5135	1.1309	139.14	7.52
22	Nematops	1.5611	0.6299	1.2161	1.5458	129.44	7.05
23	T.vancam	0.7395	0.79	0.9829	0.7644	82.49	5.71
24	Scripsie	1.608	0.9679	0.865	1.3299	122.88	11.58
25	Bri.spp.	0.7581	1.1912	0.6995	0.8402	89.29	14
26	S. quant	0.4188	0.914	0.7964	0.7816	75.1	9.41
27	S.nephro	0.8972	1.092	0.8517	1.0032	96.56	12.79
28	S.stella	0.5773	1.2701	0.8118	0.7841	89.73	6.02
29	Trinovan	0.9414	0.8255	0.9119	1.1943	97.8	10.38
30	Protoper	0.3072	0.6545	0.6753	0.8104	63.95	3.47
31	V. calvu	0.3504	0.8676	0.7657	0.5081	65.58	2.29
32	Votadini	0.4222	0.6604	1.0168	0.7086	73.32	6.83
33	Lejeunec	0.2911	0.1629	1.0037	0.7067	63.6	2.02
34	Quinquec	0.376	0.8165	0.85	0.7865	73.3	6.32
35	P. zohar	0	0	0	0	0	1

Het : Sample heterogeneity (root mean squared deviation for samples)

N	NAME	AX1	AX2	AX3	AX4	RMSTOL	N2
	FR FITTED	0.2756	0.2039	0.0976	0.0677		
1	8409	0.3926	1.2998	1.1745	0.2849	90.89	14.31
2	8397	0.5429	0.8509	0.9395	1.1574	90.01	10.51
3	8412	0.3885	0.7131	0.2701	1.3649	80.55	11.89
4	8426	0.3537	0.5922	0.2927	0.7707	53.75	9.5
5	8427	0.9455	0.7352	2.573	1.1127	152.42	5.49
6	8392	0.4513	0.4213	0.2369	0.2796	35.9	10.28
7	8408	0.419	0.807	0.8363	0.1887	62.49	11.56
8	8405	0.3665	0.5846	1.2338	0.3822	73.22	10.47
9	8401	0.3323	0.6336	0.4753	0.636	53.44	9.43
10	8394	0.5086	0.3791	0.6816	0.4137	50.94	8.12
11	8428	0.4064	0.4129	1.4225	0.7079	84.56	9.01
12	8381	0.424	0.3591	0.5586	0.5143	47.04	8.82
13	8395	1.0194	0.9344	0.4123	1.0691	89.79	5.28
14	7942	0.453	0.4402	0.2167	1.1205	65.22	7.23
15	8384	1.0837	1.2695	0.3599	0.7703	93.66	3.52
17	7954	1.8148	0.6058	1.4369	3.0438	193.58	10.15
18	7950	0.4975	1.336	0.5042	0.3932	78.12	6.14
19	7959	1.5665	1.9642	0.2446	0.3353	127.32	2.05
21	7949	0.7375	1.9138	0.3326	0.8972	113.16	5.97
22	7952	2.2365	1.4327	0.4704	1.3709	151.29	12.66
23	7945	2.7091	2.3061	1.0587	1.6526	203.16	10.9
24	7939	2.3383	0.5436	0.6695	0.4705	126.82	11.07
25	7958	0.5091	1.0166	0.2655	0.8541	72.33	5.98
26	7927	1.226	1.8702	0.2224	2.0039	150.55	3.28
27	7926	2.1622	0.9181	1.3054	0.2913	135.16	10.01
28	7953	3.5684	1.1685	3.9432	2.9154	308.82	8.35

CFit: Cumulative fit per species as fraction of variance of species

N	NAME	AX1	AX2	AX3	AX4	VAR(y)	% EXPL
	FR FITTED	0.2756	0.2039	0.0976	0.0677		
1	S.bulloi	0.0604	0.2035	0.6642	0.6769	0.33	0
2	S.ramosu	0.2503	0.6506	0.6696	0.7537	0.23	0
3	S.mirabl	0.3493	0.4464	0.5995	0.6242	0.44	0
4	S.hyperc	0.1619	0.1842	0.526	0.5589	0.3	0
5	S.membra	0.0011	0.3444	0.3449	0.3847	0.43	0
6	S.delica	0.0006	0.267	0.4404	0.4786	1.76	0
7	S.bentor	0.0012	0.0456	0.0467	0.1248	7.33	0
8	S.spp	0.1673	0.3146	0.4983	0.5418	0.22	0
10	P.reticu	0.4903	0.5408	0.5513	0.6954	0.16	0
11	O. longi	0.0018	0.1827	0.2258	0.2986	1.43	0
12	O. israel	0.1548	0.273	0.3582	0.4249	0.35	0
13	O. jandu	0.2551	0.2611	0.317	0.4847	18.69	0
14	L.machae	0.1477	0.3512	0.3785	0.4486	0.45	0
15	Lingulod	0.0739	0.2463	0.2507	0.4338	0.59	0
16	I. parad	0.6187	0.7778	0.8881	0.9175	3.96	0
17	I.patulu	0.1008	0.2044	0.2227	0.2464	7.53	0
18	I.sphaer	0.0859	0.1036	0.1523	0.1531	11.43	0
19	I. acule	0.6357	0.7464	0.9263	0.9311	11.39	0
20	I.strial	0.3646	0.4675	0.5069	0.5137	15.15	0
21	Imp spp	0.1107	0.1135	0.3008	0.3377	1.61	0
22	Nematops	0.1747	0.3914	0.3963	0.401	4.87	0
23	T.vancam	0.0183	0.5547	0.7436	0.7983	0.76	0
24	Scripsie	0.2198	0.5522	0.5858	0.8403	2.57	0
25	Bri.spp.	0.5841	0.9421	0.9482	0.9693	0.39	0
26	S. quant	0.0884	0.2185	0.224	0.3093	0.8	0
27	S.nephro	0.1718	0.1819	0.1926	0.1938	0.43	0
28	S.stella	0.1711	0.2376	0.3551	0.3556	1	0
29	Trinovan	0.0006	0.1259	0.1266	0.3717	0.7	0
30	Protoper	0.059	0.3516	0.5601	0.6995	1.82	0
31	V. calvu	0.033	0.2943	0.48	0.4879	2.9	0
32	Votadini	0.0534	0.3954	0.3954	0.4828	0.86	0
33	Lejeunec	0.0002	0.039	0.0956	0.0956	8.7	0
34	Quinquec	0.0636	0.4839	0.6117	0.6118	0.92	0
35	P. zohar	0.1569	0.1591	0.1671	0.1699	39.09	0

SqRL: Squared residual length per sample with s axes (s=1...4)

N	NAME	AX1	AX2	AX3	AX4	SQLENG	% FIT
	FR FITTED	0.2756	0.2039	0.0976	0.0677		
1	8409	0.4711	0.2261	0.1355	0.1333	0.48	72.4
2	8397	0.3447	0.255	0.1981	0.1372	0.39	64.57
3	8412	0.6104	0.5486	0.5478	0.4615	0.61	24.42
4	8426	0.2535	0.2154	0.2129	0.1863	0.25	26.62
5	8427	0.8971	0.8249	0.3694	0.3122	1.08	70.98
6	8392	0.2586	0.25	0.2499	0.2479	0.27	7.36
7	8408	0.2607	0.1744	0.1294	0.1294	0.28	53.28
8	8405	0.3572	0.3195	0.2181	0.2126	0.36	40.71
9	8401	0.1928	0.1455	0.1333	0.1153	0.19	40.24
10	8394	0.1606	0.1605	0.1316	0.1258	0.19	33.67
11	8428	0.3243	0.3116	0.1743	0.1519	0.34	54.89
12	8381	0.2513	0.251	0.2331	0.2219	0.25	11.72
13	8395	0.5263	0.4089	0.3996	0.3476	0.73	52.39
14	7942	0.1894	0.1785	0.1781	0.1203	0.19	37.33
15	8384	0.3512	0.1151	0.1082	0.0818	0.57	85.75
17	7954	1.07	1.0513	0.9153	0.485	1.74	72.16
18	7950	0.6084	0.3525	0.338	0.3341	0.61	45.12
19	7959	0.8245	0.233	0.2306	0.2275	1.35	83.1
21	7949	0.9053	0.3548	0.3538	0.3202	0.93	65.42
22	7952	0.8783	0.6014	0.5991	0.515	1.85	72.14
23	7945	2.1032	1.3184	1.2536	1.1308	3.56	68.27
24	7939	0.544	0.5321	0.5118	0.5069	1.67	69.6
25	7958	0.6566	0.5175	0.516	0.4839	0.67	27.55
26	7927	1.6502	1.1152	1.1134	0.927	1.96	52.73
27	7926	0.7104	0.6187	0.511	0.5108	1.64	68.9
28	7953	2.0517	1.8867	0.8242	0.4244	4.72	91

Site	CA score	axis 1	distance (km)	Annual pp (gC m-2a-1)
8409	-0.2813		18	319
8397	-0.5323		10	233
8412	0.034		30	233
8426	-0.0429		70	179
8427	1.0924		111	146
8392	-0.2463		184	145
8408	0.3301		23	182
8405	0.096		29	195
8401	-0.0378		23	189
8394	-0.4409		153	131
8428	0.2883		168	142
8381	-0.0208		46	111
8395	-1.1668		199	116
7942	-0.1297		214	138.7
8384	-1.2205		31	108
7954	2.1193		184	104.24
7950	-0.0452		45	108.77
7959	-1.8669		46	102.98
7949	0.3716		184	96.74
7952	2.5459		230	100.74
7945	3.1242		230	138.7
7939	2.74		413	105.76
7958	-0.2738		46	102.98
7927	-1.4412		61	114.5
7926	2.4953		168	115.48
7953	4.219		337	92.26

CHAPTER 4. 44 kyr marine palynological records from the southern South China Sea: implications for the variations in surface water productivity and climatic conditions

Hiroshi Kawamura*, Markus Kienast+, Wolfgang Kuhnt* and Stephan Steinke#

*Institut fuer Geowissenschaften der Christian Albrechts Universitaet zu Kiel

Olshausenstr. 40, 24118 Kiel, Germany

+Department of Earth and Ocean Sciences, University of British Columbia,

6339 Stores Road, Vancouver, British Columbia V6T 1Z4, Canada

Institute of Applied Geophysics, National Taiwan Ocean University, 2 Pei-Ning Road, Keelung 20224, Taiwan, R.O.C.

ABSTRACT

The timing and relative magnitude of climatic variations and surface water productivity variations during the last 44 kyr in/around the southern South China Sea are investigated with palynomorph-based proxies (pollen, organic-walled dinoflagellate cysts and freshwater algae). Species compositions of dinoflagellate cysts are used as proxies for surface water productivity. Pollen and spores are used as proxies for climatic conditions and mangrove pollen and freshwater algae *Pediastrum* are used as proxies for the flux of terrestrial organic matter and influence of freshwater plume. Palynomorph-based proxies suggest that during Marine Isotope Stage (MIS) 3, the surface water was mesotrophic and climatic conditions were somewhat colder and drier than at present. During MIS 2, surface water became eutrophic and climatic conditions became colder and drier than during MIS 3. At ca. 19 ka[#] cal BP, climatic conditions started to become abruptly warmer and more humid, and surface water productivity began to decrease toward Holocene. Productivity reached the lowest level in early Holocene and then increased again toward middle Holocene.

In general (for different MISs), the warm and moist climatic conditions corresponded to the oligotrophic surface water conditions, indicating weak winter monsoon and strong summer monsoon, and cold and dry climatic period corresponded eutrophic surface water conditions, indicating strong winter monsoon and weak summer monsoon.

All ages discussed in this chapter are calibrated BP ages.

1. INTRODUCTION

The climatic and oceanographic conditions in South East Asia (SE Asia) are primarily controlled by the semi-annual reversal of the East Asian monsoon system. At present, northern hemisphere winter monsoon (northeasterly monsoon) prevails from October to March, and is characterized by strong, cold and dry northeasterly winds originating from a high pressure system over Asia, whereas northern hemisphere summer monsoon (southwesterly monsoon) prevails from May to August, and is characterized by warm and moist southwesterly wind originating from the Indian Ocean and Australia.

The present-day climatic and oceanographic configuration of the South China Sea (SCS) is vastly different from the last glacial configuration. During the last glacial period, the vast continental shelf in the southern SCS was emerged due to the low sea-level and large fluvial systems developed on the emerged shelf (Tija, 1980). High sedimentation rates (average=17.9 g⁻¹ cm⁻¹ kyr⁻¹) were reported during the last glacial period in this area (Wang, 1999a). Many terrestrial and marine records in this region suggest that winter monsoon was intensified during the last glacial period resulting in low air and sea surface temperature (SST) in the region (Pelejero et al, 1999b, Steinke et al, 2001, Sun et al. 2000, 2001). The intensified winter monsoon and low sea level during the last period brought high productivity in the SCS (Thunell et al., 1992; Wang et al., 1999, Jian et al., 1999, Kuhnt et al, 1999; Pelejero et al., 1999b) through the intensified upwelling, high surface water mixing rates and increased flux of terrestrial nutrients from exposed large coastal lowlands. The exact timing of variations in the SST and the relative sea level has been already well constrained in the southern SCS (e.g. Hanebuth et al, 2000, Steinke et al, 2001), however, the timing of the surface water productivity variations and the climatic variations have not been well understood.

We studied a core (GIK 18267-3) collected in the southern edge of the SCS basin. Palynomorphs (organic-walled dinoflagellate cysts, pollen and spore) are used as main proxies for variations in the surface water productivity and the climatic conditions in/around the southern SCS. The main objectives of this paper are to investigate the variations in the surface water productivity and the vegetation variations of the last 44 kyr in/around the southern SCS and to study and to compare in details the timing of variations in climate and surface water productivity.

1.1 PRESENT-DAY CONDITIONS IN THE STUDY AREA

The SCS surrounded by southern China, Philippines, Vietnam, Borneo, Malaysia and Indonesia is located in the tropical/subtropical climatic zones (Figure 1). Sea surface temperature (SST) varies from 27 to 29 °C during summer and from 20 to

29 °C during winter (Levitus and Boyer, 1994). The sea surface salinity (SSS) ranges from 31.6 to 34.6 psu. throughout the year (Levitus and Boyer, 1994). The predominant current direction of the SCS is strongly controlled by semi-annual reversal of monsoon regimes. During winter monsoon (October-March), the predominant current direction is to the southwest (Figure 2a). An anticlockwise gyre develops off middle Vietnam. During summer monsoon (May-August), the inflow water enters to the SCS from the Java Sea through the Karimata Strait and forms NE-trending currents along Vietnamese coast. A clockwise eddy develops in the central SCS in April (Wyrski, 1961) (Figure 2b).

The annual primary productivity of the South China Sea is low ($<100 \text{ gCm}^{-1}\text{y}^{-1}$ in the central SCS). High annual primary productivity ($>400 \text{ gCm}^{-1}\text{y}^{-1}$) is observed only in narrow bands along coasts (Platt et al, 1995). Summer upwelling is observed off southern Vietnam (Faughn, 1974; La Fond, 1963; La Fond, 1966; La Violette and Frontenac, 1967; Vo, 1995)(Figure 2e). This upwelling is induced by summer monsoon southwesterly wind. Zones of winter upwelling are observed north of the Sunda Shelf and the area northwest of Luzon (Wiesner et al. 1996; Liu et al, 2002)(Figure 2f).

The study area is located in a climatically critical zone between equatorial and tropical climate. Equatorial climate is characterized by fairly uniform conditions throughout the year and tropical climate is characterized by existence of distinct dry and wet seasons. The boundary between these climatic regimes is located ca 6-9°N in SE Asia (Nieuwolt, 1981). Climatic conditions of the study area are controlled by a semi-annual reversal of monsoon regimes. During winter monsoon, cold, dry and stable winds are coming from the large high-pressure cell over Siberia and Mongolia and the study area experiences a dry and cold season. The mean air-temperature varies from 24-26 °C at sea level during a winter monsoon in SE Asia (Nieuwolt, 1981). During summer monsoon, the whole SCS region is under the influence of southwesterly winds. The main source area of the southwesterly wind is the Indian Ocean. Most of the annual precipitation occurs during summer. The mean air-temperature varies from 27-29°C at sea level during summer (Nieuwolt, 1981). Land topography additionally influences the precipitation and the air-temperature patterns. Temperatures decrease with a normal lapse rate of ca. 0.6 °C per 100 m. Precipitation is much higher on high mountains due to orographic precipitation.

The vegetation cover is characterized by altitudinal shifts of dominant taxa in tropical SE Asia. The intertidal zone above mean sea level is colonized by mangrove species such as *Sonneratia*, *Rhizophoraceae* and *Nypa*. *Sonneratia* is an euryhaline taxon and can adapt to wide ranges of tidal regimes whereas *Rhizophoraceae* and *Nypa* are stenohaline taxa restricted mainly to narrow tidal range areas (Duke, 1992; Smith

III, 1992). Lowland is covered by very complex and highly diverse tropical rainforest

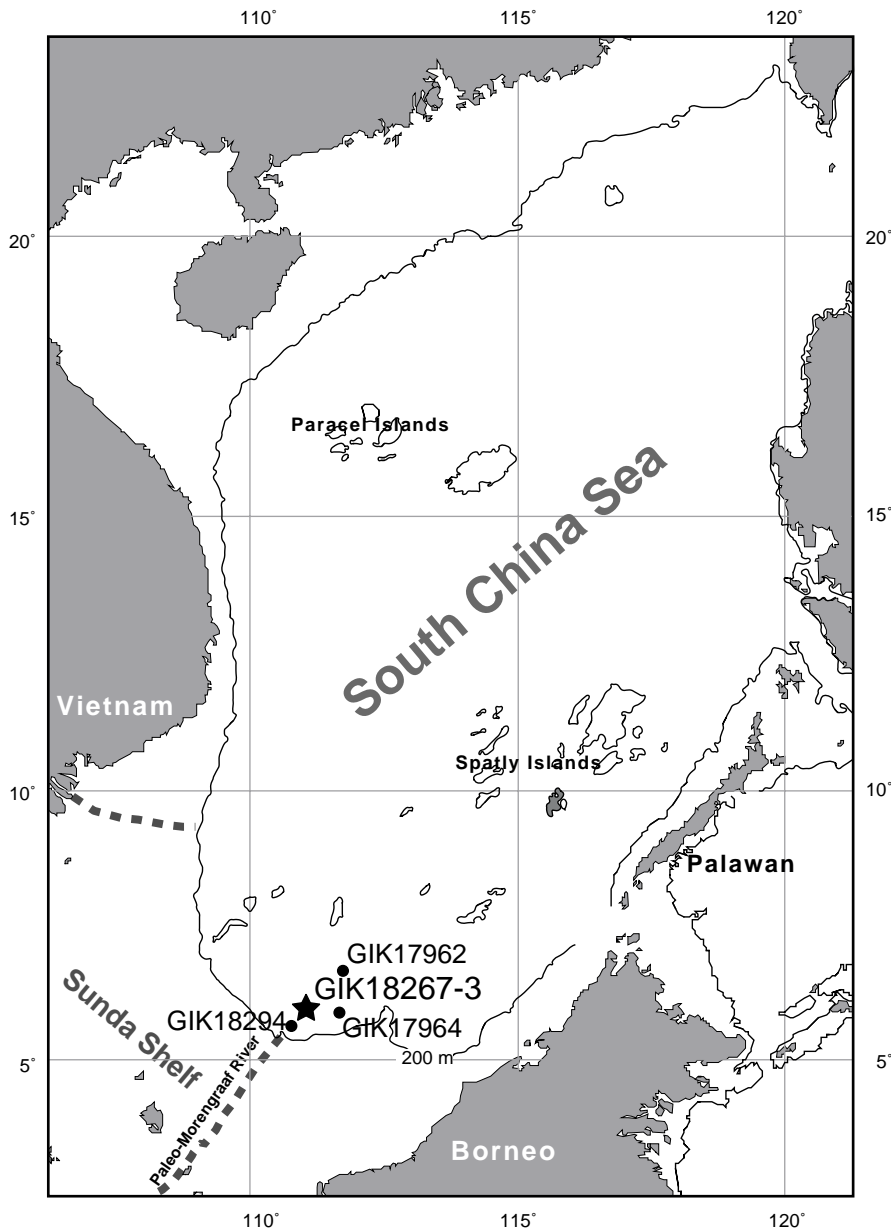


Figure 1, Locations of cores investigated (star) discussed (solid circles) in this chapter. Dotted lines indicate speculated courses of respective river during last sea-level lowstand.

taxa. The lowland rainforest occurs up to approximately 1000 m above sea-level (a.s.l.) (Flenley, 1996). Natural Savannah, dominated by Graminae, Compositae and *Cyperaceae*, occurs in some restricted areas in the Philippines and Borneo (Flenley, 1979b). Fire is probably responsible for the formation and the maintenance of Savannah (Flenley, 1979b). Lower montane forest extends up to about 2900-m a.s.l. and is characterized by occurrences of Fagaceae, Lauraceae and Hamamelidaceae. Above the lower montane forest, upper montane forest covers the area up to the forest limit (ca.

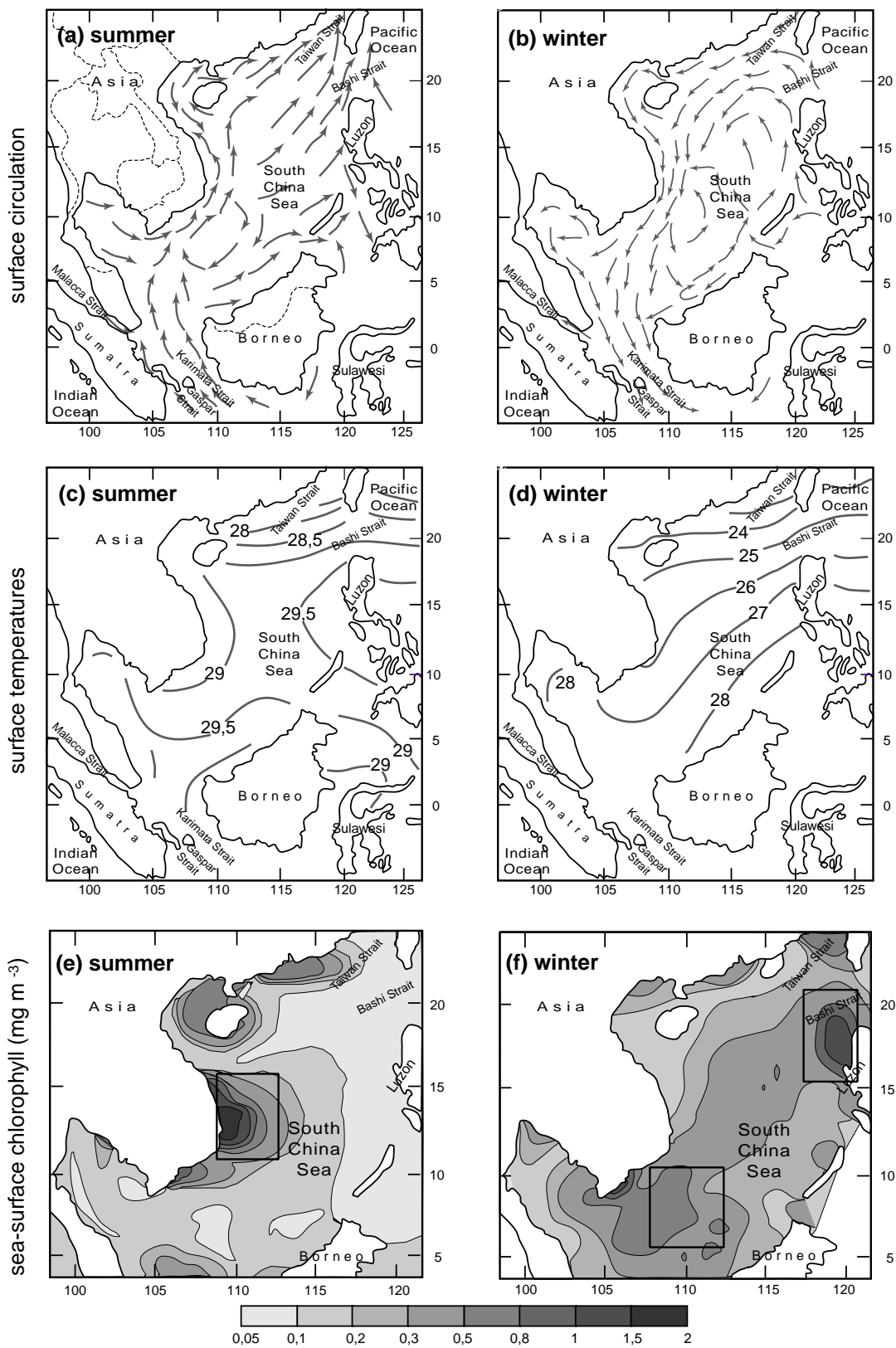


Figure 2. Present hydrographic conditions in the SCS: (a - b) surface circulation (after Wang, 1994); (c - d) sea-surface temperatures; Plots of temperatures were downloaded and redrawn from <http://ingrid.ideo.columbia.edu/SOURCES/.LEVITUS94>; (e - f) sea-surface chlorophyll (mg m^{-3}) distribution for August and December, rectangles are upwelling areas (after Liu *et al.*, 2002).

3800 m a.s.l.). *Podocarpus*, *Dacrydium*, *Dacrycarpus* and *Phyllocladus* dominate the upper montane forest (Johns, 1982). Above the forest limit, alpine grassland exists until the top. Although pines are widely present in the SE Asia, only a few taxa extend into the tropics (*P. ikedai* and *P. kwangtungensis*). Tropical pines have strong preference for seasonal climates with a dry season. The occurrences of tropical pines are so closely related to fire that these communities are often called 'fire-climax' (Goldammer and Panefiel, 1990).

2. MATERIALS AND METHODS

2.1 SAMPLE COLLECTION AND LABORATORY WORK

Core: Core GIK 18267-3(6:22.387 N, 111:49.126E; water-depth 1855 m; recovery 1409 cm) was obtained during cruise SONNE 115 "Sundaflut"(Stattegger, 1997) from the continental slope off Sunda Shelf using a 26 m piston corer (Figure 1). During the last sea-level lowstand, shallow plateaus north of core location emerged and formed islands.

The coring location was also located near the mouth of the paleo-Molengraaff River. The lithology of the core consisted of olive gray homogeneous hemi-pelagic clay with occasional dark organic-rich lenses. The actual sediment surface was lost during coring operations. Samples were taken from the core for isotopic, geochemical and palynological analysis using 10 cc pre-cleaned syringes.

Stable Isotope Analysis: Stable Oxygen and Carbon isotope analysis were performed on samples composed of 15-25 specimens of near surface dwelling planktonic foraminifera *Globigerinoides ruber* (D'ORBIGNY) s.s. (white) in the 250-400 μm size fraction. Before isotopic measurements, foraminiferal tests were manually crushed and then washed in ethanol (99.8 %) using an ultrasonic bath. Samples were dried at 40 °C overnight. Isotopic measurements were performed using a Finnigan MAT-251 mass-

spectrometry with Kiel-CARBOPREP automatic carbonate preparation line at the Leibniz Laboratory in Kiel University. The analytical precision of isotopic measurements was better than 0.04 ‰ PDB for $\delta^{13}\text{C}$ and 0.08 ‰ for $\delta^{18}\text{O}$ (Erlenkeuser, pers. comm.).

Geochemical Analysis: Total Organic Carbon (TOC) and total nitrogen (N) were measured at the University of British Columbia using flash-combustion gas chromatography on a Carlo-Erba elementary analyzer. Detailed descriptions are available from Verardo et al. (1990). Acetanelide ($\text{CH}_3\text{CONHC}^6\text{H}_5$) was used as a standard. Duplicate measurements confirm the analytical precision within $\pm 1.25\%$.

Palynological Study: Five grams of dry-sediments were treated with 10% HCl to

dissolve carbonate contents in sediments. During the HCl treatment, a tablet of *Lycopodium clavatum* was added to each sample in order to measure the concentrations of palynomorphs (Stockmarr, 1971). Then, the samples were sieved and concentrated through a 5 μ m-nylon sieve. During sieving, an ultrasonic bath of less than 30 seconds was applied to the sediments in order to disaggregate the clay contents of the sediments. The residues were then treated with 40% HF to remove siliceous sediments. The samples were left in HF without agitations until all siliceous sediments were dissolved. The samples were again sieved through 5 μ m nylon sieve with distilled water. The residues were mounted on slides with glycerine gel and sealed with paraffin wax. The use of oxidizing agents and hot acid were avoided because these agents can significantly degrade certain palynomorph groups (Dale, 1976).

Major groups of palynomorphs (dinoflagellate cyst, pollen, spore, tintinomorphs and freshwater algae) were identified and counted with a light microscope with magnifications of x400 and x800. Most organic-walled dinoflagellate cysts were identified up to species level in accordance with the classifications of Lentin and Williams (1993) and Rochen et al. (1999). *Brigantedinium* spp. was identified only up to genus level because *Brigantedinium* cysts often show poor cyst orientations that make positive identification of their archeopyle difficult. Some *Spiniferites*, which were difficult to identify, were counted as *Spiniferites* spp.

Correspondence Analysis (CA) was used to analyze cyst assemblage quantitatively. A CA was performed using the program CANOCO (ter Braak and Smilauer, 1998). Concentrations (cysts g⁻¹) of each taxa were used as input data for the CA. The samples with <70 counts were not included in the analysis.

Non-use of acetolysis during the sample processing made identification of pollen difficult. Only main montane taxa (*Podocarpus*, *Dacrydium* and *Phyllocladus*), main mangrove taxa (Rhizophoraceae, *Sonneratia* and *Nypa*), main grassland taxa (Graminae, Cyperaceae and Compositae) and main alpine taxa (*Abies*, *Picea*, *Pinus* and *Tsuga*) were identified for this study. Compositae was mainly composed of *Artemisia*. Unidentified pollen was also counted in order to calculate relative abundance of counted taxa. A CA was used to analyze pollen assemblages. Concentration values of main taxa (grains g⁻¹) were used as input file. The samples with less than 100 counts were not used for the analysis.

2.2 PROXIES

Proxies for influences of terrestrial organic matter (TOM) and of freshwater:

Ratio of terrestrial palynomorphs (pollen and spores) to marine pelagic palynomorphs (dinoflagellate cysts) (T:M ratio) and the TOC:N ratio are used as

qualitative proxies for the origin of organic matter and the influence of terrestrial nutrients in this study (Figure 5). Concentrations and accumulation rates of insect-pollinating mangrove pollen (Rhizophoraceae and *Sonneratia*) are used as proxies for the effects of offshore transport of coastal sediments, and of freshwater algae *Pediastrum* as proxies for effect of riverine freshwater plume at the coring location. T:M ratio is based on the differences in the source areas of respective palynomorph groups. The main problem associating with these palynomorph-based indices is their dependency on the sediment particle sizes. Pollen, spores, dinoflagellate cysts and *Pediastrum* are generally believed to act like silt-size particles in air and water (Dale, 1976; Traverse, 1988). According to Wagner and Dupont (1999), 45-75 % of bulk TOC is bounded to the grain-size fraction $<2\mu\text{m}$. Thus, if sediments consists of high proportions of $<2\mu\text{m}$ size sediments, these indices may not be accurate.

TOC:N ratio has been popularly used as proxies for terrestrial organic matter (TOM). TOC:N ratio is not sediment particle size dependent. However, recent studies showed that this index is very susceptible to various post-depositional processes (Wagner and Dupont, 1999). TOC:N ratio is susceptible to the preferential diagenetic remineralization of nitrogen (Emery et al., 1984), the amount of inorganic nitrogen bound in clay minerals (Calvert and Karlin, 1991) and the preferential uptake of nitrogen by benthic organisms (Wagner and Dupont, 1999). These factors can significantly alter the original signals of TOC:N ratio. Wagner and Dupont (1999) concluded that minor fluctuations in TOC:N ratio resulted likely from diagenetic effects.

Proxies for surface water productivity

Relative abundance of dinoflagellate cyst groups, sample score of the 1st CA axis and TOC are used as proxies for surface water productivity. According to Chapter 3, the distribution patterns of dinoflagellate cysts are primarily controlled either by the productivity of the surface water or effect of offshore cyst transport processes. Hence, with an assumption that the dinoflagellate distribution patterns are controlled by primary productivity, sample scores of 1st CA axis and relative abundance of dinoflagellate cyst group defined in Chapter 3 can be used as a proxy for qualitative surface water productivity. (Table 1 for group compositions).

Zonneveld et al. (2001) reported that organic-walled dinoflagellate cysts are susceptible to the species-dependent decay processes related to the variations in the bottom/pore water oxygen levels. They classified *Protoperidinium* taxa (e.g. *Brigantedinium* spp. and *Selenopemphix* spp.) as extremely sensitive. According to Thunell et al., (1992), the bottom water of the SCS was better oxygenated during the

last glacial period. Relative abundance of the Protopteridinium-dominated eutrophic group was higher during MIS 3 and 2 than during the Holocene. This may be due to the rapid burial rates during the last glacial period. However, the relative abundance of Protopteridinium-dominated eutrophic group increase during Holocene when burial rates are low (Wang, 1999b). On the basis of these results, we conclude that the effects of cyst decay relating to bottom/pore water oxygen level were minimum in cyst assemblages of core GIK 18267-3.

Proxies for climatic conditions

Relative abundance of ten major pollen types, sample scores of 1st CA axis of pollen and ratios of spore to pollen (S:P ratio) are used as proxies for climatic conditions. Van der Kaars (1991) used the S:P ratio as a proxy for humidity and/or temperature level. According to Tivy (1996), large-scale vegetation dynamics are governed mainly by temperature or/and precipitation gradients. Based on this, the sample scores of 1st CA axis of pollen are used as proxy for the temperature and/or humidity variations.

Interpretations of pollen assemblages in marine sediments are complex. Complex depositional processes often alter the original environmental signals. Pollen assemblages are especially influenced by the morphology-dependent dispersal potential of each pollen type. Therefore, it is important to consider the dispersal potential of each pollen type when pollen assemblages in marine sediments are interpreted.

Montane and tropical montane pollen in the SE Asia consist mainly of bisaccate pollen such as *Pinus* and *Podocarpus*. Bisaccate pollen is known to have high airborne and current transport potential (Mudie and McCarthy, 1994) and their relative abundance generally increases with increasing distance from the shoreline. However, a present-day pollen distribution pattern study in the SCS show that the relative abundance of *Pinus* show clear a north to south gradient, and rarely exceeds 10 % of the total pollen sum in the southern SCS (Sun et al., 1999). Thus, the distribution pattern of *Pinus* pollen mainly reflects the distribution pattern of temperate/subtropical *Pinus* taxa on land in the SCS(Sun et al. 1999).

According to Sun et al. (1999) and Van der Kaars (2001), other pollen types found in this study have low transport potentials and reflect well the vegetation types on nearby land.

2.2 STRATIGRAPHY AND AGE MODELS

The stratigraphy of GIK18267-3 is constrained by three Accelerator Mass Spectrometry (AMS) radiocarbon dates and Oxygen Isotopic record ($\delta^{18}\text{O}$) of surface

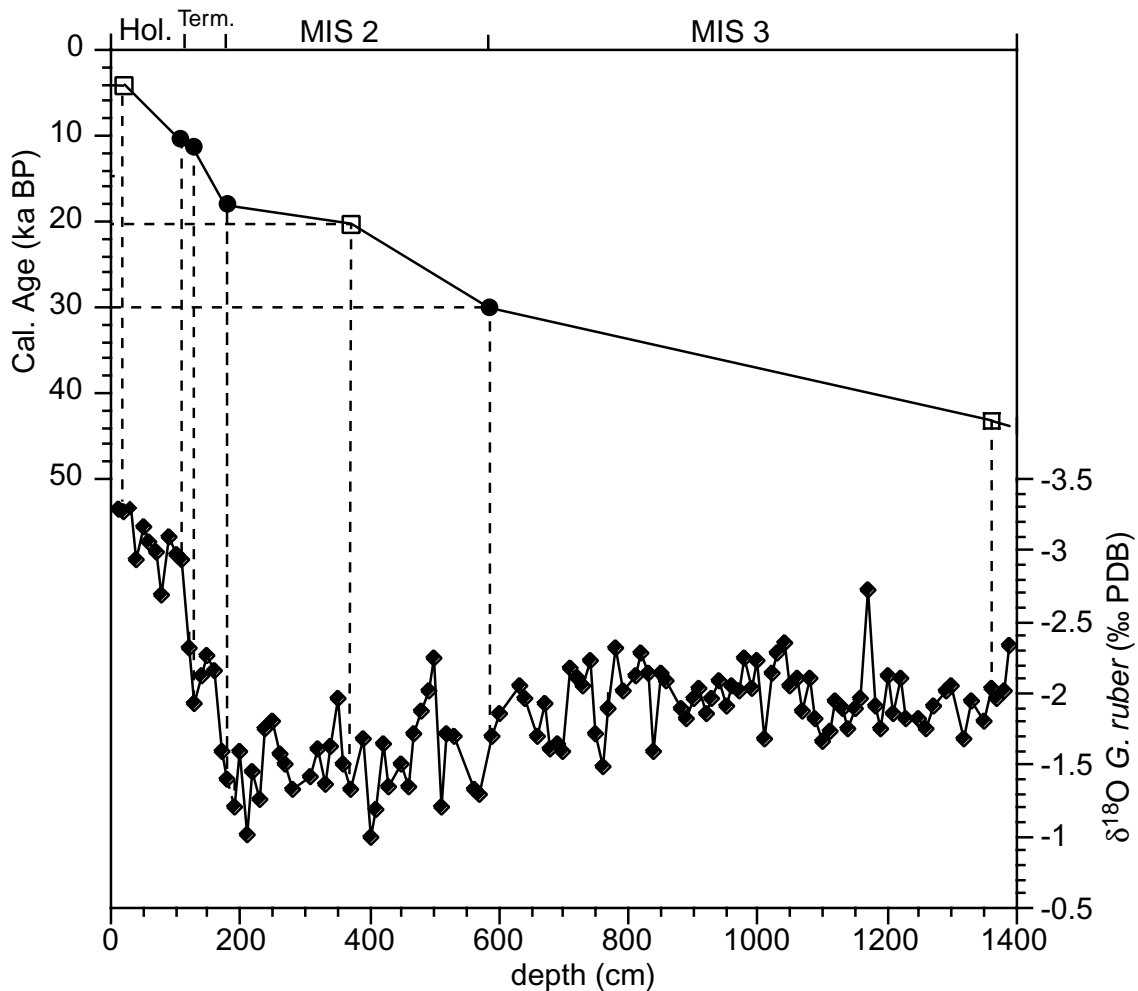


Figure 3. (a) Age-depth relationship of core GIK 18267-3, based on 3 AMS ^{14}C dates (empty squares) and 4 analogue dates (black circles) obtained by correlating $\delta^{18}\text{O}$ isotope events. (b) $\delta^{18}\text{O}$ depth profiles of planktonic foraminifera (*G. ruber*).

dwelling planktonic foraminifera species *Globigerinoides ruber* s.s. (white). AMS dating was performed at the Tandetron AMS facility at the Leibniz Laboratory at Kiel University. The youngest AMS dates were calibrated using the CALIB ver. 4.1.2. (Stuiver and Reimer, 1993) with corrections of -400 yr oceanic reservoir age (Bard, 1988) (Figure 3).

The ^{14}C age at 370 cm is calibrated using Wang et al (1999) with corrections of -400 yr oceanic reservoir age (Bard, 1988). Two other ages were calibrated using Voelker et al. (2000). In addition to the AMS dates, four dates were obtained through analogue correlations between $\delta^{18}\text{O}$ isotope events. 9.8 ka is assigned to 100 cm (core depth) as the end of Termination Ib (Winn et al, 1991). 11.6 ka is assigned to 120 cm as End of Younger Dryas Event (Stuiver et al., 1995) and 18.1 ka is assigned to 170 cm as the Termination I- MIS 2 (Voelker et al, 2000). 30.02 ka is assigned to 570 cm as the MIS2-3 boundary (Voelker et al, 2000) (see Table 2).

3. RESULTS

3.1 TOTAL ORGANIC CARBON (TOC) AND TOC/N

The signals of TOC concentrations contain distinct changes between marine isotope stages (Figure 4). During MIS 3, the concentration was low (average 0.82 % wt). During MIS 2, the concentration gradually increased. During Termination I, TOC reached maximum (1.05 % wt) at ca. 150 cm (ca.14.2 ka). The concentrations began to decrease sharply at ca. 130 cm (ca.11.6 ka). TOC remained low during the Holocene (average 0.83 % wt).

Table 1. Lists of dinoflagellate cyst taxa in eutrophic, mesotrophic and oligotrophic groups (after Chapter 3)

Eutrophic species	Mesotrophic species	Oligotrophic species
<i>Brigantedinium</i> spp.	<i>Impagidinium</i> spp.	<i>Impagidinium aculeatum</i>
<i>Operculodinium israelianum</i>	<i>Lingulodinium machaerophorum</i> (long processes)	<i>Impagidinium paradoxum</i>
<i>Quinquecuspidis concret</i>	<i>Operculodinium longispinigerum</i>	<i>Impagidinium patulum</i>
<i>Selenopemphix nephroides</i>	<i>Protoceratium reticulatum</i>	<i>Impagidinium sphaericum</i>
<i>Selenopemphix quanta</i>	<i>Lejeunecysta sabrina</i>	<i>Impagidinium striolatum</i>
<i>Stelladinium stellatum</i>	<i>Spiniferites bulloideus</i>	<i>Nematosphaeropsis labyrinthus</i>
<i>Lingulodinium machaerophorum</i> (short processes)	<i>Spiniferites bentori</i>	
<i>Votadinium calvum</i>	<i>Spiniferites delicatus</i>	
	<i>Spiniferites hypercnaethus</i>	
	<i>Spiniferites ramosus</i>	
	<i>Spiniferites mirabilis</i>	
	<i>Spiniferites membranaceus</i>	
	<i>Spiniferites</i> spp.	
	<i>Tuberculodinium vancampoeae</i>	

The ratio of TOC to total Nitrogen (TOC/N) remains in the full marine range throughout the core (6.01-8.65), but within these values TOC/N ratio shows clear variations between different marine isotope stages (Figure 5). During MIS 3, the ratios remain on a medium level between 6 and 8 (average 6.8). During Stage 2, TOC/N was high (ca. 7.5). During Termination I, the ratios reached their maximum (>8) at ca. 280 cm (ca. 19.3 ka), then decrease sharply toward the Termination-I/Holocene boundary. TOC/N remained constantly below 7 in Holocene.

3.2 DINOFLAGELLATE CYSTS

A total of 68 samples were analyzed for the palynological study. Concentrations of dinoflagellate cysts vary from 95 to 1031 cysts g⁻¹. Accumulation rates of dinoflagellate cysts vary from 1508 to 37010 cysts g⁻¹ kyr⁻¹. Dinoflagellate cyst assemblages in GIK 18267-3 are dominated by eutrophic species (for group composition, see Table 1). Relative abundance of eutrophic group varies from 42.37 to 96.72%. During MIS 3, the relative abundance of eutrophic and

Laboratory No.	depth (cm)	AMS- ¹⁴ C age (yr)	Error 1s (yr)	Foraminifera species	Description	Age (cal. Yr. B.P.)
KIA13858	20	4020	35	G. ruber & G. saculiffer		4012
	100	analogue			end of Termination Ib	9800#
	130	analogue			end of Younger Dryas	11600+
	170	analogue			beginning of H1	18100#
KIA13859	370	17020	90	Planktonic foraminifera		20520
		analogue			MIS2-3 boundary	30200*
KIA13860	1360	42420	1470/-1240	Planktonic foraminifera		43300

Table 2. AMS ¹⁴C ages and analogue ages in core GIK 18267-3. The youngest ¹⁴C age have been calibrated using Version 4.1.2 of the CALIB radiocarbon software (Stuiver and Reimer, 1993). The second ¹⁴C age have been calibrated using Wang *et al* (1999)*. The oldest AMS ¹⁴C age have been calibrated according to Voelker (2000). All AMS ¹⁴C ages were calibrated with corrections of -400 yr oceanic reservoir age (Bard, 1988). these ages are obtained through correlating $\delta^{18}\text{O}$ events with Winn *et al* (1991)¥, Stuiver *et al* (1995) +, Voelker (2000)* and Sarnthein *et al* (2000) #

mesotrophic groups fluctuated sharply. The highest relative abundance of mesotrophic group is observed during MIS 3. Between 790 and 470 cm (ca. 34-25.4 ka), relative abundance of eutrophic group increased gradually as abundance of mesotrophic group decreased. During MIS 2, the relative abundance of eutrophic group remained high until 310 cm (19.7 ka) then increased again until 260 cm (ca. 19.1 ka). Relative abundance of eutrophic groups reached their highest peak at ca. 260 cm (ca. 19.1 ka). During Termination I, eutrophic group decreased as mesotrophic and oligotrophic groups began to increase. Oligotrophic group reached it maximum relative abundance in early Holocene. Mesotrophic and eutrophic groups reached their maximum abundance at 60 cm (ca. 6.9 ka) and 30 cm (ca. 4.7 ka) successively.

The CA revealed that the 1st CA axis explains 20 % of variances in the dinoflagellate cyst data. During MIS 3, sample score of 1st CA axis scores fluctuated sharply around the medium values. The score was low during MIS 2, and remained low until the Stage 2/ Termination I boundary. After the Stage 2/Termination I boundary, the score began to increase and kept increasing until early Holocene. After reached the highest score in early Holocene, the score began to decrease at 80 cm (ca. 8.4 ka) and then stayed high until the top of the core.

3.3 POLLEN AND SPORES

A total of 10 major taxa of pollen are plotted in Figure 6. The variations of

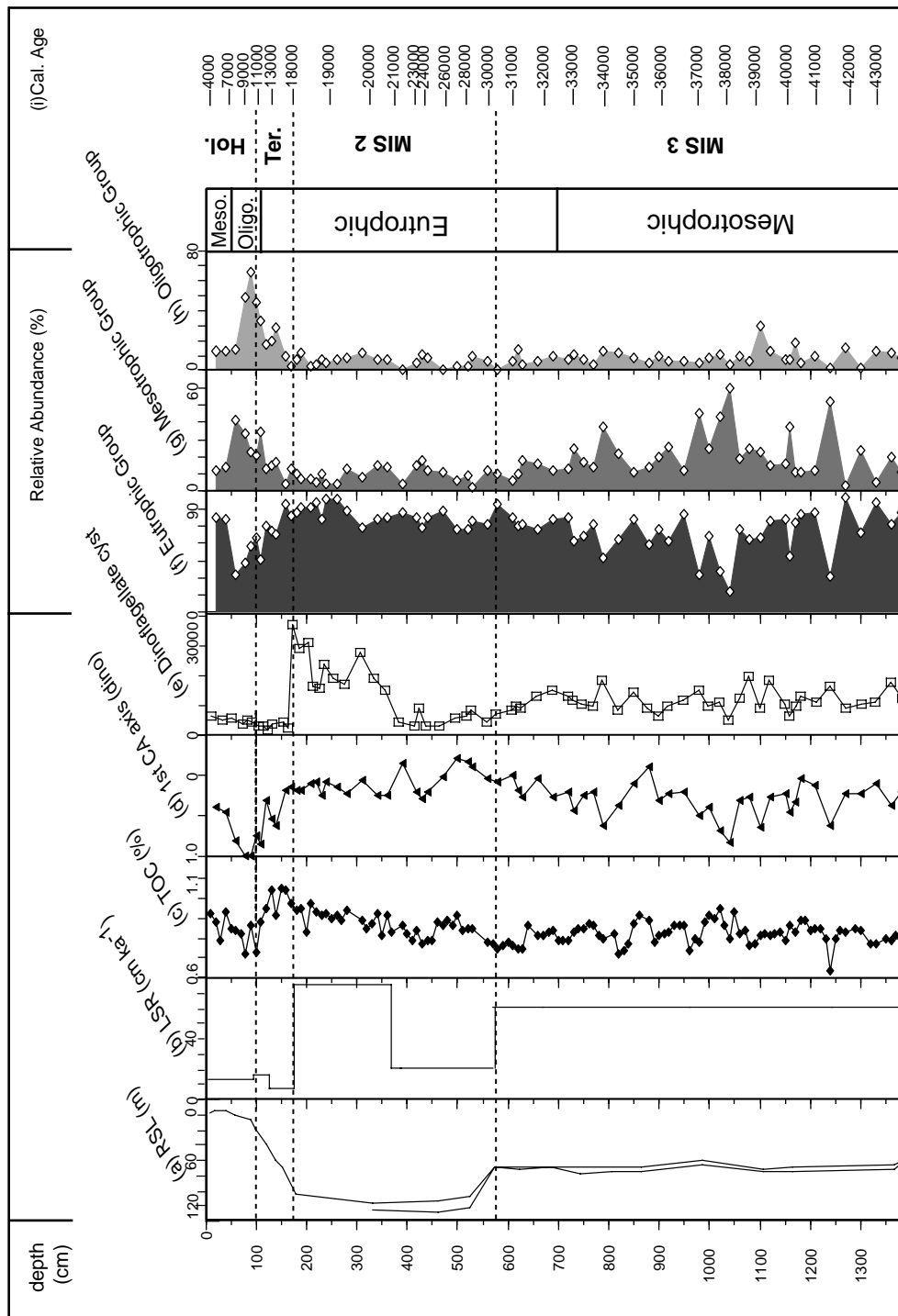


Figure 4. (a) Relative sea-level curve (adapted from Chappell, 2001), (b) changes in linear sedimentation rates (cm kyr⁻¹), (c) Total organic carbon in sediments (%), (d) Depth scores of 1st CA axis, (e) Accumulation rate of dinoflagellate cysts, Relative abundance of (f) eutrophic group, (g) mesotrophic group, (h) oligotrophic group, (i) Calibrated Ages (Cal. Ages are obtained by interpolations between 5 age-controlled points)

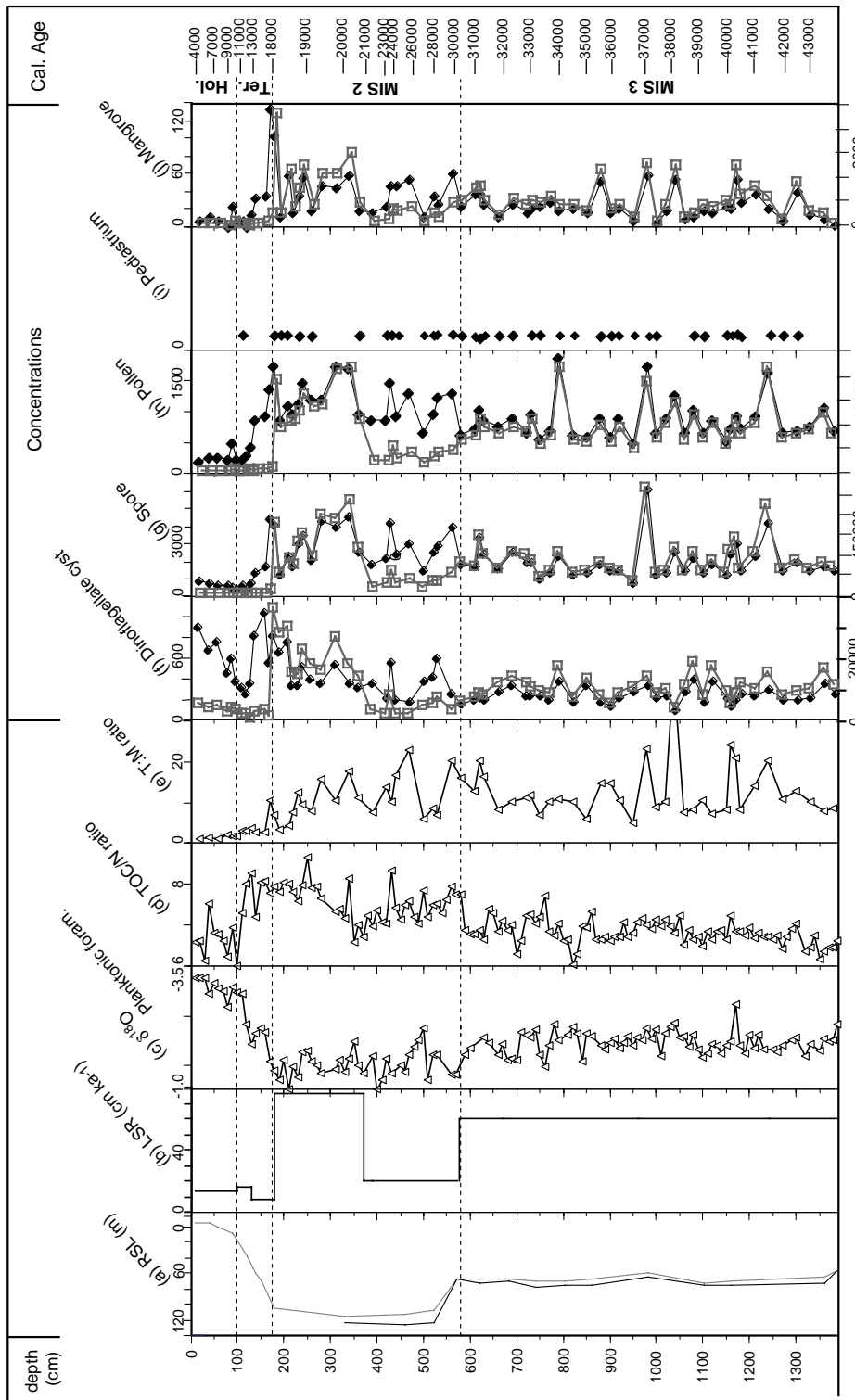


Figure 5. (a) Relative sealevel curve (adapted from Chappell, 2001), (b) Changes in linear sedimentation rates (cm kyr⁻¹), (c) δ¹⁸O ‰ (PDB) of planktonic foraminifera (*G. ruber*), (d) ratios of TOC to N in sediments, (e) ratios of terrestrial palynomorphs (pollen and spore) to marine pelagic palynomorphs (dinoflagellate cysts). Concentrations (cyst g⁻¹) (black square) and accumulation rates (cyst g⁻¹ kyr⁻¹) (empty square) of dinoflagellate cysts (f), spore (g), pollen (h), occurrence of freshwater alga Pediastrum (i), mangrove pollen (*Rhizophoraceae*, *Sonneratia* and *Nyssa*) (j), linear interpolated Cal. Age (k)

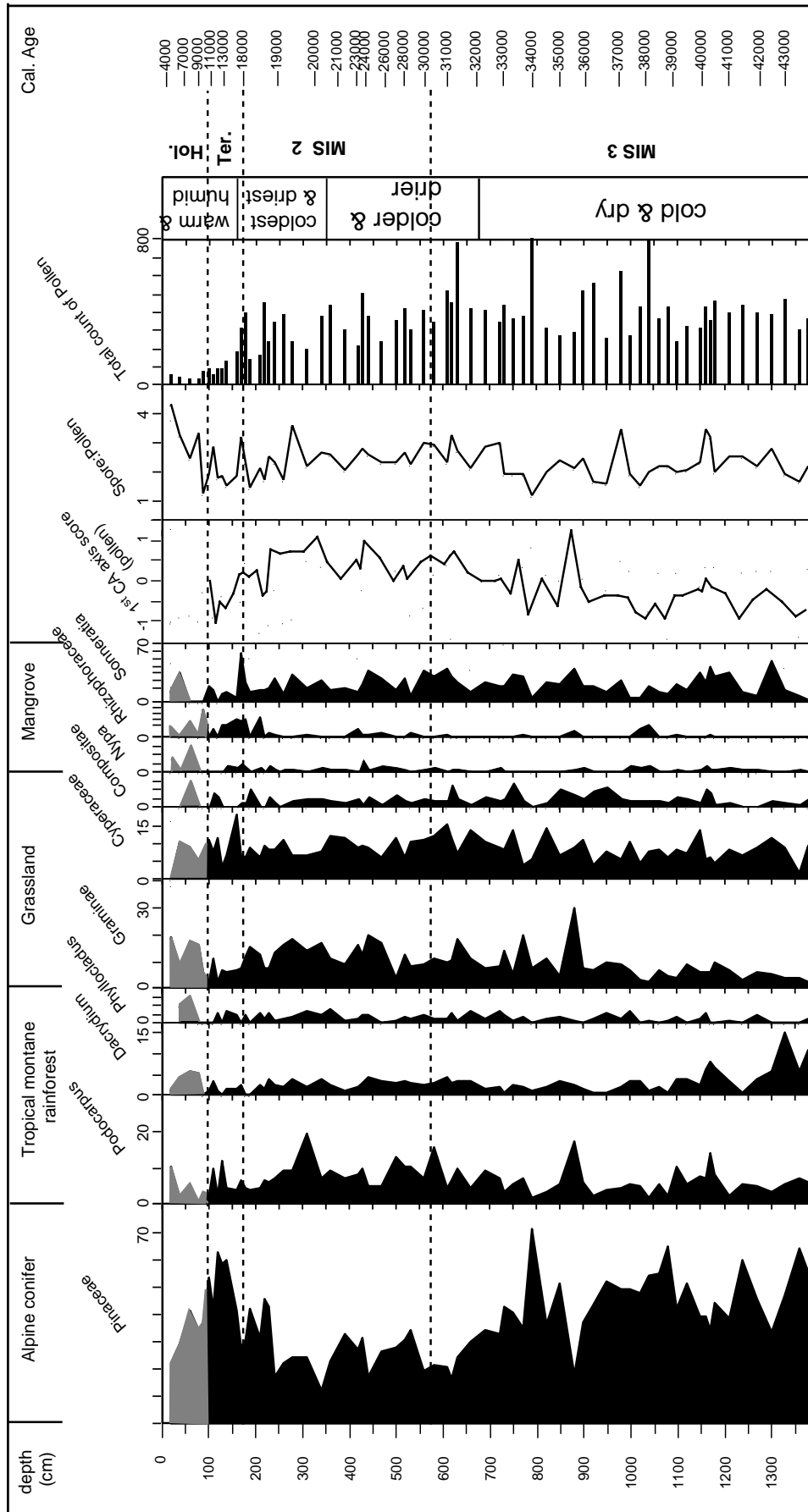


Figure 6. Relative abundances(%) of major pollen types, scores of 1st CA axis(pollen), spore:pollen ratios, total counts of pollen. The shaded sections in the pollen diagram indicate that total pollen counts were <100 grains and is likely to be unreliable. The cal. age are obtained through linear interpolations of 5 age-controlled points. The different stage boundaries are determined according to the $\delta^{18}O$ of planktonic foraminifera profiles.

pollen and spore concentrations and accumulation rates do not differ from each other much throughout the core (Figure 5). During MIS 3, the concentrations of pollen and spore remained commonly low. The concentrations began to increase gradually at MIS 3/2 boundary and reached their maximum around 320 cm (20 ka) and then began to decrease sharply toward the Termination-I/Holocene boundary. During the Holocene, the both values remained extremely low.

Alpine conifer (Pinaceae) dominates the assemblages with high relative abundance throughout the core (Figure 6ab). Pollen assemblages during MIS 3 were similar to these during MIS 2 with high relative abundance of alpine conifer. Marked differences between MIS 3 and MIS 2 are higher relative abundance of tropical montane forest and grassland, and lower relative abundance of alpine conifer during MIS 2. Relative abundance of alpine conifer decreased toward 340 cm (ca. 20.1 ka) as relative abundance of tropical montane forest pollen and gramineae began to increase. At the Stage 2/Termination I boundary, relative abundance of alpine conifer began to increase toward the Termination-I/Holocene boundary as relative abundance of tropical montane forest begin to decrease gradually. During Holocene, relative abundance of all taxa fluctuated sharply.

The CA revealed that the 1st CA axis explain 53.7 % of total variance in the data. During MIS 3, the scores were medium level. The scores began to increase gradually at 790 cm (ca.33.8 ka). During MIS 2, the sample scores remained high. The sample scores reached the highest level between 360 cm and 240 cm (20.4-18.8 ka). The scores began to decrease at 240 cm (ca. 18.8 ka). The scores continued decreasing until ca. 110 cm (10.4 ka).

OTHER PALYNOFORMS

Freshwater algae: Pediastrum occurred commonly during MIS 3 and MIS 2(Figure 5). *Pediastrum* occurred only once during Termination I. During Holocene, the occurrence of *Pediastrum* was not observed.

T:M ratio: The ratios of terrestrial palynomorphs (pollen and spore) to marine pelagic palynomorphs (dinoflagellate cysts) during MIS 3 stayed in medium level (ca. 13)(Figure 5). The ratio stayed high (ca. 18) between 630 and 560 cm (ca. 31.2-29.7 ka). Then, the ratio became low (ca. 8) between 530 and 500 cm (ca. 28.3-26.8 ka). The ratio increased again at 500 cm (ca.26.8 ka), and then decreased gradually toward Holocene. The ratio remained low through Holocene.

4. DISCUSSION

4.1 INFLUENCE OF TERRESTRIAL ORGANIC MATTER AND

FRESHWATER

During MIS 3, the T:M ratio, the concentration and accumulation rate of mangrove pollen indicated that the influence of TOM in TOC fluctuated sharply around a medium level. During MIS 2, the T:M ratio, the TOC:N ratio, the accumulation rates of mangrove pollen indicate that the influence of TOM was higher than during MIS 3. This was probably caused by the low sea level. During Termination I, T:M ratio and accumulation rate of mangrove pollen indicated that influence of TOM decreased rapidly. During MIS 3 and 2, constant occurrence of *Pediastrum* indicate that the core site was under influence of freshwater plume. *Pediastrum* occurred only once during Termination I. This indicated that freshwater plume had minimum influence during Termination I. During Holocene, the influence of both TOM and of freshwater remained low. Those variations was probably caused by increase in distance between land and the core site due to the rapid sea level rise.

4.2 VARIATIONS IN SURFACE WATER PRODUCTIVITY

4.2.1 HISTORY OF THE SURFACE WATER PRODUCTIVITY

During MIS 3, abundance of trophic group, sample scores of 1st CA axis and TOC indicate that the surface water in the studied area was mesotrophic. During MIS 2, all dinoflagellate-based proxies indicate that the surface water was eutrophic until MIS 2/Termination I boundary. The surface water became gradually oligotrophic during Termination I, and became oligotrophic in early Holocene. Productivity increased gradually again toward the late Holocene. Although only 2 points represent this change, similar change is recorded in a dinoflagellate cyst record from the northern SCS (Wu and Sun, 2000) and a coccolithophora-based paleoproductivity record from the Sulu Sea (de Garidel-Thoron et al., 2001).

4.2.2 POSSIBLE CAUSES OF PRODUCTIVITY VARIATIONS

The main causes and mechanisms of the variations in the surface water productivity in the southern SCS are not well understood to date. Several scenarios can be considered for the possible causes from the geographical settings. The 1st possibility is the variations of river-borne nutrient supply. Since the core location was near the mouth of paleo-Molengraaff River during the last glacial period, it is reasonable to think that variations in the river discharge might have caused the variations in the nutrient supply to the area and consequently leading to the productivity variations.

The 2nd scenario is variations of nutrient supply through variations in upwelling strength and/or in surface water mixing rates as in the model by Ittekkot (1991).

Upwelling occurs in the studied area during winter monsoon at present (Wiesner et al. 1996; Liu et al, 2002). The intensity of this upwelling is controlled by the strength of southward winds. During the last glacial period, many terrestrial and marine records indicate that the East Asian winter monsoon intensified and lowered air and sea surface temperature in the SE Asia and the SCS (An, 2000; Huang, 1997; Huang et al., 1997; Wang and Wang, 1990). If upwelling occurred during the last glacial period, intensified winter monsoon could induce stronger upwelling activities and/or higher mixing rates that lead to higher productivity.

4.3 TERRESTRIAL ENVIRONMENT

4.3.1 PALEOCLIMATIC RECONSTRUCTION

The pollen spectra of GIK 18267-3 show similar trends as the pollen spectra of GIK 17962 (Sun et al., 2002). During MIS 3 and MIS 2, high relative abundance of alpine conifer pollen and of tropical montane pollen indicated that alpine conifer and tropical montane forests expanded to a lower altitude in mountains in the SE Asia. This expansion is commonly observed in pollen spectra from lakes in the SE Asia, and is interpreted as temperature cooling (e.g. Flenley, 1979a; Flenley, 1996) (Figure 6). Low S:P ratio and high relative abundance of grassland pollen indicates moderately dry conditions. Lowland tropical rainforest pollen was not counted separately in this study. However, Sun et al. (2002) and Sun et al. (2000) indicate clearly the presence of lowland rainforest as the dominant vegetation cover on the emerged Sunda Shelf during MIS 3 and 2. Thus, these results may indicate that tropical lowland rainforest with small patches of grassland might have been existing on the emerged Sunda Shelf during MIS 3. This interpretation is consistent with the records in northeast Thailand lowland by Penny (2001). High relative abundance of *Sonneratia* pollen indicate that *Sonneratia*-dominated mangrove was present in the coastal area on the emerged Sunda Shelf and/or Borneo paleo-coastal areas.

During MIS 2, relative abundance of tropical montane forest and grassland pollen was higher than during MIS 3. These results indicate further cooling and somewhat drier conditions than during MIS 3. However, as during MIS 3, the dominance of tropical lowland rainforest pollen was reported by Sun et al. (2002) and Sun et al. (2000). This suggests that the dryness was only relative to today's humid conditions and was not severe enough to replace tropical lowland rainforest on the emerged Sunda Shelf. High relative abundance of tropical montane forest pollen indicate further expansion of the tropical montane forest to lower altitude, as reported from terrestrial pollen records in the South East Asia (Flenley, 1979a; Flenley, 1996;

van der Kaars, 1990; van der Kaars and Dam, 1995).

A major environmental change is observed at ca. 19 ka. The relative abundance of tropical montane forest and of grassland pollen begin to decrease at this time. This was probably caused by contraction of montane forest band, indicating warmer and more humid conditions. Constant occurrences of *Sonneratia* and increase of relative abundance of Rhizophoraceae indicate that mangrove was continuously present in the coastal area on the emerged Sunda Shelf or/and Borneo during MIS 2.

Increase in the relative abundance of alpine conifer pollen during Termination I was probably caused by the combined effects of increasing distance from the shoreline due to the sea-level rise and the high transport potentials of alpine conifer pollen. The gradual decrease in relative abundance of *Podocarpus* and *Graminae* as well as increasing S:P ratios indicate warmer and more humid conditions. The decrease in the pollen accumulation rates was also caused by the increasing distance from the paleo-shoreline and by the disappearance of Molengraaff River due to the sea-level rise.

During the Holocene, decreasing pollen and spore accumulation rates reflect increasing distance from the land. The dominance of alpine conifer is caused by the high transport potential of Pinaceae pollen. The increase in the S:P ratios indicates warmer and more humid conditions. However, low total pollen counts (<100 grains g⁻¹) of pollen during the Holocene make a sound interpretation difficult.

4.3.2 POSSIBLE CAUSES OF CLIMATIC VARIATIONS

The climatic variations (for different MIS) inferred from pollen assemblages in core GIK 18267-3 are probably related to the variations in the East Asian monsoon dynamics. During MIS 3, lower air temperature signals recorded were probably caused by strong winter monsoon which bring cold air in the region, and slightly drier signal recorded as expansion of grassland may be due to weaken summer monsoon leading to lower annual precipitation. During MIS 2, further cooling signal may indicate further intensification of winter monsoon, and further drier signal recorded may indicate further weakening of summer monsoon. Similar variations in winter and summer monsoon dynamics are reported from a loess-based reconstruction (Xiao et al, 1995). Thus, we concluded that the climatic variations recorded in pollen assemblages were caused by stronger winter monsoon or/and by weaker summer monsoon.

4.4 LAND-SEA CORRELATION

In longer scale (for different MISs), variations observed in sample scores of pollen 1st CA axis resembled with variations of 1st CA axis of dinoflagellate cysts

(Figure 7). Cold and dry climate corresponded to eutrophic surface water condition, and warm and moist climate corresponded to oligotrophic condition. However, on finer scale (millennial), some differences can be observed. During MIS 3, the changes in temperature/humidity succeed the changes in surface water productivity by a short period (<1 kyr). For example, the peaks of warm and moist climate periods at 1060 cm (ca. 38.5 ka) and 820 cm (ca. 34.5 ka) led peaks of low productivity periods. During MIS 2, peaks of brief warm and moist periods corresponded to peaks of brief high productivity periods. These results indicate that surface water productivity variations and climatic variations may not be controlled by same mechanism in finer scale. However at present, the sampling resolution is too low to determine accurate lead and lag.

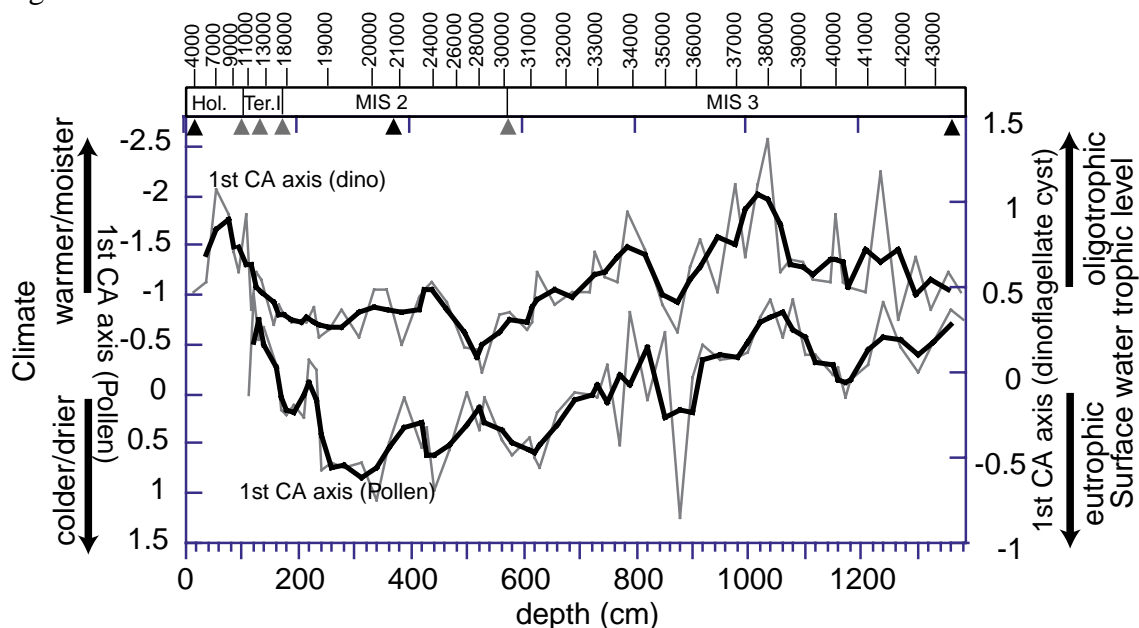


Figure 7. Variations in 1st CA axis scores of pollen and dinoflagellate cysts. Triangles indicate age-controlled points.

5. CONCLUSIONS

During the last 44 kyr, the samples from core GIK 18267-3 recorded drastic changes in surface water productivity and climatic conditions. During the MIS 3, the studied area experienced highly fluctuated environmental conditions. The condition is characterized by mesotrophic surface water and colder/slightly drier climate than present. During MIS 2, the conditions are characterized by the eutrophic surface water and colder/drier climatic conditions than during MIS 3. At ca. 19 ka, both climate and surface water productivity conditions began to change. The surface water productivity gradually decreased and the climatic conditions rapidly become warmer/more humid. The surface water productivity continues to decline until early Holocene, but then

increased toward middle Holocene. These environmental variations were probably caused by dynamics of summer and winter monsoon.

Comparison of variations in the 1st CA axis scores of dinoflagellate cyst (surface water productivity) to of the 1st CA axis scores of pollen (atmospheric temperature/humidity) showed that in the long time scale (for different MISs), the MIS of high surface productivity corresponded to cold and dry climatic conditions, and period of low surface productivity corresponded to warm and moist climatic conditions.

REFERENCES

- An, Z., 2000. The history and variability of the East Asian paleomonsoon climate. In: D. Alverson Keith, F. Oldfield and S. Bradley Raymond (Editors), Past global changes and their significance for the future. Pergamon. Oxford, United Kingdom. 2000.
- Bard, E., 1988. Correction of accelerator mass spectrometry ^{14}C ages measured in planktonic foraminifera: Paleoceanographical implications. *Paleoceanography*, 3: 635-645.
- Calvert, S.E. and Karlin, R.E., 1991. Relationship between sulfur, organic carbon, and iron in the modern sediments of the Black Sea. *Geochim Cosmochim Acta*, 55: 2483-2490.
- Chappell, J., 2001. Coral Terraces, Sea Level Changes, Ice Sheets and Isotopes. *Nova Acta Leopoldina NF*, 88, Nr. 331, 195-204.
- Dale, B., 1976. Cyst formation, sedimentation, and preservation; factors affecting dinoflagellate assemblages in Recent sediments from Trondheimsfjord, Norway. *Review of Palaeobotany and Palynology*, 22(1):
- de Garidel-Thoron, T., Beaufort, L., Linsley, B.K. and Dannenmann, S., 2001. Millennial-scale dynamics of the East Asia winter monsoon during the last 200,000 years. *Paleoceanography*, 16(5): 491-502.
- Duke, N.C., 1992. Mangrove floristics and biogeography. In: A.I. Robertson and D.M. Alongi (Editors), *Tropical Mangrove Ecosystems. Coastal and estuarine studies*. American Geophysical Union, Washington DC, pp. 63-100.
- Emery, K.O., Johns, I.A. and Honjo, S., 1984. Organic films on particulate matter in surface waters off eastern Asia. *Sedimentology*, 31(4): 503-514.
- Faughn, J.L., 1974. NAGA Expedition: Station Index and Data. NAGA Report, Vol. 1, Scripps Institute of Oceanography, La Jolla.
- Flenley, J.R., 1979. *The equatorial rain forest*. Butterworth & Co ltd, 162 pp.
- Flenley, J.R., 1996. Problems of the Quaternary on Mountains of the Sunda-Sahul region. *Quaternary Science Reviews*, 15: 549-555.
- Flenley, J.R., 1979. Present vegetation and its biogeographical problems. In: J.R. Flenley (Editor), *The equatorial rainforest*. Butterworth & Co ltd, pp. 1-14.
- Goldammer, J.G. and Penefiel, S.R., 1990. Fire in the Pine-Grassland biomes of tropical and subtropical Asia. In J.R. Goldammer (Editor), *Fire in the Tropical Biota; Ecosystem Processes and Global Challenges*. Springer Verlag, Berlin, pp.45-62.
- Hanebuth, T., Stattogger, K. and Grootes, P., 2000. Rapid flooding of the Sunda Shelf: a late-glacial sea-level record. *Science*, 288: 1033-1035.
- Huang, C., Wu, S., Zhao, M., Chen, M., Wang, C, Tu, X, Yuan, P.B., 1997. Surface ocean and monsoon climate variability in the South China Sea since the last glaciation. *Marine Micropaleontology*, 32: 71-94.

- Huang, C.Y. et al., 1997. Deep sea and lake records of the Southeast Asian paleomonsoons for the last 25 thousand years. *Earth and Planetary Science Letters*, 146(1-2): 59-72.
- Ittekkot, V., 1991. Particle flux studies in the Indian Ocean. *EOS*, 72(47): 525-527.
- Jian, Z. et al., 1999. Benthic foraminiferal paleoceanography of the South China Sea over the last 40,000 years. In: M. Sarnthein and P. Wang (Editors), *Response of West Pacific marginal seas to global climate change*. Marine Geology. Elsevier, Amsterdam, Netherlands, pp. 159-186.
- Johns, R.J., 1982. Plant zonation. In: J.L. Gressitt (Editor), *Biogeography and ecology of New Guinea*. Dr. W. Junk Publishers, Hague.
- Kuhnt, W., Hess, S. and Jian, Z., 1999. Quantitative composition of benthic foraminiferal assemblages as a proxy indicator for organic carbon flux rates in the South China Sea. In: M. Sarnthein and P. Wang (Editors), *Response of West Pacific marginal seas to global climate change*. Marine Geology. Elsevier, Amsterdam, Netherlands, pp. 123-157.
- La Fond, E.C., 1963. Physical oceanography and its relation to marine production in the South China sea. In: S.I.o. Oceanography (Editor), *Ecology of the Gulf of Thailand and the South China Sea, a report on the results of the NAGA expedition, 1959-1961*. Scripps Institute of Oceanography Contribution Series, La Jolla, USA, pp. 5-33.
- La Fond, E.C., 1966. South China Sea, *The Encyclopedia of Oceanography*. Reinhold Publishing Corp., New York, pp. 829-836.
- La Violette, P.E. and Frontenac, T.R., 1967. *Temperature, Salinity and Density of the World's Oceans: South China Sea and adjacent Gulfs*. US Naval Oceanographic Office, Washington D.C., 134 pp.
- Lentin, J.K. and Williams, G.L., 1993. *Fossil Dinoflagellates: Index to Genera to Species, 1993 Edition*. AASP Contribution Series, 28. American Association of Stratigraphical Palynologists, Dallas, 864 pp.
- Levitus, S. and Boyer, T.P., 1994. *World Ocean Atlas 1994*. U.S. Dept. of Commerce, Washington D.C., 117pp.
- Liu, K.-K., Chao, S.Y., Shaw, P.T., Gong, G.C., Chen, C.C., Tang, T.Y., 2002. Monsoon forced chlorophyll distribution and primary production in the South China Sea: observations and a numerical study. *Deep Sea Research I*, 49, 1387-1412.
- Mudie, P.J. and McCarthy, F.M.G., 1994. Late Quaternary pollen transport processes, western North Atlantic: data from box models, cross-margin and N-S transects. *Marine Geology* 118,79-105.
- Nieuwolt, S., 1981. The climates of continental Southeast Asia. In: K. Takahashi and H. Arakawa (Editors), *Climates of southern and western Asia*. World Survey of Climatology. Elsevier Scientific Publishing, Amsterdam, pp. 1-38.
- Pelejero, C., Kienast, M., Wang, L. and Grimalt, J.O., 1999. The flooding of Sundaland during the

- last deglaciation; imprints in hemipelagic sediments from the southern South China Sea. *Earth and Planetary Science Letters*, 171(4): 661-671.
- Penny, D., 2001. A 40,000 year palynological record from north-east Thailand; implication for biogeography and paleo-environmental reconstruction. *Palaeogeography, Palaeoclimatology, Palaeoecology*, 171: 97-12
- Platt, T., Sathyendranath, S. and Longhurst, A., 1995. Remote sensing of primary production in the ocean: promise and fulfillment. *Philosophical Transactions of the Royal Society of London, Series A: Mathematical and Physical Sciences*, B248,191-202.
- Rochon, A., de Vernal, A., Turon, J.L., Matthiessen, J. and Head, M.J., 1999. Distribution of recent dinoflagellate cysts in surface sediments from the North Atlantic Ocean and adjacent seas in relation to sea-surface parameters. *AASP Contribution Series 35*, 35. American Association of Stratigraphical Palynologists Foundation, Dallas, 152 pp.
- Smith III, T.J., 1992. Forest structure. In: A.I. Robertson and D.M. Alongi (Editors), *Tropical Mangrove Ecosystems*. American Geophysical Union, Washington, pp. 101-136.
- Stattegger, K., Kuhnt, W., Wong, H.K., Bühring, C. Haft, C., Hanebuth, T., Kawamura, H., Kienast, M., Lorenc, S., Lotz, B., Lüdman, T., Lurati, M., Mühlhan, N., Paulsen, A.M., Paulsen, J., Pracht, J., Putar-Roberts, A., Hung, H.Q., Richter, A., Salomon, B., Schimanski, A., Steinke, S., Szarek, R., Nhan, N.V., Weinelt, M., Winguth, C., 1997. Cruise Report SONNE 115 ``SANDAFLUT``. *Berichte - Reports, Geologisch-Palaeontologisches Institut und Museum, Christian-Albrechts-Universitaet Kiel*, 86. Christian-Albrechts-Universitaet Kiel, Geologisch-Palaeontologisches Institut und Museum, Kiel, Federal Republic of Germany, 211, pp.
- Steinke, S., Kienast, M., Pflaumann, U., Weinelt, M. and Stattegger, K., 2001. A high resolution sea-surface temperature record from the tropical South China Sea (16,500-3,000 yr B.P.). *Quaternary Research*, 55: 352-362
- Steinke, S., 2001. Sedimentological and climate changes during the Last Deglaciation recorded in cores from the Sunda Shelf margin and continental slope (southern South China Sea). Ph.D. Thesis, Institut fuer Geowissenschaften, Christian Albrechts Universitaet zu Kiel, Kiel.
- Stockmarr, J., 1971. Tablets with spores used in absolute pollen analysis. *Pollen et Spores*, 13: 615-621.
- Stuiver, M., Grootes, P.M. and Braziunas, T., 1995. The GISP $\delta^{18}\text{O}$ Climate record of the past 16,500 years and the role of the Sun, Ocean and volcanoes. *Quaternary Research*, 44: 341-354.
- Stuiver, M. and Reimer, P.J., 1993. Extended (super 14) C data base and revised CALIB 3.0 (super 14) C age calibration program. In: M. Stuiver and A. Long (Editors), *Calibration 1993. Radiocarbon*. American Journal of Science, New Haven, CT, United States, pp. 215-230.
- Sun, X., Li, X. and Beug, H.J., 1999. Pollen distribution in hemipelagic surface sediments of the

- South China Sea and its relation to modern vegetation distribution. *Marine Geology*, 156: 211-226.
- Sun, X., Li, X. and Luo, Y., 2002. Vegetation and climate on the Sunda Shelf of the South China Sea- pollen results from ODP Station 17962. *Acta Botanica Sinica*, 6.
- Sun, X., Li, X., Luo, Y. and Chen, X., 2000. The vegetation and climate at the last glaciation on the emerged continental shelf of the South China Sea. *Palaeogeography, Palaeoclimatology, Palaeoecology*, 160(3-4): 301-316.
- ter Braak, C.J.F. and Smilauer, P., 1998. *CANOCO 4*. Center of Biometry, Washington, 351 pp.
- Thunell, R.C., Miao, Q., Calvert, S.E. and Pedersen, T.F., 1992. Glacial-Holocene biogenic sedimentation patterns in the South China Sea; productivity variations and surface water pCO₂ (sub 2). *Paleoceanography*, 7(2): 143-162.
- Tjaja, H.D., 1980. The Sunda Shelf, Southeast Asia. *Zeitschrift für Geomorphologie*. N.F., 24: 405-427.
- Tivy, J., 1996. *Biogeography: A study of plants in the ecosphere*. 3rd Edition, Longman, Harlow.
- Traverse, A., 1988. *Paleopalynology*. Unwin Hyman, Boston, 600 pp.
- van Andel, T.H., Heath, G.R. and Moore, T.C., 1975. Cenozoic history and paleoceanography of the central Equatorial Pacific Ocean.
- van der Kaars, S., 1990. Late Quaternary vegetation and climate of Australasia as reflected by the palynology of eastern Indonesian deepsea piston-cores. monograph Thesis, University of Amsterdam, Amsterdam, 71 pp.
- van der Kaars, S., 2001. Pollen distribution in marine sediments from the south-eastern Indonesian waters. *Palaeogeography, Palaeoclimatology, Palaeoecology*, 171: 341-361.
- van der Kaars, W.A., 1989. Aspects of Late Quaternary palynology of eastern Indonesian deep sea cores. *Netherlands Journal of Sea Research*, 24 (4).
- van der Kaars, W.A., 1991. Palynology of eastern Indonesian marine piston-cores: a Late Quaternary vegetational and climatic record for Australasia. *Palaeogeography, Palaeoclimatology, Palaeoecology*, 85: 239-302.
- van der Kaars, W.A. and Dam, M.A.C., 1995. A 135,000-year record of vegetational and climatic change from the Bandung area, West-Java, Indonesia. *Palaeogeography, Palaeoclimatology, Palaeoecology*, 117: 55-72.
- Verardo, D.J., Froelich Philip, N. and McIntyre, A., 1990. Determination of organic carbon and nitrogen in marine sediments using the Carlo Erba NA-1500 Analyzer. *Deep-Sea Research*, 37: 157-165.
- Vo, V.L., 1995. *Coastal Upwelling off Southern Central Vietnam*. Science and Technics Publishing House, Hanoi, pp. 207.
- Voelker, A.H.L., Grootes, P.M., Nadeau, M.J. and Sarnthein, M., 2000. Radiocarbon levels in the Iceland Sea from 25-53 kyr and their link to the Earth's magnetic field intensity. In: J. van

- der Plicht (Editor), (super 14) C varve/ comparison issue. University of Arizona, Department of Geosciences. Tucson, AZ, United States. 2000.
- Wagner, T. and Dupont, L., 1999. Terrestrial organic matter in marine sediments: analytical approaches and eolian-marine records in the central equatorial atlantic. In: G. Fischer and G. Wefer (Editors), Use of proxies in paleoceanography: examples from the South Atlantic. Springer Verlag, Berlin Heidelberg, pp. 547-574.
- Wang, L. et al., 1999. East Asian monsoon climate during the late Pleistocene; high-resolution sediment records from the South China Sea. In: M. Sarnthein and P. Wang (Editors), Response of West Pacific marginal seas to global climate change. Marine Geology. Elsevier, Amsterdam, Netherlands, pp. 245-284.
- Wang, L. and Wang, P., 1990. Late Quaternary paleoceanography of the South China Sea; glacial-interglacial contrasts in an enclosed basin. *Paleoceanography*, 5(1): 77-90.
- Wang, P., 1999a. Response of Western Pacific marginal seas to glacial cycles; paleoceanographic and sedimentological features. In: M. Sarnthein and P. Wang (Editors), Response of West Pacific marginal seas to global climate change. Marine Geology. Elsevier, Amsterdam, Netherlands, pp. 5-39.
- Wang, P.X., 1999b. Response of Western Pacific marginal seas to glacial cycles: paleoceanographic and sedimentological features. *Marine Geology*, 156(1-4): 5-40.
- Wiesner, M.G., Zheng, L., Wong, H.K., Wang, Y. and Chen, W., 1996. Fluxes of particulate matter in the South China Sea. In: V. Ittekkot, P. Schaefer, S. Honjo and P.J. Depetris (Editors), Particle Flux in the Ocean. John Wiley & Sons Ltd, pp. 293-312.
- Winn, K., Sarnthein, M. and Erlenkeuser, H., 1991. $\delta^{18}\text{O}$ stratigraphy and chronology of Kiel sediment cores from the East Atlantic. 44, Geologische-Palaeontologisches Institut der Christian Albrechts Universitaet zu Kiel, Kiel.
- Wu, G. and Sun, X., 2000. Late Quaternary organic-wall phytoplankton record in northern slope of South China Sea and its paleoenvironmental significance. *Marine Geology & Quaternary Geology*, 20(2): 57-63.
- Wyrtki, K., 1961. Physical oceanography of Southeast Asian Waters, NAGA Report, Scientific Results of Marine Investigations of the South China Sea and the Gulf of Thailand, Scripps Institute of Oceanography, La Jolla, USA.
- Xiao, J., Porter, S.C., An, Z., Kumai, H. and Yoshikawa, S., 1995. Grain size of quartz as indicator of winter monsoon strength on the loess plateau of central China during the last 130,000 yr. *Quaternary Research*, 43: 22-29.
- Zonneveld, K.A.F., Versteegh, G.J.M. and de, L.G.J., 2001. Palaeoproductivity and post-depositional aerobic organic matter decay reflected by dinoflagellate cyst assemblages of the eastern Mediterranean S1 sapropel. *Marine Geology*, 172(3-4): 181-195.

Chapter 4 Appendix I. Dinoflagellate cyst counts

Sample (cm)	20	40	60	80	90	100	110	120	130	140
Sediment weight (dry g)	4	4	4	4	4	3	4	4	4	4
Lycopodium	1434	957	613	792	756	1696	1100	1339	922	736
Foramlining	1057	560	262	406	461	892	702	434	504	404
Spore	252	157	85	127	107	178	181	155	173	215
Tintinomorphs	0	0	0	0	0	3	0	3	0	0
Gonyaulacales										
Gonyaulacaceae										
Gonyaulacoid										
<i>Achomosphaera</i> spp.	0	0	0	0	0	0	0	0	0	0
<i>Spiniferites bulloideus</i>	4	4	0	3	0	4	7	3	4	4
<i>S. ramosus</i>	6	2	5	2	2	6	0	1	1	0
<i>S. mirabilis</i>	0	5	2	4	4	0	2	0	1	1
<i>S. hypercanthus</i>	1	1	2	1	1	1	1	0	0	2
<i>S. membrane</i>	1	0	2	0	1	4	3	0	0	0
<i>S. delicatus</i>	0	0	0	0	0	0	0	0	0	0
<i>S. bentori</i>	0	0	0	0	1	2	0	0	0	0
<i>S. belerius</i>	0	0	0	0	0	0	0	0	0	0
<i>Spiniferites</i> spp.	5	5	6	2	5	8	4	1	1	7
<i>Protoceratium reticulatum</i>	15	1	11	13	9	7	10	4	3	8
<i>Operculodinium longispinigerum</i>	0	0	0	0	0	0	0	0	0	0
<i>O. crassum</i>	1	0	0	0	1	0	0	0	0	0
<i>Operculodinium</i> spp.	0	0	0	0	0	2	0	4	0	0
<i>Lingulodinium machaerophorum</i>	0	0	0	1	0	0	0	0	0	0
<i>L. machaerophorum</i> (short process)	1	2	0	1	0	9	0	2	0	0
<i>Impagidinium paradoxum</i>	3	3	3	1	3	4	0	0	2	1
<i>I. patulem</i>	0	0	0	3	2	0	0	0	1	3
<i>I. striatum</i>	1	0	3	0	1	0	3	1	2	1
<i>I. aculeatum</i>	1	0	0	1	1	2	1	1	0	1
<i>Impagidinium</i> spp.	0	0	6	0	0	0	0	1	1	0
<i>Nematopshaera labyrinthus</i>	0	0	0	0	0	0	0	0	0	0
<i>Tectatodinium</i> spp.	0	0	0	0	0	0	0	0	0	0
<i>Polysphaeridium zoharyi</i>	0	0	1	0	0	0	0	0	0	3
Tuberculodinioid										
<i>Tuberculodinium vancampoae</i>	0	0	4	1	0	0	0	0	0	0
Peridinales										
Proto-peridiniaceae										
Proto-peridinioid										
pre-encysted Proto-peridium	0	0	0	0	0	0	0	0	0	0
<i>Brigantedinium</i> spp.	196	96	45	43	66	94	42	55	50	95
<i>P. americanum</i>	0	0	0	1	1	0	0	0	0	1
<i>Selenopemphix quanta</i>	4	0	0	0	0	1	1	0	2	0
<i>S. nephroides</i>	9	5	4	2	1	3	4	6	3	2
<i>Trinovantedinium capitatum</i>	0	0	1	0	0	0	0	0	0	0
<i>Stelladium stelladium</i>	9	4	0	1	0	3	0	0	0	0
<i>Proto-peridinium latissimum</i>	1	0	0	0	0	0	0	0	0	0
<i>Lejeunecysta sabrina</i>	0	0	0	0	0	0	0	0	0	0
<i>Quinquecuspis concret</i>	0	0	0	0	0	0	0	0	0	0
<i>Votadinium carvum</i>	6	12	5	3	0	0	2	0	2	0
Diplopsalid										
<i>Diplopelta purva</i>	1	1	1	1	0	0	0	0	0	0
Calciodinellid group										
<i>Scripsiella</i> spp.	30	16	10	35	60	66	22	12	11	31
<i>Pheopolykos hartmannii</i>	0	0	0	0	0	1	0	0	0	0
Total count of dino	295	157	111	119	159	217	102	91	84	160
Other										
<i>Cladopyxis</i> sp.	2	0	0	0	0	0	0	0	0	0
9 <i>Cymatiosphaera</i>	0	0	0	0	3	7	0	4	0	10
<i>Cyclopsiella</i> spp.	6	2	6	5	0	2	1	0	1	0
<i>Halodium major</i>	0	0	0	0	0	0	0	2	0	0
<i>Pediastrum</i>	0	0	0	0	0	0	1	0	0	0
Unidnetified Acritarchs	3	6	0	4	0	0	3	0	0	0

Sample (cm)	140	160	170	180	190	210	220	230	240	260
Sediment weight (dry g)	4	4	4	4	4	4	4	4	4	4
Lycopodium	736	945	1091	989	732	733	1956	872	983	1357
Foramlining	404	478	173	231	315	285	765	203	694	538
Spore	215	343	998	945	219	361	796	612	806	685
Tintinomorphs	0	0	0	0	0	0	5	0	1	0
Gonyaulacales										
Gonyaulacaceae										
Gonyaulacoid										
<i>Achomosphaera</i> spp.	0	0	0	0	0	0	0	0	0	0
<i>Spiniferites bulloideus</i>	4	1	0	6	0	1	0	1	1	2
<i>S. ramosus</i>	0	0	0	1	2	0	2	0	0	0
<i>S. mirabilis</i>	1	1	0	3	1	2	1	1	0	0
<i>S. hypercanthus</i>	2	1	0	0	0	0	0	0	0	0
<i>S. membrane</i>	0	1	0	4	1	1	1	0	1	1
<i>S. delicatus</i>	0	0	1	0	0	0	0	0	0	0
<i>S. bentori</i>	0	0	1	0	0	0	0	0	0	0
<i>S. belerius</i>	0	0	0	0	0	0	0	0	0	0
<i>Spiniferites</i> spp.	7	2	1	3	1	0	1	3	1	0
<i>Protoceratium reticulatum</i>	8	2	6	0	1	3	3	2	1	3
<i>Operculodinium longispinigerum</i>	0	0	0	0	0	0	1	0	0	0
<i>O. crassum</i>	0	0	0	0	0	0	0	0	0	0
<i>Operculodinium</i> spp.	0	0	0	0	0	0	0	0	0	0
<i>Lingulodinium machaerophorum</i>	0	0	6	1	1	0	0	0	0	0
<i>L. machaerophorum</i> (short process)	0	1	0	0	6	1	4	1	1	0
<i>Impagidinium paradoxum</i>	1	2	1	0	0	0	3	3	0	1
<i>I. patulem</i>	3	0	0	0	0	0	0	0	0	0
<i>I. striatum</i>	1	2	0	0	0	0	0	0	0	0
<i>I. aculeatum</i>	1	0	0	1	1	1	0	1	0	0
<i>Impagidinium</i> spp.	0	0	0	0	0	1	0	0	1	0
<i>Nematopshaera labyrinthus</i>	0	0	0	0	0	0	0	0	0	0
<i>Tectatodinium</i> spp.	0	0	0	0	0	0	0	0	0	0
<i>Polysphaeridium zoharyi</i>	3	0	1	3	0	0	0	0	0	0
Tuberculodinioid										
<i>Tuberculodinium vancampoae</i>	0	0	1	1	0	0	0	0	0	0
Peridinales										
Proto-peridiniaceae										
Proto-peridinioid										
pre-encysted Proto-peridium	0	0	0	0	0	0	0	0	0	0
<i>Brigantedinium</i> spp.	95	172	98	161	90	103	133	56	112	124
<i>P. americanum</i>	1	4	0	0	2	2	0	0	0	0
<i>Selenopemphix quanta</i>	0	1	1	1	0	0	2	0	0	1
<i>S. nephroides</i>	2	10	9	6	4	2	10	1	2	1
<i>Trinovantedinium capitatum</i>	0	0	0	0	1	0	0	0	0	0
<i>Stelladium stelladium</i>	0	2	0	1	0	0	1	0	0	1
<i>Proto-peridinium latissimum</i>	0	0	0	0	0	0	0	0	0	0
<i>Lejeunecysta sabrina</i>	0	0	0	0	0	0	0	0	0	0
<i>Quinquecuspis concret</i>	0	2	0	0	1	0	1	0	0	1
<i>Votadinium carvum</i>	0	1	0	0	0	1	0	0	0	1
Diplopsalid										
<i>Diplopelta purva</i>	0	2	0	0	0	4	1	0	1	0
Calcioidinellid group										
<i>Scripsiella</i> spp.	31	18	3	12	12	2	6	4	6	9
<i>Pheopolykos hartmannii</i>	0	0	4	0	0	0	0	0	0	0
Total count of dino	160	225	133	204	124	124	170	73	127	145
Other										
<i>Cladopyxis</i> sp.	0	0	0	0	0	0	0	0	0	0
9 <i>Cymatiosphaera</i>	10	0	4	4	0	0	0	0	0	0
<i>Cyclopsiella</i> spp.	0	0	0	7	0	1	0	0	0	0
<i>Halodinium major</i>	0	1	0	1	0	0	0	0	0	0
<i>Pediastrum</i>	0	0	0	2	1	1	0	2	0	1
Unidnetified Acritarchs	0	4	0	0	2	4	1	4	0	5

Sample (cm)	280	310	340	360	390	420	430	440	470	500
Sediment weight (dry g)	4	4	4	4	4	4	4	4	4	4
Lycopodium	804	436	817	1879	1440	1031	1162	1565	687	1985
Foramlining	195	371	217	362	269	180	652	269	169	399
Spore	854	444	1010	1190	632	579	1449	984	559	835
Tintinomorphs	0	0	0	0	0	0	0	0	0	0
Gonyaulacales										
Gonyaulacaceae										
Gonyaulacoid										
<i>Achomosphaera</i> spp.	0	0	0	0	0	0	0	0	0	0
<i>Spiniferites bulloideus</i>	0	1	1	0	1	1	6	1	2	2
<i>S. ramosus</i>	0	1	1	2	0	1	2	0	0	1
<i>S. mirabilis</i>	0	1	2	1	1	0	4	1	0	2
<i>S. hypercanthus</i>	1	0	1	2	0	0	4	2	0	0
<i>S. membrane</i>	1	0	3	1	1	0	2	2	0	1
<i>S. delicatus</i>	1	0	0	0	0	0	0	0	0	0
<i>S. bentori</i>	0	0	0	0	0	0	1	0	0	0
<i>S. belerius</i>	0	0	0	0	0	0	0	0	0	0
<i>Spiniferites</i> spp.	1	2	3	6	2	1	10	1	1	1
<i>Protoceratium reticulatum</i>	4	0	1	9	0	4	1	2	0	5
<i>Operculodinium longispinigerum</i>	0	0	0	0	0	0	0	0	0	0
<i>O. crassum</i>	0	0	0	0	0	0	0	1	0	0
<i>Operculodinium</i> spp.	0	7	0	0	9	0	3	0	0	27
<i>Lingulodinium machaerophorum</i>	0	0	0	0	0	0	1	1	0	0
<i>L. machaerophorum</i> (short process)	3	4	4	6	3	1	4	11	0	28
<i>Impagidinium paradoxum</i>	0	1	2	1	1	0	1	1	0	2
<i>I. patulem</i>	0	0	1	1	0	0	0	0	0	0
<i>I. striatum</i>	0	0	0	0	0	0	0	0	0	1
<i>I. aculeatum</i>	0	0	0	1	0	0	0	0	0	0
<i>Impagidinium</i> spp.	0	0	0	0	0	0	1	0	0	1
<i>Nematopshaera labyrinthus</i>	0	0	0	0	0	0	0	0	0	0
<i>Tectatodinium</i> spp.	0	0	0	0	0	0	0	0	0	0
<i>Polysphaeridium zoharyi</i>	0	0	0	0	0	0	0	0	0	0
Tuberculodinioid										
<i>Tuberculodinium vancampoae</i>	0	0	0	0	0	0	1	0	0	0
Peridinales										
Proto-peridiniaceae										
Proto-peridinioid										
pre-encysted Proto-peridium	0	0	0	0	0	0	0	0	0	0
<i>Brigantedinium</i> spp.	58	39	58	109	93	45	129	46	25	120
<i>P. americanum</i>	0	0	0	0	0	0	1	0	0	0
<i>Selenopemphix quanta</i>	0	1	0	3	5	0	5	5	1	6
<i>S. nephroides</i>	1	5	2	3	5	4	12	7	5	3
<i>Trinovantedinium capitatum</i>	0	0	0	0	0	2	1	0	1	0
<i>Stelladium stelladium</i>	0	0	0	0	0	0	0	0	0	1
<i>Proto-peridinium latissimum</i>	0	0	0	0	0	0	1	1	0	0
<i>Lejeunecysta sabrina</i>	1	0	0	0	0	0	0	0	0	0
<i>Quinquecuspis concret</i>	0	0	2	2	0	0	1	0	0	0
<i>Votadinium carvum</i>	0	0	0	0	0	0	0	1	0	2
Diplopsalid										
<i>Diplopelta purva</i>	0	1	1	1	0	0	2	0	1	2
Calcioidinellid group										
<i>Scripsiella</i> spp.	6	7	5	8	0	3	20	7	0	4
<i>Pheopolykos hartmannii</i>	0	0	0	0	0	0	0	0	0	0
Total count of dino	77	70	87	156	121	62	213	90	36	209
Other										
<i>Cladopyxis</i> sp.	0	0	0	0	0	0	0	2	0	0
9 <i>Cymatiosphaera</i>	0	0	0	0	0	0	0	0	0	0
<i>Cyclopsiella</i> spp.	0	0	2	1	1	1	0	0	2	1
<i>Halodium major</i>	0	1	0	0	0	0	0	0	0	0
<i>Pediastrum</i>	0	0	0	2	0	1	4	1	0	3
Unidnetified Acritarchs	0	0	1	0	1	0	2	2	1	1

Sample (cm)	520	530	560	580	610	620	630	660	690	720
Sediment weight (dry g)	4	4	4	3	4	4	4	4	4	4
Lycopodium	1614	934	1078	1889	2491	1500	3087	1955	1620	1515
Foramlining	347	202	279	319	494	321	797	317	454	309
Spore	1123	696	1223	1034	1238	1484	2146	896	1184	1035
Tintinomorphs	0	0	0	0	0	0	0	0	0	0
Gonyaulacales										
Gonyaulacaceae										
Gonyaulacoid										
<i>Achomosphaera</i> spp.	0	0	0	0	0	0	0	0	0	0
<i>Spiniferites bulloideus</i>	2	0	0	1	0	0	7	4	4	2
<i>S. ramosus</i>	1	0	0	0	1	0	1	2	3	4
<i>S. mirabilis</i>	0	1	0	0	2	1	0	4	2	1
<i>S. hypercanthus</i>	2	0	0	0	0	1	1	1	1	0
<i>S. membrane</i>	5	1	1	1	1	2	1	0	2	1
<i>S. delicatus</i>	0	0	0	0	0	0	0	0	0	0
<i>S. bentori</i>	0	0	0	0	0	0	0	2	1	1
<i>S. belerius</i>	0	0	0	0	0	0	0	0	0	0
<i>Spiniferites</i> spp.	2	0	5	2	2	4	7	5	1	4
<i>Protoceratium reticulatum</i>	5	1	4	3	1	1	15	0	5	1
<i>Operculodinium longispinigerum</i>	0	1	0	0	0	0	0	0	0	0
<i>O. crassum</i>	0	0	2	0	0	0	0	0	0	0
<i>Operculodinium</i> spp.	28	20	8	0	9	7	0	11	0	0
<i>Lingulodinium machaerophorum</i>	0	0	0	0	0	0	0	0	0	0
<i>L. machaerophorum</i> (short process)	7	6	6	1	9	1	5	7	4	2
<i>Impagidinium paradoxum</i>	0	0	0	0	1	1	2	1	1	1
<i>I. patulem</i>	0	0	0	0	0	1	1	1	2	0
<i>I. striatum</i>	0	0	0	0	1	0	1	0	1	0
<i>I. aculeatum</i>	0	1	0	0	1	1	1	1	1	0
<i>Impagidinium</i> spp.	0	0	0	2	1	0	0	2	0	0
<i>Nematopshaera labyrinthus</i>	0	0	0	0	0	0	0	0	1	0
<i>Tectatodinium</i> spp.	0	0	0	0	0	0	0	0	0	0
<i>Polysphaeridium zoharyi</i>	0	0	0	0	0	0	1	0	0	1
Tuberculodinioid										
<i>Tuberculodinium vancampoae</i>	0	0	0	0	0	0	0	0	0	0
Peridinales										
Proto-peridiniaceae										
Proto-peridinioid										
pre-encysted Proto-peridium	0	0	0	0	0	0	0	0	0	0
<i>Brigantedinium</i> spp.	119	104	47	70	96	67	119	93	119	87
<i>P. americanum</i>	0	0	0	0	0	0	0	0	0	1
<i>Selenopemphix quanta</i>	4	1	2	1	4	1	5	12	3	8
<i>S. nephroides</i>	6	6	6	4	7	7	13	9	8	9
<i>Trinovantedinium capitatum</i>	0	0	0	0	1	1	1	5	0	2
<i>Stelladium stelladium</i>	0	2	0	1	0	0	0	0	0	0
<i>Proto-peridinium latissimum</i>	0	0	0	0	0	0	0	0	0	0
<i>Lejeunecysta sabrina</i>	0	0	0	0	0	0	0	1	0	0
<i>Quinquecuspis concret</i>	5	0	3	3	1	1	4	4	0	0
<i>Votadinium carvum</i>	0	0	0	0	1	0	0	0	1	1
Diplopsalid										
<i>Diplopelta purva</i>	1	0	0	1	0	0	0	0	1	1
Calcioidinellid group										
<i>Scripsiella</i> spp.	5	12	5	0	7	11	5	7	10	9
<i>Pheopolykos hartmannii</i>	0	0	0	0	0	0	0	0	0	0
Total count of dino	192	156	89	90	146	108	190	172	171	136
Other										
<i>Cladopyxis</i> sp.	0	0	0	0	0	0	2	1	0	0
9 <i>Cymatiosphaera</i>	0	0	0	0	0	0	0	0	0	0
<i>Cyclopsiella</i> spp.	0	2	0	0	2	1	4	0	0	0
<i>Halodium major</i>	0	0	1	0	0	0	0	0	1	0
<i>Pediastrum</i>	1	2	1	1	2	1	3	1	3	0
Unidnetified Acritarchs	4	1	7	0	9	4	5	5	14	7

Sample (cm)	730	750	770	790	820	850	880	900	920	950
Sediment weight (dry g)	4	4	4	4	4	4	4	4	4	4
Lycopodium	1469	2406	1818	2613	1671	1636	1118	2902	2266	1830
Foramlining	444	498	468	519	256	626	240	442	152	239
Spore	876	725	727	1880	622	661	624	1280	959	413
Tintinomorphs	0	0	0	0	0	0	0	1	0	0
Gonyaulacales										
Gonyaulacaceae										
Gonyaulacoid										
<i>Achomosphaera</i> spp.	0	0	0	0	0	0	0	0	0	0
<i>Spiniferites bulloideus</i>	10	2	2	17	3	0	0	2	6	2
<i>S. ramosus</i>	1	1	2	4	2	0	0	2	5	1
<i>S. mirabilis</i>	3	4	1	22	2	2	1	1	7	6
<i>S. hypercanthus</i>	0	1	0	4	1	0	0	1	3	3
<i>S. membrane</i>	2	1	2	5	2	1	0	1	2	0
<i>S. delicatus</i>	0	0	0	0	0	1	0	0	0	0
<i>S. bentori</i>	0	0	0	0	0	0	0	0	0	0
<i>S. belerius</i>	0	0	0	0	0	0	0	1	0	0
<i>Spiniferites</i> spp.	3	3	2	17	5	6	4	9	7	3
<i>Protoceratium reticulatum</i>	6	11	4	36	5	2	3	7	6	1
<i>Operculodinium longispinigerum</i>	0	0	0	0	0	0	0	0	0	0
<i>O. crassum</i>	1	1	0	2	0	0	0	0	0	0
<i>Operculodinium</i> spp.	0	5	0	0	0	3	10	0	0	0
<i>Lingulodinium machaerophorum</i>	1	1	0	5	0	0	0	0	0	0
<i>L. machaerophorum</i> (short process)	0	11	2	5	6	20	7	11	45	9
<i>Impagidinium paradoxum</i>	1	2	3	3	0	2	0	1	1	1
<i>I. patulem</i>	3	2	1	3	2	1	0	1	3	1
<i>I. striatum</i>	0	2	0	3	0	0	0	0	0	0
<i>I. aculeatum</i>	1	1	0	5	1	0	0	0	0	0
<i>Impagidinium</i> spp.	0	0	0	2	0	3	1	0	0	0
<i>Nematopshaera labyrinthus</i>	0	0	0	0	1	0	0	0	0	0
<i>Tectatodinium</i> spp.	0	0	0	0	0	0	0	0	0	0
<i>Polysphaeridium zoharyi</i>	0	0	0	0	0	0	0	0	0	0
Tuberculodinioid										
<i>Tuberculodinium vancampoae</i>	1	0	0	1	0	1	0	0	0	1
Peridinales										
Protopteridiniaceae										
Protopteridinioid										
pre-encysted Protopteridium	0	0	1	0	0	0	0	0	0	0
<i>Brigantedinium</i> spp.	69	93	71	144	47	95	30	71	44	96
<i>P. americanum</i>	0	0	1	0	0	0	0	0	0	0
<i>Selenopemphix quanta</i>	3	4	7	14	5	2	1	4	4	5
<i>S. nephroides</i>	6	9	8	17	8	9	6	8	10	8
<i>Trinovantedinium capitatum</i>	1	3	2	3	0	1	0	0	1	0
<i>Stelladium stelladium</i>	1	1	1	1	0	1	0	0	0	0
<i>Protopteridinium latissimum</i>	0	2	0	0	1	3	0	1	0	0
<i>Lejeunecysta sabrina</i>	0	0	0	2	0	0	0	0	0	0
<i>Quinquecuspis concret</i>	1	0	0	10	0	2	0	1	0	1
<i>Votadinium carvum</i>	0	2	0	3	0	0	0	0	0	3
Diplopsalid										
<i>Diplopelta purva</i>	1	0	0	1	0	0	0	1	0	0
Calcioidinellid group										
<i>Scripsiella</i> spp.	8	7	3	28	7	11	3	10	6	8
<i>Pheopolykos hartmannii</i>	0	0	0	0	0	0	1	0	0	0
Total count of dino	123	169	113	357	98	166	67	133	150	149
Other										
<i>Cladopyxis</i> sp.	0	0	1	0	0	1	0	2	0	0
9 <i>Cymatiosphaera</i>	0	0	0	0	0	0	0	0	5	0
<i>Cyclopsiella</i> spp.	2	1	0	7	0	1	0	0	7	0
<i>Halodium major</i>	0	1	0	0	0	0	0	1	0	0
<i>Pediastrum</i>	1	1	0	18	2	0	1	1	5	6
Unidnetified Acritarchs	7	1	0	1	3	2	0	5	1	2

Sample (cm)	980	1000	1020	1040	1060	1080	1100	1120	1150	1160
Sediment weight (dry g)	4	4	4	4	4	4	4	4	4	4
Lycopodium	1242	1405	1584	2030	1986	1360	1261	1191	1892	2032
Foramlining	83	394	281	81	172	184	320	129	282	164
Spore	2193	528	672	1630	832	964	504	688	737	1502
Tintinomorphs	0	0	0	0	0	0	0	0	0	0
Gonyaulacales										
Gonyaulacaceae										
Gonyaulacoid										
<i>Achomosphaera</i> spp.	0	0	1	0	0	0	0	0	0	0
<i>Spiniferites bulloideus</i>	8	5	7	2	5	15	3	5	6	5
<i>S. ramosus</i>	7	0	3	2	4	3	0	2	2	7
<i>S. mirabilis</i>	4	0	5	1	3	11	3	1	2	1
<i>S. hypercanthus</i>	4	3	1	2	1	1	1	2	1	0
<i>S. membrane</i>	5	2	9	5	4	1	1	3	3	3
<i>S. delicatus</i>	1	1	0	0	0	0	0	0	0	0
<i>S. bentori</i>	5	0	0	0	0	0	1	0	2	2
<i>S. belerius</i>	0	0	0	0	0	0	2	0	0	0
<i>Spiniferites</i> spp.	9	5	6	9	3	3	2	3	2	10
<i>Protoceratium reticulatum</i>	7	4	17	14	4	5	2	4	2	2
<i>Operculodinium longispinigerum</i>	0	0	0	0	0	0	0	0	1	0
<i>O. crassum</i>	0	0	1	1	0	0	1	0	0	0
<i>Operculodinium</i> spp.	1	0	0	0	1	3	0	0	0	0
<i>Lingulodinium machaerophorum</i>	2	0	0	0	1	1	1	0	0	0
<i>L. machaerophorum</i> (short process)	12	1	8	0	5	12	1	20	7	10
<i>Impagidinium paradoxum</i>	0	3	1	0	1	0	1	0	1	0
<i>I. patulem</i>	1	0	0	0	0	2	1	0	0	1
<i>I. striatum</i>	0	0	0	0	1	2	0	2	1	0
<i>I. aculeatum</i>	1	0	0	0	0	0	1	1	0	0
<i>Impagidinium</i> spp.	0	2	0	0	1	1	0	1	0	0
<i>Nematopshaera labyrinthus</i>	0	0	0	0	0	0	0	0	0	0
<i>Tectatodinium</i> spp.	0	0	1	0	0	0	1	0	0	0
<i>Polysphaeridium zoharyi</i>	0	0	0	0	0	0	0	0	0	0
Tuberculodinioid										
<i>Tuberculodinium vancampoae</i>	2	0	0	0	3	0	0	0	0	0
Peridinales										
Proto-peridiniaceae										
Proto-peridinioid										
pre-encysted Proto-peridium	0	0	0	0	0	0	0	0	0	0
<i>Brigantedinium</i> spp.	31	52	37	17	96	90	44	82	81	32
<i>P. americanum</i>	0	0	0	0	0	0	0	0	0	0
<i>Selenopemphix quanta</i>	2	5	6	3	4	7	1	2	3	4
<i>S. nephroides</i>	18	5	7	3	17	15	4	13	13	4
<i>Trinovantedinium capitatum</i>	1	0	0	0	1	0	0	0	0	0
<i>Stelladium stelladium</i>	0	1	0	0	0	0	0	0	1	0
<i>Proto-peridinium latissimum</i>	1	0	0	0	2	0	0	0	0	0
<i>Lejeunecysta sabrina</i>	0	0	0	0	0	1	0	0	0	0
<i>Quinquecuspis concret</i>	0	2	0	1	0	0	1	0	2	1
<i>Votadinium carvum</i>	1	0	0	0	0	0	0	0	0	0
Diplopsalid										
<i>Diplopelta purva</i>	1	1	1	0	0	1	0	1	0	0
Calcioidinellid group										
<i>Scripsiella</i> spp.	4	7	12	2	14	6	19	15	8	5
<i>Pheopolykos hartmannii</i>	0	0	0	0	0	0	0	0	0	0
Total count of dino	128	99	123	62	171	180	91	157	138	87
Other										
<i>Cladopyxis</i> sp.	0	0	0	0	0	0	0	0	0	0
9 <i>Cymatiosphaera</i>	5	0	0	0	2	5	0	2	0	0
<i>Cyclopsiella</i> spp.	2	0	11	1	0	2	3	0	1	0
<i>Halodium major</i>	0	0	3	0	0	1	0	0	0	0
<i>Pediastrum</i>	7	1	0	0	0	4	1	0	5	3
Unidentified Acritarchs	0	6	5	1	0	0	2	0	3	5

Sample (cm)	1170	1180	1210	1240	1270	1300	1330	1360	1380
Sediment weight (dry g)	4	4	4	4	4	4	4	4	4
Lycopodium	1204	2104	1449	760	2053	1817	2013	928	1721
Foramlining	130	144	210	118	168	233	150	98	175
Spore	1163	934	1025	1149	903	1088	922	523	812
Tintinomorphs	0	0	1	2	0	0	0	1	0
Gonyaulacales									
Gonyaulacaceae									
Gonyaulacoid									
<i>Achomosphaera</i> spp.	0	0	0	0	0	0	0	0	0
<i>Spiniferites bulloideus</i>	6	0	1	3	0	4	2	2	1
<i>S. ramosus</i>	0	1	0	2	0	0	1	0	2
<i>S. mirabilis</i>	1	0	5	5	1	4	1	2	3
<i>S. hypercanthus</i>	0	1	0	1	1	1	0	1	1
<i>S. membranaceus</i>	0	3	2	9	0	2	4	0	1
<i>S. delicatus</i>	0	0	1	0	0	0	0	0	0
<i>S. bentori</i>	0	0	0	0	0	4	0	0	0
<i>S. belerius</i>	0	0	0	0	0	0	0	0	0
<i>Spiniferites</i> spp.	0	8	2	8	0	8	0	9	3
<i>Protoceratium reticulatum</i>	1	6	1	11	2	3	0	5	3
<i>Operculodinium longispinigerum</i>	0	0	0	0	0	0	0	0	0
<i>O. crassum</i>	0	0	0	0	0	0	0	0	0
<i>Operculodinium</i> spp.	0	0	0	0	0	0	0	0	0
<i>Lingulodinium machaerophorum</i>	0	0	0	2	0	2	0	0	0
<i>L. machaerophorum</i> (short process)	5	44	20	2	4	9	28	4	5
<i>Impagidinium paradoxum</i>	2	2	0	0	1	0	1	1	1
<i>I. patulem</i>	0	0	0	0	0	0	0	0	1
<i>I. striatum</i>	0	0	0	0	0	0	0	1	0
<i>I. aculeatum</i>	4	2	0	0	0	0	0	0	1
<i>Impagidinium</i> spp.	0	1	0	0	0	0	0	0	0
<i>Nematopshaera labyrinthus</i>	0	0	0	0	0	0	1	0	0
<i>Tectatodinium</i> spp.	0	0	0	0	0	0	0	0	0
<i>Polysphaeridium zoharyi</i>	0	0	0	0	0	0	0	0	1
Tuberculodinioid									
<i>Tuberculodinium vancampoae</i>	0	0	0	0	0	0	0	1	1
Peridinales									
Protopteridiniaceae									
Protopteridinioid									
pre-encysted Protopteridium	0	0	0	0	0	0	0	0	0
<i>Brigantedinium</i> spp.	42	86	54	25	95	63	86	66	93
<i>P. americanum</i>	0	0	0	0	0	0	0	0	0
<i>Selenopemphix quanta</i>	5	4	9	4	5	3	1	4	4
<i>S. nephroides</i>	7	14	5	6	13	14	13	9	18
<i>Trinovantedinium capitatum</i>	0	0	0	0	0	0	0	0	0
<i>Stelladium stelladium</i>	0	0	1	1	0	0	0	0	0
<i>Protopteridinium latissimum</i>	0	0	0	0	0	0	1	0	0
<i>Lejeunecysta sabrina</i>	0	0	0	0	0	0	0	1	0
<i>Quinquecuspis concret</i>	1	1	0	2	1	0	2	2	2
<i>Votadinium carvum</i>	1	0	0	0	0	2	1	0	0
Diplopsalid									
<i>Diplopelta purva</i>	0	1	0	2	0	1	0	0	2
Calcioidinellid group									
<i>Scripsiella</i> spp.	9	7	10	1	18	2	17	11	9
<i>Pheopolykos hartmannii</i>	0	0	0	0	0	0	0	0	0
Total count of dino	84	181	111	84	141	122	159	119	152
Other									
<i>Cladopyxis</i> sp.	0	3	0	0	0	0	0	0	0
9Cymatiosphaera	0	0	0	0	0	0	0	0	0
<i>Cyclopsiella</i> spp.	1	1	0	0	0	0	3	1	0
<i>Halodium major</i>	0	0	0	0	0	0	0	0	3
<i>Pediastrum</i>	2	2	0	2	1	2	0	0	0
Unidnetified Acritarchs	0	7	4	0	5	1	4	1	6

Sample (cm)	280	310	340	360	390	420	430	440	470	500
Araliaceae	0	0	2	1	0	0	0	1	0	0
Betulaceae	0	2	0	0	0	0	0	0	0	0
Compositae	2	2	4	3	2	2	2	5	1	5
Cyperraceae	16	13	30	54	35	20	49	33	15	41
Dacrydium	9	4	14	12	3	5	15	16	8	10
Ericaceae	0	2	3	4	0	2	1	1	1	0
Euphobiaceae	1	3	0	0	0	1	0	1	0	0
Graminae	43	28	63	51	27	35	63	75	39	14
Kateleeria	0	3	0	0	0	0	1	0	0	0
Lithocarpus	0	1	0	0	0	0	0	0	0	0
Meliaceae	0	8	0	0	0	0	0	2	0	0
Nypa	1	0	2	1	1	0	7	1	2	2
Phyllocladus	2	3	4	7	1	1	5	4	0	1
Pinaceae(divided)	58	48	46	104	101	61	158	66	63	99
Podocarpus(divided)	22	39	27	41	22	18	50	20	12	47
Quercus	0	4	0	0	0	0	0	0	0	0
Rhizophoraceae	0	1	1	1	0	3	3	2	2	0
Rubiaceae	0	2	0	0	0	0	1	0	0	0
Sapotaceae	0	1	0	0	0	0	0	0	0	0
Sonnetatia	9	4	12	8	6	3	13	17	8	6
Taxodiaceae	1	0	0	0	0	0	0	0	0	0
Tiliaceae	0	1	0	0	0	0	0	0	0	0
Unidentified Pollen	73	28	168	160	106	71	139	132	85	132
Total count of Pollen	237	197	376	447	304	222	507	376	236	357
Sporegia	0	0	1	0	0	0	0	0	0	0

Sample (cm)	520	530	560	580	610	620	630	660	690	720
Araliaceae	0	0	0	0	1	0	0	0	0	1
Betulaceae	0	0	0	6	0	0	6	0	0	0
Compositae	3	2	4	3	4	11	8	1	5	3
Cyperraceae	27	31	46	42	79	53	57	57	44	31
Dacrydium	14	9	11	10	23	13	28	15	7	7
Ericaceae	2	0	3	3	3	2	0	3	1	2
Euphobiaceae	0	0	0	5	0	0	0	0	0	0
Graminae	54	25	36	39	50	47	142	45	32	28
Kateleeria	1	0	0	1	0	0	0	0	0	0
Lithocarpus	0	0	0	0	0	0	0	0	0	0
Meliaceae	0	0	0	0	0	0	0	0	0	0
Nypa	1	0	1	2	0	1	2	0	0	2
Phyllocladus	3	2	4	2	3	5	3	6	2	5
Pinaceae(divided)	131	103	80	76	107	76	192	125	143	114
Podocarpus(divided)	45	32	30	55	25	31	79	19	38	24
Quercus	0	0	0	0	0	0	0	0	0	0
Rhizophoraceae	1	3	1	0	2	0	0	0	0	1
Rubiaceae	1	0	0	0	0	0	0	0	0	0
Sapotaceae	0	0	0	0	0	0	0	0	1	0
Sonnetatia	14	3	18	13	24	16	22	6	12	8
Taxodiaceae	0	0	0	0	0	0	0	0	0	0
Tiliaceae	0	0	0	0	0	0	0	0	0	0
Unidentified Pollen	124	91	172	94	198	194	245	141	128	118
Total count of Pollen	421	301	406	351	519	449	784	418	413	344
Sporegia	0	0	0	2	0	0	0	0	0	0

Chapter 4. Appendix III

Sample (cm)	$\delta^{18}\text{O}$	$\delta^{13}\text{C}$	TOC (%)	bulk density	TOC/N ratio	T:M ratio
10	-3.28	1.27	0.92	0.51	6.61	
20	-3.27	1.24	0.88	0.50	6.63	1.20
30	-3.28	1.28	0.79	0.51	6.13	
40	-2.94	1.22	0.93	0.49	7.54	1.60
50	-3.16	1.17	0.85	0.47	6.82	
60	-3.06	1.01	0.84	0.51	6.79	1.25
70	-2.99	0.97	0.82	0.54	6.63	
80	-2.69	0.91	0.72	0.54	6.24	2.06
90	-3.09	0.79	0.86	0.55	6.95	1.90
100	-2.97	0.55	0.73	0.58	6.01	1.79
110	-2.94	0.44	0.88	0.57	7.30	3.12
120	-2.32	0.68	0.95	0.56	8.01	3.05
130	-1.92	0.57	1.04	0.55	8.26	3.72
140	-2.13	0.73	0.91	0.53	7.20	2.72
150	-2.26	0.75	1.05	0.57	8.05	
160	-2.16	0.56	1.04	0.52	8.08	2.60
170	-1.59	0.63	0.97	0.52	7.80	10.38
180	-1.40	0.83	0.94	0.59	7.96	7.02
190	-1.21	0.85	0.95	0.58	7.81	3.29
200	-1.60	0.71	0.83	0.66	8.04	
210	-1.01	0.49	0.97	0.52	8.00	4.50
220	-1.46	0.91	0.93	0.60	7.83	7.70
230	-1.25	0.83	0.91	0.59	7.61	12.29
240	-1.76	1.10	0.92	0.59	7.97	9.57
250	-1.80	0.80	0.90	0.65	8.65	
260	-1.57	0.90	0.91	0.61	7.92	8.03
270	-1.51	0.92	0.89	0.67	7.94	
280	-1.33	1.05	0.94	0.61	7.66	15.59
290						
300						
310	-1.42	0.98	0.89	0.65	7.34	10.34
320	-1.61	0.91	0.85	0.60	7.40	
330	-1.37	0.89	0.87	0.62	7.19	
340	-1.62	0.86	0.92	0.68	8.16	17.54
350	-1.97	0.99	0.81	0.60	6.60	
360	-1.50	0.78	0.91	0.62	7.01	11.29
370	-1.33	0.93	0.83	0.62	6.73	
380					7.23	
390	-1.69	0.93	0.86	0.60	6.97	7.74
400	-0.99	0.88	0.82	0.64	7.37	
410	-1.19	0.89	0.79	0.64	7.07	
420	-1.64	0.65	0.84	0.63	7.05	13.58
430	-1.34	0.56	0.77	0.74	8.33	10.30
440			0.79	0.65	7.45	16.59
450	-1.50	0.91	0.79	0.68	7.15	
460	-1.35	0.85	0.88	0.66	7.51	
470	-1.72	0.84	0.86	0.67	7.60	22.71
480	-1.88	1.09	0.89	0.64	7.20	
490	-2.02	0.95	0.86	0.63	7.05	
500	-2.25	0.61	0.91	0.67	7.87	5.93

Sample (cm)	$\delta^{18}O$	$\delta^{13}C$	TOC (%)	bulk density	TOC/N ratio	T:M ratio
510	-1.20	0.92	0.84	0.66	7.22	
520	-1.71	1.23	0.85	0.68	7.50	8.53
530	-1.70	1.02	0.85	0.65	7.53	6.92
540					7.30	
550					7.63	
560	-1.32	0.75	0.78	0.72	7.95	20.11
570	-1.30	0.68	0.77	0.69	7.77	
580			0.75	0.73	7.77	16.11
590	-1.70	0.72	0.76	0.75	6.88	
600	-1.86	1.10	0.78	0.70	6.78	
610			0.76	0.71	6.79	12.83
620			0.75	0.72	6.90	20.14
630	-2.06	1.00	0.75	0.72	6.66	16.19
640	-1.96	0.63	0.86	0.70	7.39	
650					7.32	
660	-1.70	0.75	0.81	0.71	6.84	8.21
670	-1.93	0.96	0.81	0.69	7.12	
680	-1.61	0.67	0.83	0.71	6.88	
690	-1.64	0.86	0.84	0.71	7.01	10.04
700	-1.60	0.46	0.79	0.70	6.31	
710	-2.17	0.91	0.79	0.67	6.62	
720	-2.11	0.88	0.79	0.87	7.25	11.03
730	-2.05	0.92	0.83	0.77	7.28	11.68
740	-2.23	0.65	0.85	0.66	7.04	
750	-1.71	0.60	0.85	0.70	7.21	6.86
760	-1.48	1.00	0.87	0.77	7.74	
770	-1.90	0.72	0.86	0.72	6.86	10.01
780	-2.32	0.97	0.81	0.71	6.76	
790	-2.02	0.90	0.80	0.79	7.05	10.90
800					6.62	
810	-2.12	0.84	0.82	0.71	6.67	
820	-2.28	1.24	0.72	0.72	6.05	10.24
830	-2.14	1.29	0.74	0.81	6.30	
840	-1.59	0.65	0.77	0.75	6.98	
850	-2.14	1.03	0.87	0.70	6.96	6.11
860	-2.09	0.80	0.91	0.70	7.33	
870					6.65	
880	-1.89	0.84	0.89	0.74	6.67	14.54
890	-1.82	0.87	0.78	0.71	6.72	
900	-1.96	1.08	0.81	0.72	6.62	14.81
910	-2.03	1.19	0.82	0.73	6.72	
920	-1.85	1.11	0.83	0.69	6.72	10.54
930	-1.96	0.82	0.86	0.71	7.07	
940	-2.08	0.85	0.86	0.69	6.74	
950	-1.91	0.99	0.86	0.69	6.82	4.90
960	-2.05	0.89	0.74	0.75	7.09	
970	-2.01	1.09	0.80	0.76	7.19	
980	-2.24	1.17	0.78	0.73	7.02	23.13
990	-2.04	1.06	0.88	0.73	6.92	
1000	-2.22	0.92	0.91	0.72	7.13	9.00

Sample (cm)	$\delta^{18}\text{O}$	$\delta^{13}\text{C}$	CaCO ₃ (%)	TOC (%)	bulk density	TOC/N ratio	T:M ratio
1010	-1.69	0.88	2.99	0.90	0.71	6.98	
1020	-2.14	0.84	4.07	0.95	0.75	7.13	10.06
1030	-2.28	0.87	4.07	0.86	0.74	6.98	
1040	-2.36	0.71	3.55	0.80	0.77	6.81	41.10
1050	-2.06	0.67	4.12	0.93	0.74	7.25	
1060	-2.10	0.79	3.03	0.82	0.70	6.53	7.65
1070	-1.88	0.87	2.83	0.84	0.76	6.88	
1080	-2.11	0.86	2.76	0.76	0.78	6.65	8.15
1090	-1.83	0.72	2.64	0.77	0.75	6.74	
1100	-1.66	1.00	3.34	0.81	0.74	6.49	10.55
1110	-1.74	0.75	3.77	0.82	0.77	6.87	
1120	-1.94	0.89	2.83	0.81	0.77	6.66	7.17
1130	-1.89	1.12	2.52	0.82	0.75	6.87	
1140	-1.75	0.97	2.60	0.83	0.76	6.88	
1150	-1.90	0.99	2.33	0.79	0.77	6.66	8.18
1160	-1.97	1.05	2.10	0.86	0.74	7.24	23.89
1170	-2.73	0.56	1.89	0.83	0.79	6.84	20.86
1180	-1.91	0.82	2.55	0.89	0.76	6.84	8.10
1190	-1.75	0.65	2.44	0.89	0.76	6.77	
1200	-2.12	1.10	2.40	0.84	0.78	6.96	
1210	-1.85	0.90	2.99	0.85	0.75	6.70	14.10
1220	-2.11	0.90	2.16	0.85	0.78	6.83	
1230	-1.82	0.89	1.85	0.80	0.74	6.71	
1240			2.90	0.64	0.89	6.72	20.15
1250	-1.83	0.98	2.26	0.80	0.75	6.65	
1260	-1.76	0.82	2.30	0.84	0.78	6.76	
1270	-1.91	0.87	2.86	0.83	0.73	6.45	10.72
1280						6.74	
1290	-2.01	1.08	2.59	0.85	0.75	6.93	
1300	-2.05	1.17	2.15	0.84	0.77	7.05	12.59
1310							
1320	-1.68	0.92	1.97	0.77	0.76	6.37	
1330	-1.94	1.02	1.96	0.77	0.76	6.46	10.04
1340						6.75	
1350	-1.80	1.09	2.71	0.80	0.77	6.18	
1360	-2.04	0.75	3.30	0.79	0.78	6.37	7.88
1370	-1.97	0.78	2.84	0.81	0.76	6.47	
1380	-2.02	0.86	3.37	0.80	0.76	6.46	8.46
1390	-2.34	0.72	3.33	0.79	0.83	6.63	

Chapter 4 Appendix IV

Sample (cm)	Dino CA 1	Axis Dino CA Axis 2	Dino CA WEIGHT	Pollen CA Axis 1	Pollen CA Axis 2	Pollen CA WEIGHT
20	-0.5293	-0.8206	52.67			
40	-0.6129	-1.0543	46.22			
60	-0.883	-0.617	56.72			
80	-0.9199	-0.0504	49.91			
90	-0.7057	0.2599	43.41			
100	0.2305	0.1928	42.05			
110	-0.6707	-0.7016	39.28			
120	0.7694	-0.489	29.11	0.012	-0.061	224.04
130	-0.6633	-0.9298	38.95	-1.014	-0.060	244.20
140	-0.8826	0.0058	40.4	-0.539	-0.390	405.62
160	-0.2938	-0.8928	44.86	-0.678	-0.471	784.52
170	-0.7891	2.2672	30.66	-0.289	-0.352	781.00
180	-0.5997	0.7018	36.1	0.164	-0.181	963.89
190	0.0429	0.8375	35.38	0.217	-0.902	1259.55
210	-0.2937	-0.9853	35.01	0.106	-0.505	762.16
220	0.2343	-0.2882	28.08	0.246	-0.758	842.36
230	-0.1369	-0.1271	25.36	-0.340	0.009	775.86
240	0.2037	-0.5154	23.46	-0.239	0.090	950.74
260	-0.1732	-0.7075	23.3	0.764	-0.076	990.44
280	0.0199	0.3394	25.5	0.694	-0.117	933.34
310	0.9666	-0.2523	40.48	0.739	-0.038	1048.49
340	-0.1224	-0.0342	36.51	0.699	0.297	1504.69
360	-0.0206	0.0574	32.56	1.072	0.003	1201.01
390	1.6332	0.0592	24.02	0.482	0.225	717.01
420	0.1153	0.3747	21.79	0.036	0.029	653.23
430	0.2145	0.4921	51.14	0.528	-0.316	706.72
440	-0.184	0.2285	32.8	0.329	0.039	1248.54
470	0.1935	0.1434	18.2	0.966	-0.182	774.28
500	0.9607	-0.8036	36.44	0.561	-0.353	1029.98
520	1.3251	0.001	35.24	-0.013	0.903	450.77
530	1.6161	-0.2848	31.67	0.359	0.124	793.07
560	1.4467	0.2493	29.89	0.031	0.226	970.97
580	0.3157	-0.5965	21.03	0.467	0.402	862.89
610	0.9225	-0.3334	29.26	0.606	0.587	511.15
620	0.8023	0.2154	31.29	0.427	0.466	520.51
630	-0.0655	0.1233	29.11	0.631	0.435	696.78
660	0.8608	0.4638	39.14	0.733	-0.026	761.78
690	-0.4273	-0.1137	37.03	0.188	0.137	576.48
720	-0.1937	0.2178	31.53	-0.006	0.268	686.96
730	-0.459	0.48	37.4	0.008	0.088	477.68
750	0.1614	0.0638	39.15	0.028	-0.432	860.43
770	-0.0442	0.0899	30.19	-0.295	0.355	448.30
790	-0.4825	0.0951	56.75	0.511	-0.502	664.97
820	-0.1223	0.2296	33.09	-0.827	-0.501	1793.56
850	0.7096	0.2072	38.04	0.059	-0.144	535.82
				-0.621	0.294	490.64

Sample (cm)	Dino CA Axis 1	Dino CA Axis 2	Dino CA WEIGHT	Pollen CA Axis 1	Pollen CA Axis 2	Pollen CA WEIGHT
880	1.644	0.0415	25.67	1.241	-0.259	1012.67
900	0.0437	0.0676	27.91	-0.173	0.095	463.40
920	-0.1064	0.2116	36.01	-0.492	-0.305	619.26
950	-0.329	-0.1483	33.7	-0.348	-0.280	454.92
980	-0.2935	1.0262	51.55	-0.358	-0.164	1449.72
1000	-0.0011	-0.3457	35.7	-0.420	0.108	585.19
1020	-0.1208	-0.0456	38.64	-0.772	-0.047	646.10
1040	-0.1424	0.2358	23.28	-0.948	-0.407	959.65
1060	0.0123	0.4143	38.46	-0.585	-0.029	571.98
1080	0.1666	-0.0045	44.84	-0.942	-0.314	882.01
1100	-0.3478	0.8019	33.69	-0.386	0.594	510.74
1120	-0.1035	-0.4239	40.45	-0.385	0.042	779.54
1150	-0.0173	0.0619	33.34	-0.199	0.396	432.17
1160	-0.0216	0.5139	29.73	-0.263	0.641	555.50
1170	-0.0803	-0.3917	30.31	0.027	1.046	783.25
1180	0.2459	-0.1524	31.96	-0.142	0.346	636.89
1210	0.3615	0.1367	27.57	-0.300	0.123	660.14
1240	-0.25	0.238	45.05	-0.926	-0.116	1335.04
1270	0.2688	-0.0338	22.3	-0.473	0.199	527.22
1300	-0.3566	0.5761	32.9	-0.210	0.675	489.46
1330	0.2936	-0.1339	25.96	-0.518	1.291	677.16
1360	-0.1573	-0.0089	38.91	-0.857	0.241	935.66
1380	-0.1839	0.1996	34.43	-0.749	0.931	623.28

CHAPTER 5. CONCLUSIONS

1. Distribution patterns of organic-walled dinoflagellate cysts

- * Forty-five taxa of organic-walled dinoflagellate cysts were identified from eighty-six surface sediment samples.
- * High proportions of *Spiniferites* sp. characterize dinoflagellate cyst assemblages in the tropical Sunda Shelf.
- * Dinoflagellate cyst assemblages in the Vietnamese Shelf are characterized by the dominance of protoperidinioids such as *Brigantedinium* sp., *S. stellatum*, *S. quanta*, *Q. concreta* and *S. nephroides*.
- * Dinoflagellate cyst assemblages in the oceanic part of the SCS are characterized by occurrences of *Impagidinium* sp. and *N. labyrinthus*.

2. Relations between distribution patterns and environmental parameters

- * Concentration of dinoflagellate cysts on the Sunda Shelf increases with increasing abundance of grain-size ϕ^0 5.75-6.25 sediments. This result indicates that winnowing processes mainly control distribution patterns of dinoflagellate cysts on the Sunda Shelf. High concentration of dinoflagellate cysts is recorded in sediments composed of high proportions of fine-silt size grains.
- * Distribution patterns of dinoflagellate cysts in the SCS related strongly to distance from the shallow coastal area. This relation may be explained with either gradients of surface water productivity or effect of offshore transport from shallow coastal area. Both productivity and effect of offshore transport showed a correlation with 1st CA axis scores. More samples are necessary to determine which of these factors is the main factor controlling the distribution patterns of dinoflagellate cysts.
- * **Presumably cysts found in oceanic area are autochthonous**, dinoflagellate cyst species can be divided into three trophic groups (eutrophic/coastal, mesotrophic/shelf and oligotrophic/oceanic), and scores of 1st CA axis can be used as qualitative proxies for the surface water productivity level. Eutrophic/coast-slope group is characterized by the dominance of protoperidinioid group. Mesotrophic/shelf-slope group is characterized by the dominance of *Spiniferites* sp. and oligotrophic/oceanic group is characterized by the dominance of *Impagidinium* spp. and *Nematosphaera labyrinthus*.

3. Environmental variations in/around the southern SCS over the last 44 kyr

- * Dinoflagellate cyst assemblages of core GIK 18267-3 revealed that surface water was mesotrophic during MIS 3 in the southern SCS. Productivity level was high

during MIS 2. At ca. 19 ka BP, productivity gradually decreased toward early Holocene. After a short oligotrophic period in early Holocene, surface water returned to mesotrophic. Since the core was recovered from an area of the SCS that is today dominated by a monsoon driven winter upwelling, this productivity record may be closely related to the changes in winter monsoon intensity.

* Pollen analysis of core GIK 18267-3 revealed that climatic condition during MIS 3 was colder and drier than at present. During MIS 2, climate became colder and drier than during MIS 3. Starting at 19 ka BP, climate began to be warmer and moister in two steps toward Holocene.

* Ratio of terrestrial palynomorphs (pollen and spore) to marine pelagic palynomorphs (dinoflagellate cysts), accumulation rates of insect pollinating mangrove pollen and of freshwater algae *Pediastrum* were used as qualitative proxies for the influence of terrestrial organic matter, for the effect of offshore transport of coastal fine-sediments and for the influence of freshwater plume at the core site respectively. The results suggested that during MIS 3, influences of offshore sediment transport and of terrestrial organic matters were medium level. During MIS 2, influences of offshore sediment transport and of terrestrial organic matters were high. The coring site 18267-3 was constantly under influence of freshwater plume during MIS3 and 2. During Termination-I, influence of terrestrial organic matters and of offshore sediment transport decreased and no influences of freshwater plume was recognized. These results are caused probably by the rapid rise of sea level. During Holocene, influence of terrestrial organic matter and the effect of offshore sediment transport were low. No influence of freshwater plume was recognized during the Holocene.

* Comparison of surface water productivity record with climate records shows some similarities and dissimilarities. In general (for different MISs), cold/dry climatic conditions corresponded to eutrophic surface water condition, indicating strong winter monsoon/weaker summer monsoon, and warm/moist climatic condition corresponded to oligotrophic surface water condition, indicating strong summer monsoon/weak winter monsoon. However, on millennial scale, changes in climatic conditions and in surface-water productivity-level do not correlate each other. During MIS 3, the changes in climatic conditions led shortly (<1 kyr) the changes in productivity level. During MIS 2, brief warm/moist periods corresponded with brief high productivity periods and vice versa. Climatic condition and surface water productivity also shows different deglaciation processes. At ca. 19 ka, climate amelioration processes and gradual lowering of productivity toward Holocene began. Climatic amelioration was drastic while lowering of productivity was gradual. These results may indicate that different monsoonal forcing controlled surface water productivity and climatic conditions on

millennial scale the southern SCS.